Excitatory Interneurons in the Mouse Spinal Cord with Emphasis on those Expressing Gastrin-Releasing Peptide.

Andrew McKenzie Bell

Bachelor of Veterinary Medicine & Science (University of Glasgow 2004)

September 2020

Submitted in fulfilment of the requirements for the Degree of Doctor of Philosophy

Institute of Neuroscience and Psychology

College of Medical, Veterinary and Life Sciences

University of Glasgow

Summary

The neurons of the dorsal horn of the spinal cord are critically important components of neural circuits for pain and itch. The vast majority of cells in this area are interneurons and these have axons that remain in the cord and do not project to supra-spinal targets. It is likely that specific classes of interneurons are functionally highly specialised to process specific somatosensory modalities and mediate cross-modality interactions. However, we have a poor understanding of the dorsal horn circuitry that underlies pain and itch sensation and defining functional populations of interneurons remains a challenge. Dorsal horn excitatory interneurons display a marked heterogeneity in terms of their lineage, morphology, physiology, neurochemistry, transcriptomic identity and connectivity. A proposed class of lamina II excitatory interneurons includes cells that express gastrin-releasing peptide (GRP), and these can be identified by the expression of enhanced green fluorescent protein (EGFP) in a GRP-EGFP transgenic mouse line. These cells are distinct from other defined neurochemical classes of interneuron in the dorsal horn and have been proposed to act as secondary pruritoceptors in a labelled-line for itch. The underlying hypothesis of the work presented here is that these cells are not simply neurochemically distinct but rather represent a distinct functional population of excitatory interneurons. We present a series of studies that aims to provide evidence for this by further categorising these neurons in terms of their morphology, responses to stimuli, synaptic inputs and molecular identity.

In order to investigate the morphology of GRP-EGFP cells, neurobiotin-filled neurons were reconstructed following patch-clamp recording. Many of the GRP-EGFP cells were classed as having central type morphology. As the majority of these cells also displayed transient firing patterns, they are likely to represent 'transient central cells', which are a component of a previously proposed circuit for tactile allodynia. We also compared the morphology of GRP-EGFP cells to cells of another neurochemical class defined by the expression of substance P. Substance P-expressing cells were revealed using virally mediated Brainbow labelling in the $Tac1^{Cre}$ mouse. Many of these cells had radial morphology. Additionally, the two populations of neurons were shown to have distinct somatodendritic morphology using hierarchical cluster analysis.

Furthermore, we aimed to determine the responses of GRP-EGFP cells to noxious and pruritic stimuli using activity-dependent markers as surrogate measures of neuronal activation. Despite observing a robust expression of Fos and phosphorylation of ERK following intradermal injection of the pruritogen chloroquine, we found that GRP-EGFP cells were significantly less likely to show these markers than other neurons. We also seldom observed phosphorylation of ERK in GRP-EGFP cells in response to the pruritogen histamine or to a variety of noxious stimuli.

The patterns of synaptic input to a cell have implications for function. Here the proportions of synapses arising from specific classes of primary afferent neurons to the GRP-EGFP cells were determined using an anatomical quantification technique. Excitatory synapses were identified using the post-synaptic density protein Homer. We show that these cells receive much of their excitatory synaptic input from MrgprA3/MrgprD-expressing pruritoceptive/nociceptive afferents or from C-low threshold mechanoreceptors. Although the cells were not innervated by a class of pruritoceptors that express brain natriuretic peptide (BNP) most of them contained mRNA for NPR1, the receptor for BNP. These cells received only around 10% of their excitatory input from other interneurons, and this is in stark contrast to the equivalent proportion in SP-expressing cells, for which around 50% of excitatory synapses arise from other local neurons.

Finally, recent transcriptomic studies have shown that mRNA for GRP is widely distributed among excitatory interneurons in the superficial dorsal horn. This finding is at odds with observations based on the GRP-EGFP mouse, which reveals a homogenous and distinct group of neurons. We show using multiplex *in situ* hybridisation that *Grp* mRNA is present in several transcriptomically-defined populations including those expressing *Tac1*, *Tac2* and a newly recognised class expressing *Npff*. However, EGFP is restricted to a discrete subset of *Grp*-expressing cells in the GRP-EGFP mouse. These are different from those that express *Tac1*, *Tac2* and *Npff*, although some of them express *Nmur2* and likely belong to a cluster defined as Glut8.

Altogether, these findings demonstrate that the GRP-EGFP cells constitute a discrete population of excitatory interneurons. In support of this we provide evidence of distinctive somatodendritic morphology, and a characteristic pattern of synaptic inputs. Many of these

findings are consistent with the proposed role of these cells in itch circuits. However, the functional implications of the mechano-nociceptive and low threshold inputs identified here are still to be established

Acknowledgements

Firstly, I would like to thank my supervisor, Professor Andrew Todd. I am incredibly grateful for his support and guidance during this PhD. I could not have wished to have been supervised by a better role model, and his time, effort and the opportunities that have arisen as a result are truly appreciated. I would also like to thank my second supervisor Dr David Hughes for his advice and support.

I would also like to extend my thanks to all members of the Spinal Cord group for their assistance and support throughout the project. It has been a joy working within such a generous and friendly lab group. In particular, I'd like to extend thanks to Allen Dickie and Noboru Iwagaki for their contributions to the electrophysiology data in the project; Robert Kerr and Christine Watt for their invaluable technical support; Maria Gutierrez-Mecinas, Erika Polgar and Kieran Boyle for their patience and assistance with techniques; John Riddell for his encouragement in his role as assessor; and my fellow PhD students Robert Ganley, Marami Binti Mustapa and Olivia Davis for their support.

I am also grateful to all my colleagues in the clinical anaesthesia department in the School of Veterinary Medicine. Without their understanding and backing, I simply would not have been able to contemplate this project. I am particularly grateful to Dr Pat Pawson for her support, dedication and unerring sound judgement.

I would also like to acknowledge the funders of various parts of this project, each of which are detailed in the submitted manuscripts.

Finally, I am tremendously grateful to my wife Hannah and our children Finlay and Noah. Undertaking a part-time PhD alongside veterinary clinical work is no easy task and their understanding, support and encouragement have been invaluable.

Declaration

I declare that the work presented in this thesis is my own work, except where explicit reference is made. Each of the publications submitted as part of this thesis is preceded by an individual declaration that states my contribution to the work. This thesis has not been submitted in any previous application for any other degree in the University of Glasgow or any other institution.

Andrew McKenzie Bell
September 2020

Table of Contents

List of Figures

Publications

The following four publications comprise this work. These are included in this thesis with the permission of the respective publishers where appropriate.

Paper I

Bell, A.M., Gutierrez-Mecinas, M., Polgár, E., Todd, A.J., 2016. Spinal neurons that contain gastrin-releasing peptide seldom express Fos or phosphorylate extracellular signal-regulated kinases in response to intradermal chloroquine. Molecular Pain 12, 1744806916649602.

Paper II

Dickie, A.C.*, **Bell, A.M.*,** Iwagaki, N., Polgár, E., Gutierrez-Mecinas, M., Kelly, R., Lyon, H., Turnbull, K., West, S.J., Etlin, A., Braz, J., Watanabe, M., Bennett, D.L.H., Basbaum, A.I., Riddell, J.S., Todd, A.J., 2019. Morphological and functional properties distinguish the substance P and gastrin-releasing peptide subsets of excitatory interneuron in the spinal cord dorsal horn. Pain 160, 442–462.

Paper III

Gutierrez-Mecinas, M.*, **Bell, A.M.*,** Polgár, E., Watanabe, M., Todd, A.J., 2019. Expression of Neuropeptide FF Defines a Population of Excitatory Interneurons in the Superficial Dorsal Horn of the Mouse Spinal Cord that Respond to Noxious and Pruritic Stimuli. Neuroscience 416, 281–293.

Paper IV

Bell, A.M., Gutierrez-Mecinas, M., Stevenson, A., Casas-Benito, A., Wildner, H., West, S.J., Watanabe, M., Todd, A.J., 2020. Expression of green fluorescent protein defines a specific population of lamina II excitatory interneurons in the GRP::eGFP mouse. Scientific Reports 10, 13176.

*Equal contribution

Other Papers arising from work (not included in this thesis)

Gutierrez-Mecinas, M., **Bell, A.M**., Marin, A., Taylor, R., Boyle, K.A., Furuta, T., Watanabe, M., Polgár, E., Todd, A.J., 2017. Preprotachykinin A is expressed by a distinct population of excitatory neurons in the mouse superficial spinal dorsal horn including cells that respond to noxious and pruritic stimuli. Pain 158, 440–456.

Gutierrez-Mecinas, M., Polgár, E., **Bell, A.M.,** Herau, M., Todd, A.J., 2018. Substance P-expressing excitatory interneurons in the mouse superficial dorsal horn provide a propriospinal input to the lateral spinal nucleus. Brain Struct Funct 223, 2377–2392.

Gutierrez-Mecinas, M.*, **Bell, A.M.*,** Shepherd, F., Polgár, E., Watanabe, M., Furuta, T., Todd, A.J., 2019. Expression of cholecystokinin by neurons in mouse spinal dorsal horn. Journal of Comparative Neurology 527, 1857–1871.

Polgár, E.*, **Bell, A.M.*,** Gutierrez-Mecinas, M., Dickie, A.C., Akar, O., Costreie, M., Watanabe, M., Todd, A.J., 2020. Substance P-expressing neurons in the superficial dorsal horn of the mouse spinal cord: insights into their functions and their roles in synaptic circuits. Neuroscience, *in press*.

List of Abbreviations

5-HT	5-hydroxytrypamine
ALT	Anterolateral tract
AP	Action potential
Bhlhb5	Basic helix-loop-helix b5
BMP	Bone morphogenic protein
BNP	Brain natriuretic peptide
CCK	Cholecystokinin
CGRP	Calcitonin gene-related peptide
COOH	Carboxyl group
CQ	Chloroquine
CYSLTR2	Cysteinyl Leukotriene Receptor 2
DLF	Dorsolateral funiculus
DRG	Dorsal root ganglion
EGFP	Enhanced green fluorescent protein
EPSC	Excitatory postsynaptic current
ERK	Extracellular signal-regulated kinase
GABA	Gamma aminobutyric acid
GAD67	Glutamic acid decarboxylase 67
GDNF	Glial cell-derived neurotrophic factor
GENSAT	Gene expression nervous system atlas
GFP	Green fluorescent protein
GFRα	GDNF family receptor alpha
Glut	Glutamatergic
GLYT2	Glycine transporter 2
GRP	Gastrin-releasing peptide
GRPR	Gastrin-releasing peptide receptor
HTRF1	5-hydroxytryptamine receptor F1
IB4	Isolectin B4
IL-31RA	Interleukin-31 receptor A
LSN	Lateral spinal nucleus
LTMR	Low threshold mechanoreceptor

MOR	Mu opioid receptor
MrgprA3	Mas-related G protein–coupled receptor A3
MrgprB4	Mas-related G protein–coupled receptor B4
MrgprD	Mas-related G protein–coupled receptor D
mRNA	Messenger Ribonucleic acid
NF	Neurofilament
NGF	Nerve growth factor
NKB	Neurokinin B
NMB	Neuromedin B
NMBR	Neuromedin B receptor
nNOS	Neuronal nitric oxide synthase
NP	Non peptidergic
NPFF	Neuropeptide FF
Nppb	Natriuretic Peptide Precursor B
Npra	Natriuretic Peptide Receptor
NPY	Neuropeptide Y
NTS	Neurotensin
OSMR	Oncostatin M Receptor
PEP	Peptidergic
pERK	Phosphorylated extracellular signal-regulated kinase
PKCγ	Protein kinase C gamma
PrP	Prion protein
RC:DV	Rostrocaudal:Dorsoventral
Ret	Rearranged during transfection
RORβ	RAR-related orphan receptor beta
RVM	Rostral ventromedial medulla
scRNAseq	Single cell RNA sequencing
SP	Substance P
SST	Somatostatin
sst2A	Somatostatin 2a receptor
TF	Transcription factor
TH	Tyrosine hydroxylase
TrkA	Tropomyosin receptor kinase A

TRP	Transient receptor potential
TRPA1	Transient receptor potential ankyrin 1
TRPM3	Transient receptor potential melastatin 3
TRPM8	Transient receptor potential melastatin 8
TRPV1	Transient receptor potential vanilloid 1
VGAT	Vesicular GABA transporter
VGLUT1	Vesicular glutamate transporter 1
VGLUT2	Vesicular glutamate transporter 2
VGLUT3	Vesicular glutamate transporter 3

1 Introduction

The somatosensory system allows animals to perceive both their internal and external environments and respond appropriately. The sensations of pain and itch are fundamentally important for survival, and permit organisms to avoid injurious or damaging stimuli. Nociceptive and pruritic stimuli are transduced in the periphery by specific classes of primary afferent neuron and the dorsal horn of the spinal cord is the site of their first synapse in the central nervous system. Although this information may cause immediate nocifensive reflexes, the spinal dorsal horn acts not simply as a relay site for these impulses but rather serves to integrate and modulate this information before it is projected to higher structures and ultimately perceived. The vast majority of neurons in the dorsal horn are interneurons with axons that remain in the spinal cord, and these form circuits essential for the behavioural expression of pain and itch. However, we have a poor understanding of the circuits that underlie these phenomena, and this is fuelled by a marked heterogeneity of neurons in terms of their lineage, morphology, physiology, neurochemistry, transcriptomic identity, and connectivity.

Defining functional populations of interneurons remains a challenge and we must question what defines neuronal diversity and how does this contribute to sensory coding and function? This introduction comprises a brief summary of the anatomy of the dorsal horn, followed by a critical appraisal of those characteristics that may allow classification of dorsal horn neurons into distinct classes. The proposed circuits that these cells engage and their functional relevance is highlighted.

1.1 Composition of the Dorsal Horn

The dorsal horn can be divided into six parallel layers based on differences in neuronal size and density which occur in the dorso-ventral axis (Rexed, 1952). Laminae I (the marginal layer) and II (the substantia gelatinosa) make up the superficial dorsal horn and appear translucent due to the minimal levels of myelination in this area. The somas of lamina I neurons are variable in size, and this thin layer is distinguishable from lamina II where small neurons are densely packed. Lamina II can be divided into inner and outer bands (IIi & IIo) and the former may be further divided into a dorsal and ventral zone (IIid & IIiv) (Abraira et

al., 2017). The deeper dorsal horn comprises the nucleus proprius (laminae III-V), the neck (V) and the base (VI). At the lamina III/IV border neurons become markedly heterogeneous in size and lamina V is then distinguished by the presence of myelinated afferents forming a reticulated area. Finally, lamina VI is characterised by smaller and more regularly arranged cells than lamina V (Peirs et al., 2020).

Cutaneous primary afferent fibres have cell bodies which reside in the dorsal root ganglia, but the central branches of their axons terminate in the dorsal horn. These afferents convey stimuli which may be classed as innocuous, nociceptive or pruritoceptive, and these are transmitted by generally distinct sensory neuron populations (more detail in 1.7.1). Primary afferent fibres have classically been categorised by their size and degree of myelination. Large myelinated Aβ fibres transmit innocuous touch, functioning as LTMRs, while small myelinated Aδ fibres and unmyelinated C fibres predominantly convey noxious and pruritic information. However, this is an oversimplification, with multiple differentially expressed molecular markers highlighting the diversity of these afferents (again see 1.7.1). However, these afferents terminate in the dorsal horn in a highly ordered somatotopic and modality specific pattern (Koch et al., 2018). In contrast to LTMRs which generally terminate in lamina III and deeper, those afferents transmitting noxious and pruritic stimuli synapse in laminae I and II (Todd, 2010). This highlights the importance of the superficial dorsal horn in pain and itch processing.

A minority of cells within the superficial dorsal horn have axons that project to the brain via the anterolateral tract and are termed projection neurons. These are concentrated in lamina I and are also present in the deeper laminae. The great majority of cells within the superficial dorsal horn have axons that remain within the cord and are classified as interneurons. These cells represent 95% of neurons in lamina I and virtually all neurons in lamina II (Bice and Beal, 1997; Spike et al., 2003). Interneurons may broadly be classed as excitatory or inhibitory based on the neurotransmitter they principally use. Excitatory neurons in the dorsal horn are glutamatergic and express VGLUT2 (Todd et al., 2003), while inhibitory neurons use GABA and/or glycine as neurotransmitters (Todd and Sullivan, 1990). Many inhibitory cells in the superficial laminae use GABA and glycine as co-transmitters, while inhibitory cells using glycine alone are more prevalent in the deeper laminae. Quantitative studies using technically challenging immunostaining for GABA and glycine estimate that inhibitory cells account for

26% of neurons in laminae I & II and 38% of those in lamina III (Polgár et al., 2013a). Genetically modified mice expressing GFP in cells that express either GABA synthesising enzymes or glycine transporters (GAD67 or GLYT2, respectively) have also been used to identify these populations and their distributions (Punnakkal et al., 2014). Other investigators have also used staining for transcription factors such as Pax2 and Lmx1b which identify inhibitory and excitatory cells respectively (Del Barrio et al., 2013; Larsson, 2017) or *in situ* hybridisation for mRNAs associated with each class (Figure 1-1) (Häring et al., 2018; Gutierrez-Mecinas et al., 2019).

It is thought that integration and modulation of information in the dorsal horn is heavily reliant on interneuron activity. This concept dates back to the gate theory of pain (Melzack and Wall, 1965) which proposed that the extent to which a stimulus produced pain was not just a function of the magnitude of the signal in nociceptive specific primary afferents, rather this activity could be modulated at the level of the spinal cord by non-nociceptive afferents. At the centre of the gate control circuit lies an inhibitory interneuron which can be activated by the large touch fibres resulting in feed-forward inhibition of the nociceptive input to the projected output. Dorsal horn neurons display a notable heterogeneity in their characteristics (Todd, 2017), and given the now apparent complexity of the interneurons, the original gate theory would appear to be an oversimplification. However, inhibitory interneurons are still thought to have critical roles in the modulation of pain and itch behaviour; although the exact circuits involved remain largely unknown (Foster et al., 2015). Circuits involving excitatory interneurons are also important for the detection of itch and pain, and the development of tactile allodynia (Wang et al., 2013; Xu et al., 2013; Duan et al., 2014). Beyond these broad categories it is likely that some neurons of the dorsal horn are functionally highly specialised to process specific modalities of pain and mediate complex cross modality interactions (Peirs et al., 2020). What follows is an appraisal of the lineage, physiology, morphology, neurochemistry, genomic identity, and connectivity factors that allow classification of superficial dorsal horn neurons, and in particular those in lamina II, into functional populations.

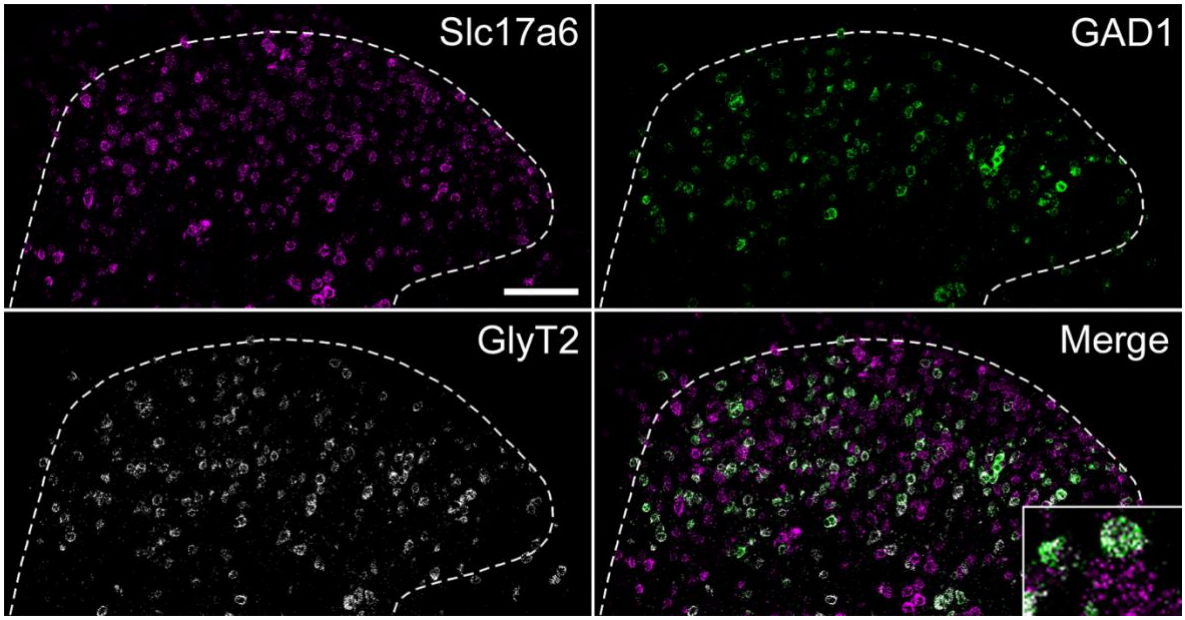

Figure-1-1. Distribution of Neurotransmitter Expression in the Dorsal Horn

The image shows a transverse section of the dorsal horn. Fluorescent multiplex *in situ* hybridisation with probes against *Slc17a6* (VGLUT2), *Gad1* (GAD67) and *Slc6a5* (GlyT2) has been carried out. Excitatory neurons comprise approximately 75% of the superficial dorsal horn neurons, and around 60% of cells in the deeper laminae. These can be identified by VGLUT2 expression. Inhibitory cells can be identified by expression of GlyT2 or GAD67. Many inhibitory cells co-express GABA and Glycine as evidenced by GAD67 and GlyT2 expression, respectively. However, inhibitory neurons in the deeper laminae may be exclusively glycinergic. Image courtesy of Dr David Hughes.

1.2 Developmental Lineage

The spinal cord is formed from the developing neural tube which arises following invagination and closure of the neuroepithelium. The brain develops from the rostral parts and the caudal portion becomes the spinal cord. The caudal neural tube differentiates in to a diverse array of neuronal classes where dorso-ventral patterning is a major determinant of cellular identity (Lai et al., 2016). A number of lineage tracing studies have sought to determine the combinatorial patterns of transcription factor expression that define specific cell types. Neurogenesis occurs between embryonic days 9 and 13 in the mouse and is initially directed by signals emanating from the dorsal and ventral poles of the caudal neural tube which divide progenitors into 13 distinct domains ordered along the dorso-ventral axis. Each domain has a unique gene expression program, with significant cross-repressive actions between TFs, which determine the neuronal type generated (Jessell, 2000). Progenitors of the ventral horn are specified by Sonic hedgehog, while BMPs and Wnts produced by roof plate cells specify the development of six cardinal dorsal interneuron cell types (dI1-6). Amongst these, Class A neurons are marked by the expression of Olig3 and depend on BMP and Wnt signalling (Müller et al., 2005). The progenitors that ultimately make up the superficial dorsal horn are termed class B interneurons and which arise in a BMP independent manner and comprise the Lbx1-expressing dI4 and dI5 and their later-born counterparts, the dILA and dILB interneurons (Müller et al., 2002). Inhibitory GABAergic or glycinergic interneurons arise from dI4/dILA within which Ptf1a is required for the expression of the transcription factors Pax2, Lhx1/5, and Gbx1 (Glasgow et al., 2005). The excitatory glutamatergic interneurons of the dorsal horn develop from dI5/dILB interneurons which express the Lmx1b and Tlx1/3 transcription factors independently of Ptf1a which antagonise Pax2 and result in an excitatory phenotype (Guo et al., 2012; Xu et al., 2013).

Markers such as Pax2 and Tlx3 can be used to distinguish inhibitory and excitatory cells, although of these only Pax2 expression is retained in the post-natal animal. However, some transcription factors expressed during development may be the basis for the differentiation of more restricted cell populations. In the mechanosensory dorsal horn (lamina III-IV), a combinatorial transcription factor code defines nine different post-natal populations of interneurons (Del Barrio et al., 2013). No single transcription factor determined a cells' fate and Lbx1, RORβ, MafB and c-Maf were expressed in both excitatory and inhibitory neurons,

highlighting the combinatorial nature of identity development. However, the authors hypothesise that these molecularly distinct classes are functionally important, and this characterisation sets the stage for dissecting mechanosensory circuits. In the superficial dorsal horn, the dI4/dILA interneurons develop into inhibitory neurons which can express dynorphin, galanin, NPY, nociceptin and enkephalin depending on Ptf1a, indicating that these neuropeptides are expressed in inhibitory neurons (Bröhl et al., 2008). Furthermore, Bröhl et al. demonstrate that the factors Neurod1/2/6, acting downstream of Ptf1a, are essential for dynorphin and galanin expression, while NPY expression depends on Lhx1/5. This demonstrates that developmental transcriptional networks can control both neurotransmitter phenotype and peptidergic fate, and this may underlie the function of the resultant neurons. In a further study, a genome-wide expression profiling approach in mice lacking the transcription factors Ptf1a and Ascl1 has been used to identify novel genetic markers for inhibitory dorsal horn interneurons (Wildner et al., 2013). Ptf1a is required for the development of all inhibitory interneurons in the dorsal horn and hence Ptf1a$^{-/-}$ mice lack these cells, while only late born inhibitory interneurons are missing in Ascl1$^{-/-}$ mice. Gene expression in the dorsal horn was compared between these mice and wild-type mice and the non-overlapping markers Tfap2b, Rorb, Kcnip2 and pDyn were proposed as novel markers for distinct inhibitory interneuron populations.

Developmental features such as transcription factors are attractive markers for functional populations of interneurons. As they are unlikely to persist in the adult animal, genetically modified strains may be required to investigate the function of these neurons, and the combinatorial nature of TF action may make it difficult to easily untangle the provenance of a particular cell type. That said, a number of examples of functionally distinct dorsal horn neuronal classes have been linked to transcription factor expression (Ross et al., 2010; Roome et al., 2020). Intriguingly, single cell transcriptomic analysis of the developing mouse spinal cord has been conducted (Delile et al., 2019) and this data allows prediction of novel transcriptional codes that should at least correlate with neuronal identity.

1.3 Electrophysiology

Dorsal horn neurons may also be categorised by their firing patterns in response to suprathreshold depolarising current steps. Within the neurons of lamina I, four firing patterns

are recognised: tonic - which fire continuously but slowly, phasic (also termed transient) - firing with a high frequency burst of variable duration, delayed – firing with an obvious delay to the first spike, and single spike – characterised by a single action potential (Prescott and Koninck, 2002). In lamina II interneurons, two additional firing patterns are recognised: gap - which have a long first interspike interval, and reluctant which do not spike upon depolarization (Yasaka et al., 2010). Reluctant and single spike patterns may represent an extreme version of phasic firing. Different firing patterns relate to differential potassium channel expression and distribution (Balachandar and Prescott, 2018), with delayed, gap and reluctant firing patterns in excitatory lamina II neurons associated with A-type potassium currents (Yasaka et al., 2010). As shown below, many experiments have dually established firing pattern and somatodendritic morphology for lamina II cells, and some morphologies have been associated with specific patterns. For example, tonic patterns are often attributed to inhibitory interneurons. However the distinction is not all that clear as some subsets of excitatory neurons may also show this pattern (Yasaka et al., 2010; Peirs et al., 2015). Technical considerations such as recording condition or stimulus intensity may also alter the firing pattern of a cell (Tadros et al., 2018), an example being delayed or gap firing becoming tonic when resting membrane potential is held less negative (Yasaka et al., 2010). Patch clamp electrophysiology also allows functional interrogation of cells beyond the determination of firing pattern. Synaptic inputs, receptive fields and cell connectivity may be determined (see 1.7.3) and responses to receptor agonists and antagonists can be revealed. These techniques can be used not only to validate findings of molecular and immunocytochemical studies (e.g. verify a functional receptor is present) but to address whether a specific cell type possesses attributes that may suggest it belongs to a functional population.

1.4 Neuronal Morphology

In many regions of the nervous system, diverse neuronal populations have been categorised by their morphology (Parekh and Ascoli, 2013). Neurons of the dorsal horn may be classified by their somatodendritic morphology and this was originally achieved using Golgi staining (Gobel, 1978). However, most experiments which have provided information about cell morphology have used ex-vivo whole cell patch clamp recording followed by anatomical reconstruction. Because of this, morphology is often compared with electrophysiological properties. The most widely used classification system for lamina II neurons was developed by

Grudt and Perl (2002) and comprises 4 major classes; islet, vertical, radial and central cells. Each of these morphologies relates to dendritic arbors visualised in sagittal sections (Figure 1-2).

Islet cells have characteristic complex dendrites which are elongated in sagittal plane and extend distances greater than 400μm rostro-caudally in the rat despite limited dorsoventral and mediolateral spread (Maxwell et al., 2007; Yasaka et al., 2007). The dendritic trees arborise extensively within lamina II, the axon invariably remains within the dendritic tree. Islet cells are consistently inhibitory and possess tonic firing patterns (Prescott and Koninck, 2002). They receive monosynaptic primary afferent input from C-fibres and some also receive Aδ inputs (Grudt and Perl, 2002) While all islet cells are inhibitory, they do not account for all inhibitory neurons (Heinke et al., 2004). Two neurochemical classes have been shown to include islet cells; some of those expressing parvalbumin (Abraira et al., 2017; Boyle et al., 2019) and the inhibitory calretinin population (Smith et al., 2015, 2019). However the galanin/dynorphin, nNOS and NPY subsets of inhibitory interneurons are morphologically and electrophysiologically heterogeneous (Ganley et al., 2015; Iwagaki et al., 2016).

Vertical cells, have previously been termed stalked cells (Gobel, 1978) and possess large dendritic tress which extend ventrally in a cone shape. Their somas generally lie at the lamina I/II border, although dendrites may reach lamina III (Maxwell et al., 2007). The majority of vertical cells are excitatory neurons, although a small inhibitory populations exists characterised by smaller and less compact dendritic arbors (Yasaka et al., 2010). The axons of excitatory vertical cells extend into lamina I and are presynaptic to ALT cells (Lu and Perl, 2005; Cordero-Erausquin et al., 2009). Vertical cells typically display tonic or delayed AP firing (Prescott and Koninck, 2002; Yasaka et al., 2010), and receive inputs from Aδ and C fibres based on dorsal root stimulation experiments (Yasaka et al., 2007). However, the presence of VGLUT1 staining on dendrites supports the notion that they also receive input from Aβ-LTMRs (Yasaka et al., 2014). A number of neurochemical classes may include vertical cells including excitatory dynorphin and calretinin expressing cells (Smith et al., 2015; Huang et al., 2018).

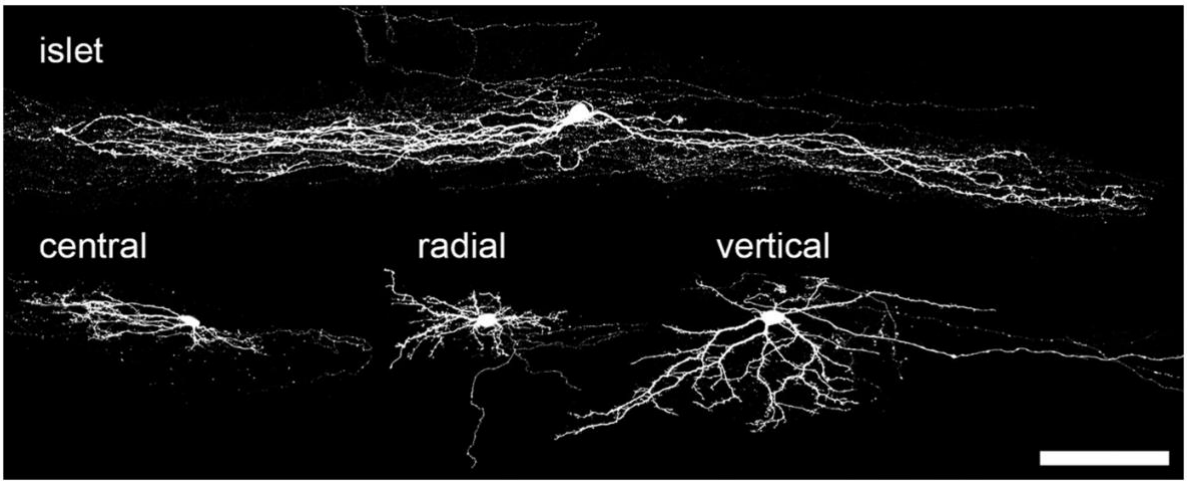

Figure-1-2. Morphological Classification of Lamina II Interneurons

Examples of cells from each of the four main morphological classes of lamina II interneuron as described by Grudt and Perl (2002). Islet cells have complex dendritic trees with extensive rostrocaudal spread. Central cells are similar to islet cells in terms of shape, although they are less extensive in the rostrocaudal axis. Radial cells have compact dendritic trees with primary dendrites radiating in several directions. Vertical cells typically have a dorsally placed soma and dendrites that fan out in a cone shape ventrally. Scale bar = 100 μm, Modified from Todd (2010)

Radial cells possess short and compact dendrites which radiate in all directions and are flattened in the mediolateral axis. Yasaka et al. (2007) propose using a RC:DV ratio of less than 3.5 as a criterion for classifying these cells. Their axons arborise locally and also enter the DLF. These cells are excitatory and display delayed firing (Yasaka et al., 2010). They receive inputs from Aδ (indirectly) and C fibres (Grudt and Perl, 2002; Yasaka et al., 2010). Excitatory substance P-expressing cells in lamina II have been shown to have radial-type morphology (Dickie et al., 2019) as have a sub-population of PKCγ interneurons (Alba-Delgado et al., 2015). Little is known about excitatory circuits involving radial cells, although they may also undergo disinhibition in neuropathic pain (Imlach et al., 2016).

Central cells are similar to islet cells in that they have rostrocaudally orientated arbors, although these are significantly less extensive than those of islet cells. The axonal plexus also frequently extends beyond the dendritic tree, two types of central cell have been identified in terms of firing pattern, which may be tonic or transient (Prescott and Koninck, 2002). There is considerable heterogeneity within this cell type and central cells may be either excitatory or inhibitory in roughly equal proportions (Yasaka et al., 2010). In terms of inputs, They receive excitatory input from C fibres (Grudt and Perl, 2002; Yasaka et al., 2007). One third of PKCγ interneurons, have been shown to have central morphology (Alba-Delgado et al., 2015) along with a number of calretinin-expressing cells (Smith et al., 2015).

Classification according to morphology may have some role in identifying functional populations. As described above, there is a significant association between morphology and firing pattern, and this should govern at least some of a cell's functional role (Prescott and Koninck, 2002; Yasaka et al., 2010). Additionally, dendritic and axonal distribution inevitably has some bearing on the potential inputs and outputs of a cell within a dorsal horn arranged in a modality specific laminar pattern. However, around 25% of lamina II cells are unclassified according to this system (Grudt and Perl, 2002; Yasaka et al., 2010). Furthermore, recent transcriptomic studies which assign neurons to clusters have revealed the rich diversity present in dorsal horn neurons, while conversely, performing unbiased clustering based on electrophysiological and morphological parameters results in a number of clusters which falls well short of those predicted by molecular techniques (Browne et al., 2020); this suggests a limited ability of these schemes to detail the true heterogeneity in dorsal horn neurons. However, paired recording from cells has enabled important neural circuits defined by

morphology to be elucidated. For example, Lu et al. (2013) propose a circuit which conveys Aβ input from PKCγ interneurons to lamina I ALT neurons via transient central cells and then vertical cells. The PKCγ connection is usually held silent under strong glycinergic control, but this is removed in nerve injury allowing low threshold information to activate the nociceptive pathway (Lu et al., 2013).

1.5 Neurochemistry

An alternative approach to neuronal classification has been to use the expression of neurochemical markers such as neuropeptides, transcription factors, receptors, and calcium binding proteins to define populations (Todd, 2010, 2017). Some markers, such as dynorphin or enkephalin are present in both excitatory and inhibitory neurons (Marvizón et al., 2009) but many markers are localised to one class, e.g. somatostatin which is present only in excitatory neurons (Duan et al., 2014; Chamessian et al., 2018). As it is likely that neurons of the dorsal horn are highly specialised, the neurochemical markers chosen to define populations should reflect this granularity. The expression of markers, such as somatostatin and calretinin (Duan et al., 2014; Petitjean et al., 2019) have been suggested as defining features of functional populations despite being expressed in a high proportion of dorsal horn excitatory interneurons (Gutierrez-Mecinas et al., 2016a, 2019b). In terms of defining functional populations with adequate resolution to interrogate circuits meaningfully, these subsets of cells are undeniably mixed in terms of their neurochemical makeup. Notably however, neither calretinin nor somatostatin are expressed in ALT neurons. Therefore, studies that have investigated the effects of manipulation of these broad classes of cells have demonstrated the importance of dorsal horn interneurons for the expression of pain and itch phenotypes. Ablation of somatostatin-expressing neurons results in the loss of acute mechanical pain behaviours and these mice also fail to develop tactile allodynia following either neuropathy of inflammation (Duan et al., 2014). Optogenetic activation of somatostatin-expressing cells causes nocifensive and aversive behaviours while chemogenetic inhibition increased withdrawal thresholds and reduced allodynia in inflammation (Christensen et al., 2016). Additionally, somatostatin-expressing neurons may have a role in the transmission of chemical itch (Fatima et al., 2019). Chemogenetic activation of calretinin-expressing cells reduced mechanical thresholds and resulted in nocifensive behaviour (Peirs et al., 2015; Petitjean et al., 2019; Smith et al., 2019).

These cells were also shown to be directly connected to lamina I ALT cells (Smith et al., 2019).

One must bear in mind that defining a population is not simply a function of the expression of a particular peptide marker (Smith and Ross, 2020). Rather, investigations are required to provide evidence that cells have a homogeneous pattern of anatomical, electrophysiological and behavioural features which collectively represent a signature enabling them to function as a distinct class. In a seminal study, this approach has led to the identification of 11 separate classes of neuron in the LTMR recipient zone in lamina III of the dorsal horn (Abraira et al., 2017). These authors propose an integrative model where touch processing begins at the earliest stages of sensory neuron input into the LTMR recipient zone. Using genetic tools, they identify 7 excitatory and 4 inhibitory neuronal subtypes and document their properties, alongside conducting functional studies to demonstrate essential roles in touch perception. Non-overlapping neurochemical classification schemes have also been proposed for both excitatory and inhibitory interneurons in lamina II (Gutierrez-Mecinas et al., 2016a; Boyle et al., 2017). Within the excitatory cells, a scheme involving restricted expression of 6 neurochemical markers defines around 75% of dorsal horn cells (Figure 1-3) (Gutierrez-Mecinas et al., 2019a). These markers are substance P, neurotensin, cholecystokinin, neurokinin B and neuropeptide FF together with EGFP expression in a GRP-EGFP mouse line (Figure 1-3). Each of these categories and their functional relevance will be discussed below (with the exception of NPFF, which is the subject of paper III of this thesis).

One advantage of neurochemical classification compared to previous electrophysiological or morphological schemes is the potential to use molecular genetic techniques to manipulate the function of the neurons and hence elucidate their roles in circuits. Expression of recombinases in specific cell populations driven by the defining neurochemical promotors may be used to facilitate neuronal silencing, activation and ablation via systems including chemogenetic/optogenetic agents and toxins (Graham and Hughes, 2019). A number of examples of these techniques are evident in the literature investigating the functional roles of dorsal horn interneurons, and these are highlighted where relevant in the discussion of individual classes below. However, confusion may arise depending on the methodology used to manipulate the cell types, and one particular issue can be the inadvertent manipulation of cells which do not express a particular marker in adulthood but rather do so during

development. In these cells, developmental Cre expression leads to recombination and expression of floxed reporters, ion channels or receptors which then persists in adulthood. Where transient expression influences the cell type selected for, it invariably increases the size and potentially the heterogeneity of the population (Branda and Dymecki, 2004), and these studies should term their classes differently using the term ‘lineage’ (Serafin et al., 2019). The effects of transient expression can be avoided by either inducing Cre recombinase activity (Feil et al., 1997), or injecting viruses containing Cre-dependent constructs in the mature animal (Foster et al., 2015). Also, of note when interpreting the results of functional studies is the potential for the method of activation (e.g. ionotropic vs metabotropic constructs) to effect the sensory modality perceived following stimulation (Sharif et al., 2020).

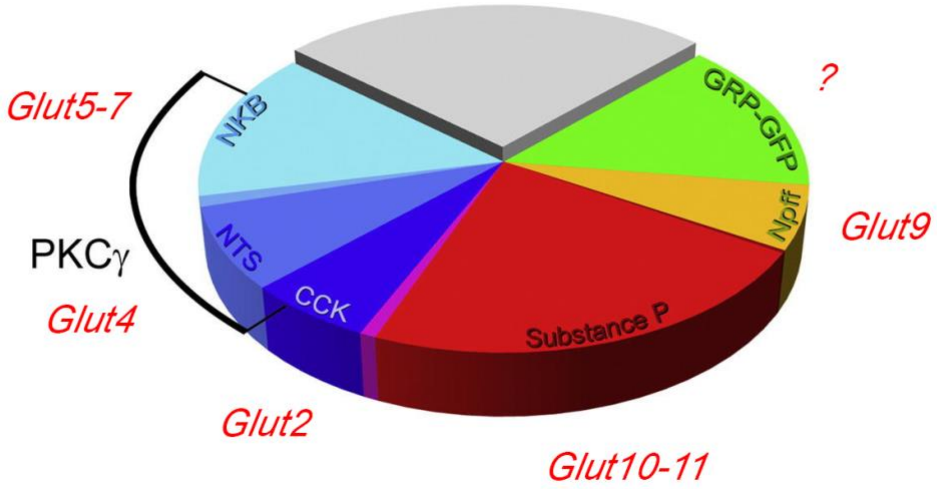

Figure-1-3. Neurochemical Classification of Superficial Dorsal Horn Excitatory Interneurons

Pie chart showing the relative sizes of different neurochemical classes of excitatory interneurons in laminae I & II of the mouse dorsal horn. NKB, NTS, CCK, Substance P, NPFF and GRP-EGFP form largely non-overlapping populations. Many of the cells which express NTS and some that express CCK and NKB are PKCγ immunoreactive. Each of these populations, with the exception of the GRP-EGFP cells, correspond to clusters identified in Häring et al. (2018) and these are shown in red. Adapted from Gutierrez-Mecinas et al. (2019)

1.5.1 Gastrin-releasing Peptide expressing Interneurons

Gastrin-releasing peptide is a bombesin-like peptide which is biologically active and has been shown to affect many biological processes both in the gastrointestinal tract and in the central nervous system (Ramos-Álvarez et al., 2015). Bombesin and other bombesin-like peptides were originally isolated from the European frog (Rana temporaria) between 1970 and 1990 (Erspamer, 1988). While bombesin itself is not present in mammals, a number of mammalian bombesin-like peptides have been discovered. These include the 27 amino acid peptide GRP ($GRP_{1\text{-}27}$), several forms of neuromedin B ($NMB_{1–32}$, $NMB_{2–32}$, and $NMB_{23–32}$) and the decapeptide COOH terminal of GRP ($GRP_{18\text{-}27}$) which is termed neuromedin C (McDonald et al., 1979; Minamino et al., 1984). Bombesin and GRP share their 7 peptide COOH terminal, which is the biologically active end of the peptide. NMB contains a portion of these amino acid residues but more closely resembles the amphibian peptides, ranatensin, and litorin (Lin et al., 1995).

The source of GRP in the dorsal horn of the spinal cord has been the topic of significant and longstanding controversy. While it is broadly accepted that GRP is expressed by dorsal horn interneurons and not primary afferent fibres in naïve mice, some studies continue to challenge this view (Barry et al., 2020; Chen and Sun, 2020). Early immunohistochemical studies consistently demonstrated that GRP was expressed in a subset of small DRG neurons (Sun and Chen, 2007; Takanami et al., 2014), and consistent with this, that dorsal root rhizotomy significantly reduced GRP immunoreactivity in the ipsilateral dorsal horn (Zhao et al., 2013). However, these findings may have resulted from cross-reaction of GRP antibodies with substance P (Goswami et al., 2014; Gutierrez-Mecinas et al., 2014; Solorzano et al., 2015) and these studies additionally confirm that GRP is localised to dorsal horn interneuron terminals and refute the finding that rhizotomy or TRPV1+ ablation alters dorsal horn GRP immunoreactivity (Wada et al., 1990; Solorzano et al., 2015). Molecular studies using *in situ* hybridisation have shown that mRNA for GRP is expressed in dorsal horn cells and not in the DRG (Fleming et al., 2012; Mishra and Hoon, 2013; Solorzano et al., 2015), although this has been contested (Liu et al., 2014; Barry et al., 2016). Additional qPCR and bulk next-gen mRNAseq studies have localised *Grp* expression to the dorsal horn and not the DRG (Mishra and Hoon, 2013; Goswami et al., 2014). Furthermore, large single cell transcriptomic datasets have consistently failed to demonstrate expression of mRNAs for GRP in the DRG, while

demonstrating expression in dorsal horn cells (Usoskin et al., 2015; Li et al., 2016; Sathyamurthy et al., 2018; Häring et al., 2018; Zeisel et al., 2018). BAC transgenic mice which express either EGFP or Cre under control of the *Grp* promotor can be used to directly label GRP-expressing neurons, and these are present in the dorsal horn but not the DRG (Mishra and Hoon, 2013; Gutierrez-Mecinas et al., 2014; Sun et al., 2017; Albisetti et al., 2019; Pagani et al., 2019). However, a recent study using a GRP-Cre mouse produced using a potentially more faithful knock-in strategy, demonstrates putative GRP-expressing cells in both the DRG and spinal cord and argues that the DRG cells are more functionally important for itch transmission (Barry et al., 2020).

Using a GRP-EGFP mouse from the GENSAT project (Gong et al., 2003), studies have demonstrated that the cell bodies of GRP-EGFP cells are present predominantly in lamina II (Mishra and Hoon, 2013) and that they do not express Pax2 and are excitatory interneurons (Gutierrez-Mecinas et al., 2014). Furthermore, GRP-EGFP axonal boutons frequently express VGLUT2 and not VGAT (Gutierrez-Mecinas et al., 2014). It has been estimated that these GRP-EGFP cells make up 11% of all neurons in laminae I & II, which would correspond to approximately 15% of excitatory neurons in that area (Gutierrez-Mecinas et al., 2016a). While 59% of GRP-EGFP cells in laminae I & II were shown to express somatostatin, this population does not show significant overlap with those expressing neurotensin, neurokinin B, substance P, or cholecystokinin (Gutierrez-Mecinas et al., 2016a; Gutierrez-Mecinas et al., 2019). Interestingly, GRP-EGFP neurons are often weakly stained for the pan-neuronal marker NeuN, suggesting they belong to a unique developmental population. There has been some suggestion in the literature that BAC transgenic mice used to label GRP-expressing cells may not capture all cells that express mRNA for the peptide, with only 25% of mRNA containing neurons being Cre-positive in one study (Albisetti et al., 2019), and this apparent discrepancy has not yet been resolved.

GRP and its receptor, GRPR, have been strongly implicated in the transmission of pruritogen induced itch signals in the dorsal horn. In a seminal study, Sun and Chen (2007) showed that mice lacking GRPR showed significantly reduced responses to a variety of pruritogens but normal responses to painful stimuli. In agreement with this, the intrathecal injection of GRP elicited scratching, while antagonists markedly reduced responses to pruritogens in both mice and primates (Sun and Chen, 2007; Lee and Ko, 2015). A subsequent study where GRPR-

expressing cells were ablated using intrathecal bombesin-saporin also resulted in specifically reduced itch behaviours in response to pruritogens with no evident changes in nocifensive responses (Sun et al., 2009). Supplementary data in this follow-up study also highlighted that in mice lacking GRPR, it is non-histaminergic itch responses which are more affected when compared to those responses following the injection or endogenous release of histamine. This is consistent with the findings that non-histaminergic itch behaviour in mice could be reduced by the administration of GRPR antagonists, while this had little effect on scratch bouts elicited by histamine (Akiyama et al., 2014). Further studies using both GRPR and NMBR knock out mice have, again demonstrated the necessity of GRPR for CQ-induced scratching but have also found that GRPR may upregulate and compensate for the loss of NMBR in non-histaminergic itch (Zhao et al., 2014). Also, of interest in this study is the finding that GRP may also exert its itch inducing actions via NMBR+ neurons, albeit to a lesser extent than via GRPR+ neurons. Although these pathways are thought to be distinct by other authors (Sukhtankar and Ko, 2013).

Given the importance of GRP-GRPR signalling and the majority view that the source of GRP in the dorsal horn is a subset of interneurons, the function of these cells has been interrogated in a number of studies. In a series of experiments involving saporin based ablation and pharmacological activation, Mishra and Hoon (2013) propose a model where GRP-expressing cells act as secondary pruritoceptors in a labelled line for itch (Figure 1-4). A specific subset of TRPV1-expressing, itch specific primary afferents signal by releasing BNP (also termed NPPB) in the superficial dorsal horn (Huang et al., 2018). BNP acts on GRP-expressing cells via the BNP receptor NPRA, which in turn activates these cells and causes the release of GRP (Mishra and Hoon, 2013). Consistent with this, localised spinal ablation of GRP neurons reduces itch behaviour in response to a variety of pruritogens while chemogenetic excitation provoked spontaneous itch-like behaviours and facilitated the response to pruritogens (Albisetti et al., 2019). Responses to painful stimuli were not altered. These authors also demonstrated that GRP-expressing cells receive direct monosynaptic inputs from another pruritoceptive primary afferent subtype, those C-fibres expressing MrgprA3 (Han et al., 2013). The same group have also investigated the signalling mechanisms which link GRP+ with GRPR+ cells, demonstrating the importance of peptide release alongside glutamatergic signalling in itch transmission (Pagani et al., 2019). Initially Pagani et al. (2019) conducted electrophysiology recordings from GRP-EGFP cells while optogenetically stimulating

MrgprA3 pruritoceptors. Surprisingly, single pulse stimulation of the primary afferents resulted in bursts of action potentials in the GRP+ neurons. The authors then optogenetically stimulated GRP+ cells while recording from GRPR+ cells. While single pulses of activity in the GRP+ cells were not sufficient to drive APs in the GRPR+ cells, simulated burst activity in the GRP neurons led to gradual depolarisation of the GRPR neurons followed by AP firing which persisted for minutes after synaptic stimulation stopped. This depolarisation continued in the presence of glutamate receptor antagonists but was abolished by GRPR antagonists, thus emphasising the role of peptidergic signalling at this synapse. The investigators were then able to confirm their findings in freely moving animals using fibre optic activation of GRP+ neurons by showing that only burst stimulation was associated with aversive behaviours. Consistent with these findings, Sun et al. (2017) also show in an isolated DRG and spinal cord preparation that pruritic stimuli activate GRP cells. However, they also show that these cells are strongly activated by painful stimuli and that GRP cells activate enkephalinergic interneurons which act as a feedforward inhibitory mechanism to decrease the magnitude of strongly painful stimuli. Consistent with this model, the global ablation of GRP cells decreased itch while increasing the magnitude of pain responses (Sun et al., 2017). However, using a different mouse line, as mentioned above, Barry et al. (2020) did not find any effect on itch or pain responses following ablation of spinal GRP+ neurons, in contrast to ablation of DRG GRP+ cells, which resulted in a diminished itch phenotype.

Despite some conflicting evidence it seems highly likely that GRP release form dorsal horn excitatory interneurons is central to at least non-histaminergic chemical itch transmission and that these cells may represent a unique functional class. Cells expressing GRPR may also represent a distinct functional class as their ablation reveals they are selectively tuned to both acute and chronic itch transmission (Sun et al., 2009; Koga et al., 2020). This class of cells has a distinctive laminar distribution, with the cells concentrated at the laminae I and IIo border and the cells are predominantly excitatory (Sun et al., 2009; Pagani et al., 2019). Despite their location in the most superficial laminae of the dorsal horn, GRPR+ cells do not project to the brain, rather are local interneurons (Sun et al., 2009; Aresh et al., 2017; Bardoni et al., 2019). However, they do form the terminal part of a dorsal horn itch circuit as GRPR+ neurons synapse directly with spinoparabrachial projection neurons (Mu et al., 2017). Studies have sought to define the modulatory inputs to GRPR+ and have demonstrated a complex inhibitory network, composed of synaptic and tonic currents that gates the excitability of GRPR neurons

(Freitag et al., 2019). These inhibitory inputs arise both locally from nNOS+ cells and via synaptic descending mechanisms from the RVM (Liu et al., 2019). These inhibitory inputs may underlie the inhibition of activity in GRPR+ cells by TRPM8 and TRPA1 agonists, which presumably act via circuits initially involving primary afferents (Bardoni et al., 2019).

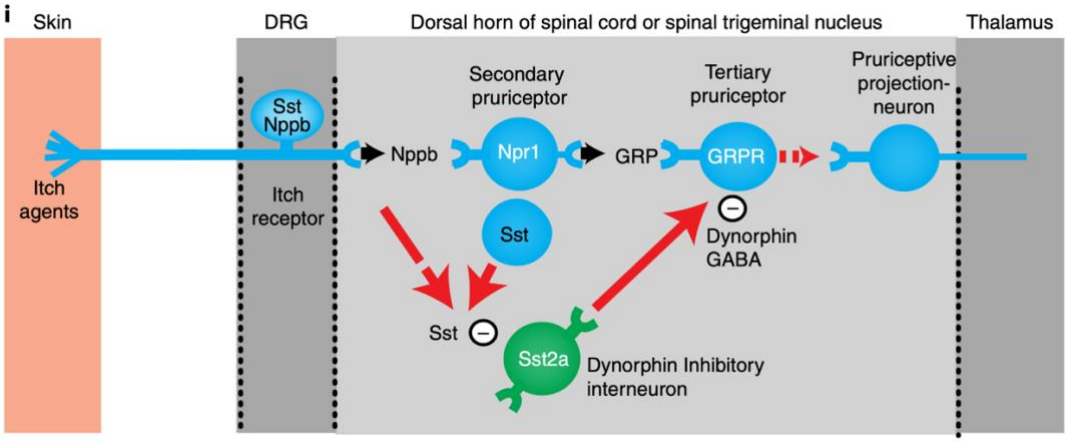

Figure-1-4. Proposed Neural Circuits for Itch in the Dorsal Horn

GRP-expressing cells are secondary pruritoceptors in a circuit proposed by Mishra and Hoon (2013). They receive peptidergic signalling from primary afferent fibres that express SST and Nppb. Nppb acts via the Npr1 receptor which is present on these cells. GRP release then acts via GRPR-expressing cells which are then disynaptically linked to supraspinal targets via projection neurons. This figure also shows the involvement of dynoprphin-expressing inhibitory neurons in this circuit. Somatostatin acts via the SST2A receptor to inhibit these cells, thereby disinhibiting GRPR+ cells and potentiating itch. From Huang et al. (2018).

1.5.2 Substance P-expressing Excitatory Interneurons

Substance P immunoreactivity is present in the superficial dorsal horn and the majority of this peptide is found in axon terminals of primary afferent fibres (Hokfelt et al., 1975; Cuello et al., 1977). However, following rhizotomy, around 20% of the peptide remains in the ipsilateral dorsal horn and hence is of non-primary origin (Jessell et al., 1979). SP-immunoreactive cells have been identified in the dorsal horn (Ribeiro-da-Silva et al., 1991), and these findings have more recently been confirmed using an antibody to pre-protachykinin A, *in situ* hybridisation, and genetically modified mice expressing Cre under control of the *Tac1* promotor (Xu et al., 2013; Gutierrez-Mecinas et al., 2017). These cells are mostly excitatory and account for 24% of excitatory interneurons in laminae I and II. Many of these cells respond to noxious and pruritic stimuli as shown by expression of Fos or phosphorylation of ERK (Gutierrez-Mecinas et al., 2017).

It has recently been shown that these SP cells have a specific pattern of connectivity that underlies their function. These interneurons have been identified as having radial morphology and consistent with previously described features of radial cells (Grudt and Perl, 2002) have long propriospinal axons which travel in the DLF and target the LSN (Gutierrez-Mecinas et al., 2018; Dickie et al., 2019). Using an anatomical approach based on immunostaining for the post-synaptic protein homer, Polgár et al. (2020) find that SP-radial cells receive half their excitatory synaptic input from other interneurons and this arises preferentially from cells that express EGFP in the GRP-EGFP mouse line (Polgár et al., 2020). In addition, substance P is expressed by 40% of ALT projection neurons in lamina I as well as by some of those in lamina III, although as these cells are much rarer than interneurons, this accounts for a small percentage of SP cells (Polgár et al., 2020). A recent study reported that ablation of SP-expressing cells in the $Tac1^{Cre}$ mouse resulted in the loss of both persistent licking and conditioned aversion evoked by stimuli which produce sustained pain, but without altering acute nocifensive reflexes (Huang et al., 2019). The authors suggest this is due to ablation of ALT cells which project to the thalamus and underlie coping behaviours. However, this is surprising as the majority of SP cells are interneurons which are activated by noxious and pruritic stimuli. As such, this finding associated with coping responses has been challenged, with one study showing silencing of $Tac1^{Cre}$ cells affecting acute nocifensive responses to both cold and radiant heat (Polgár et al., 2020).

1.5.3 Neurotensin-expressing Excitatory Interneurons

Neurotensin expressing cells are located at the lamina II/III border and represent 9% of excitatory cells in laminae I-II and 13% of those in lamina III (Gutierrez-Mecinas et al., 2016a). Virtually all of these cells are PKCγ-expressing, and levels of expression of this kinase are high. Furthermore, 85% of strong PKCγ-expressing cells can be accounted for by largely non-overlapping NTS or CCK expression (Gutierrez-Mecinas et al., 2019). PKCγ-expressing cells have been identified as an important population of excitatory cells as mice in which the kinase has been knocked out or antagonised show reduced hypersensitivity following nerve injury or strychnine injection (Malmberg et al., 1997; Miraucourt et al., 2007). Although chemogenetic or optogenetic functional studies of PKCγ-expressing cells have not been carried out, circuit interrogation with electrophysiology and pharmacology suggests these cells form part of a circuit conveying low threshold stimuli to lamina I projection neurons which becomes functional during disinhibition in neuropathy (Neumann et al., 2008; Lu et al., 2013; Wang et al., 2020).

1.5.4 Cholecystokinin-expressing Excitatory Interneurons

Excitatory cells expressing cholecystokinin represent around 7% of excitatory interneurons in laminae I & II (Gutierrez-Mecinas et al., 2019). However, they are frequently encountered in deeper laminae, representing around a third of the excitatory cells in lamina III. A number of these cells, particularly those in lamina IIi, co-express PKCγ and it has been shown that 85% of strongly PKCγ-expressing neurons can be accounted for by expression of CCK or NTS (Gutierrez-Mecinas et al., 2019). The release of CCK from these cells principally acts to reduce the antinociceptive action of opioids via CCK_B receptors (Wiesenfeld-Hallin et al., 2002; Yang et al., 2018). However, this function does not account for the glutamatergic role these cells have in spinal circuits. Ablation of the CCK-expressing cells in the dorsal horn has demonstrated their importance in both processing of tactile stimuli and mechanical allodynia in neuropathic pain. Using a novel behavioural paradigm, Abraira et al. (2017) showed that mice in which the cells had been ablated could not distinguish between objects of different textures. In a separate study, ablation of these cells reduced mechanical allodynia in neuropathic pain models (Liu et al., 2018). Based on the extensive expression of CCK across

the dorsal horn and transcriptomic evidence (Häring et al., 2018), it is likely that there are a number of functional subpopulations amongst the CCK cells. One such subset is present at the lamina IIi/III border and is defined by the expression of urocortin 3 (Pan et al., 2019). These cells have been shown to have a role in the transmission of mechanical itch, in a circuit gated by NPY-expressing inhibitory cells.

1.5.5 Neurokinin B-expressing Excitatory Interneurons

Neurons expressing NKB have a very similar distribution to NTS cells and lie either side of the II/III border. These cells comprise around 16% of the excitatory interneurons in lamina II (and 7% in lamina III) and may express PKCγ, albeit at a low level (Gutierrez-Mecinas et al., 2016a). Ablation of these cells did not result in any alterations to nociceptive thresholds, and thus very little is known about their function (Duan et al., 2014).

1.5.6 Inhibitory Interneurons

In laminae I and II, recent studies have identified five largely non-overlapping, neurochemically defined subsets that account for nearly all dorsal horn inhibitory interneurons (Boyle et al., 2017). These groups comprise those inhibitory neurons expressing Galanin or Dynorphin, nNOS, NPY, calretinin or parvalbumin.

Galanin and dynorphin cells are present in lamina I-IIo and have a very high degree of co-expression of the two peptides, therefore they are considered as a single class (Todd, 2017). Dynorphin is present in 31% of all inhibitory cells in the superficial dorsal horn and this class of cells can be identified in the PrP-EGFP mouse, which reveals both this population and those expressing nNOS (Iwagaki et al., 2013; Ganley et al., 2015). Interestingly, all of this population express the sst_{2A} receptor, which is expressed by around half of all SDH inhibitory neurons (Polgár et al., 2013b, 2013a). This is consistent with their proposed functional role in itch circuits (Kardon et al., 2014; Huang et al., 2018). This role was first suggested by the finding that Dynorphin cells (along with those expressing nNOS) are absent in mice lacking the transcription factor Bhlhb5 (Kardon et al., 2014). These mice develop spontaneous itch behaviour (Ross et al., 2010) and it is proposed that the activity of dynorphin released from these cells at KOR supresses itch (Kardon et al., 2014). Chemogenetic activation of

dynorphin-expressing cells suppresses itch but also causes mechanical allodynia; an effect thought to be mediated via the small population of excitatory dynorphin cells (Huang et al., 2018). Duan et al. (2014) ablated dynorphin lineage cells and this resulted in a mechanical allodynia phenotype. This discrepancy is perhaps explained by the recent finding that dynorphin cells attenuate mechanical sensitivity throughout development, but this population dampens acute nonhistaminergic itch only during adulthood (Brewer et al., 2020).

Inhibitory cells expressing nNOS are present in lamina II but also occur in adjacent laminae. They represent 17% of inhibitory cells in the superficial dorsal horn (Iwagaki et al., 2013; Boyle et al., 2017) In terms of function, chemogenetic activation has demonstrated antinoceptive but not antipruritic functions of these cells (Huang et al., 2018). Another class; those inhibitory cells expressing calretinin account for 25% of all inhibitory cells, but this represents a small percentage (~15%) of cells expressing calretinin overall; the majority of which make up a broad and non-specific class of excitatory interneurons. Perhaps as might be expected with a broad heterogenous class, these cells are functionally involved in the generation and amplification of pain (Duan et al., 2014; Peirs et al., 2015; Petitjean et al., 2019; Smith et al., 2019).

Expression of NPY occurs in around one third of inhibitory cells and these are distributed between lamina I and III (Boyle et al., 2017). Ablation of NPY lineage cells has suggested a role for them in the gating of mechanical itch (Bourane et al., 2015), although activation of these cells does appear to increase nociceptive thresholds (Acton et al., 2019); an effect which the authors of that study attribute to NPY actions on primary afferents. However the release of NPY itself in the dorsal horn has been shown to dampen both mechanical and chemical itch (Gao et al., 2018) and has been implicated in supressing neuropathic pain (Solway et al., 2011). The Y1 receptor for NPY is expressed on a subset of superficial dorsal horn excitatory interneurons which are a mixed population overlapping to a moderate degree with GRP-EGFP cells (Acton et al., 2019). The functional role of this Y1-expressing population is unclear, with conflicting evidence suggesting both a role in neuropathic pain and mechanical itch (Acton et al., 2019; Nelson et al., 2019), although these differences could relate to the methodology used for manipulation.

Cells belonging to the final class of inhibitory interneuron express parvalbumin and these are located at the lamina II/III border (Hughes et al., 2012). While some parvalbumin cells are excitatory, the majority are inhibitory and represent around 10% of the superficial dorsal horn inhibitory cells, and a much higher proportion of cells in lamina III (Abraira et al., 2017; Boyle et al., 2017). Many of these cells show islet morphology, and their axons form inhibitory axoaxonic synapses on the central terminals of A-LTMRs (Hughes et al., 2012). These cells are therefore a source of presynaptic inhibition of low threshold inputs and also provide post-synaptic inhibitory input to vertical cell dendrites (Boyle et al., 2019). Petitjean et al. proposed that a pattern of reduced innervation of PKCγ cells by parvalbumin inhibitory cells contributed to allodynia in neuropathic pain (Petitjean et al., 2015). However this reduction in contacts could not be reproduced in another study, which suggested that parvalbumin cells undergo reductions in activity in neuropathic pain rather than changes to their connectome (Boyle et al., 2019).

1.6 Transcriptomics

Recent advances in DNA sequencing technology have allowed analysis of the transcriptome of single cells and have paved the way for exploration of how the molecular profiles of neural populations are linked to their functional and morphological diversity. Microfluidic platforms have dramatically reduced the cost per cell of sequencing and the advantages of this have been seen in characterisation of other areas of the nervous system. For example, recent scRNAseq of retinal cells has revealed 15 neuronal types, 13 of which were previously identified and two of which were novel classes (Shekhar et al., 2016). In the spinal cord several studies have defined clusters of dorsal horn neurons based on the constellations of genes that they express (Häring et al., 2018; Sathyamurthy et al., 2018; Zeisel et al., 2018). Häring et al. (2018) define 15 classes of excitatory neuron and 15 classes of inhibitory neuron in the dorsal horn (Figure 1-5). Sathyamurthy et al. (2018) define a similar number of dorsal excitatory cell types, but only 9 classes of dorsal horn inhibitory neuron. While there are a number of similarities in the clusters from the two studies, the clusters are not all comparable and this may be due to technical differences. Firstly Häring et al. sequenced mRNAs from the whole neuron, while Sathyamurthy et al. performed nuclear only sequencing. The Häring et al. study also sequenced to a greater depth with a significantly higher number of reads per cell/nucleus which led to a higher number of detected genes per cell (3400 vs 1400). As such, Häring et al.

(2018) represents a more comprehensive classification of dorsal horn neurons. Another sequencing study from the same group involving neurons from the entire mouse nervous system also provided a less comprehensive classification due to lower sequencing depth and total cell numbers (Zeisel et al., 2018). In addition to clustering based on transcriptional identity, Häring et al. (2018) performed multiplex *in situ* hybridisation using combinatorial marker genes for each population to validate their results and define the laminar distribution of each cell type.

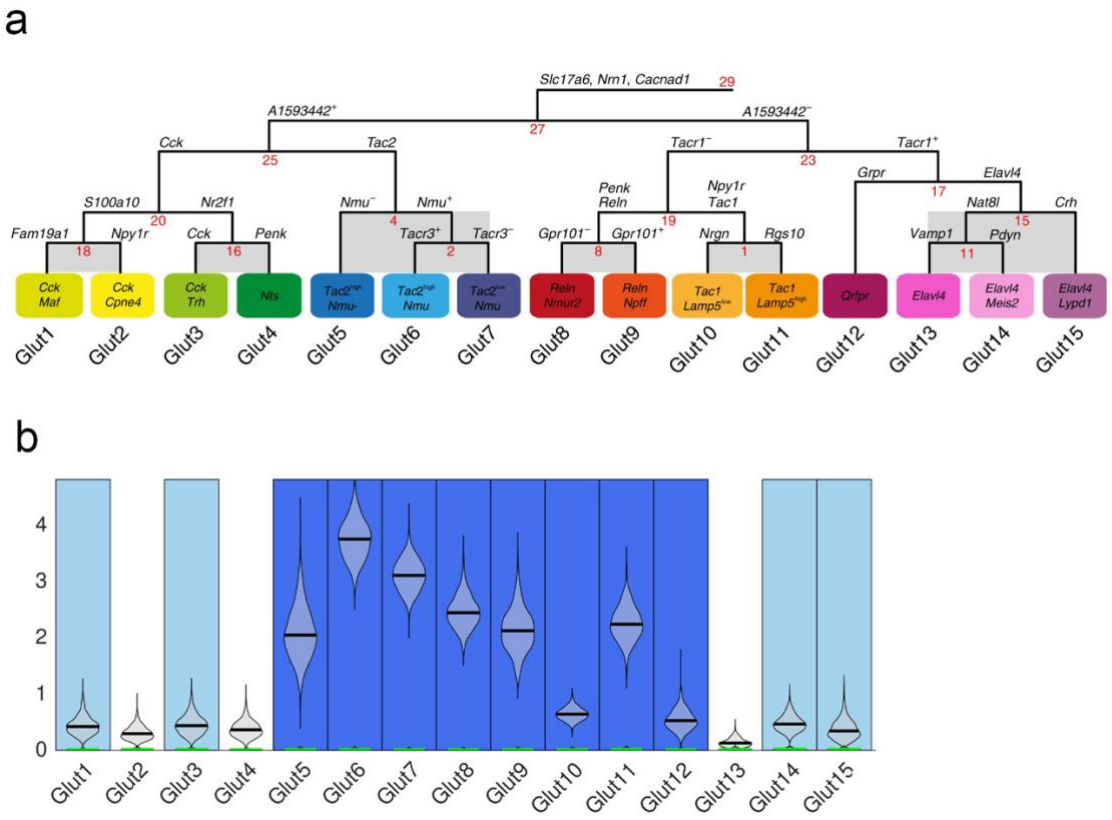

Figure-1-5. Transcriptomic clusters of Dorsal Horn Neurons from Häring et al. (2018)

The neurons of the dorsal horn may be classified on the basis of their transcriptome. (a) shows a hierarchical representation of the different glutamatergic neuronal types. 15 clusters of neurons are proposed and the marker genes for each are shown in the coloured boxes. The genes named at divisions of the dendrogram define the splits between types. The distribution of *Grp* expression across the classes is shown in (b). The violin plots show the distribution of molecular counts within the cells of each cluster. The blue colouring indicates a Bayesian prediction of the probability of expression within a cluster. Light blue colouring indicates a posterior probability greater than 99.9%. Dark blue also indicates this but indicates a further level of stringency requiring a median predicted expression greater than 0.5. Adapted with permission from Häring et al. (2018).

Transcriptomic datasets identifying dorsal horn neurons are useful for investigating the expression of different markers, developing genetic tools to investigate cell types and validating experimental results (Denk, 2017; Crow and Denk, 2019). However it is not yet clear just how molecular identity is linked to function. In many cases the task of linking molecular properties to functional, anatomical, morphological, and electrophysiological properties remains (Nguyen et al., 2017). Careful interpretation of transcriptomic cell classes is necessary as a number of technical issues may prevent accurate classification of the full neural repertoire. Some degree of cell selection bias may be inherent to the technique, such that certain cell types do not survive harvesting and dissociation (e.g. large Purkinje cells may not survive to be sequenced in representative numbers as they are often damaged due to their size (Zeisel et al., 2018)). Furthermore depending on the number of cells and the clustering algorithm, it may be that only abundant cell types are sequenced in adequate numbers. Under sampling can also lead to subclasses of a population not being resolved adequately and the assumption being made that a particular gene is ubiquitous in a population, where it may only be expressed highly in a subpopulation (Nguyen et al., 2017). Also, spatial distribution data is not preserved when cells are sequenced. Therefore, it is advantageous to perform *in situ* validation of any co-expression of molecular markers. Ultimately, the question of whether a transcriptomic cluster truly represents a fundamentally different neuronal type, is complex and requires careful validation and further multi-disciplinary studies.

The scheme proposed by Häring et al. aligns reasonably with the existing neurochemical scheme proposed above for excitatory dorsal horn neurons (Figure 1-3). There are some discrepancies evident however. Notably, *Tac1*, the gene for substance P, is present in two clusters and *Tac2*, the gene for NKB is present in 3 clusters. This supports the notion that there may be functionally distinct subclasses amongst these neurons. However, similar findings in the DRG, where much more is known about modality specificity of neurons, have not yet translated to the discovery of additional functional subclasses (Zeisel et al., 2018; Nguyen et al., 2019). Additionally, some clusters (e.g. Glut10) extend over multiple laminae, and this is hard to reconcile with the notion that these clusters represent functional populations of cells given the modality specific arrangement of the dorsal horn. Of particular interest is the distribution of *Grp* expression amongst neuronal classes in transcriptomic studies of the dorsal horn. While Sathyamurthy et al. (2018) shows a cluster defined by *Grp* expression, this finding is not replicated in Häring et al. (2018). Rather *Grp* expression is widespread

throughout the dorsal horn and present in multiple classes (Figure 1-5). This discrepancy between transcriptomic findings and those using BAC transgenic animals to identify GRP cells, as described above, has not been reconciled.

1.7 Connectivity

Primary afferent sensory neurons of the trunk and limbs project from tissues including skin, muscle, joints and viscera to the spinal cord. Anatomically, the cell bodies of these cells are located in the dorsal root ganglia (DRG) adjacent to the spinal cord. The cells are pseudounipolar, that is the axon has both a peripheral branch that innervates the tissues and a central branch that arborises in the dorsal horn of the spinal cord. It is generally accepted that distinct classes of primary afferent neurons are specialized to detect various sensory modalities and the existence of neurons with different response profiles allows discrimination between the sensations of warmth, cold, pain, itch and touch (Emery and Ernfors, 2020). Given this specialisation, the inputs a dorsal horn neuron receives from different classes of primary afferent may underlie the functional role of that neuron. However, to gain insights into function in this way requires not only appropriate methodological approaches to determine the input to cells, but also a classification scheme for primary afferents that adequately reflects their diversity and function.

1.7.1 Classifying Primary Afferent Neurons

Classically, primary afferent fibres have been classified by their size and degree of myelination, both of which determine their conduction velocity. This scheme results in four broad classes; heavily and moderately myelinated Aα and Aβ fibres, thinly myelinated Aδ fibres and unmyelinated C fibres. Simplistically, Aα and Aβ fibres transmit proprioceptive and low threshold touch information, respectively, while the Aδ and C classes transmit noxious and pruritic stimuli. However, there are a number of exceptions to this rule that make comprehensive classification by conduction velocity challenging. A small class of C fibres does not transmit nociceptive information, rather encodes pleasant or gentle touch sensations, and these are termed C-low threshold mechanoreceptors (C-LTMRs) (Abraira and Ginty, 2013). The Aδ class also contains non-nociceptive fibres that are associated with hair follicles and termed D-hair afferents or Aδ-LTMRs (Abraira and Ginty, 2013). A number of studies

have also identified neurons preferentially tuned to noxious stimuli (nociceptors) within the Aβ class (Djouhri and Lawson, 2004). LTMRs do not innervate laminae I & II of the dorsal horn, rather they project to lamina III and deeper. Consequently, their patterns of input are unlikely to be a defining feature of superficial dorsal horn interneurons. Therefore the remainder of this section focusses on the classification of afferents that project to laminae I & II.

A common approach to classifying primary sensory neurons has been to do so on the basis of electrophysiological determination of their sensitivity to sensory modalities. The sensitivity and threshold to noxious mechanical (M), heat (H) and cold (C) can be defined during recordings, and while estimates vary between studies, polymodal units (ie. those responding to multiple stimuli) represent the majority of the C fibre neurons (Dubin and Patapoutian, 2010). A small proportion of C-MH fibres are silent and only become responsive to noxious stimuli after being sensitised by inflammation (Schmidt et al., 1995). A-fibre nociceptors are predominantly heat and or mechanosensitive although some respond to cold (Dubin and Patapoutian, 2010). The A-MH nociceptors can also be further subdivided into two functional groups based on their response properties. Type I Aδ nociceptors respond to mechanical and chemical stimuli and have high heat thresholds but will sensitise in the context of tissue injury. These fibres are probably responsible for ‘first’ pain from mechanical stimuli such as a pin prick. Type II fibres have a much lower heat threshold and a high mechanical threshold and are involved in ‘fast’ pain responses to heat. The traditionally held view of polymodality as defined by microneurography or electrophysiology has recently been challenged in high-throughput in-vivo studies using calcium imaging; with one group finding that the vast majority of DRG neurons are modality specific (Emery et al., 2016). While this more modality specific finding may align well with the recently elucidated genetic diversity of DRG cells (see below), it has not been supported by other similarly conducted studies and remains controversial (Chisholm et al., 2018; Wang et al., 2018).

Another approach to classifying sensory neurons relies on their neurochemistry and this has been extensively studied and correlated to function. A major subdivision within nociceptors lies between peptidergic and non-peptidergic cells. Peptidergic neurons by definition express neuropeptides such as substance P and CGRP, while non-peptidergic neurons do not express these but bind the lectin Griffonia simplicifolia IB4 (Hokfelt et al., 1975; Snider and

McMahon, 1998). Many peptidergic neurons also express the tyrosine kinase receptor TrkA, which is the receptor for NGF (Denk et al., 2017), and some may express the NPY 2 receptor (Arcourt et al., 2017). Non-peptidergic neurons express the glial-derived neurotrophic factor Ret and the coreceptors GFRα1 and GFRα2 (Bennett et al., 1998; Franck et al., 2011). Subpopulations within the non-peptidergic class also differentially express a number of Mas-related G protein–coupled receptors such as MrgprA3 and MrgprD (Dong et al., 2001) and the proposed functional significance of this is detailed below. As mentioned above, some C fibres transmit pleasant touch sensations and many of these express TH and VGLUT3 (Seal et al., 2009), while a smaller population expresses MrgprB4 (Vrontou et al., 2013). Another popular classification scheme is based on the differential expression of TRP channels that confer sensitivity to heat, and cold. There is overwhelming evidence that TRPM8 is necessary for the transduction of cold (Bautista et al., 2007; McKemy, 2012), but the expression patterns and signalling mechanisms of other temperature sensitive channels in the DRG are complex and do not themselves singularly define functional classes (Paricio-Montesinos et al., 2020).

Given the extensive literature that associates single molecular markers with function in primary afferents, the use of newer unbiased and comprehensive classification strategies of DRG neurons is warranted. Several single cell RNA sequencing studies have sought to define classes of DRG neurons (Usoskin et al., 2015; Li et al., 2018; Zeisel et al., 2018). As single cell RNA sequencing allows for tens of thousands of transcripts to be quantified per cell, it has the capacity to define neuronal classes comprehensively. However, a number of technical factors can influence the results and particularly the ability to compare classes between studies (Emery and Ernfors, 2020). The number of neurons sequenced, and the sequencing depth are particularly important causes of variability. Here I present the scheme proposed by Usoskin et al. (2015), who sequenced 622 neurons to a moderate depth. This is in contrast to a scheme proposed by Li et al. (2016), where much deeper sequencing was used but on fewer (197) cells and the authors did not validate their results in vivo. When this data was re-analysed recently (Li et al., 2018), it predicted 9 neuronal classes in contrast to the 11 of Usoskin et al. The 11 neuronal types proposed by Usoskin et al. are: five types of neurofilament heavy chain-expressing myelinated A fibres, of which three are LTMRs (NF1, NF2 & NF3) and two are proprioceptors (NF4 & NF5). One C-LTMR population that expresses tyrosine hydroxylase named TH. One unmyelinated peptidergic C fibre class termed PEP1 and one lightly myelinated Aδ population, called PEP2. And finally, three types of non-peptidergic neurons;

the NP1, NP2 and NP3 clusters, that are defined by the expression of MrgprD, MrgprA3 and NPPB/SST, respectively. This classification system was refined by Zeisel et al. (2018), and these authors sequenced more neurons (1580) but to a shallower depth. This resulted in some variability between their results and those of Usoskin et al. (2015). LTMRs were underrepresented and as such NF2 and NF3 could not be separated. However, this more recent analysis was able to define three additional TRPM8-expressing cold-sensing clusters and separate a number of the peptidergic and non-peptidergic classes into subclasses. For example, NP1 and NP2 were both split into 2 subclusters (NP1.1/1.2 & NP2.1/2.2 respectively) although the functional significance of these subclusters is not yet known (Emery and Ernfors, 2020).

Each of the clusters of Usoskin et al. (2015) is thought to have functional significance based on previous work defining the roles of single neurochemical features of DRG neurons. Here I highlight the functional roles of the PEP, NP and TH classes as it is these fibres which project to the superficial dorsal horn (Todd and Wang, 2020). Neurons in the PEP1 cluster express high levels of *Tac1* (the gene for Substance P) and Calca (the gene for CGRP) and are therefore peptidergic. Previous work has shown that virtually all SP-expressing neurons are polymodal and respond to both noxious heat and mechanical stimuli (Lawson et al., 1997). Therefore PEP1 neurons are best classed as MH-C fibres and consistent with this they abundantly express TRPV1 and other TRP channels required for noxious heat sensation (Vandewauw et al., 2018). The PEP2 neuron class are lightly myelinated as they express NEFH and likely correspond to Aδ-nociceptors. They express *Calca* but not *Tac1*, and some express TRPV1 but a limited complement of other heat sensitive TRP channels. The TH class, express TH and *Slc17a8* (the gene for VGLUT3) and correspond to the previously defined C-LTMR class that are only present in hairy skin and convey pleasant touch sensations (Löken et al., 2009; Seal et al., 2009; Liljencrantz and Olausson, 2014).

The NP classes are best characterised as itch-mechano-heat neurons (Emery and Ernfors, 2020). The NP1 class are the only class expressing high levels of MrgprD. Ablation of MrgprD-expressing cells results in a deficit in response to mechanical stimuli with heat responses left unchanged (Cavanaugh et al., 2009). Very few of these fibres express TRPV1, although some express TRPM3 or TRPA1, which perhaps explains their limited responses to heat during in vivo recordings (Liu et al., 2012). MrgprD is also the receptor for β-alanine, a

compound that induces itch, and this highlights a pruritoceptive role for this class (Liu et al., 2012). The NP2 cells are the only class that express MrgprA3, and despite being polymodal nociceptors, these neurons have a well-defined role in chloroquine induced itch (Liu et al., 2009; Han et al., 2013). Ablation of these cells results in no changes in pain sensitivity despite substantial reductions in pruritogen evoked scratching (Han et al., 2013). The NP3 class is defined by the expression of a number of genes which also implicate them as neurons with broad itch functions. These cells express both NPPB and SST which act as itch neurotransmitters in the dorsal horn (Mishra and Hoon, 2013; Huang et al., 2018). Ablation of these cells reduces scratching in response to multiple pruritogens (Stantcheva et al., 2016), while optogenetic activation causes scratching (Huang et al., 2018). The NP3 cells also express a number of other molecules that have been implicated in acute and chronic itch such as IL-31RA, OSMR, CYSLTR2, and HTRF1 (Akiyama and Carstens, 2013; Usoskin et al., 2015; Dong and Dong, 2018).

1.7.2 Projections to the Dorsal Horn

Primary afferents project to the dorsal horn in a type and modality specific laminar pattern (Figure 1-6). Myelinated LTMRs terminate mainly in lamina III and deeper with specific distribution patterns (Abraira and Ginty, 2013). Within the superficial dorsal horn, C-LTMRs terminate at the lamina IIi/III border and it is mainly nociceptive and pruritoceptive fibres that are represented dorsal to this band (Peirs and Seal, 2016). Most Aδ-myelinated nociceptors have a compact termination zone in lamina II and IIo (Light and Perl, 1979) although some may arborise more diffusely (Boada and Woodbury, 2008; Arcourt et al., 2017). The remaining peptidergic and non-peptidergic C fibre nociceptors terminate in mid lamina II in defined bands depending on fibre type (Zylka et al., 2005). All primary afferents are glutamatergic and their central terminals express vesicular glutamate transporters which are differentially expressed amongst these cells. Both corticospinal projections and A-LTMRs express VGLUT1 (Todd et al., 2003). Although Aδ and C nociceptors utilise VGLUT2, the expression level of this transporter is such that the amount that can be detected in central terminals is generally low (Todd et al., 2003). The highest levels of VGLUT2 are seen in the axonal boutons of local excitatory interneurons (Todd et al., 2003). The adult expression of VGLUT3 defines the C-LTMR class of DRG cells and their central terminals are strongly immunoreactive for this protein (Seal et al., 2009).

Some primary afferent classes form complex synaptic arrangements termed synaptic glomeruli as they project to the dorsal horn (Ribeiro-da-Silva and Coimbra, 1982). These contain a central terminal representing the axonal bouton of the afferent, and this is surrounded by post-synaptic dendrites and pre-synaptic axonal terminals. The dendrites are postsynaptic to the central terminal, although they may form reciprocal synaptic arrangements. The pre-synaptic axons are GABAergic and represent the neuroanatomical substrate for pre-synaptic inhibition (Todd, 1996). Classically there are two types of glomeruli that can be ultrastructurally recognised in the rodent dorsal horn (Ribeiro-da-Silva and Coimbra, 1982). Type I glomeruli have small, dark and indented central terminals with few mitochondria and closely packed vesicles of variable diameter. These are thought to be associated with C-MrgprD nociceptors and are consequently prevalent in mid lamina II. Type II glomeruli have a large and more regularly contoured central terminal with fewer synaptic vesicles of a more regular diameter. These glomeruli are thought to arise from myelinated afferents and are found in lamina IIi and III. Other types of afferent may also give rise to synaptic glomeruli, including C-LTMRs although the classical glomerular type of these terminations is disputed (Larsson and Broman, 2019; Salio et al., 2020).

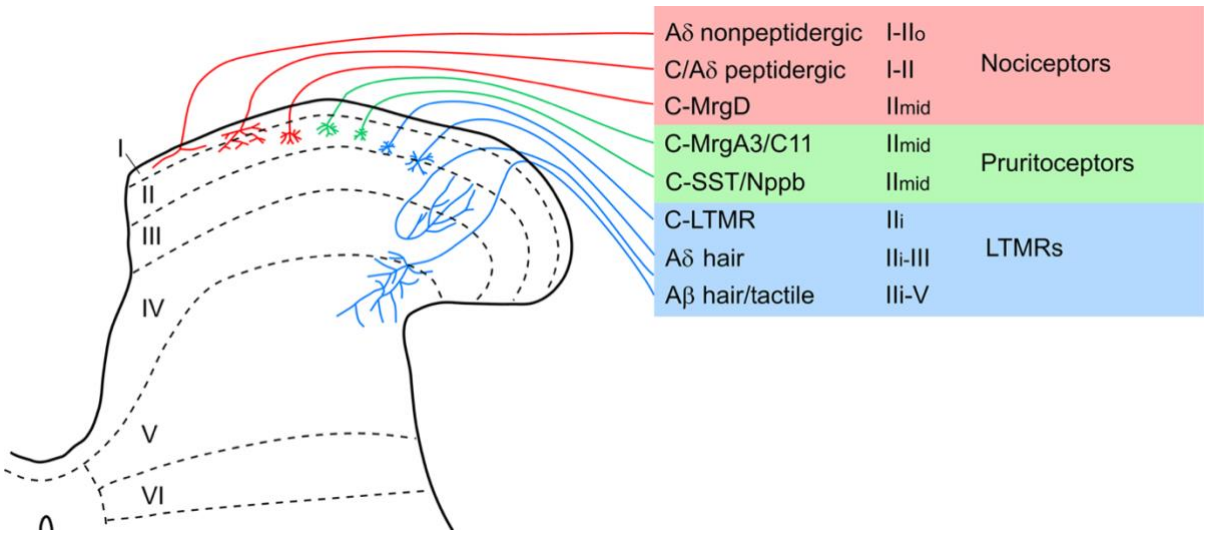

Figure-1-6. Terminations of Primary Afferent Neurons in the Dorsal Horn

Primary afferent neurons terminate in the dorsal horn in a modality specific laminar pattern. Aδ nociceptors terminate in laminae I and IIo, while peptidergic nociceptors arborise in laminae I and II. LTMR classes terminate in lamina IIi and deeper. The NP classes of Usoskin et al. (2015), which are defined by the expression of MrgprD, MrgprA3 or SST/NPPB all terminate in mid lamina II. From Todd and Wang (2020).

1.7.3 Methods used to Determine Synaptic Inputs

A number of techniques have been used to identify the synaptic inputs to dorsal horn neurons and these may be based on electrophysiology, optogenetics, anatomical tracing, viral tracing techniques or some combinations of the above. Patch clamp electrophysiology, when paired with dorsal root stimulation, can be used to determine whether individual cells receive Aβ, Aδ or C fibre inputs by mono or polysynaptic connections. This methodology has been used to determine the primary afferent input patterns of classically defined neuronal morphological types (Grudt and Perl, 2002; Yasaka et al., 2007) (and see 1.4 above). However, this approach is not specific enough to distinguish inputs from the diverse array of molecularly defined primary afferent fibres. In order to provide further insights into this, optogenetic stimulation of molecularly defined primary afferents has been used during patch clamp electrophysiology. In one study this approach did not show any specificity in the connections between MrgprD-expressing afferents and different morphologically defined classes of substantia gelatinosa neurons (Wang and Zylka, 2009). In terms of the pattern of inputs to GRP-expressing neurons, both of the techniques above have provided valuable insights. Sun et al. (2017) recorded from GRP-EGFP neurons and demonstrated a high proportion received monosynaptic C fibre input, while very few of these cells showed EPSCs in response to Aβ or Aδ stimulation. Both Pagani et al. (2019) and Sun et al. (2017) have also recorded from GRP-EGFP neurons while optogenetically stimulating MrgprA3 fibres, and both of these studies demonstrate that these cells have monosynaptic connections from this fibre type.

Anatomical techniques may be used to determine the presence and also extent of synaptic input to a cell from a specific primary afferent population. These studies may use fluorescent immunohistochemistry to identify pre and post synaptic markers adjacent to cells (Abraira et al., 2017; Larsson and Broman, 2019; Polgár et al., 2020), or may identify synapses using electron microscopy with specific labelling of pre and post synaptic structures (Peirs et al., 2014). Viral tracing techniques may also be used to identify cells which are pre-synaptic to a given cell type (Luo et al., 2018; Saleeba et al., 2019). Retrograde tracing with modified rabies virus has been used for this purpose in dorsal horn neurons (Albisetti et al., 2017; Sun et al., 2017). The modified rabes virus used in this strategy has its glycoprotein deleted so it is incapable of spreading from one neuron to another. The rabies virus can be directed to a specific population of starter cells by expressing both its cognate receptor (TVA) and the

rabies glycoprotein in a Cre-dependent fashion. Thus the rabies virus can multiply in this specific population of cells but also retrogradely infects those neurons which are pre-synaptic to the starter population where it causes expression of a fluorescent reporter (Callaway and Luo, 2015). A number of technical limitations make this technique challenging and these include variable susceptibility of pre-synaptic neurons to transfection (Albisetti et al., 2017), neurotoxicity, and variable proportions of labelling of pre-synaptic neurons (Callaway and Luo, 2015; Kim et al., 2016). It is also of note that the quantitative nature of the data is different to that gained from other anatomical techniques as the results pertain to inputs to a population rather than an individual cell. In the case of GRP-expressing neurons, rabies tracing has generated conflicting results and this perhaps arises from technical difficulties with the method (Albisetti et al., 2017; Sun et al., 2017). While both of these studies demonstrated that greater than 50% of the labelled DRG neurons were peptidergic, there were large and significant discrepancies in the numbers of neurofilament-expressing and non-peptidergic cells labelled. A number of other novel methods based on either specific synaptic reconstitution of fluorescent proteins or barcode sequencing have been proposed as high-throughput molecular techniques to determine synaptic connectivity, but these have not yet been demonstrated in the mammalian spinal cord (Feng et al., 2014; Kebschull, 2019).

1.8 Overall Aims of the Project

Excitatory dorsal horn interneurons that express GRP can be identified by the expression of EGFP in the GRP-EGFP mouse. These cells have been shown to be distinct from other neurochemical populations identified in the superficial dorsal horn (Gutierrez-Mecinas et al., 2014; Todd, 2017; Gutierrez-Mecinas et al., 2019). They are also likely to act as secondary pruritoceptors in a putative labelled-line for itch (Mishra and Hoon, 2013; Huang et al., 2018). The underlying hypothesis of the work presented here is that these cells are not simply neurochemically distinct, but rather represent a distinct functional population of excitatory interneurons. The aim of this series of studies is to further categorise these neurons in terms of their morphology, responses to stimuli, connectivity and molecular identity to determine whether they possess unique properties which are consistent with, and provide further evidence for, EGFP expression defining a functional population of cells. A series of major aims are addressed;

1. Neuronal morphology can be used to categorise dorsal horn interneurons (Grudt and Perl, 2002; Yasaka et al., 2010) and somato-dendritic morphometric parameters alongside axonal projections may have important implications for neuronal function. One aim of this project was to perform detailed morphological analysis on the GRP-EGFP cell population using neurobiotin filled cells following patch-clamp electrophysiological recordings. We aimed to determine whether these represent a morphologically homogeneous population of cells, but also to compare their morphology with that of another distinct population of lamina II excitatory interneurons; those cells expressing substance P.

2. Given the proposed role of these cells in itch pathways, we would expect them to be active following itch inducing stimuli delivered to the skin. Neuronal activity can be inferred using immunostaining for the Fos protein or phosphorylated ERK (Ji et al., 1999; Coggeshall, 2005). We aimed to determine whether GRP-EGFP cells consistently expressed Fos or phosphorylated ERK following the injection of pruritogens into the skin. Additionally, as it has been proposed that GRP-EGFP neurons form an itch specific circuit, we sought to determine if ERK phosphorylation was present following a variety of nociceptive stimuli.

3. Given the apparent modality-preferential nature of primary afferents, the pattern of inputs to a given dorsal horn cell type implies functional consequences. The inputs to GRP-EGFP cells have previously been defined using a rabies virus based approach (Sun et al., 2017). However, rabies based approaches may have technical limitations as some primary afferent fibre types appear resistant to infection (Albisetti et al., 2017). Also, these approaches are not quantitative at the individual cell level and retrograde labelling may be biased as it is more likely to arise from potentially atypical cells with more synaptic input; hence there is not always a direct correspondence between rabies findings and other anatomical and functional measures of connection strength (Luo et al., 2018). Given these limitations, here we aimed to determine the relative contributions of different primary afferent and local excitatory interneuron inputs to GRP-EGFP cells. Furthermore, we sought to quantify in particular the level of connectivity from putative pruritoceptive primary afferent neurons. This was achieved with an anatomical approach that used the post-synaptic protein Homer to identify synapses (Gutierrez-Mecinas et al., 2016b; Abraira et al., 2017).

4. Recent transcriptomic studies have identified clusters amongst dorsal horn interneurons which may represent discrete functional classes. Häring et al. (2018) describe 15 excitatory interneuron classes and these align well with the existing neurochemical classes defined by CCK, substance P, NKB and NTS expression. However, GRP expression does not define a class in this transcriptomic scheme. Instead, GRP expression is widespread and is documented in 8 of the 15 clusters, including Glut9 – a cluster defined by the expression of Npff. As little was known about the properties of Npff-expressing neurons, we aimed to characterise them using both *in situ* hybridisation and immunohistochemical approaches. This study therefore aimed to determine the overlap of Npff expression with existing neurochemical classes, and in particular the relationship to GRP-EGFP cells.

5. The finding of widespread expression of GRP across neuronal classes by Häring et al. (2018), is at odds with findings from the GRP-EGFP mouse where EGFP expression appears to mark a discrete population (Gutierrez-Mecinas et al., 2014). This discrepancy may be explained by the finding that, at least in the closely related GRP-Cre transgenic line, only around a quarter of GRP-expressing cells are labelled by a floxed reporter (Albisetti et al., 2019). Using an *in situ* hybridisation based approach we aimed to determine whether this was also the case for the GRP-EGFP mouse and whether, despite GRP mRNA being present in several transcriptomically-defined populations, EGFP is restricted to a discrete subset of cells.

2 Paper I

Bell, A.M., Gutierrez-Mecinas, M., Polgár, E., Todd, A.J., 2016. Spinal neurons that contain gastrin-releasing peptide seldom express Fos or phosphorylate extracellular signal-regulated kinases in response to intradermal chloroquine. Molecular Pain 12, 1744806916649602.

CRediT statement

Conceptualization, A.M.B., M.G.M. and A.J.T.; Methodology, A.M.B, E.P. and A.J.T.; Formal analysis, A.M.B.; Investigation, A.M.B, E.P. and M.G.M.; Writing – Original Draft, A.M.B. and A.J.T.; Writing – Review & Editing, A.M.B., M.G.M., E.P. and A.J.T.; Visualization, A.M.B. and A.J.T.; Supervision, A.J.T.; Funding Acquisition, A.J.T.

Summary of practical involvement in each component of study

All experiments and analysis – A.M.B primary role.

Research Article

MOLECULAR PAIN

Molecular Pain
Volume 12: 1–9

DOI: 10.1177/1744806916649602
mpx.sagepub.com
SAGE

Spinal neurons that contain gastrin-releasing peptide seldom express Fos or phosphorylate extracellular signal-regulated kinases in response to intradermal chloroquine

Andrew M Bell, BVMS[1,2], Maria Gutierrez-Mecinas, PhD[1], Erika Polgár, PhD[1] and Andrew J Todd, PhD[1]

Abstract

Background: Gastrin-releasing peptide (GRP) is thought to play a role in the itch evoked by intradermal injection of chloroquine. Although some early studies suggested that GRP was expressed in pruriceptive primary afferents, it is now thought that GRP in the spinal cord is derived mainly from a population of excitatory interneurons in lamina II, and it has been suggested that these are involved in the itch pathway. To test this hypothesis, we used the transcription factor Fos and phosphorylation of extracellular signal-regulated kinases (ERK) to look for evidence that interneurons expressing GRP were activated following intradermal injection of chloroquine into the calf, in mice that express enhanced green fluorescent protein (EGFP) in these cells.

Results: Injection of chloroquine resulted in numerous Fos- or phospho-ERK (pERK) positive cells in the somatotopically appropriate part of the superficial dorsal horn. The proportion of all neurons in this region that showed Fos or pERK was 18% and 21%, respectively. However, among the GRP–EGFP, only 7% were Fos-positive and 3% were pERK-positive. As such, GRP–EGFP cells were significantly less likely than other neurons to express Fos or to phosphorylate ERK.

Conclusions: Both expression of Fos and phosphorylation of ERK can be used to identify dorsal horn neurons activated by chloroquine injection. However, these results do not support the hypothesis that interneurons expressing GRP are critical components in the itch pathway.

Keywords

Itch, spinal cord, pERK, interneuron

Date received: 12 January 2016; revised: 10 March 2016; accepted: 8 April 2016

Background

Itch has been defined as an unpleasant sensation that causes a desire to scratch. Chronic itch (pruritus) can result from several dermatological and systemic diseases and represents a major unmet clinical need. Despite this, we still know relatively little about the neuronal circuits that are responsible for the sensation of itch.[1–4] A major distinction can be made between those forms of itch that are relieved by antihistamines (histamine-dependent) and those that are not (histamine-independent). Many substances (pruritogens) can evoke itch, when injected into the skin, and these can operate through either histamine-dependent or histamine-independent mechanisms.[5–7]

An early insight into the peripheral and spinal pathways responsible for itch came from the observation that mice lacking the receptor for gastrin-releasing peptide

[1]Institute of Neuroscience and Psychology, College of Medical, Veterinary and Life Sciences, University of Glasgow, Glasgow, UK
[2]School of Veterinary Medicine, College of Medical, Veterinary and Life Sciences, University of Glasgow, Glasgow, UK

Corresponding author:
Andrew Todd, Institute of Neuroscience and Psychology, College of Medical, Veterinary and Life Sciences, University of Glasgow, Glasgow, G12 8QQ, UK.
Email: Andrew.Todd@glasgow.ac.uk

(GRP) showed significantly reduced responses to certain pruritogens, but normal responses to a variety of painful stimuli.[8] Three lines of evidence suggested that GRP signalling at the spinal level was required for itch: (a) intrathecal administration of GRP receptor (GRPR) agonists evoked scratching, while antagonists reduced scratching in response to injected pruritogens; (b) *in situ* hybridisation revealed that the GRPR was expressed by neurons in lamina I of the dorsal horn; (c) a subsequent study from the same group showed that ablation of spinal GRPR-expressing neurons with saporin conjugated to bombesin (an amphibian homologue of GRP) resulted in reduced responsiveness to a variety of pruritogens.[9] This study also demonstrated that itch behaviours following administration of histamine-independent pruritogens such as chloroquine were substantially reduced in GRPR knockout mice, whereas histamine-dependent responses were much less affected.[9] Further evidence for a role of spinal GRP signalling in histamine-independent itch came from the finding that a GRPR antagonist delivered directly to the spinal cord significantly reduced the responses of superficial dorsal horn neurons to intradermal chloroquine but not to intradermal histamine.[10]

There has been considerable debate concerning the source of GRP in the spinal cord. A number of studies have provided evidence that GRP is expressed by a specific subset of peptidergic primary afferents,[8,11–13] and it has been suggested that the GRP released by these afferents acts through spinal GRPR to mediate itch.[8] However, several other groups have failed to detect GRP mRNA in primary afferents, using a variety of methods, including in situ hybridisation, RT and real-time polymerase chain reaction, and RNA seq.[14–18] In addition, it has been reported that the antibodies that had been used to reveal GRP in the dorsal root ganglion[8,13] can cross react with substance P,[14,19] which is expressed by many peptidergic primary afferents.[20,21]

mRNA for GRP has been identified in the dorsal horn[14–16,18,22,23] and the GRP-expressing cells can be identified in a mouse line (Tg-GRP-EGFP) in which enhanced green fluorescent protein (EGFP) is expressed under control of the GRP promoter.[14,19,24] It has recently been shown that these cells represent a specific population of excitatory interneurons in lamina II.[19,25] Taken together with the evidence against primary afferent expression of GRP, these findings have led to the alternative suggestion that GRP released by itch-activated spinal interneurons plays an important role in histamine-independent itch.[14,24,26] To test this hypothesis, we have looked for evidence that chloroquine can activate GRP-expressing dorsal horn interneurons. As GRP cannot be detected in the cell bodies of these neurons with immunocytochemistry,[19] we used the Tg(GRP-EGFP) line. $EGFP^+$ cells in this mouse are mainly present in lamina II,[19] and it has been shown that >90% of these possess GRP mRNA.[14]To reveal activated neurons, we stained for the transcription factor Fos,[27] which has been used in several previous studies,[28–32] and for phosphorylated extracellular signal-regulated kinases (pERK).[33,34]

Methods

All animal experiments were approved by the Ethical Review Process Applications Panel of the University of Glasgow and were performed in accordance with the European Community directive 86/609/EC and the UK Animals (Scientific Procedures) Act 1986.

Fos induction

Six adult Tg(GRP-EGFP) mice of either sex (16–25 g; Gene Expression Nervous System Atlas [GENSAT]) were used to investigate Fos expression after intradermal injection of chloroquine or vehicle. The skin on the lateral aspect of the hindlimb was shaved on the day before stimulation, and in order to prevent scratching or biting of the injected area during the postinjection survival time (which would result in nociception-activated Fos), an Elizabethan collar (Harvard Apparatus, #72-0056) was applied at the time of shaving. Animals were briefly anaesthetised with isoflurane, and injections of either chloroquine (40 µg dissolved in 10 µl of phospate-buffered saline [PBS], $n = 3$ mice) or vehicle (10 µl PBS, $n = 3$ mice) were made into the lateral aspect of the left calf, after which the mice were allowed to recover from anaesthesia. The success of the intradermal injection was assessed by the formation of a small bleb[6,7] in the calf skin. They were reanaesthetised with pentobarbitone (20 mg i.p.) and perfused through the left ventricle with fixative that contained 4% freshly depolymerised formaldehyde 2 h after the stimulus.

The L3 spinal segment (which contains the great majority of cells activated by these stimuli) was removed and postfixed for 2 h in the same fixative. The contralateral (right) side was notched to allow identification, and the tissue was cut into 60 µm thick transverse sections with a vibrating blade microtome (Leica VT1200). These were immersed in 50% ethanol for 30 min to enhance antibody penetration and then multiple-labelling immunofluorescence staining was performed as described previously.[19,35] The sections were incubated for three days in the following combination of primary antibodies: mouse monoclonal antibody NeuN (Millipore; MAB377; diluted 1:500), chicken anti-EGFP (Abcam, ab13970; diluted 1:1000), and rabbit anti-Fos (Santa Cruz Biotechnology, sc-52; diluted 1:5,000). They were then incubated overnight in species-specific secondary antibodies that were raised in donkey and conjugated to

Alexa 647, Alexa 488, or Rhodamine Red (Jackson Immunoresearch, West Grove, PA, USA). Secondary antibodies were diluted 1:500 (Alexa 647 and Alexa 488) or 1:100 (Rhodamine Red). All antibodies were diluted in PBS that contained 0.3% Triton X-100 and incubations were at 4°C. Following the immunocytochemical reaction, sections were stained with 4′,6-diamidino-2-phenylindole (DAPI) to reveal nuclei, mounted in antifade medium and stored at −20°C.

Sections were scanned with a Zeiss LSM 710 confocal microscope equipped with Argon multiline, 405 nm diode, 561 nm solid state, and 633 nm HeNe lasers. They were initially viewed with epifluorescence optics, and three sections from the chloroquine-injected mice that contained numerous Fos^+ cells were selected from each animal, before EGFP was observed. Z-series (2 μm spacing) were then scanned through the full thickness of each section with the 40× oil-immersion lens (numerical aperture 1.3), with the confocal aperture set to 1 Airy unit. These scans included the central part of the dorsal horn, which contained the activated cells. The z-stacks from chloroquine-injected mice were analysed with Neurolucida for Confocal (MBF Bioscience, Williston, VT, USA). The outline of the grey matter was drawn, and the ventral border of the GRP plexus (which corresponds approximately to the boundary between the inner and outer parts of lamina II[19]) was determined from a maximum intensity projection and plotted onto the drawing. The mediolateral extent of the region that contained a high density of Fos^+ cells was delineated by drawing two parallel lines that were orthogonal to the laminar boundaries (see Figure 1).

Initially, only the channels corresponding to NeuN and DAPI were viewed, and the locations of all neurons ($NeuN^+$ cells) that lay within this region were plotted onto the drawing. To avoid overcounting cells that were split during sectioning,[36] we included cells if at least part of the nucleus (stained with DAPI) was present in the first optical section of the z-series and excluded them if part of the nucleus was present in the last optical section.[37] The channel corresponding to Fos was then viewed, and the presence or absence of staining in each of the neurons in the sample was recorded. Finally, the EGFP channel was viewed and all neurons that were $EGFP^+$ were identified on the drawing. As Fos^+ cells were present at highest density in lamina I and the outer part of lamina II (lamina IIo), we determined the proportion of all neurons that were located within this region and between the two parallel lines that were Fos-immunoreactive. We then determined the proportion of GFP^+ neurons within this volume that were Fos-immunoreactive. Sections from the PBS-injected mice were also examined with the confocal microscope to test for the presence of Fos-immunoreactive neurons.

Phosphorylation of ERK

In initial studies, we performed intradermal injections of chloroquine or PBS and allowed a 5-min survival time before perfusion fixation, as phosphorylation of ERK occurs rapidly following stimulation.[33–35,38] However, although we observed numerous pERK-positive cells in the superficial dorsal horn of the ipsilateral L3 segment in the chloroquine-injected mice, there were also many $pERK^+$ cells in the corresponding region in PBS-injected mice. This is likely to have been caused by the mechanical noxious stimulus that results from needle insertion and distension of the skin during the intradermal injection.[6] In subsequent experiments, we therefore allowed a longer postoperative survival time (30 min). Six adult Tg(GRP-EGFP) mice of either sex (16–23 g; GENSAT) were anaesthetised with isoflurane and received intradermal injections of chloroquine (40 μg in 10 μl, $n = 3$ mice) or PBS (10 μl, $n = 3$ mice) into the left calf, which had been shaved the day before, as described earlier. The mice were maintained under isoflurane anaesthesia throughout the survival period. They then received pentobarbitone (20 mg i.p.) prior to perfusion fixation (a described earlier), which was carried out 30 min after the intradermal injection. The tissue was processed exactly as described for the Fos experiments, except that the Fos antibody was replaced with rabbit anti-pERK (Cell Signaling Technology, 9101; diluted 1:500). Confocal scanning and analysis were performed as described for the Fos experiments.

Characterisation of antibodies

The EGFP antibody was raised against recombinant full--length EGFP, and the distribution of staining matches that of native EGFP. The mouse monoclonal antibody NeuN was raised against cell nuclei extracted from mouse brain[39] and apparently labels all neurons but no glial cells in the rat spinal dorsal horn.[40] The Fos antibody was raised against a peptide corresponding to the *N*-terminus of human Fos. The pERK antibody detects p44 and p42 MAP kinase (Erk1 and Erk2) when these are phosphorylated either individually or dually at Thr202 and Tyr204 of Erk1 or Thr185 and Tyr187 of Erk2. It does not cross-react with the corresponding phosphorylated residues of JNK/SAPK or of p38 MAP kinase or with nonphosphorylated Erk1/2 (manufacturer's specification). Specificity of both Fos and pERK antibodies was demonstrated by the lack of staining in nonstimulated areas (e.g. the contralateral dorsal horn).

Statistics

Data were formatted into 2 × 2 contingency tables for each animal, with rows corresponding to presence or absence of EGFP and columns to presence or absence of Fos or

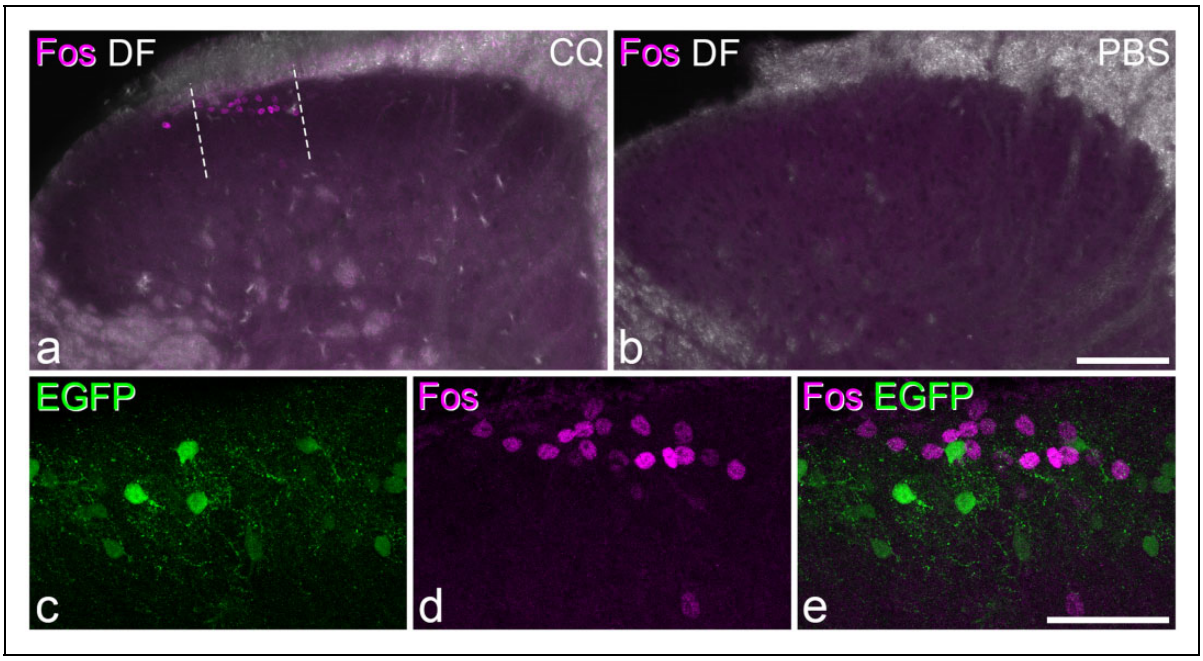

Figure 1 Fos in the dorsal horn following intradermal injection of chloroquine.
(a) A transverse section through the dorsal horn from the L3 segment of a GRP-EGFP mouse, ipsilateral to the side in which chloroquine (CQ) had been injected intradermally 2 h prior to perfusion fixation. Fos immunoreactivity (magenta) is superimposed on a dark-field (DF) image. There is a cluster of Fos^+ cells in the superficial part of the dorsal horn, and these are concentrated between the two dashed lines. (b) An equivalent section from a mouse that had received an intradermal injection of PBS, in which no Fos^+ cells are visible. (c–e) Higher magnification views from the section shown in a to show the relationship between EGFP (green) and Fos. Note that although the cells are intermingled, there are none that are double labelled in this section. All sections are maximum intensity projections of confocal z-series (2 μm z-separation) through the full thickness of the 60 μm section. Scale bars: a, b = 100 μm; c–e = 50 μm.

Table 1 pERK and Fos following intradermal chloroquine.

pERK/Fos	Total neurons	$pERK^+/Fos^+$ neurons	$GRP\text{-}EGFP^+$ neurons	$GRP\text{-}EGFP^+$ and $pERK^+/Fos^+$	% Neurons $pERK^+/Fos^+$	% GRP-EGFP neurons $pERK^+/Fos^+$
Fos	417.7 (386–440)	74 (67–78)	55 (42–62)	4.0 (1–7)	17.7 (17.4–18.3)	6.8 (2.4–11.3)
pERK	398 (309–475)	82.7 (59–110)	50 (45–60)	1.3 (1–2)	20.9 (16.6–26.8)	2.8 (1.7–4.4)

Note. pERK: phospho extracellular signal-regulated kinase; GRP: gastrin-releasing peptide; EGFP: enhanced green fluorescent protein. The table shows quantitative data from the region delineated by high levels of Fos or pERK, and were obtained from three mice in each case.

pERK. To determine whether there was a consistent difference in the proportions across the tables for the different cell types, we used the Mantel–Haenszel analysis.[41] Breslow–Day testing for homogeneity of the odds ratio was conducted prior to computation of the Mantel–Haenszel odds ratio and 95% confidence intervals.

Results

Fos

Injection of chloroquine into the calf, followed by a survival time of 2 h, resulted in expression of Fos in neurons in the superficial part of the dorsal horn of the L3 segment ipsilateral to the injection site. The cells were found throughout the length of the segment but were restricted to a narrow mediolateral band (around 100 μm wide) in the middle part of the dorsal horn (Figure 1a), which corresponds to the central projection zone of primary afferents from the lateral part of the calf.[42] They were largely restricted to laminae I and IIo and were rarely seen in deeper parts of the dorsal horn. Within the delineated region, the mean total number of neurons in laminae I–IIo pooled from three sections from each animal varied from 386–440 ($n = 3$ mice), and the proportion of these that showed Fos was 18% (Table 1). In the PBS-injected mice, only very occasional cells showing Fos were evident (Figure 1b).

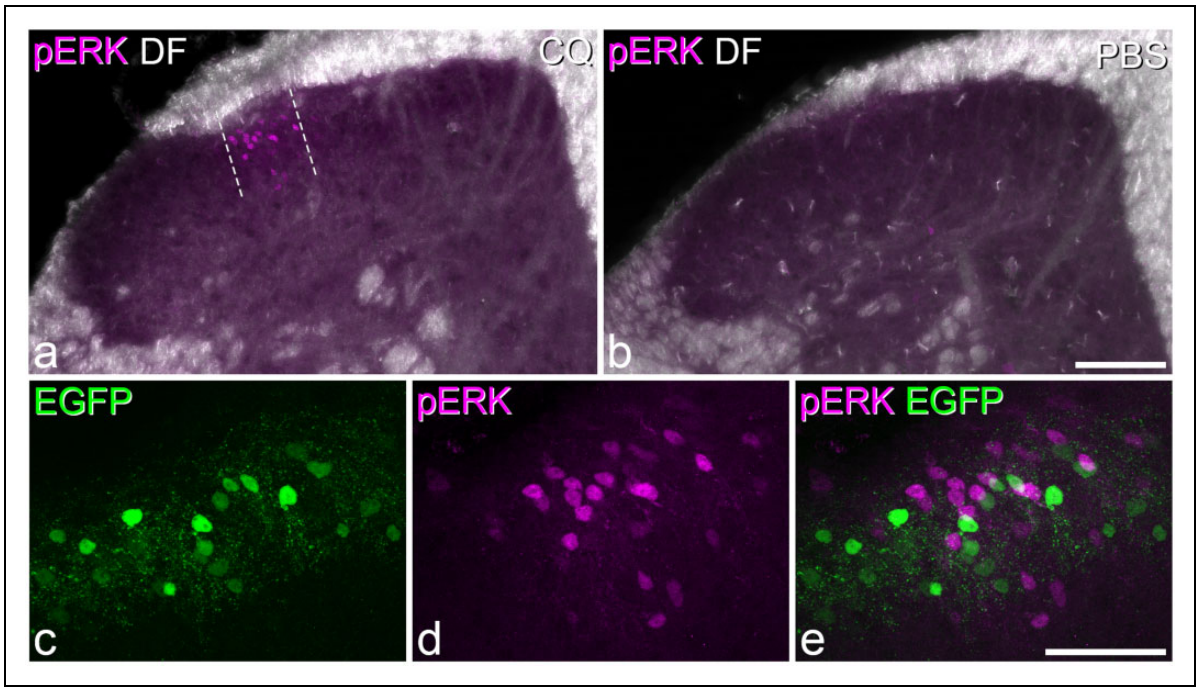

Figure 2 pERK in the dorsal horn following intradermal injection of chloroquine.
(a) A transverse section through the dorsal horn from the L3 segment of a GRP-EGFP mouse, ipsilateral to the side in which chloroquine (CQ) had been injected intradermally 30 min prior to perfusion fixation. pERK immunoreactivity (magenta) is superimposed on a dark-field (DF) image. There is a cluster of $pERK^+$ cells in the superficial dorsal horn, which is concentrated between the two dashed lines. (b) An equivalent section from a mouse that had received an intradermal injection of PBS, in which no $pERK^+$ cells are visible in the superficial laminae. (c–e) Higher magnification views from the section illustrated in a show the relationship between EGFP (green) and pERK. Note that although the cells are intermingled, there are none that are double labelled in this section. All sections are maximum intensity projections of confocal z-series (2 μm z-separation) through the full thickness of the 60 μm section. Scale bars: a, b = 100 μm; c–e = 50 μm.

Table 2 Analysis of odds ratios for coexpression of EGFP and activity-dependent markers.

Activity-dependent marker	Breslow–Day significance	Mantel–Haenszel test of conditional independence			Estimate of common odds ratio	95% confidence interval
		χ^2_{MH}	*df*	Significance		
Fos	0.259	13.92	1	<0.001	0.32	0.17–0.59
pERK	0.937	32.56	1	<0.001	0.09	0.03–0.25

As reported previously,[14,19,24,25] GRP-EGFP neurons were particularly numerous in lamina II, but were occasionally seen in lamina I, and were also scattered through the deeper parts of the dorsal horn (Figures 1c,e and 2). Although there was considerable overlap in the distribution of GRP-EGFP and Fos, relatively few of the GRP-EGFP cells were Fos-immunoreactive (Figure 1). The mean number of GRP-EGFP cells that were sampled in lamina I-IIo in the delineated area was 55, and of these, 7% were Fos-immunoreactive (Table 1).

To determine whether the presence of Fos among GRP-EGFP cells was significantly less frequent than that in the general population of neurons, we measured the common odds ratio for the three mice (Table 2). The 95% confidence interval was below 1, indicating that the GRP-EGFP cells were significantly less likely than other neurons in this region to express Fos.

pERK

Thirty minutes after chloroquine injection, numerous pERK-positive cells were seen in the ipsilateral L3 segment, while in contrast, very few pERK cells were seen in the mice that had received injection of PBS (Figure 2). The distribution of pERK cells in the chloroquine-injected mice was similar to that of Fos-positive neurons

described earlier, forming a narrow mediolateral band in the middle part of the dorsal horn throughout the L3 segment. The total number of neurons in laminae I-IIo within the region delineated by pERK-immunoreactivity varied from 309 to 475 ($n = 3$ mice), and the proportion of these that were pERK-immunoreactive was 21% (Table 1). Again, although numerous GRP^+ cells were present in this region (mean 50 cells), relatively few of these (3%) were pERK-immunoreactive (Figure 2c–e). The 95% confidence interval for the common odds ratio was below 1, indicating that GRP-EGFP cells were significantly less likely than other neurons to have phosphorylated ERK (Table 2).

Discussion

The main findings of this study are that following intradermal injection of 40 μg chloroquine into the calf, around 20% of neurons in laminae I-IIo in the somatotopically appropriate region of L3 upregulate Fos and phosphorylate ERK. However, although the activated cells showed an overlapping distribution with GRP-EGFP neurons, the latter were seldom Fos- or pERK-positive.

Fos and pERK as markers for itch activation

Several previous studies have used expression of Fos to identify neurons in the spinal dorsal horn that were activated by various pruritogens, including chloroquine, or in models of chronic itch.[30,32,34,43–50] Between them, these studies have involved intradermal injections into several body regions: the cheek, neck, back, calf, and hindpaw. In each case, Fos^+ neurons have been identified in laminae I–II of the corresponding spinal cord segments or spinal trigeminal nucleus. The distribution of Fos^+ cells seen in the present study was therefore entirely consistent with these reports. As very few Fos cells were seen following an equivalent injection of the vehicle (PBS), it is highly likely that the Fos was induced as a result of the chloroquine and therefore represents the response to a pruritic stimulus.

There have apparently been very few reports of ERK phosphorylation in itch models. Zhang et al.[34] showed that histamine injected intradermally in the neck or hindpaw caused phosphorylation of ERK, which could be detected in the superficial dorsal horn, peaking 30 min after the stimulus. However, they found that intradermal injections of chloroquine that were sufficient to induce scratching did not evoke pERK. It is difficult to explain the discrepancy between their findings and those reported here, although in their study, the mice were not anaesthetised, and it is therefore possible that scratching of the affected area or activity in descending systems that are inactive during general anaesthesia suppressed ERK phosphorylation. It is unlikely that differences in the site of injection (neck in Zhang et al. and calf in the present study) were responsible for the different results, as Fos studies have shown very similar patterns of expression when pruritogens were injected into different sites. We found very little pERK in animals that had survived 30 min after PBS injection, which suggests that the phosphorylation was evoked by the chloroquine and therefore represents a pruritic response. However, our preliminary experiments with 5-min survival times indicated that the injection itself could cause significant phosphorylation of ERK. This was clearly very short lived, as it had completely subsided by 30 min.

Comparing our findings with Fos and pERK shows that there was a very similar distribution of labelled cells and that a comparable proportion of lamina I-IIo neurons within the somatotopically appropriate region was affected (~20% in each case). Since ERK phosphorylation is an upstream regulator of Fos in the dorsal horn,[51] it is likely that the two markers were labelling equivalent populations of neurons, and the finding that GRP-EGFP cells were underrepresented with both markers is consistent with this suggestion.

Interestingly, Zhang et al.[34] reported that blocking phosphorylation of ERK with a MEK inhibitor reduced scratching behaviour in response to histamine but not to chloroquine. Our findings indicate that ERK is phosphorylated following intradermal injection of chloroquine but presumably it is not required for the resulting behaviour.

The identity of the itch-activated neurons in laminae I-IIo is not yet known, although it is likely that the great majority are interneurons,[28] and it will therefore be important for future studies to determine which neurochemical classes of interneuron show Fos or pERK following pruritogen injections. We have recently provided evidence that four nonoverlapping populations, defined by expression of GRP, neurotensin, neurokinin B, and substance P, can be identified among the excitatory interneurons in laminae I–III.[19,25] However, the neurotensin and neurokinin B populations are both concentrated in the inner part of lamina II and lamina III and are therefore unlikely to be involved in itch. At present, the substance P-expressing cells are difficult to identify with immunocytochemistry due to the low level of peptide present in their cell bodies.

A role for GRP-expressing interneurons in chloroquine-evoked itch?

There is considerable evidence that the GRPR plays an important role in several forms of itch,[1] including that evoked by chloroquine.[8,10] As it has been suggested that GRP-expressing dorsal horn interneurons are part of the itch pathway,[14,24,26] we were surprised to find that

GRP-EGFP cells were underrepresented among those that showed either Fos or pERK. It is likely that the dose of chloroquine we used was sufficient to cause itching, as similar doses have evoked scratching or biting in other studies in the mouse.[52,53] In addition, we have found that intradermal injection of 40 μg of chloroquine into the calf in mice without Elizabethan collars leads to biting of the injected area (EP unpublished data), and this dose was sufficient to evoke Fos or pERK in a substantial proportion (~20%) of the neurons in laminae I–IIo in this study.

This leaves several possible explanations for this paradox. (1) A significant number of GRP-EGFP cells may have been activated without expressing Fos or phosphorylating ERK, and the risk of false-negative results should always be considered with studies involving these activity-dependent markers. It is also possible that a relatively low level of activation is required to induce release of neuropeptides, including GRP. (2) It may be that sufficient GRP is released from the relatively few GRP-EGFP cells that were activated. (3) Solorzano et al.[14] reported that only ~70% of neurons with GRP mRNA were $EGFP^+$ in this mouse line and therefore EGFP-negative GRP-expressing neurons may have been activated. However, this explanation would require that there was a specific subpopulation of GRP-expressing neurons that lacked EGFP and that these were selectively activated by chloroquine.

Alternatively, the GRP-expressing dorsal horn interneurons may not be critically involved in itch pathways. There continues to be considerable debate about whether GRP is released from primary afferents,[12,24] and if it is then this would be consistent with our findings. However, the majority view now appears to be against primary afferents as a source of GRP,[15–18] at least in naïve animals.[14]

Finally, it is possible that the GRPR on lamina I neurons is activated by a different peptide. Although the other main bombesin-like peptide, neuromedin B, is expressed in primary afferents,[15–18] it has a very low affinity for the GRPR[54] and is therefore unlikely to mediate its activation following pruritic stimulation. However, there may be another, as yet unknown, peptide that forms the link between pruriceptive primary afferents and the GRPRs that are expressed by lamina I neurons, and the fact that there is an orphan receptor (BB3) would be consistent with this suggestion.[54]

Conclusions

The results of this study show that both Fos and pERK can be used to identify cells that have been activated by intradermal injections of the pruritogen chloroquine and that similar numbers of cells are labelled for each marker. However, they do not support the suggestion that GRP-expressing interneurons in the superficial dorsal horn are preferentially activated by chloroquine.

Authors' contributions

AMB, MGM, and AJT designed the study. AMB, MGM, and EP performed the anatomical experiments and analysed the resulting data. All authors contributed to the writing of the manuscript and approved the final version.

Acknowledgements

The authors are grateful to Mr R Kerr and Ms C Watt for excellent technical assistance and to Dr R Ganley for helpful discussion. The mouse strain Tg(GRP-EGFP) was originally obtained from the Mutant Mouse Regional Resource Centre (MMRRC), a National Centre for Research Resources- and NIH-funded strain repository and was donated to the MMRRC by the NINDS-funded GENSAT BAC transgenic project.

Declaration of Conflicting Interests

The author(s) declared no potential conflicts of interest with respect to the research, authorship, and/or publication of this article.

Funding

The author(s) disclosed receipt of the following financial support for the research, authorship, and/or publication of this article: The work was supported by the Wellcome Trust (grant 102645) and the MRC (grant L003430).

References

1. Bautista DM, Wilson SR and Hoon MA. Why we scratch an itch: the molecules, cells and circuits of itch. *Nat Neurosci* 2014; 17: 175–182.
2. LaMotte RH, Dong X and Ringkamp M. Sensory neurons and circuits mediating itch. *Nat Rev Neurosci* 2014; 15: 19–31.
3. Ross SE. Pain and itch: insights into the neural circuits of aversive somatosensation in health and disease. *Curr Opin Neurobiol* 2011; 21: 880–887.
4. Akiyama T and Carstens E. Neural processing of itch. *Neuroscience* 2013; 250: 697–714.
5. Davidson S, Zhang X, Yoon CH, et al. The itch-producing agents histamine and cowhage activate separate populations of primate spinothalamic tract neurons. *J Neurosci* 2007; 27: 10007–10014.
6. Moser HR and Giesler GJ Jr. Characterization of pruriceptive trigeminothalamic tract neurons in rats. *J Neurophysiol* 2014; 111: 1574–1589.
7. Roberson DP, Gudes S, Sprague JM, et al. Activity-dependent silencing reveals functionally distinct itch-generating sensory neurons. *Nat Neurosci* 2013; 16: 910–918.
8. Sun YG and Chen ZF. A gastrin-releasing peptide receptor mediates the itch sensation in the spinal cord. *Nature* 2007; 448: 700–703.

9. Sun YG, Zhao ZQ, Meng XL, et al. Cellular basis of itch sensation. *Science* 2009; 325: 1531–1534.
10. Akiyama T, Tominaga M, Takamori K, et al. Roles of glutamate, substance P, and gastrin-releasing peptide as spinal neurotransmitters of histaminergic and nonhistaminergic itch. *Pain* 2014; 155: 80–92.
11. Zhao ZQ, Huo FQ, Jeffry J, et al. Chronic itch development in sensory neurons requires BRAF signaling pathways. *J Clin Invest* 2013; 123: 4769–4780.
12. Liu XY, Wan L, Huo FQ, et al. B-type natriuretic peptide is neither itch-specific nor functions upstream of the GRP-GRPR signaling pathway. *Mol Pain* 2014; 10: 4.
13. Takanami K, Sakamoto H, Matsuda KI, et al. Distribution of gastrin-releasing peptide in the rat trigeminal and spinal somatosensory systems. *J Comp Neurol* 2014; 522: 1858–1873.
14. Solorzano C, Villafuerte D, Meda K, et al. Primary afferent and spinal cord expression of gastrin-releasing peptide: message, protein, and antibody concerns. *J Neurosci* 2015; 35: 648–657.
15. Fleming MS, Ramos D, Han SB, et al. The majority of dorsal spinal cord gastrin releasing peptide is synthesized locally whereas neuromedin B is highly expressed in pain- and itch-sensing somatosensory neurons. *Mol Pain* 2012; 8: 52.
16. Goswami SC, Thierry-Mieg D, Thierry-Mieg J, et al. Itch-associated peptides: RNA-Seq and bioinformatic analysis of natriuretic precursor peptide B and gastrin releasing peptide in dorsal root and trigeminal ganglia, and the spinal cord. *Mol Pain* 2014; 10: 44.
17. Usoskin D, Furlan A, Islam S, et al. Unbiased classification of sensory neuron types by large-scale single-cell RNA sequencing. *Nat Neurosci* 2015; 18: 145–153.
18. Wada E, Way J, Lebacq-Verheyden AM, et al. Neuromedin B and gastrin-releasing peptide mRNAs are differentially distributed in the rat nervous system. *J Neurosci* 1990; 10: 2917–2930.
19. Gutierrez-Mecinas M, Watanabe M and Todd AJ. Expression of gastrin-releasing peptide by excitatory interneurons in the mouse superficial dorsal horn. *Mol Pain* 2014; 10: 79.
20. Hokfelt T, Kellerth JO, Nilsson G, et al. Substance-P—localization in central nervous system and in some primary sensory neurons. *Science* 1975; 190: 889–890.
21. Todd AJ and Spike RC. The localization of classical transmitters and neuropeptides within neurons in laminae I-III of the mammalian spinal dorsal horn. *Prog Neurobiol* 1993; 41: 609–645.
22. Wang X, Zhang J, Eberhart D, et al. Excitatory superficial dorsal horn interneurons are functionally heterogeneous and required for the full behavioral expression of pain and itch. *Neuron* 2013; 78: 312–324.
23. Allen Spinal Cord Atlas, http://mousespinal.brain-map.org/. .
24. Mishra SK and Hoon MA. The cells and circuitry for itch responses in mice. *Science* 2013; 340: 968–971.
25. Gutierrez-Mecinas M, Furuta T, Watanabe M, et al. A quantitative study of neurochemically-defined excitatory interneuron populations in laminae I-III of the mouse spinal cord. *Mol Pain* 2016. DOI: 10.1177/1744806916629065.
26. Hoon MA. Molecular dissection of itch. *Curr Opin Neurobiol* 2015; 34C: 61–66.
27. Hunt SP, Pini A and Evan G. Induction of c-fos-like protein in spinal cord neurons following sensory stimulation. *Nature* 1987; 328: 632–634.
28. Akiyama T, Curtis E, Nguyen T, et al. Anatomical evidence of pruriceptive trigeminothalamic and trigeminoparabrachial projection neurons in mice. *J Comp Neurol* 2016; 524: 244–256.
29. Nojima H, Carstens MI and Carstens E. c-fos expression in superficial dorsal horn of cervical spinal cord associated with spontaneous scratching in rats with dry skin. *Neurosci Lett* 2003; 347: 62–64.
30. Han L, Ma C, Liu Q, et al. A subpopulation of nociceptors specifically linked to itch. *Nat Neurosci* 2013; 16: 174–182.
31. Nakano T, Andoh T, Lee JB, et al. Different dorsal horn neurons responding to histamine and allergic itch stimuli. *Neuroreport* 2008; 19: 723–726.
32. Yao GL, Tohyama M and Senba E. Histamine-caused itch induces Fos-like immunoreactivity in dorsal horn neurons: effect of morphine pretreatment. *Brain Res* 1992; 599: 333–337.
33. Ji RR, Baba H, Brenner GJ, et al. Nociceptive-specific activation of ERK in spinal neurons contributes to pain hypersensitivity. *Nat Neurosci* 1999; 2: 1114–1119.
34. Zhang L, Jiang GY, Song NJ, et al. Extracellular signal-regulated kinase (ERK) activation is required for itch sensation in the spinal cord. *Mol Brain* 2014; 7: 25.
35. Polgar E, Sardella TC, Tiong SY, et al. Functional differences between neurochemically defined populations of inhibitory interneurons in the rat spinal dorsal horn. *Pain* 2013; 154: 2606–2615.
36. Guillery RW. On counting and counting errors. *J Comp Neurol* 2002; 447: 1–7.
37. Cameron D, Gutierrez-Mecinas M, Gomez-Lima M, et al. The organisation of spinoparabrachial neurons in the mouse. *Pain* 2015; 156: 2061–2071.
38. Polgár E, Campbell AD, MacIntyre LM, et al. Phosphorylation of ERK in neurokinin 1 receptor-expressing neurons in laminae III and IV of the rat spinal dorsal horn following noxious stimulation. *Mol Pain* 2007; 3: 4.
39. Mullen RJ, Buck CR and Smith AM. NeuN, a neuronal specific nuclear protein in vertebrates. *Development* 1992; 116: 201–211.
40. Todd AJ, Spike RC and Polgar E. A quantitative study of neurons which express neurokinin-1 or somatostatin sst2a receptor in rat spinal dorsal horn. *Neuroscience* 1998; 85: 459–473.
41. McDonald JH. *Handbook of biological statistics*, 3rd ed. Baltimore, MD: Sparky House Publishing, 2014.
42. Takahashi Y, Chiba T, Kurokawa M, et al. Dermatomes and the central organization of dermatomes and body surface regions in the spinal cord dorsal horn in rats. *J Comp Neurol* 2003; 462: 29–41.
43. Akiyama T, Curtis E, Nguyen T, et al. Anatomical evidence of pruriceptive trigeminothalamic and trigeminoparabrachial projection neurons in mice. *J Comp Neurol* 2016; 524: 244–256.

44. Akiyama T, Merrill AW, Zanotto K, et al. Scratching behavior and Fos expression in superficial dorsal horn elicited by protease-activated receptor agonists and other itch mediators in mice. *J Pharmacol Exp Ther* 2009; 329: 945–951.
45. Hamada R, Seike M, Kamijima R, et al. Neuronal conditions of spinal cord in dermatitis are improved by olopatadine. *Eur J Pharmacol* 2006; 547: 45–51.
46. Han N, Zu JY and Chai J. Spinal bombesin-recognized neurones mediate more nonhistaminergic than histaminergic sensation of itch in mice. *Clin Exp Dermatol* 2012; 37: 290–295.
47. Inan S, Dun NJ and Cowan A. Inhibitory effect of lidocaine on pain and itch using formalin-induced nociception and 5'-guanidinonaltrindole-induced scratching models in mice: behavioral and neuroanatomical evidence. *Eur J Pharmacol* 2009; 616: 141–146.
48. Lieu T, Jayaweera G, Zhao P, et al. The bile acid receptor TGR5 activates the TRPA1 channel to induce itch in mice. *Gastroenterology* 2014; 147: 1417–1428.
49. Nojima H, Cuellar JM, Simons CT, et al. Spinal c-fos expression associated with spontaneous biting in a mouse model of dry skin pruritus. *Neurosci Lett* 2004; 361: 79–82.
50. Nojima H, Simons CT, Cuellar JM, et al. Opioid modulation of scratching and spinal c-fos expression evoked by intradermal serotonin. *J Neurosci* 2003; 23: 10784–10790.
51. Kawasaki Y, Kohno T, Zhuang ZY, et al. Ionotropic and metabotropic receptors, protein kinase A, protein kinase C, and Src contribute to C-fiber-induced ERK activation and cAMP response element-binding protein phosphorylation in dorsal horn neurons, leading to central sensitization. *J Neurosci* 2004; 24: 8310–8321.
52. Akiyama T, Nagamine M, Carstens MI, et al. Behavioral model of itch, alloknesis, pain and allodynia in the lower hindlimb and correlative responses of lumbar dorsal horn neurons in the mouse. *Neuroscience* 2014; 266: 38–46.
53. Akiyama T, Nguyen T, Curtis E, et al. A central role for spinal dorsal horn neurons that express neurokinin-1 receptors in chronic itch. *Pain* 2015; 156: 1240–1246.
54. Ramos-Alvarez I, Moreno P, Mantey SA, et al. Insights into bombesin receptors and ligands: highlighting recent advances. *Peptides* 2015; 72: 128–144.

3 Paper II

Dickie, A.C., **Bell, A.M.,** Iwagaki, N., Polgár, E., Gutierrez-Mecinas, M., Kelly, R., Lyon, H., Turnbull, K., West, S.J., Etlin, A., Braz, J., Watanabe, M., Bennett, D.L.H., Basbaum, A.I., Riddell, J.S., Todd, A.J., 2019. Morphological and functional properties distinguish the substance P and gastrin-releasing peptide subsets of excitatory interneuron in the spinal cord dorsal horn. Pain 160, 442–462.

CRediT statement

Conceptualization, A.J.T., J.S.R., A.M.B. and A.C.D; Methodology, A.J.T.; Formal analysis, A.C.D. and A.M.B.; Investigation, A.C.D., A.M.B., N.I., E.P., M.G.M., R.K., H.L., K.T., S.J.W., A.E. and J.B.; Resources, M.W.; Writing – Original Draft, A.C.D., A.M.B. and A.J.T.; Writing – Review & Editing, A.C.D., A.M.B., N.I., E.P., M.G.M., D.L.H.B., A.I.B., J.S.R. and A.J.T.; Visualization, A.C.D., A.M.B., M.G.M. and A.J.T.; Supervision, A.J.T., A.M.B., M.G.M. and E.P.; Funding Acquisition, A.J.T.

Summary of practical involvement in components of study

Immunohistochemical characterisation of GRP-EGFP somatotopy – A.M.B. primary role.
In situ hybridisation experiments – S.J.W. & J.B. primary role – A.M.B. secondary role.
Neuronal reconstructions of GRP-EGFP cells – A.M.B. primary role.
Neuronal reconstructions of SP cells – A.M.B. primary role and supervisory role (some reconstructions performed by R.K., H.L, and K.T under supervision).
Morphology data analysis – A.M.B. primary role.
pERK response studies – A.M.B. primary role.
CTb tracing studies – E.P. and M.G.M. primary practical roles, A.M.B secondary role (analysis)
All electrophysiology experiments – A.C.D., N.I. and A.E. primary roles. A.M.B. no significant involvement.

Research Paper

PAIN®

OPEN

Morphological and functional properties distinguish the substance P and gastrin-releasing peptide subsets of excitatory interneuron in the spinal cord dorsal horn

Allen C. Dickie[a], Andrew M. Bell[a], Noboru Iwagaki[a], Erika Polgár[a], Maria Gutierrez-Mecinas[a], Rosalind Kelly[a], Heather Lyon[a], Kirsten Turnbull[a], Steven J. West[b], Alexander Etlin[c], Joao Braz[c], Masahiko Watanabe[d], David L.H. Bennett[b], Allan I. Basbaum[c], John S. Riddell[a], Andrew J. Todd[a,*]

Abstract

Excitatory interneurons account for the majority of neurons in the superficial dorsal horn, but despite their presumed contribution to pain and itch, there is still limited information about their organisation and function. We recently identified 2 populations of excitatory interneuron defined by expression of gastrin-releasing peptide (GRP) or substance P (SP). Here, we demonstrate that these cells show major differences in their morphological, electrophysiological, and pharmacological properties. Based on their somatodendritic morphology and firing patterns, we propose that the SP cells correspond to radial cells, which generally show delayed firing. By contrast, most GRP cells show transient or single-spike firing, and many are likely to correspond to the so-called transient central cells. Unlike the SP cells, few of the GRP cells had long propriospinal projections, suggesting that they are involved primarily in local processing. The 2 populations also differed in responses to neuromodulators, with most SP cells, but few GRP cells, responding to noradrenaline and 5-HT; the converse was true for responses to the μ-opioid agonist DAMGO. Although a recent study suggested that GRP cells are innervated by nociceptors and are strongly activated by noxious stimuli, we found that very few GRP cells receive direct synaptic input from TRPV1-expressing afferents, and that they seldom phosphorylate extracellular signal–regulated kinases in response to noxious stimuli. These findings indicate that the SP and GRP cells differentially process somatosensory information.

Keywords: Glutamatergic interneuron, Radial cell, Central cell, GRP, Pain

1. Introduction

The superficial laminae (I-II) of the spinal dorsal horn are the main target for nociceptive and pruriceptive primary afferents. Consequently, neurons within this region are involved in transmitting and modulating signals perceived as pain and itch. Although some of these cells project to the brain, most (~99%) are interneurons.[1,8,65] Although early models emphasised the importance of inhibitory interneurons in gating nociceptive inputs,[45] the majority of interneurons in these laminae are glutamatergic excitatory cells,[66] and these are both functionally and morphologically heterogeneous.[22,49,56,71,73] Recent studies demonstrated that the excitatory interneurons are essential for normal perception of pain and itch, and suggested that particular subgroups process distinct sensory modalities.[16,69] It is therefore important to define functional populations among these cells.

Among the morphologically distinct classes of excitatory interneurons are vertical cells, which have ventrally directed dendrites; radial cells, which have compact, highly branched dendritic trees; and central cells, which have rostrocaudally orientated dendrites. These differ in physiological properties[22,71] and may therefore correspond to functional populations. However, many excitatory interneurons cannot be assigned to a particular morphological class,[73] and we have developed an alternative classification scheme based on the largely non-overlapping expression of 4 neuropeptides: neurotensin, neurokinin B (NKB), gastrin-releasing peptide (GRP), and substance P (SP).[23,24] Together, these account for over half of the excitatory interneurons in laminae I and II. Neurotensin and NKB neurons are concentrated in inner lamina II (IIi), and overlap extensively

Sponsorships or competing interests that may be relevant to content are disclosed at the end of this article.

A.C. Dickie, A.M. Bell, and N. Iwagaki contributed equally to this work.

[a] Spinal Cord Group, Institute of Neuroscience and Psychology, College of Medical, Veterinary and Life Sciences, University of Glasgow, Glasgow, United Kingdom, [b] The Nuffield Department of Clinical Neurosciences, University of Oxford, John Radcliffe Hospital, Oxford, United Kingdom, [c] Department of Anatomy, University of California, San Francisco, San Francisco, CA, United States, [d] Department of Anatomy, Hokkaido University School of Medicine, Sapporo, Japan

**Corresponding author. Address: Spinal Cord Group, Institute of Neuroscience and Psychology, College of Medical Veterinary and Life Sciences, University of Glasgow, West Medical Building, University Ave, Glasgow G12 8QQ, United Kingdom. Tel.: (+44) 141 330 5868; fax: (+44) 141 330 2868. E-mail address: andrew.todd@glasgow.ac.uk (A.J. Todd).*

Supplemental digital content is available for this article. Direct URL citations appear in the printed text and are provided in the HTML and PDF versions of this article on the journal's Web site (www.painjournalonline.com).

PAIN 160 (2019) 442–462

http://dx.doi.org/10.1097/j.pain.0000000000001406

with cells expressing protein kinase Cγ (PKCγ). Gastrin-releasing peptide–expressing neurons are found throughout lamina II and can been identified in a GRP::eGFP BAC transgenic mouse.[57] Gastrin-releasing peptide cells have attracted particular interest because of their contribution to itch.[46,60] Gastrin-releasing peptide released from these cells targets the GRP receptor (GRPR), which is expressed by a different population of excitatory interneurons in lamina I and outer lamina II (IIo).[61,62] Gastrin-releasing peptide cells are innervated by pruriceptive afferents that express MrgA3, a receptor for the pruritogen chloroquine,[60] and are believed to act as "secondary pruriceptors" in a pathway linking pruriceptive afferents to GRPR-expressing interneurons,[46] which innervate lamina I projection neurons. Substance P is cleaved from a precursor, preprotachykinin A (PPTA) coded by *Tac1*, and SP-expressing neurons can be identified by intraspinal injection of adeno-associated viruses (AAVs) containing Cre-dependent expression cassettes into mice in which Cre-recombinase is knocked into the *Tac1* locus (Tac1^{Cre}). Using this approach, we found that SP-expressing cells are located mainly in lamina IIo, somewhat dorsal to GRP cells, although the populations show some spatial overlap.[23] Although SP-expressing neurons include some projection neurons and inhibitory cells, the great majority are excitatory interneurons.[23,25]

Despite the nonoverlapping expression pattern of these neuropeptides, we cannot be certain that GRP and SP cells represent distinct functional populations. Here, we used a variety of techniques to characterise and compare GRP- and SP-expressing neurons in the mouse superficial dorsal horn. We find that these 2 populations differ widely in anatomical, electrophysiological, and pharmacological properties, suggesting that they represent distinct populations that are likely to contribute differentially to somatosensory processing.

2. Methods

Experiments were approved by the Ethical Review Process Applications Panel of the University of Glasgow and were performed in accordance with the UK Animals (Scientific Procedures) Act 1986 and the University of California, San Francisco's Institutional Animal Care and Use Committee guidelines.

2.1. Animals

We used 2 genetically modified mouse strains: a BAC transgenic Tg(GRP-EGFP) from GENSAT in which GFP is expressed under control of the GRP promoter,[19,26,46,57] and a line in which Cre-recombinase is inserted into the *Tac1* locus (Tac1-IRES2-Cre-D; Jackson Laboratory, Bar Harbor, ME; Stock number 021877).[28] These lines are referred to as GRP::eGFP and Tac1^{Cre}, respectively. GRP::eGFP mice were maintained as heterozygotes, whereas most of the Tac1^{Cre} mice were homozygous. Both strains were maintained on a C57BL/6 background. For some experiments, the 2 lines were crossed to produce double transgenic mice (Tac1^{Cre};GRP::eGFP). Unless otherwise stated, mice of either sex weighing between 14 and 28 g were used in all parts of the study. Most of the mice that were used for anatomical studies underwent perfusion fixation. They were deeply anaesthetised with pentobarbitone (20 mg, intraperitoneally [i.p.]) and perfused through the heart with a fixative that contained 4% freshly depolymerised formaldehyde in phosphate buffer. Spinal cord tissue was rapidly dissected out and postfixed at 4°C for 2 hours (unless stated otherwise).

2.2. Intraspinal injection

Intraspinal injections were performed to deliver viral vectors coding for Cre-dependent constructs into Tac1^{Cre} or Tac1^{Cre};GRP::eGFP mice, and to deliver the retrograde tracer cholera toxin B (CTb) subunit into GRP::eGFP mice. **Table 1** lists the viral vectors used. To identify SP cells, we used AAVs coding for Cre-dependent eGFP or tdTomato, and to investigate the somatodendritic morphology of these cells, we used AAV-Brainbow vectors.[9] The injections used a modification of the method of Foster et al.[17] as described previously.[23] The mice were anaesthetised with 1% to 2% isoflurane and placed in a stereotaxic frame. For the experiments involving AAVs, 2 injections were made in each animal, either into the L3 and L5 segments on one side, or else bilaterally into either the L3 or L5 segments. The vertebral column was exposed, and vertebral clamps were attached to the T12 and L1 vertebrae. The space between the laminae of T12 and T13 was used for L3 injections and that between laminae of T13 and L1 for L5 injections. In each case, a small incision was made in the dura to the side of the midline, and injections were made through glass micropipettes (inner diameter of tip 40 μm) into the spinal dorsal horn. Injections were made 300 to 500 μm lateral to the midline at a depth of 300 μm below the pial surface and were administered at a rate of 30 nL/minute. The wound was then closed, and animals were allowed to recover with appropriate analgesia (buprenorphine 0.3 mg/kg and carprofen 5 mg/kg). Injections of CTb into the GRP::eGFP mice were targeted on the T13 spinal segment. These injections were performed as described above, except that they were made through the space between the laminae of T11 and T12 vertebrae.[25] In each case, a single injection (300 nL of 1% CTb) was made into the dorsal horn on the right side, and the animals survived for 4 days before perfusion fixation.[25]

2.3. General features of immunocytochemistry and characterisation of antibodies

Multiple labelling immunofluorescence microscopy was performed as described previously.[23] **Table 2** lists the sources and concentrations of the antibodies used. Briefly, spinal cord segments were cut into 60-μm-thick transverse or parasagittal sections with a vibrating blade microtome (Leica VT1200, Leica Microsystems (UK) Ltd, Milton Keynes, United Kingdom), and these were treated with 50% ethanol for 30 minutes to enhance antibody penetration. Sections were incubated for 3 days at 4°C in mixtures of primary antibodies and then overnight in mixtures of species-specific secondary antibodies that were raised in donkey. The secondary antibodies were conjugated to Alexa 488, Alexa 647, Rhodamine Red, Pacific Blue, or biotin (Jackson ImmunoResearch, West Grove, PA) and were used at 1:500 (Alexa 488, Alexa 647, and biotin), 1:200 (Pacific Blue), or 1:100 (Rhodamine Red). Biotinylated secondary antibodies were detected with a tyramide signal-amplification method (TSA kit tetramethylrhodamine NL702; PerkinElmer Life Sciences, Boston, MA) as described previously.[24] After immunoreaction, the sections were mounted in antifade medium and stored at −20°C. Unless otherwise stated, sections were scanned with a Zeiss LSM710 confocal microscope equipped with Argon multi-line, 405 nm diode, 561 nm solid state, and 633 nm HeNe lasers. In all cases, the confocal aperture was set to 1 Airy unit or less.

The CTb antibody was raised against the purified protein, and specificity is demonstrated by the lack of staining in regions that did not contain injected or transported tracer. The chicken and rabbit antibodies against GFP were raised against recombinant

Table 1

Adeno-associated virus vectors.

	Serotype	Promoter	Construct	Details of injection	
				No. of GCs	Volume
AAV.flex.tdTom	AAV1	CAG	tdTomato	5-18 × 10^8	300 nL
AAV.flex.eGFP	AAV1	CAG	eGFP	8.6-17.2 × 10^9	300 nL
AAV.Brainbow1	AAV9	hEF1a	eYFP and TagBFP	7.6-18.9 × 10^7	500 nL
AAV.Brainbow2	AAV9	hEF1a	TFP and mCherry	7.4-18.6 × 10^7	500 nL

All AAV vectors were obtained from Penn Vector Core (Philadelphia, PA).
AAV, adeno-associated virus; eYFP, enhanced yellow fluorescent protein; GC, gene copies; TagBFP, tag blue fluorescent protein; TFP, teal fluorescent protein.

full-length eGFP, and the staining matches that of native GFP fluorescence. The PKCγ antibodies, which were raised against amino acids 648 to 697 of the mouse protein, detect a single band at 75 kDa in tissue from wild-type (but not PKCγ$^{-/-}$) mice, and the guinea pig antibody stains identical structures to those detected by a well-characterised rabbit antibody.[52,74] The VGLUT3 antibody was raised against amino acids 522 to 588 of the mouse protein and detects a single band at 60 to 62 kDa. The mouse monoclonal NeuN antibody was raised against cell nuclei extracted from the mouse brain and found to react with a protein specific for neurons,[47] which has subsequently been identified as the splicing factor Fox-3.[36] The guinea pig antibody was raised against a recombinant protein consisting of amino acids 1 to 97 of Fox-3 and immunostains the same cells as the mouse antibody. The mCherry antibody was raised against a full-length recombinant protein, whereas the teal fluorescent protein (TFP) and tagRFP antibodies were raised against the corresponding purified proteins. Their specificity is demonstrated by the lack of staining in tissue that lacks these fluorescent proteins. The Pax2 antibody is directed against amino acids 188 to 385 of the mouse protein and recognizes bands of the appropriate size on Western blots of the mouse embryonic kidney.[15] The phosphorylated extracellular signal–regulated kinase (pERK) antibody detects p44 and p42 MAP kinase (Erk1 and Erk2) when these are phosphorylated either individually or dually at Thr202 and Tyr204 of Erk1 or Thr185 and Tyr187 of Erk2. This antibody does not cross-react with the corresponding phosphorylated residues of JNK/SAPK or of p38 MAP kinase, or with non-phosphorylated Erk1/2 (manufacturer's specification). Specificity is demonstrated by the lack of staining in nonstimulated areas (eg, in the contralateral dorsal horn).

2.4. Distribution of gastrin-releasing peptide::eGFP cells and their relation to gastrin-releasing peptide mRNA

To assess differences in the distribution of GRP-eGFP cells in different regions of the lumbar spinal cord, we examined the lateral and medial regions of the superficial dorsal horn in the L1 and L4 segments using immunostained sections. These segments were chosen because they differ in the extent to which they receive input from glabrous skin,[30] and preliminary observations indicated that GFP$^+$ cells were less numerous in glabrous skin territory. Scans were analysed with Neurolucida for Confocal (MBF Bioscience, Williston, VT). We used a modification[48] of the disector method[59] to quantify the proportion of all neurons that were GFP-positive in sections from 3 perfusion-fixed GRP::eGFP mice. These sections had been immunoreacted to reveal GFP (chicken antibody), VGLUT3, and NeuN (mouse antibody), and counterstained with 4′,6-diamidino-2-phenylindole (DAPI). Three sections from the L1 and L4 segments of each mouse were scanned with the confocal microscope through a 40× oil-immersion lens (numerical aperture 1.3) to include the entire

Table 2

Antibodies.

Antibody	Species	Dilution	Source	Catalogue #
CTb	Goat	1:200,000	List Biological	703
GFP	Chicken	1:1000	Abcam	ab13970
GFP	Rabbit	1:200-500	M Watanabe	
PKCγ	Goat	1:200	M Watanabe	
PKCγ	Guinea pig	1:500	M Watanabe	
VGLUT3	Guinea pig	1:10,000-20,000*	M Watanabe	
NeuN	Mouse	1:500	Millipore	MAB377
NeuN	Guinea pig	1:500	Synaptic Systems	266 004
mCherry	Chicken	1:5000	Abcam	ab205402
mTFP	Rat	1:500	Kerafast	EMU103
tagRFP	Guinea pig	1:500	Kerafast	EMU107
Pax2	Rabbit	1:1000	Life Technologies	716000
pERK	Rabbit	1:500	Cell Signaling Technology	9101

* Used with the tyramide signal-amplification method.
CTb, cholera toxin B; pERK, phosphorylated extracellular signal–regulated kinase; TFP, teal fluorescent protein.

mediolateral extent of the dorsal horn through the whole depth of the section (2-μm z-spacing). The reference and look-up sections were placed 20 μm apart, and all optical sections between these were carefully examined. All neuronal nuclei (defined by the presence of NeuN and DAPI) with their bottom surface between the reference and look-up sections were identified and plotted onto an outline of the dorsal horn. The channel corresponding to GFP was then viewed, and the presence or absence of immunoreactivity was noted for each selected neuron. Scans from L4 were divided into medial and lateral compartments based on the pattern of VGLUT3 immunoreactivity, which is expressed by C–low-threshold mechanoreceptors that are restricted to the lateral "hairy skin" region.[38,54] Because the whole of the L1 segment is innervated from hairy skin, we divided the dorsal horn into medial and lateral halves in this segment.

In situ hybridisation was used to examine the relationship between GRP mRNA and GFP in the L4 and L5 segments from 3 perfusion-fixed GRP::eGFP mice. Tissue from these mice was postfixed for 4 to 12 hours, cryoprotected in 30% sucrose, embedded in optimal cutting temperature mounting medium, and stored at −80°C. Transverse sections (12-μm thick) were cut with a cryostat, mounted onto SuperFrost Plus slides (48311-703, VWR), and air dried. The RNAscope procedure was performed according to the supplied protocol. Briefly, tissue was incubated in peroxide solution, dehydrated in 100% ethanol, and reacted with protease in aqueous buffer. The RNAscope probe against GRP (Mm-GRP, 317861, RNAscope, Bio-Techne, Abingdon, United Kingdom) and a negative control probe were incubated with tissue sections at 40°C for 2 hours, followed by washing in RNAscope wash buffer and a series of incubations in amplification buffers (1-6, 15-30 minutes at 40°C—room temperature), and finally detected using the Red Assay kit (322360; RNAscope). Sections were then incubated for 24 hours at room temperature in GFP antibody (rabbit), and then in secondary antibody conjugated to Alexa 488. They were then counterstained with DAPI and mounted in antifade medium. Sections were scanned with a Zeiss LSM 700 laser-scanning confocal microscope. The images were acquired by scanning a single optical plane through the centre of the section depth with a 40× oil-immersion lens (numerical aperture 1.3), to include both dorsal horns for each section.

Cells that were positive for GRP mRNA and GFP were quantified manually in ImageJ by using the Cell Counter Plugin. Cells in laminae I and II of the dorsal horn were counted, and a minimum of 3 sections were assessed per animal. The dorsal horn was divided into medial glabrous and lateral hairy skin innervation territories, defined by the intense plexus of GFP labelling seen in hairy skin territory in the GRP:eGFP mice (see below). Initially, the mRNA channel was examined, and cell bodies (defined by DAPI labelling) that contained 3 or more intense mRNA puncta were counted. Next, the GFP labelling was viewed to reveal the proportion of GFP cells that were positive for GRP mRNA. Finally, the number of GFP-positive cells that lacked GRP mRNA was determined. Images were assessed against the negative control probe, which did not show any specific or intense in situ hybridisation product.

2.5. Relationship between gastrin-releasing peptide– and substance P–expressing cells

To determine the extent of overlap between GRP::eGFP and SP populations, we injected AAV coding for a Cre-dependent form of tdTomato (AAV.flex.tdTom) into 2 $Tac1^{Cre}$;GRP::eGFP male mice. The virus encodes an inverted sequence for tdTomato between pairs of heterotypic LoxP sites with antiparallel orientation,[4] resulting in expression of tdTomato only in transfected cells that contain Cre. After a 2-week survival period, the mice were reanaesthetised and perfused with fixative. Sections through the injection site of both mice were immunostained with antibodies against GFP (rabbit) and PKCγ (goat), and 2 sections containing numerous $tdTom^+$ cells were selected and scanned with the confocal microscope. The scans were analysed with Neurolucida. Initially, the channel corresponding to tdTom was viewed, and all labelled cells were plotted onto an outline of the superficial dorsal horn (laminae I and II). The other 2 channels were then viewed, and the presence or absence of GFP and PKCγ was noted for each tdTom cell. Any additional cells that were GFP^+ and/or $PKC\gamma^+$ were then added to the drawing. Although a stereological method was not used in this part of the study, the low level of double labelling for tdTom and GFP (see below) is unlikely to have been affected by sampling bias. We have previously shown that after intraspinal injection of AAV coding for a Cre-dependent form of eGFP into $Tac1^{Cre}$ mice, virtually all the cells near the injection site that are immunoreactive for the SP precursor PPTA are GFP-positive, indicating that this procedure captures a high proportion of SP-expressing cells.[23] We have also reported that it results in GFP labelling of ~20% of neurons in the superficial dorsal horn within 4 days of the injection, and that this percentage does not change when animals are allowed to survive for 8 days after the spinal injection,[25] suggesting that a stable expression pattern is reached very soon after the injection.

To compare expression of SP with the distribution of GRP mRNA, we injected AAV.flex.eGFP into 3 male $Tac1^{Cre}$ mice. One or 2 weeks later, the mice were reanaesthetised and fixed by perfusion. Tissue from these mice was processed with in situ hybridisation histochemistry to reveal GRP mRNA and GFP. Both the tissue processing and analysis were performed as described above.

To provide further evidence about the extent of coexpression of SP and GRP, we performed double-label fluorescence in situ hybridisation on tissue from 4 adult wild-type (C57Bl/6) mice, using RNAscope probes against mRNAs for GRP and substance P. The reaction was performed on 12-μm-thick cryostat sections from C4 to C6 segments (from 3 mice) and the L3 to L5 segment (from one mouse) according to the supplied protocol. Sections were counterstained with DAPI to allow for identification of cell nuclei. Single RNA transcripts for each target gene appeared as punctate dots (usually around the DAPI-stained nucleus), and we considered a cell to be positive if it contained more than 5 dots. Quantification was performed on a series of spinal cord sections (1 in every 4) from 3 separate animals. We analysed between 5 and 8 sections per animal. Only positive cells containing a DAPI-stained nucleus in the dorsal horn (laminae I-V) were included in the analysis. The percentage of double-labeled cells was calculated by dividing the number of double-labeled neurons by the number of single-labeled neurons for each probe.

2.6. Slice preparation and electrophysiology

Electrophysiological recordings from both SP and GRP neurons were performed on spinal cord slices. For those involving SP neurons, we used $Tac1^{Cre}$ mice that had received intraspinal injection of either AAV.flex.eGFP or AAV.flex.tdTom between 1 and 3 weeks previously. Spinal cord slices were obtained from 40 injected $Tac1^{Cre}$ mice and from 105 GRP::eGFP mice aged 4 to 10 weeks old, as described previously.[14,34] The spinal cord was removed either after laminectomy performed under isoflurane

anaesthesia or in ice-cold dissection solution after decapitation of the mice under brief isoflurane or tribromoethanol anaesthesia. Mice from which the cord was removed under anaesthesia were decapitated immediately afterwards. Parasagittal (300-500 μm), transverse (400-600 μm), or horizontal (400 μm) slices from the lumbar spinal cord were cut with a vibrating blade microtome and allowed to recover in recording or modified dissection solution for at least 30 minutes at room temperature.[14,34] In some cases, the slices were placed in an NaCl-based recovery solution or an *N*-methyl-D-glucamine (NMDG)-based recovery solution[64] at 32°C for 15 minutes before being placed in recording solution at room temperature. The solutions used contained the following (in mM): dissection, 3.0 KCl, 1.2 NaH_2PO_4, 0.5 to 2.4 $CaCl_2$, 1.3 to 7.0 $MgCl_2$, 26.0 $NaHCO_3$, 15.0 to 25.0 glucose, and 240.0 to 251.6 sucrose; modified dissection, 3.0 KCl, 1.2 NaH_2PO_4, 0.5 $CaCl_2$, 1.3 $MgCl_2$, 8.7 $MgSO_4$, 26.0 $NaHCO_3$, 20.0 HEPES, 25.0 glucose, and 215.0 sucrose, with or without 1.0 kynurenic acid; NaCl recovery solution, 125.0 NaCl, 2.5 KCl, 1.25 NaH_2PO_4, 1.5 $CaCl_2$, 6.0 $MgCl_2$, 26.0 $NaHCO_3$, and 25.0 glucose; NMDG recovery solution, 93.0 NMDG, 2.5 KCl, 1.2 NaH_2PO_4, 0.5 $CaCl_2$, 10.0 $MgSO_4$, 30.0 $NaHCO_3$, 25.0 glucose, 5.0 Na-ascorbate, 2.0 thiourea, 3.0 Na-pyruvate, and 20.0 HEPES; and recording, 125.0 to 127.0 NaCl, 2.5 to 3.0 KCl, 1.2 to 1.25 NaH_2PO_4, 2.0 to 2.4 $CaCl_2$, 1.0 to 1.3 $MgCl_2$, 26.0 $NaHCO_3$, and 15.0 to 25.0 glucose. In some cases, dissection was performed in NaCl recovery solution with 1 mM kynurenic acid. All solutions were bubbled with 95% O_2/5% CO_2.

Targeted whole-cell patch-clamp recordings were made from GFP-positive cells (slices from GRP::eGFP mice or $Tac1^{Cre}$ mice with AAV.Flex.eGFP injection) or tdTomato-positive cells ($Tac1^{Cre}$ mice with AAV.Flex.tdTom injection) in the superficial dorsal horn, using patch pipettes that had a typical resistance of 3 to 7 MΩ when filled with an intracellular solution containing (in mM): 130.0 K-gluconate, 10.0 KCl, 2.0 $MgCl_2$, 10.0 HEPES, 0.5 EGTA, 2.0 ATP-Na_2, 0.5 GTP-Na, and 0.2% Neurobiotin, pH adjusted to 7.3 with 1.0M KOH. In some cases, the pipette solution contained (in mM): 120.0 K-methanesulphonate, 10.0 NaCl, 1.0 $CaCl_2$, 10.0 HEPES, 10 EGTA, 5.0 ATP-Mg, and 0.5 GTP-Na. Data were recorded and acquired with a Multiclamp 700B amplifier and pClamp 10 software (both Molecular Devices), and were filtered at 4 kHz and digitised at 10 kHz.

After achieving stable whole-cell configuration, the cells were voltage clamped at −60 mV, and a series of 100-millisecond voltage steps from −70 to −50 mV (2.5 mV increments) delivered to determine the current–voltage relationship, which was used to calculate resting membrane potential and input resistance. Cells that had a resting membrane potential that was less negative than −30 mV were excluded from all analysis.

The action potential firing pattern was assessed in the current-clamp mode, in response to 1-second depolarising current steps of increasing amplitude, from a membrane potential of around −60 mV. Firing patterns were classified on the basis of previously published criteria.[18,20,22,51,56,73] Cells were classed as tonic firing if they exhibited continuous action potential discharge throughout the depolarising step; transient if the action potential discharge occurred only during the early part of the step; delayed if there was a clear delay between the start of the depolarising step and the first action potential; single spike if only 1 or 2 action potentials occurred at the onset of the step; gap if there was a long first interspike interval; and reluctant if current injection did not result in action potential firing. It has recently been reported that reluctant firing may result from high levels of expression of both a low-threshold noninactivating potassium conductance and an inactivating (A-type) potassium conductance.[5]

Subthreshold voltage-activated currents were investigated by voltage clamping the cell at −60 mV before stepping to −90 mV for 1 second and then to −40 mV for 200 milliseconds, and automated leak subtraction was used to remove capacitive and leak currents.[21,56] This step protocol enables the identification of 2 types of transient outward current and 2 types of inward current.[21] The outward currents that occur during the depolarising step (−90 to −40 mV) are consistent with A-type potassium currents (I_A), and on the basis of their kinetics can be distinguished as rapid (I_{Ar}) or slow (I_{As}). A transient inward current can be observed during the depolarising step, which is considered to reflect the low-threshold "T-type" calcium current ($I_{ca,T}$). A slow inward current can occur during the hyperpolarisation step (−60 to −90 mV) that is consistent with the hyperpolarisation-activated (I_h) current. The amplitude of I_{Ar} was measured as the peak of the transient outward current. The amplitude of the I_h current was measured during the final 200 milliseconds of the hyperpolarising step, and inward currents were classified as I_h if the amplitude was greater than −5 pA.

Excitatory synaptic input to GRP-eGFP and SP neurons was assessed by recording spontaneous excitatory postsynaptic currents (sEPSCs) at a holding potential of −60 or −70 mV. The functional expression of TRP channels on the afferents providing synaptic input was investigated by voltage-clamping cells at −60 or −70 mV and recording sEPSCs or miniature EPSCs (mEPSCs), the latter in the presence of tetrodotoxin (TTX) (0.5 μM), bicuculline (10 μM), and strychnine (5 μM), before and during the bath application of the TRPV1 agonist capsaicin (2 μM) or the TRPM8 agonist icilin (20 μM; mEPSCs only). In the case of icilin application, the temperature of the bath was raised to 32°C.[18] These data were analysed using Mini Analysis (Synaptosoft), and sEPSC/mEPSC events were automatically detected by the software and were then rejected or accepted after visual examination. Neurons were considered to receive input from capsaicin- or icilin-sensitive afferents if capsaicin/icilin application resulted in a significant leftwards shift in the distribution of interevent intervals, indicating an increase in frequency. They were considered nonresponsive if this threshold was not reached.

The response of GRP-eGFP and SP cells to a number of pharmacological agents was investigated by voltage-clamping cells at −60 or −70 mV, and bath applying one of the following: 5-HT (10-20 μM), noradrenaline (NA) (20 μM), the μ-opioid receptor (MOR) agonist DAMGO (3 μM), the κ-opioid (KOR) agonist U69593 (1 μM), or the δ-opioid (DOR) agonist [D-Ala^2]-Deltorphin II (1 μM). Cells were considered responsive if drug application resulted in a clear slow outward current and nonresponsive if no current was seen.

All chemicals were obtained from Sigma except: TTX (Alomone, Jerusalem, Israel), bicuculline (Tocris, Abingdon, UK), and Neurobiotin (Vector Labs Peterborough, UK).

2.7. Morphological analysis of gastrin-releasing peptide and substance P cells

Reconstruction of the GRP neurons (n = 45) was performed on Neurobiotin-labelled cells that had been recorded in electrophysiological experiments. For the SP neurons (n = 31), analysis of cell bodies and dendritic trees was performed on tissue from mice that had been injected with Brainbow viruses.[9] In addition, a few Neurobiotin-labelled SP neurons (n = 12) from electrophysiological experiments were examined to allow for reconstruction of their local axonal arbors.

Processing to reveal Neurobiotin in patched cells was performed as described previously.[18,34] Briefly, fixed slices containing recorded cells were incubated in avidin-rhodamine (1:1000; Jackson ImmunoResearch) in phosphate-buffered saline containing 0.3% Triton X-100 and mounted on slides. In a few cases, recordings had been made from $Tac1^{Cre}$ mice that were injected with AAV.flex.tdTom, and in these cases, avidin-Alexa 488 was used instead of avidin-rhodamine. The sections were scanned with the confocal microscope through a 63× oil-immersion lens (numerical aperture 1.4) at 0.5-μm z-spacing. These scans included all the dendritic and axonal arbors that were visible at this stage. For each cell, the presence of GFP or tdTom was confirmed by scanning for the native protein. The dendritic and axonal arbors were reconstructed in Neurolucida. Axons could easily be distinguished from dendrites based on their thin nontapering profiles and the presence of irregularly spaced boutons. By contrast, dendrites showed progressive tapering and invariably gave rise to dendritic spines.[34] Slices were then resectioned at 60-μm thickness with the vibrating blade microtome, and sections were kept in a serial order. Sections were examined with the confocal microscope, and if additional parts of the dendritic or axonal tree located deep within the slice were found, these were added to the reconstruction. To determine laminar boundaries, we immunostained one section from each slice to reveal PKCγ, using a guinea pig antibody. PKCγ is present in a plexus of dendrites that occupies the inner half of lamina II (IIi).[31] The boundaries between laminae II/III were then added to the reconstructions, by aligning sections containing the recorded cells with nearby sections stained for PKCγ. The lamina I/II border was taken to be 20 μm below the dorsal white matter,[18] and this was also added to the reconstruction. To investigate the axonal morphology of SP neurons, we also reconstructed axonal arbors of 12 of these cells that had undergone whole-cell patch-clamp recording. These cells were processed, scanned, and analysed as described above, except that in this case, the PKCγ immunoreaction was performed on the intact slice.

Two $Tac1^{Cre}$ mice (one male and one female) received injections of 2 Brainbow AAV vectors.[9] One of these codes for enhanced yellow fluorescent protein and Tag blue fluorescent protein (TagBFP), and the other for TFP and mCherry. In both cases, the sequences are for farnesylated fluorescent proteins in reverse orientation between antiparallel LoxP sites. Cre-mediated recombination leads to random expression of one of the fluorescent proteins (or neither fluorescent protein) for each virus, and the presence of multiple copies of both viruses within cells results in a wide range of hues, resulting from varying amounts of each membrane-targeted fluorescent protein. Two weeks after the spinal injection, the mice were perfused with fixative, and tissue from these animals was used to investigate the morphology of SP-expressing neurons. Sagittal sections (60-μm thick) from the lumbar enlargement were reacted with antibodies against mCherry, mTFP, tagRFP (which recognises tagBFP), and Pax2, and these were revealed with secondary antibodies. Regions close to the injection site that contained numerous labelled cells were selected and scanned with the confocal microscope through the 63× lens at 0.5-μm z-spacing. Tile scans were obtained through the full thickness of the section to include approximately 400 μm along the rostrocaudal (RC) axis and the entire dorsoventral (DV) extent of laminae I and II. Thirty-one cells (15 and 16 from the 2 mice) were selected, based on the following criteria: (1) relatively strong staining for at least one of the fluorescent proteins; (2) location of the soma in the mid region of the z-axis, such that the entire dendritic tree was likely to be contained within the section; (3) the presence of a distinctive colour hue that contrasted with that of nearby labelled cells. Cell bodies and dendritic trees of SP neurons were drawn in Neurolucida by following colour-coded processes originating from the soma of the selected cells. Although this allowed for reconstruction of dendritic trees, it was not possible to follow axons beyond their initial segments, due to their very small diameter.

Morphometric data for dendritic trees of all the reconstructed cells were obtained from Neurolucida Explorer. The dendritic parameters extracted were the same as those used in our previous study.[18] To make an objective comparison between the GRP and SP cells, we performed cluster analysis using Ward's method,[70] as described previously.[18] To reduce the dimensionality of the original data while preserving variance, we calculated principal components from the data set.[13] The number of principal components to be retained for cluster analysis was then determined from a scree test.

2.8. Potential propriospinal projections of gastrin-releasing peptide–eGFP cells

Bice and Beal[7] reported that a proportion of neurons in the superficial dorsal horn have long propriospinal axons. We recently reported that around 40% of excitatory interneurons in laminae I and II of the mouse L5 segment have axons that project at least 5 segments rostrally, and that SP cells are overrepresented among the neurons with these propriospinal projections.[25] To determine whether GRP-expressing neurons also give rise to long propriospinal axons, we examined the L5 segments of 4 GRP::eGFP mice that had received injections of CTb into the T13 segment.

Injection sites were assessed by reacting transverse sections through T13 with an immunoperoxidase method.[10] The sections were incubated in anti-CTb at 1:200,000, followed by biotinylated secondary antibody and avidin-peroxidase, which was revealed with diaminobenzidine in the presence of H_2O_2. Transverse sections from the L5 segments were reacted with antibodies against CTb, NeuN (mouse or guinea pig), and GFP (chicken). These antibodies were detected with fluorescent secondary antibodies, and the sections were stained with DAPI. Four sections from each mouse were selected for analysis before the relationship between CTb and GFP was observed. The sections were scanned through the 40× oil-immersion lens to generate z-series (at least 20 optical sections at 1 μm z-separation) such that the entire cross-sectional area of the ipsilateral dorsal horn was included. The confocal scans were analysed with Neurolucida by using the modified disector method (see above). The reference and look-up sections were set 10 μm apart. Because the quantitative analysis was performed on laminae I and II, we first plotted the outline of the dorsal horn gray matter, and then located the lamina II/III border, based on the relatively low density of neurons in lamina IIi. The channels corresponding to NeuN and DAPI were initially viewed, and all neurons for which the bottom surface of the nucleus lay between the reference and look-up sections were marked on the drawing. The GFP and CTb channels were then examined, and for each of the selected neurons, the presence or absence of both GFP and CTb was determined. In this way, we determined the proportions of all lamina I/II neurons, and of GRP-eGFP neurons, in the L5 segment that were retrogradely labelled with CTb.

Because few GRP cells in L5 were retrogradely labelled from the T13/L1 injection site (see Results), a more limited analysis was also performed on sections from the L2 segment of 2 of these mice, to look for evidence of short intersegmental projections.

2.9. Phosphorylation of extracellular signal–regulated kinase after noxious and pruritic stimuli

We previously demonstrated that SP cells in laminae I and II often express the transcription factor Fos[32] or phosphorylate ERKs[35] in response to a variety of noxious and pruritic stimuli.[23] In addition, we reported that GRP cells seldom show pERK after injection of the pruritogen chloroquine.[6] Here, we used phosphorylation of ERK to test whether the GRP cells respond to other pruritic or to noxious stimuli.

Fifteen GRP::eGFP mice were used in these experiments (n = 3 mice per stimulus type). In all cases, stimuli involved the left calf (which had been shaved on the day before stimulation), because of the relatively low density of GRP-eGFP cells in regions of the dorsal horn that are innervated from glabrous skin (see below). Twelve of the mice received noxious stimuli or vehicle injection. These animals had been anaesthetised with urethane (40-80 mg i.p.), and the stimulus was applied 5 minutes before perfusion fixation. The stimuli were: (1) immersion of the leg up to the level of the knee in 52˚C water for 15 seconds (noxious heat); (2) pinching of 5 skin folds on the calf with forceps applied for 5 seconds at each site (pinch); (3) subcutaneous injection of capsaicin (10 μL) into the lateral surface of the calf (capsaicin); and (4) subcutaneous injection (10 μL) of the vehicle used to deliver capsaicin (vehicle). Capsaicin was initially prepared at 1% by dissolving in 7% Tween 80, 20% ethanol in saline, and then diluted to 0.25%. Three of the mice were anaesthetised with urethane and used to investigate phosphorylation of ERK after intradermal injection of histamine (100 μg/10 μL) into the lateral calf. The success of the intradermal injection was assessed by the formation of a small bleb in the calf skin.[50] To avoid detecting pERK that had resulted from the intradermal injection itself, in these cases, perfusion fixation was performed 30 minutes after the stimulus. We have previously shown that intradermal injection of vehicle (phosphate-buffered saline) causes ERK phosphorylation when animals are perfused with fixative 5 minutes after the injection. This presumably results from the noxious stimulus caused by insertion of the needle and distension of the skin.[6] By contrast, we found that injection of pruritogens, but not vehicle, resulted in pERK-immunoreactivity in neurons in laminae I and II when the mice were perfusion-fixed 30 minutes after the injection. This is likely to reflect the relatively prolonged activation of these cells by pruritogens.

The L3 spinal segment, which contains the great majority of cells activated by these stimuli, was cut into 60-μm-thick transverse sections, and these were reacted with antibodies against NeuN (mouse), GFP (chicken), and pERK. These markers were revealed with fluorescent secondary antibodies, and sections were stained with DAPI. Sections that contained numerous pERK-positive neurons were initially selected and scanned with the confocal microscope through the 40× oil-immersion lens, to generate z-stacks (2-μm z-separation) through the full thickness of the section so as to include the region that contained pERK cells. The z-stacks were analysed with Neurolucida. Initially, the outline of the gray matter was plotted, together with the ventral border of the GRP plexus (which corresponds approximately to the boundary between the inner and outer parts of lamina II). The mediolateral extent of the region that contained a high density of pERK cells was delineated by drawing 2 parallel lines that were orthogonal to the laminar boundaries. The channels corresponding to NeuN and DAPI were viewed, and the locations of all neurons that lay within this region were plotted onto the drawing. To avoid overcounting

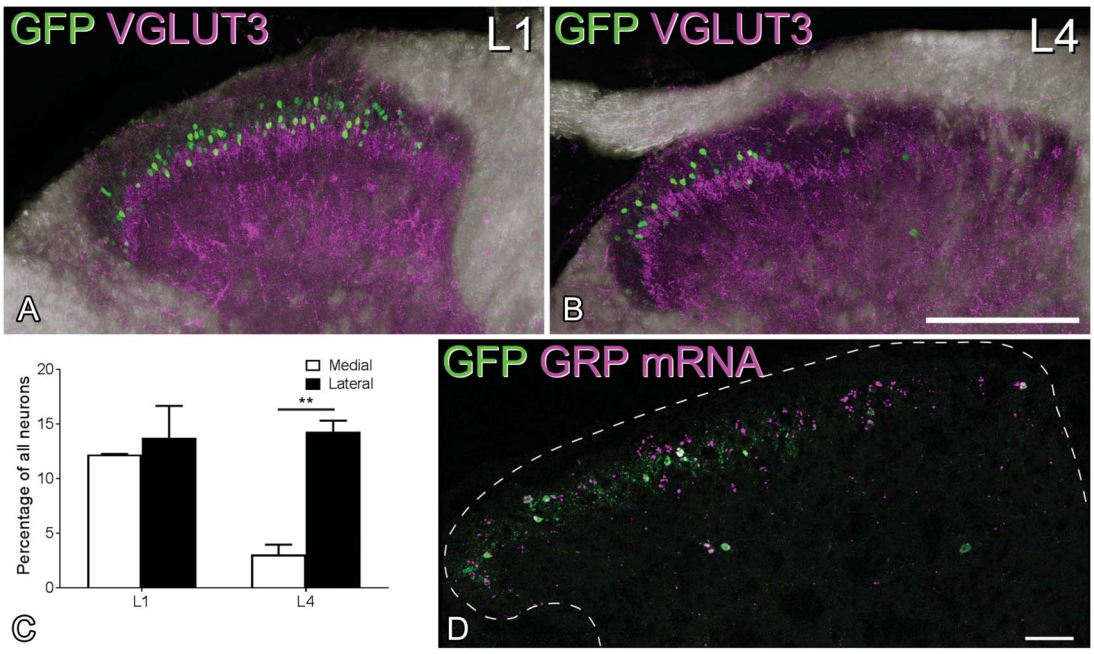

Figure 1. Differences in the mediolateral distribution of GFP and GRP mRNA in GRP::eGFP mice. (A and B) Immunostaining for GFP (green) and VGLUT3 (magenta) in the dorsal horn of GRP::eGFP mice in the L1 and L4 segments. A dense plexus of VGLUT3 staining is present in the inner part of lamina II, and this corresponds to the central terminals of C-LTMR afferents, which are associated with hairy skin. The plexus is evenly distributed across the L1 dorsal horn but is restricted to the lateral part in L4. The medial region, where the plexus is absent, is innervated from glabrous skin of the hind paw. Note that GFP^+ cells are largely restricted to those regions with hairy skin input. These images are projections from z-stacks through the full thickness of 60-μm sections. (C) Quantification of GFP^+ cells as a proportion of all neurons in the medial and lateral halves of the dorsal horn in L1 and the glabrous (medial) and hairy (lateral) territories in L4 (mean ± SD). ** denotes significant difference ($P<0.01$). (D) In situ hybridisation histochemistry on the L4 segment reveals that GRP mRNA (magenta) is present in many cells in the medial half of the dorsal horn, although there are very few GFP^+ (green) cells. The dashed line represents the gray matter–white matter border. Scale bars: (A and B) = 200 μm, (D) = 50 μm. C-LTMR, C–low-threshold mechanoreceptor; GRP, gastrin-releasing peptide.

neurons, we included them if at least part of the nucleus (stained with DAPI) was present in the first optical section of the z-series and excluded them if part of the nucleus was present in the last optical section.[2,58] The channel corresponding to pERK was then viewed, and the presence or absence of staining in each of the neurons in the sample was recorded. Finally, the GFP channel was viewed and all neurons that were GFP$^+$ were identified on the drawing. As pERK$^+$ cells were present at highest density in laminae I and IIo, we determined the proportion of all neurons that were located within this region and between the 2 parallel lines that were pERK-immunoreactive. We then determined the proportion of GFP$^+$ neurons within this volume that were pERK-immunoreactive.

2.10. Terminology

For convenience, we refer to cells that expressed fluorescent proteins after intraspinal injections of AAVs coding for Cre-dependent forms of these proteins into the Tac1^{Cre} mouse line as "substance P (SP) cells." Similarly, we refer to cells that were GFP-positive in the GRP::eGFP mouse as "GRP cells," although not all cells with GRP mRNA were GFP-positive in this line (see below).

2.11. Statistics

Two-way repeated-measures ANOVA with the *post hoc* Sidak test was used to determine whether there were significant differences in the proportions of neurons that were GFP$^+$ in medial and lateral parts of the dorsal horn at L1 and L4 in the GRP::eGFP mice and a *t* test was used to compare medial and lateral counts from in situ hybridisation data. Differences in electrophysiological properties between the GRP and SP cells were compared using Mann–Whitney *U* or Wilcoxon signed-rank tests. Recorded neurons were classified as responsive to capsaicin or icilin by comparing the cumulative probability distribution of sEPSC/mEPSC interevent intervals with a 2-sample Kolmogorov–Smirnov test. T tests were used to compare morphometric parameters from reconstructed axons and dendritic trees of GRP and SP populations. To determine whether there was a significant difference in the proportions of GRP$^+$ and GRP$^-$ neurons in L5 that were retrogradely labelled from T13/L1, a contingency table was analysed with the Mantel–Haenszel test.[44] Breslow–Day testing for homogeneity of the odds ratio was conducted before computation of the Mantel–Haenszel odds ratio and 95% confidence intervals. The Mantel–Haenszel test was also used to determine whether the proportions of GRP$^+$ and GRP-negative cells that showed pERK in response to noxious or pruritic stimuli differed significantly. Data are expressed as mean ± SEM, unless stated otherwise. *P* values of less than 0.05 were considered to be significant. Statistical tests were performed in Prism 7 (GraphPad) or SPSS (Version 22, IBM, for the Mantel–Haenszel test).

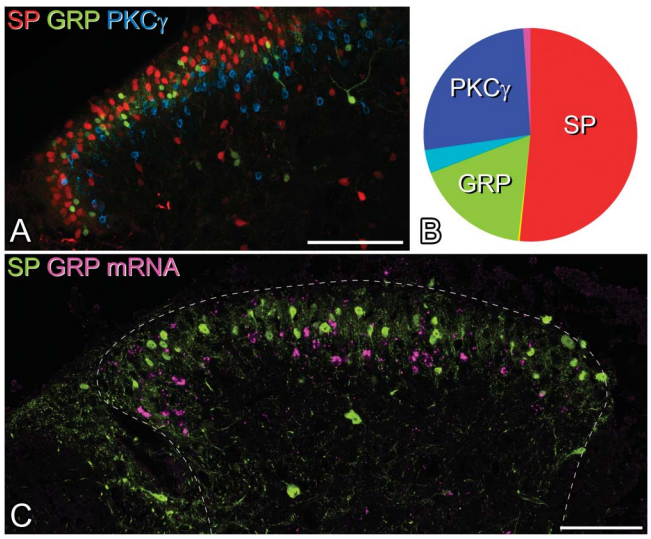

Figure 2. Distribution of cells expressing substance P (SP), GRP, and PKCγ. (A) A confocal image showing part of a transverse section through the dorsal horn of the L3 segment from a Tac1^{Cre};GRP::eGFP mouse that had received an intraspinal injection of AAV.flex.tdTom 2 weeks previously. The section has been immunostained for GFP (green) and PKCγ (blue), while the native fluorescence of tdTom is shown in red. Cells containing each of these markers form largely separate populations. Although these overlap, the tdTom$^+$ (SP-expressing) cells are generally dorsal, and the PKCγ cells ventral, to the GRP-eGFP cells. (B) Pie chart showing the relative sizes and extent of overlap of these populations. (C) Lack of coexpression of GRP and SP is further supported by the finding that there is virtually no overlap between GRP mRNA (magenta) and GFP (green) in the L3 segment of a Tac1^{Cre} mouse that had received an intraspinal injection of AAV.flex.eGFP. Scale bars: (A and B) = 100 μm. AAV, adeno-associated virus; GRP, gastrin-releasing peptide.

3. Results

3.1. Mediolateral distribution of gastrin-releasing peptide–eGFP cells

During the course of experiments with the GRP::eGFP mouse, we noted that there was some variability in the number of GFP$^+$ cells in the superficial dorsal horn in different mice. In addition, we observed a consistently lower number of GFP-positive cells in the medial part of the dorsal horn in caudal lumbar segments (especially L4 and L5) (**Figs. 1A and B**). Because this region is innervated by glabrous skin of the hind paw, we compared the proportion of neurons that were GFP$^+$ in regions innervated by hairy and glabrous skin. This analysis was performed in the L4 segment (which receives input from both hairy and glabrous skin) and L1, which receives its cutaneous input only from hairy skin. The mean numbers of neurons counted per segment were 934 (882-1122) for L4 and 738 (702-808) for L1 (n = 3 mice). Although the percentage of laminae I and II neurons that were GFP$^+$ in L1 and in the lateral (hairy skin) part of L4 was very similar (12%-14%), only 3% of those in the medial (glabrous skin) part of L4 expressed GFP (**Fig. 1C**). A 2-way repeated-measures ANOVA demonstrated a significant effect of lumbar location ($F(1, 2) = 37.15$, $P = 0.026$) and mediolateral location ($F(1, 2) = 27.3$, $P = 0.035$). The interaction between these factors was significant ($F(1, 2) = 86.61$, $P = 0.011$), and the *post hoc* Sidak test shows a significant mediolateral difference at L4 ($t(2) = 2.08$, $P = 0.0085$) but not at L1 ($t(2) = 15.24$, $P = 0.32$).

The lack of GRP::eGFP cells in medial L4 and L5 could reflect the absence of cells that express GRP or a lack of GFP in some GRP-expressing neurons in the BAC transgenic line. To distinguish between these possibilities, we performed in situ hybridisation histochemistry on tissue from GRP::eGFP mice. We identified a mean of 43.7 (35-54) GFP$^+$ cells and 96.0 (90-107) GRP mRNA cells in sections from 3 mice and found that virtually all (98%) GFP$^+$ cells had detectable GRP mRNA, whereas 44.5% (39%-51%) of cells with the mRNA were GFP-positive. Gastrin-releasing peptide mRNA$^+$ cells were found throughout the mediolateral extent of the dorsal horn in the midlumbar region (**Fig. 1D**) and the medial part of the L4 and L5 segments contained numerous GRP mRNA$^+$/GFP-negative cells. We could not determine the proportion of neurons with

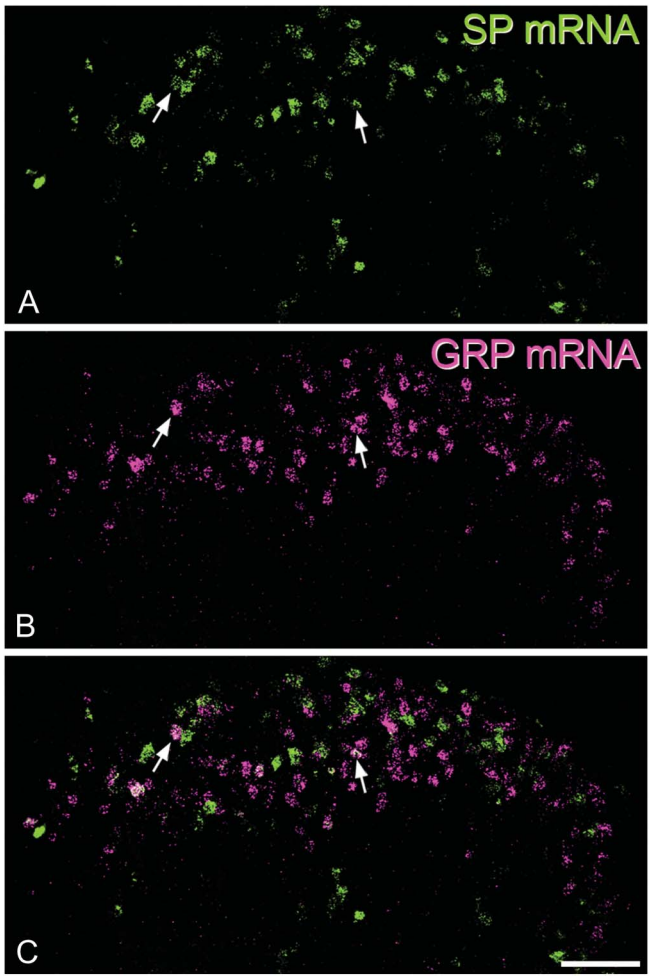

Figure 3. Limited coexistence of mRNAs for SP and GRP in a section of the cervical dorsal horn that had been reacted with a double-label in situ hybridisation method. (A) Substance P mRNA is shown in green. (B) The same field scanned to reveal GRP mRNA (magenta). (C) A merged image shows that most cells that are labelled contain only one of the mRNA types. However, some cells are double-labelled, and 2 of these are indicated with arrows. Scale bar = 50 μm. GRP, gastrin-releasing peptide; SP, substance P.

GRP mRNA, due to the lack of a neuronal marker in these sections, but we noted that although the lateral and medial parts (defined by the presence and absence of the intense GFP plexus) were approximately equal in size, GRP mRNA cells were more numerous in the lateral part (57-84 cells, mean 65.3 for the lateral part; 23-36 cells, mean 30.6 for the medial part; n = 3 mice). However, the extent of overlap between GRP mRNA and GFP was significantly different, depending on mediolateral location. In the medial part, only 30.5% (28%-33%) of GRP mRNA-positive cells were GFP-positive, compared with 50.8% (46%-56%) in the lateral part, and this difference was significant (*t* test, $t(4) = 5.93$, $P = 0.004$). We may have underestimated the proportion of GRP mRNA cells that express GFP due to some loss of GFP signal resulting from the in situ hybridisation protocol.[57] However, these results suggest that although there may be fewer GRP mRNA-positive cells in the glabrous skin territory, lack of expression of GFP in GRP-expressing neurons is partially responsible for the low numbers of GFP cells seen in this region in the GRP::eGFP mouse.

Because we do not have a convenient way of identifying cells with GRP mRNA that did not express GFP, our subsequent analysis was restricted to the GFP-positive population. It should be borne in mind that these cells may differ functionally from the GFP-negative cells that contain GRP mRNA.

3.2. Limited coexpression of gastrin-releasing peptide and substance P

We previously identified SP-expressing neurons by using immunocytochemistry to reveal PPTA and reported that there was minimal overlap between PPTA-immunoreactive neurons and those that were GFP-positive in the GRP::eGFP mouse.[23] However, we also found that the PPTA antibody labelled fewer neurons than were seen after intraspinal injection of AAV.flex.tdTom into $Tac1^{Cre}$ mice. It is therefore possible that we underestimated the degree of overlap between these populations. To better separate these populations, we performed experiments on $Tac1^{Cre}$;GRP::eGFP and $Tac1^{Cre}$ mice that had received intraspinal injections of AAVs coding for either tdTom or eGFP (**Fig. 2**). We first examined tissue from 2 $Tac1^{Cre}$;GRP::eGFP mice that had been injected with AAV.flex.tdTom, and measured the extent of overlap between $tdTom^+$ (SP cells) and GFP^+ (GRP cells) in laminae I and II. We also stained for PKCγ, which is found in a different population of excitatory interneurons.[26,57] This analysis provided further evidence that the SP, GRP, and PKCγ cells are largely separate populations (**Figs. 2A and B**). The mean number of cells that were $tdTom^+$, GFP^+, and/or $PKC\gamma^+$ in sections from the 2 mice was 356 (364 and 347 in the 2 mice). Of these, 189 (199, 178) were tdTom-positive, 75 (80, 70) were GFP-positive, and 110 (114, 105) were PKCγ-immunoreactive. As reported previously,[24,26] we found some overlap between GRP-eGFP cells and PKCγ-immunoreactive cells (corresponding to 17% of the GFP cells and 11% of those with PKCγ), but minimal overlap between tdTom and PKCγ cells (corresponding to 2.1% of the tdTom cells and 3.6% of those with PKCγ). In addition, we saw very little overlap of the tdTom (SP) population with the GRP-GFP cells (1.3% of the GRP-GFP cells and 0.6% of the tdTom cells).

Because some GRP cells may not be detected in the GRP::eGFP mouse, we also compared the distribution of GRP mRNA with that of GFP in 3 $Tac1^{Cre}$ mice that had been injected with AAV.flex.eGFP (**Fig. 2C**). We identified a mean of 75.3 (68-85) GFP^+ cells and 46.3 (44-49) GRP mRNA cells and found only 2.3 (2-3) double-labelled cells (corresponding to 3.2% of the GFP population and 5.2% of the GRP mRNA cells).

In sections of the cervical cord that had undergone double-labelling in situ hybridisation (**Fig. 3**), we identified a mean of 678 cells with SP mRNA (range 561-783, n = 3 mice) and 618 (483-715) cells with GRP mRNA. The mean number of cells in these sections that contained both SP and GRP mRNAs was 72 (range 54-85), and this corresponded to 10.7% (9.6%-11.3%) of the cells with SP mRNA and 11.7% (10.9%-12.9%) of those with GRP mRNA. A similar pattern was seen in the sections of the lumbar cord (1 mouse): we identified 572 cells with SP mRNA, 497 cells with GRP mRNA, and 60 of these cells had both mRNAs. In this case, cells with both mRNAs corresponded to 10.5% of the GRP^+ cells and 12.2% of the SP^+ cells. We conclude that although there is a limited overlap between SP and GRP cells, they are largely separate populations.

3.3. Electrophysiological properties of gastrin-releasing peptide and substance P cells

As we did not observe any differences between male and female mice, all data presented are from a combination of both sexes.

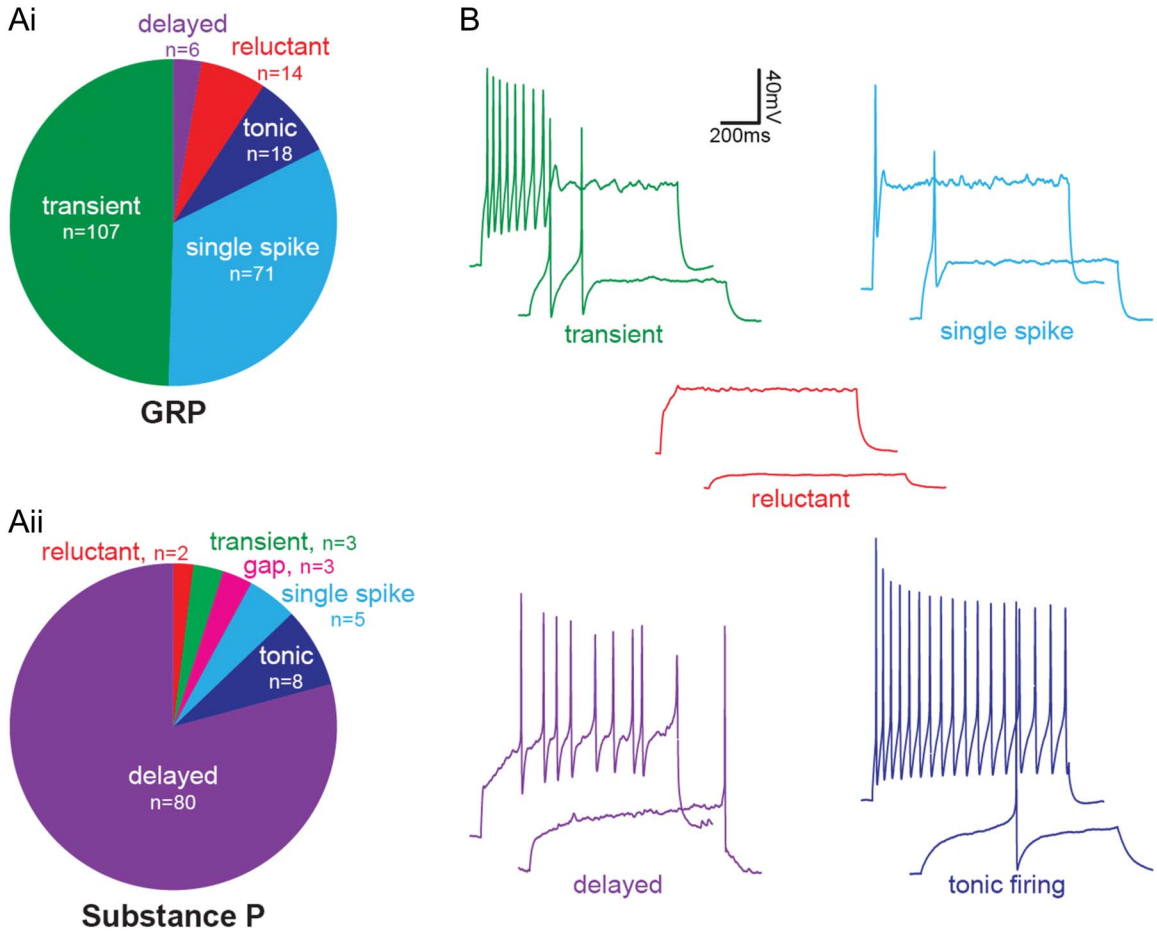

Figure 4. Action potential firing patterns in GRP and SP cells. GRP cells were identified by the presence of GFP in slices taken from GRP::eGFP mice. Substance P cells were identified by expression of either GFP or tdTom in Tac1^{Cre} mice that had received injections of AAV coding for Cre-dependent forms of the corresponding fluorescent protein. (Ai) In response to a suprathreshold current injection (1 second), most GRP cells displayed transient (107/216, 49.5%) or single-spike (71/216, 32.9%) firing, with a smaller proportion of cells showing tonic (18/216, 8.3%), reluctant (14/216, 6.5%), or delayed (6/216, 2.8%) firing. (Aii) The majority of SP cells exhibited delayed firing (80/101, 79.2%), with smaller proportions displaying tonic (8/101, 7.9%), single-spike (5/101, 5%), transient (3/101, 3%), gap (3/101, 3%), or reluctant (2/101, 2%) firing patterns. (B) Examples of transient, single-spike, and reluctant firing GRP cells, and delayed and tonic-firing SP cells. AAV, adeno-associated virus; GRP, gastrin-releasing peptide; SP, substance P.

For the electrophysiological parts of the study, GRP cells were identified by GFP expression in slices from the GRP::eGFP mice, whereas SP cells were identified by expression of either GFP or tdTom in slices obtained from Tac1^{Cre} mice that had received intraspinal injections of AAVs coding for Cre-dependent forms of the corresponding fluorescent protein. Because GRP-eGFP cells were relatively infrequent in the medial part of the L4 and L5 segments, parasagittal slices through these segments were cut in such a way as to allow recordings from cells located in the more lateral parts of the segment.

The incidence of action potential firing patterns differed substantially between GRP and SP cells (**Fig. 4**). Gastrin-releasing peptide cells generally displayed transient (107/216, 49.5%) or single-spike (71/216, 32.9%) firing patterns, which were rarely seen in SP cells (3/101, 3% and 5/101, 5%, respectively). By contrast, the great majority of SP cells (80/101, 79.2%) exhibited the delayed firing pattern, which was very seldom seen in the GRP cells (6/216, 2.8%). Both cell populations contained a small proportion of tonic-firing cells (GRP: 18/216, 8.3% and SP: 8/101, 7.9%), together with a few cells that were classified as reluctant (GRP: 14/216, 6.5% and SP: 2/101, 2%), while 3 of the SP cells (3.0%) showed a long first interspike interval and were classified as gap-firing.[29]

We have shown that when Tac1^{Cre} mice received intraspinal injections of AAV.flex.eGFP, around 10% of the GFP^{+} cells are Pax2^{+} (inhibitory) neurons, and these are therefore likely to have been included among the neurons recorded in these experiments. Previous studies have shown that delayed, gap, and reluctant firing patterns, which are believed to result from the presence of A-type potassium currents, are particularly associated with excitatory interneurons in lamina II.[29,49,73] For all subsequent electrophysiological and pharmacological parts of the study, we therefore restricted the analysis to the 84% of SP cells (85/101) that showed delayed, gap, or reluctant firing. This approach reduced the risk that recordings were from inhibitory SP neurons.

Consistent with the much higher proportion of SP cells that showed gap or delayed firing, the latency between the onset of the current injection and the first action potential at rheobase was significantly greater for the SP cells (595.0 ± 28.26 ms) compared with the GRP cells (137.1 ± 6.2 ms) (Mann–Whitney, $U = 504$, $P < 0.001$, n = 155 GRP cells and 80 SP cells). The rheobase of SP cells was 46.45 ± 2.15 pA, and this was significantly larger than that of GRP cells, 18.30 ± 1.07 pA (Mann–Whitney, $U = 1275$, $P < 0.001$, n = 155 GRP cells and 80 SP cells).

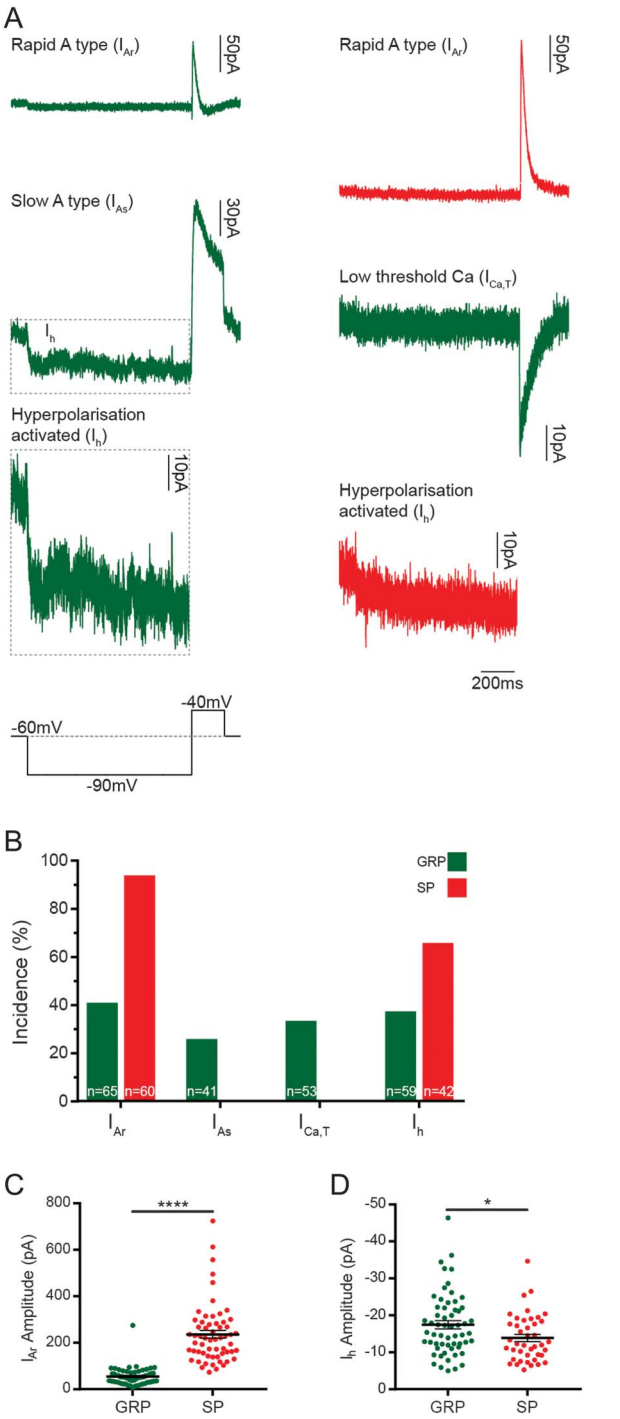

Figure 5. Subthreshold voltage-activated currents in GRP and SP cells, which were identified as described in the legend for Figure 4. (A) Subthreshold currents were examined in GRP and SP cells using a voltage step protocol that hyperpolarised cells from −60 to −90 mV for 1 second and then to −40 mV for 200 milliseconds (lower left trace). The responses to this protocol were classified as rapid (I_{Ar}) or slow (I_{As}) A-type potassium currents, hyperpolarisation-activated currents (I_h), or low-threshold calcium currents ($I_{Ca,T}$). Examples from both GRP (green) and SP (red) cells show an average of 5 traces. The example of I_h for the GRP cell (dashed outline) is shown at 2 different y-axis scales. (B) Almost all SP cells displayed I_{Ar} (60/64, 93.8%) and most had I_h (42/64, 65.6%), with many cells exhibiting both (38/64, 59.4%). I_{Ar} was the most commonly seen current in GRP cells (65/159, 40.9%), with fewer cells showing I_h (59/159, 37.3%), I_{As} (41/159, 25.8%), or $I_{Ca,T}$ (53/159, 33.3%). (C) The amplitude of I_{Ar} was significantly greater in SP cells (C, 263.3 ± 16.5 vs 58.6 ± 4.6 pA), $^{****}P < 0.0001$, Mann–Whitney *U* test. (D) I_h amplitude was significantly larger in GRP cells (D, −17.5 ± 1.1 vs −13.9 ± 1.0 pA). $^{*}P = 0.024$, Mann–Whitney *U* test. GRP, gastrin-releasing peptide; SP, substance P.

The subthreshold I–V relationship was determined by voltage clamping the cells at −60 mV and applying 100-millisecond voltage steps from −70 to −50 mV in 2.5 mV increments. The resting membrane potential, as calculated from the I–V relationship for individual cells, was −52.89 ± 0.78 mV for GRP cells and −55.77 ± 0.90 mV for SP cells, with the GRP cells having a significantly more depolarised resting membrane potential (Mann–Whitney, $U = 7758$, $P = 0.0074$, n = 230 GRP cells and 84 SP cells). The capacitance of GRP cells was significantly smaller than that of SP cells (5.12 ± 0.11 vs 7.07 ± 0.33 pF; Mann–Whitney, $U = 5904$, $P < 0.001$, n = 232 GRP cells and 85 SP cells), with GRP cells also displaying a greater input resistance (1588 ± 85 vs 836 ± 52 MΩ; Mann–Whitney, $U = 5315$, $P < 0.001$, n = 232 GRP cells and 84 SP cells).

Almost all SP neurons tested (60/64, 93.8%, **Figs. 5A and B**) displayed a rapid I_A current (I_{Ar}), and most showed a hyperpolarisation-activated current (I_h) (42/64, 65.6%), with many exhibiting both I_{Ar} and I_h (38/64, 59.4%). Although I_{Ar} was the most commonly seen subthreshold current in GRP cells (65/159, 40.9%, **Figs. 5A and B**), the incidence was lower than that in SP cells, and the amplitude was significantly smaller (54.9 ± 4.6 vs 263.3 ± 16.5 pA, Mann–Whitney, $U = 64$, $P < 0.0001$, **Fig. 5C**). Many GRP cells displayed I_h (59/159, 37.3%), with some cells exhibiting both I_h and I_{Ar} (13/159, 8.2%). The amplitude of I_h in GRP cells was significantly larger than that recorded in SP cells (−17.5 ± 1.1 vs −13.9 ± 1.0 pA, Mann–Whitney, $U = 911.5$, $P = 0.024$, **Fig. 5D**). Although not detected in the SP cells, slow I_A current (I_{As}) (41/159, 25.8%) and low-threshold Ca currents ($I_{Ca,T}$) (53/159, 33.3%) were recorded in some GRP cells. Some GRP cells that showed I_{As} also exhibited I_h (36/159, 22.6%) or I_h and $I_{Ca,T}$ (1/159, 0.6%), and $I_{Ca,T}$ was found to overlap with I_{Ar} (5/159, 3.1%) and with I_h (3/159, 1.9%).

3.4. Excitatory inputs to gastrin-releasing peptide and substance P cells

As stated above, analysis of SP cells was restricted to those with delayed, gap, or reluctant firing patterns. Substance P cells showed a higher frequency of both sEPSCs and mEPSCs (6.04 ± 0.96 Hz sEPSCs, 3.24 ± 0.67 Hz mEPSCs, n = 27 and 11, respectively) than GRP cells (0.2 ± 0.05 Hz sEPSCs, 0.02 ± 0.01 Hz mEPSCs, n = 120 and 32, respectively), and these differences were both highly significant (sEPSC, Mann–Whitney, $U = 68$, $P < 0.0001$; mEPSC, Mann–Whitney, $U = 0$, $P < 0.0001$; **Fig. 6**). For 11 of the SP cells, we were able to compare sEPSC frequency with mEPSC frequency in the same cell. The sEPSC frequency for these cells (5.39 ± 0.93 Hz) was higher than the mEPSC frequency (3.24 ± 0.67 Hz), and this difference was highly significant (Wilcoxon signed-rank test; W = 66, $P = 0.0036$). This finding suggests that the SP cells receive excitatory synaptic input from neurons that were spontaneously firing action potentials in the slice.

Capsaicin caused a leftwards shift in the distribution of mEPSC interevent intervals in 1 of 11 GRP and 4 of 9 SP cells (**Figs. 6C and D**). Capsaicin increased mEPSC frequency from 0.04 to 0.17 Hz in the single responsive GRP cell, and from 3.58 ± 0.91 to 8.78 ± 1.79 Hz in the responsive SP cells (example traces shown in **Fig. 6Dii**). When sEPSCs were recorded, 4 of 16 GRP and 3 of 5 SP cells were found to be sensitive to capsaicin (**Fig. 6C**). For those cells that were classed as sensitive, capsaicin increased sEPSC frequency from 0.36 ± 0.10 to 3.58 ± 2.09 Hz in GRP cells, and 1.64 ± 0.16 to 3.29 ± 0.30 Hz in SP cells (example traces shown in **Fig. 6Di**). Application of icilin did not increase

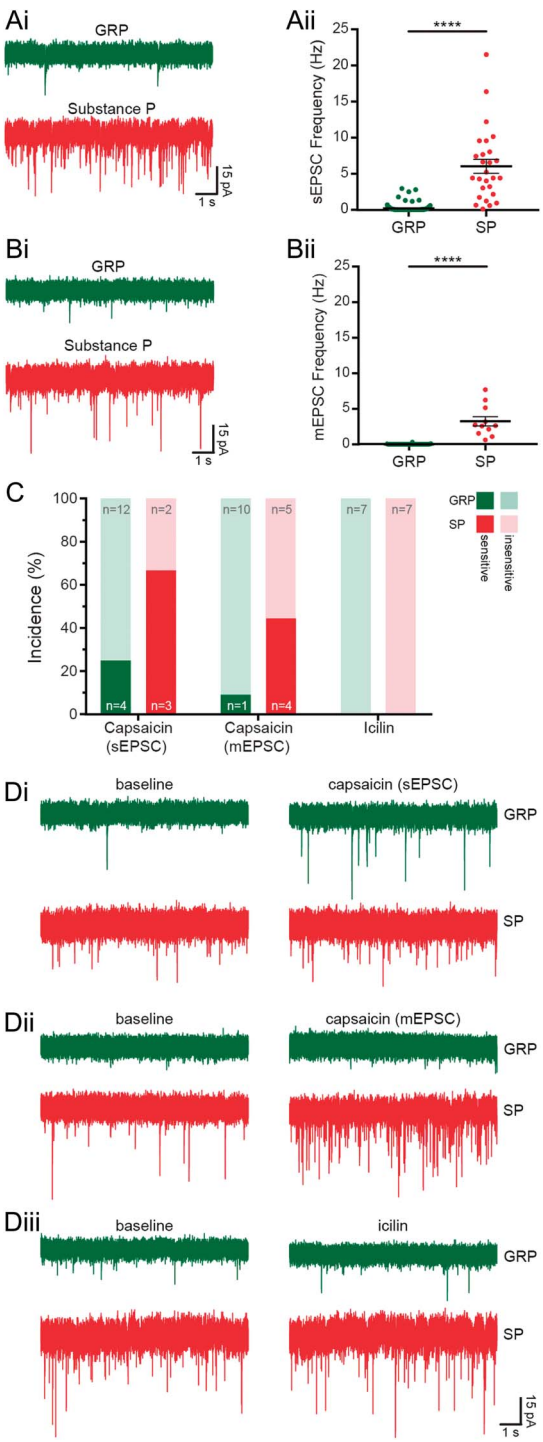

Figure 6. Excitatory inputs to GRP and SP cells, which were identified as described in the legend for Figure 4. Spontaneous EPSCs (Ai) and mEPSCs (Bi) were recorded in GRP and SP cells. Substance P cells were found to receive greater excitatory drive, having a higher frequency of both types of excitatory event (6.04 ± 0.96 Hz sEPSCs, Aii, 3.24 ± 0.67 Hz mEPSCs, Bii, n = 27 and 11, respectively) than GRP cells (0.2 ± 0.05 Hz sEPSCs, Aii, 0.02 ± 0.01 Hz mEPSCs, Bii, n = 120 and 32, respectively). These differences were both highly significant (****$P < 0.0001$, Mann–Whitney U test). (C and Di-iii) Primary afferent input to GRP and SP cells was assessed by recording sEPSCs and mEPSCs in response to the TRP channel agonists capsaicin (TRPV1, Di–ii) and icilin (TRPM8, mEPSCs only, Diii). (C) When mEPSCs were recorded, capsaicin caused a significant leftwards shift in the distribution of interevent intervals in 1 of 11 GRP cells and 4 of 9 SP cells; when sEPSCs were recorded, 4 of 16 GRP cells and 3 of 5 SP cells were found to be capsaicin-sensitive. Icilin did not increase mEPSC frequency in any of the GRP (n = 7) or SP cells (n = 7) tested. GRP, gastrin-releasing peptide; mEPSC, miniature excitatory postsynaptic current; sEPSC, spontaneous excitatory postsynaptic current; SP, substance P.

mEPSC frequency in any of the GRP (n = 7) or SP cells (n = 7) that were tested (**Figs. 6C and Diii**). Because TRPM8 and TRPV1 expression in the dorsal horn are believed to be restricted to primary afferents, these data suggest that neither GRP nor SP cells receive monosynaptic input from TRPM8-expressing afferents. These findings also indicate that both cell types receive input from TRPV1-expressing afferents, and that this includes monosynaptic input, although this is considerably more prevalent in SP cells than GRP cells.

3.5. Responses of gastrin-releasing peptide and substance P cells to neuromodulators

To investigate the effect of neuromodulators (NA, 5-HT, and opioids) on GRP and SP cells, we bath-applied different agonists (**Fig. 7**). DAMGO (3 μM) caused an outward current (7.36 ± 0.99 pA) in all but one of the GRP cells tested (14/15); none of the 7 SP cells tested were responsive. None of the GRP cells responded to the KOR agonist, U69593 (1 μM), and this caused an outward current (7.23 pA) in only 1 of the 8 SP cells tested. The DOR agonist [D-Ala^2]-Deltorphin II (1 μM) was tested on 7 GRP cells and 8 SP cells, but had no effect on any of these. Application of NA (20 μM) caused an outward current in the majority (7 of 9) of the SP cells (15.59 ± 2.54 pA), but in only 1 of 6 GRP cells (8.86 pA). None of the 6 GRP cells tested responded to 5-HT (10 or 20 μM), whereas all 8 SP cells tested displayed an outward current (19.22 ± 2.55 pA). These findings demonstrate that GRP and SP cells differ in their response profiles to the monoamines and MOR agonist, whereas few or none of these cells respond to KOR or DOR agonists. Specifically, most putative excitatory SP cells are hyperpolarised by both NA and 5-HT, but not by any of the opioid agonists. By contrast, most GRP cells do not respond to NA, 5-HT, DOR, or KOR agonists, but are hyperpolarised by MOR agonists.

3.6. Morphological properties of gastrin-releasing peptide and substance P cells

Morphological analysis was performed on 45 GRP cells that underwent whole-cell recording, and from a total of 43 SP cells (31 from perfusion-fixed Brainbow tissue and 12 from electrophysiological experiments). In the tissue from Tac1^{Cre} mice injected with Brainbow AAVs, initial scans revealed that the distribution and density of labelled cells was generally consistent with that seen after injection of AAV.flex.tdTom[23] (**Fig. 8A**). However, although ~10% of the labelled cells in our previous study were Pax2-immunoreactive, only 1 of 100 Brainbow-labelled neurons examined was Pax2-positive, although numerous Pax2$^+$ nuclei were present within the dorsal horn (**Figs. 8B–D**). Clearly, this strategy selectively targets the excitatory SP-expressing neurons. All 31 reconstructed SP neurons had nuclei that were Pax2-negative.

Preliminary observation of the Neurolucida reconstructions suggested that the 2 populations differed in terms of somatodendritic morphology. Although the GRP cells were morphologically heterogeneous, they generally had dendritic trees that were considerably longer in the RC axis than in DV or mediolateral axes, but were shorter than those of islet cells. At least some of these cells could therefore be classed as central cells.[22,71,73] By contrast, **Figure 8E** shows that many of the SP cells reconstructed from the Brainbow experiments resembled radial cells, with relatively numerous primary dendrites that did not extend far from the cell body, and compact dendritic trees. This initial

observation was confirmed by principal component analysis and subsequent cluster analysis of dendritic morphometric parameters extracted from the Neurolucida drawings. These parameters are listed in detail in Table 5 of Ref. 18. A scree test revealed that 5 principal components accounted for 80% of the total variance in the data set, and these were therefore used for cluster analysis. This separated the reconstructed neurons into 2 distinct clusters, one of which (n = 30) consisted entirely of SP cells, and the other (n = 46) of which included all the GRP cells, together with one SP cell (**Fig. 8F**).

Because the 2 populations were obtained from different types of experiment, we were concerned that this might have influenced the clustering results. For example, due to the difficulty of following fine distal dendrites, we may have underestimated the sizes of dendritic trees in the Brainbow material. We therefore looked for factors that correlated well with the principal components distinguishing the clusters and found that the number of primary dendrites was a major factor. We therefore compared the number of primary dendrites between the 2 populations and found a highly significant difference (**Table 3**). We also found that both the DV extent of dendritic trees and the ratio of DV to RC extent[71] differed significantly. The SP cells had more primary dendrites and a lower RC:DV ratio (**Table 3**), both of which are consistent with radial cell morphology. Although we did not analyse the dendritic trees of the recorded SP cells in detail, we noted that these resembled those of the SP neurons seen in the Brainbow tissue (**Figs. 9C and D**). These cells also gave rise to numerous primary dendrites (mean 6.9 ± 1.5 SD), which is similar to the number of primary dendrites on the reconstructed Brainbow neurons (7.4 ± 1.4, **Table 3**).

Because of the difficulty of following axons belonging to individual neurons in Brainbow material, axonal morphology for the SP cells was only analysed on those that had undergone whole-cell recording. For many of the GRP cells, we found that although a well-filled axon could be seen emerging from the soma or a primary dendrite, the axon rapidly turned either medially or laterally and left the slice either without branching (n = 14) or after giving rise to a small arbor (n = 9). For this reason, axonal morphology was only analysed on 22 of the 45 GRP cells. Examples of axonal arbors are illustrated in **Figure 9**. The total length of axon that was reconstructed was significantly greater for the GRP than for the SP cells (*t* test, $t(32) = 3.68$, $P = 0.0008$; **Fig 9E**). However, in both cases, 95% of the axonal length remained in lamina II, with only a small amount in laminae I or III (2% and 4%, respectively, for GRP cells, 4% and 1%, respectively, for SP cells).

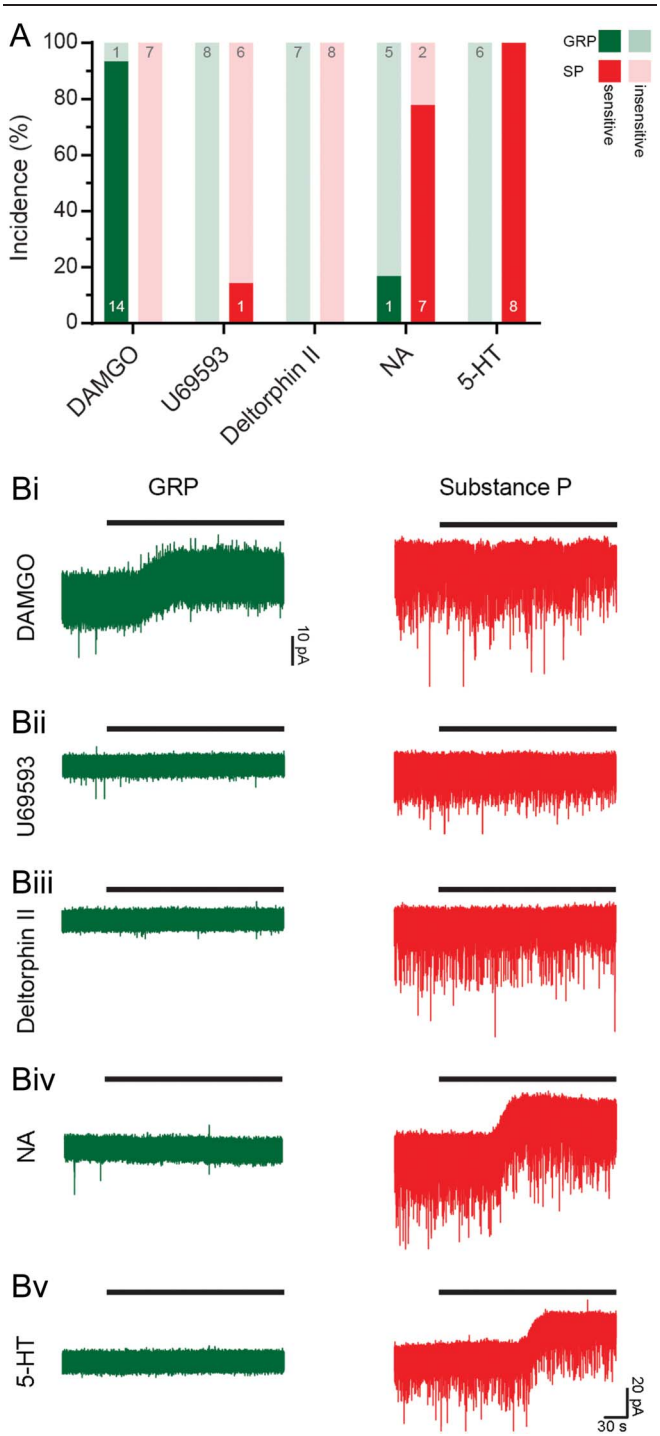

Figure 7. Responses of GRP and SP cells to neuromodulators. Cells were identified as described in the legend for Figure 4. (A) The proportions of tested GRP and SP cells that responded to various neuromodulators are shown. (Bi) The MOR agonist DAMGO caused an outward current in most GRP cells (14/15) but was without effect in SP cells. (Bii) No GRP cells and only 1 of 7 SP cells responded to the KOR agonist, U69593. (Biii) No cells of either type responded to the DOR agonist, [D-Ala^2]-Deltorphin II. (Biv) Noradrenaline (NA) elicited a response in most SP cells (7/9), but only 1 of 6 GRP cells. (Bv) 5-HT evoked an outward current in all 8 SP cells, whereas the 6 GRP cells tested were unresponsive. GRP, gastrin-releasing peptide; SP, substance P.

3.7. Lack of long propriospinal projections of gastrin-releasing peptide cells

The finding that the axons of recorded GRP cells often turned medially or laterally raised the possibility that these had propriospinal projections,[7,25] and we therefore addressed this in the retrograde labelling experiments. The CTb injection sites in the T13 segment in these experiments included the whole of laminae I to V of the right dorsal horn as well as the lateral spinal nucleus (LSN) (**Fig. 10A**). The pattern of retrograde labelling with CTb in the L5 segment was very similar to that described previously.[25] There were numerous CTb-labelled neurons evenly distributed throughout the mediolateral extent of the superficial dorsal horn, as well as in deeper laminae (**Fig. 10B**). Few retrogradely labelled cells were seen on the contralateral (left) side. The mean number of laminae I and II neurons included in the disector sample in the 4 mice was 589 (range 547-620), and 26.6% were CTb-immunoreactive (range 22.1%-29.6%), indicating that at least a quarter of superficial dorsal horn neurons in L5 have axons that extend rostrally for 5 segments.

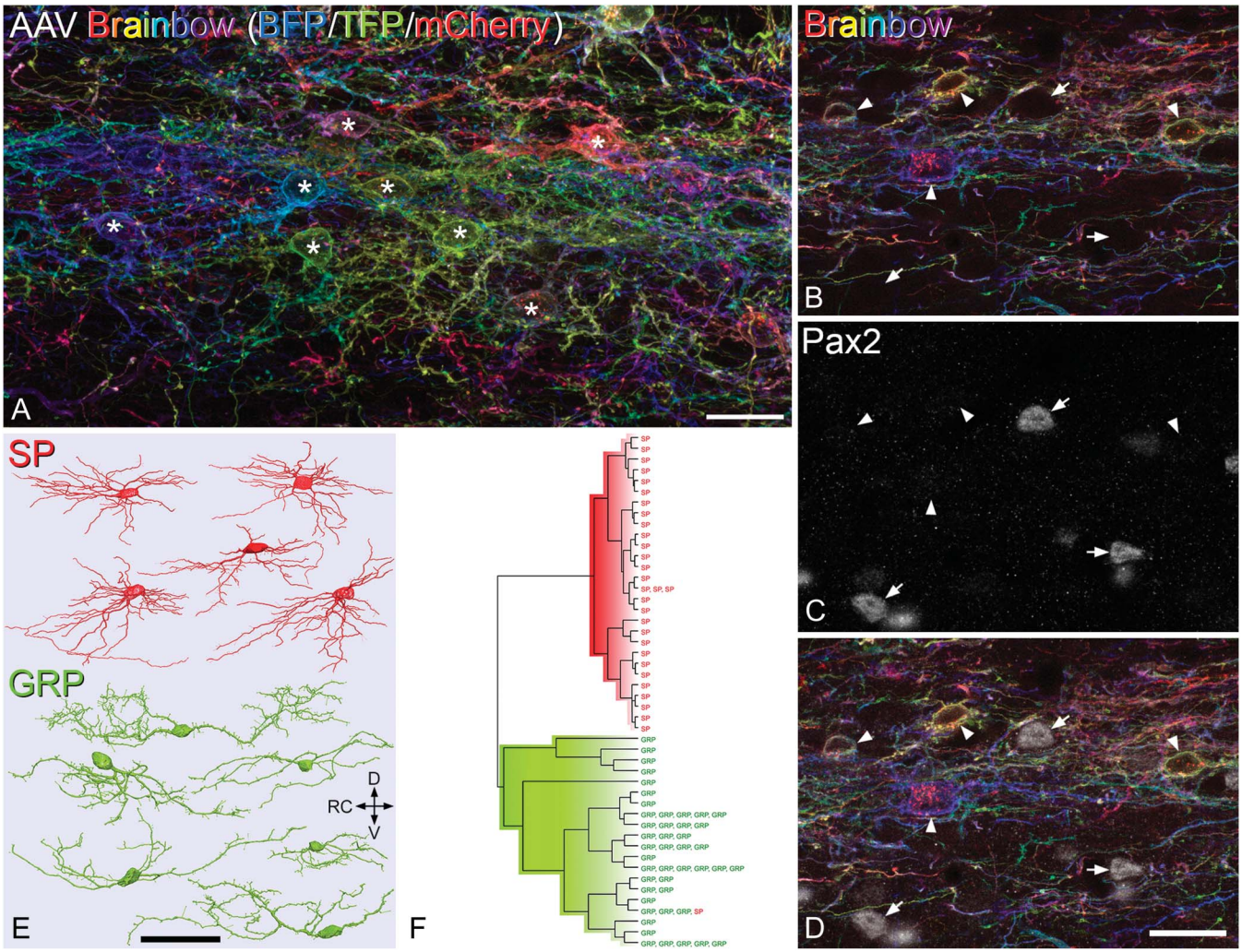

Figure 8. Morphology of SP and GRP cells. (A) The labelling that results from injection of AAV Brainbow into the dorsal horn of a Tac1^{Cre} mouse. This field shows part of lamina II in a projected image of 38 optical sections at 0.5-μm z-separation. Numerous neuronal cell bodies are visible (some marked with asterisks), and these show different hues, resulting from differential expression of blue fluorescent protein (BFP), teal fluorescent protein (TFP), and mCherry. Note that apart from some cytoplasmic staining for mCherry, the labeling is largely restricted to the plasma membrane and therefore outlines the cells. (B–D) A projection of 5 optical sections at 1-μm z-separation from a Tac1^{Cre} mouse injected with AAV Brainbow. This has been scanned to reveal the fluorescent proteins (shown in B and D) and Pax2 (C and D). Although there are Pax2-positive cells in this field (some marked with arrows), none of these correspond to the Brainbow-labelled cells (arrowheads). (E) Neurolucida reconstructions of the cell bodies and dendritic trees of representative SP and GRP cells. Note that the SP cells were obtained from Brainbow experiments, whereas the GRP cells were from electrophysiological recordings in the GRP::eGFP mice. (F) Hierarchical cluster analysis (Ward's method) based on morphometric dendritic parameters results in almost complete separation of the SP and GRP cells, with only 1 of 31 SP cells appearing in the lower cluster, which contains all 45 of the GRP cells. Scale bars: (A) = 20 μm, (B–D) = 20 μm, and (E) = 50 μm. AAV, adeno-associated virus; D, dorsal; GRP, gastrin-releasing peptide; RC, rostrocaudal; SP, substance P; V, ventral.

Cells that were positive for eGFP in the L5 segment accounted for 10.3% (7.6%-12.6%) of all laminae I and II neurons, which is similar to our previous estimate (11%).[24] Very few of the GFP$^+$ cells, 3.5% (2.6%-4.7%), were CTb-immunoreactive, while GFP-immunoreactive cells accounted for only 1.3% (1.1%-1.5%) of the CTb-labelled neurons in laminae I and II (**Figs. 10C and D**). This difference in proportion was highly significant (Mantel–Haenszel test, $\chi^2(1) = 73.0$, $P < 0.0001$), with an odds ratio for a GRP cell to be retrogradely labelled calculated as 0.08 (0.04-0.17; 95% confidence interval, Breslow–Day significance; $P = 0.944$). We conclude that GRP-expressing cells are significantly underrepresented among the superficial dorsal horn neurons that have long ascending propriospinal axons.

To test whether GRP cells give rise to short intersegmental connections, we also analysed sections from the L2 segment in 2 of the mice. We found that the proportion of all neurons in laminae I and II that were retrogradely labelled with CTb from the T13 injection sites was 58% (range 55.9%-60.1%), and that among GRP-eGFP cells, the proportion that were CTb-labelled was 15.1% (range 13%-17.1%). This indicates that a few of the GRP cells have axons that extend for at least 2 segments rostrally.

3.8. Responses of gastrin-releasing peptide cells to noxious and pruritic stimuli

Noxious and pruritic stimuli induced pERK in cells of the ipsilateral dorsal horn, mainly in the superficial laminae with a mediolateral extent that reflected the somatotopic location of a stimulus delivered to the lateral calf.[6,23] Few, if any, pERK cells were located on the contralateral side or in the dorsal horn of mice that received vehicle injection.

First, we determined the proportion of all neurons that were pERK-positive after stimulation with histamine, capsaicin, pinch, and noxious heat. The percentage of all neurons within the activated zone in laminae I and II that were pERK-immunoreactive varied between 23%

Table 3

Morphological properties of dendrites of GRP and SP cells.

Dendritic measure	GRP	SP	*t*	*df*	*P*
Total primary dendrite number	3.4 ± 1.3	7.4 ± 1.4	12.4	74	0.0001
Total dendritic length (μm)	845.7 ± 527.8	1012.6 ± 249.8	1.61	74	0.110
RC extent (μm)	159.8 ± 54.3	141.5 ± 28.9	1.69	74	0.094
DV extent (μm)	46.6 ± 13.3	58.0 ± 11.2	3.72	74	0.0004
ML extent (μm)	34.9 ± 16.2	30.5 ± 7.2	1.40	74	0.164
RC:DV ratio	3.65 ± 1.4	2.5 ± 0.7	4.06	74	0.0001
Spine density (per 100 μm)	17.2 ± 5.8	18.6 ± 4.2	1.11	74	0.267

The table shows quantitative morphological data from the 45 GRP cells (from whole-cell patch-clamp recordings) and 31 SP cells (from Brainbow experiments) that were morphologically reconstructed. Data are shown as mean ± SD.

DV, dorsoventral; GRP, gastrin-releasing peptide; ML, mediolateral; RC, rostrocaudal; SP, substance P.

and 37% depending on the stimulus (**Table 4**). We then compared the proportions of GFP^+ and GFP-negative cells that showed pERK after the different types of noxious and pruritic stimulus. We found that in all cases, the GFP^+ cells were significantly underrepresented compared with GRP-negative neurons (**Table 4**). Examples of pERK staining in the GRP-eGFP mice are shown in **Figure 11**.

4. Discussion

Our main findings are that SP- and GRP-expressing cells form largely nonoverlapping populations among the excitatory interneurons in laminae I and II, and that these differ significantly in morphology, firing patterns, EPSC frequency, and responses to

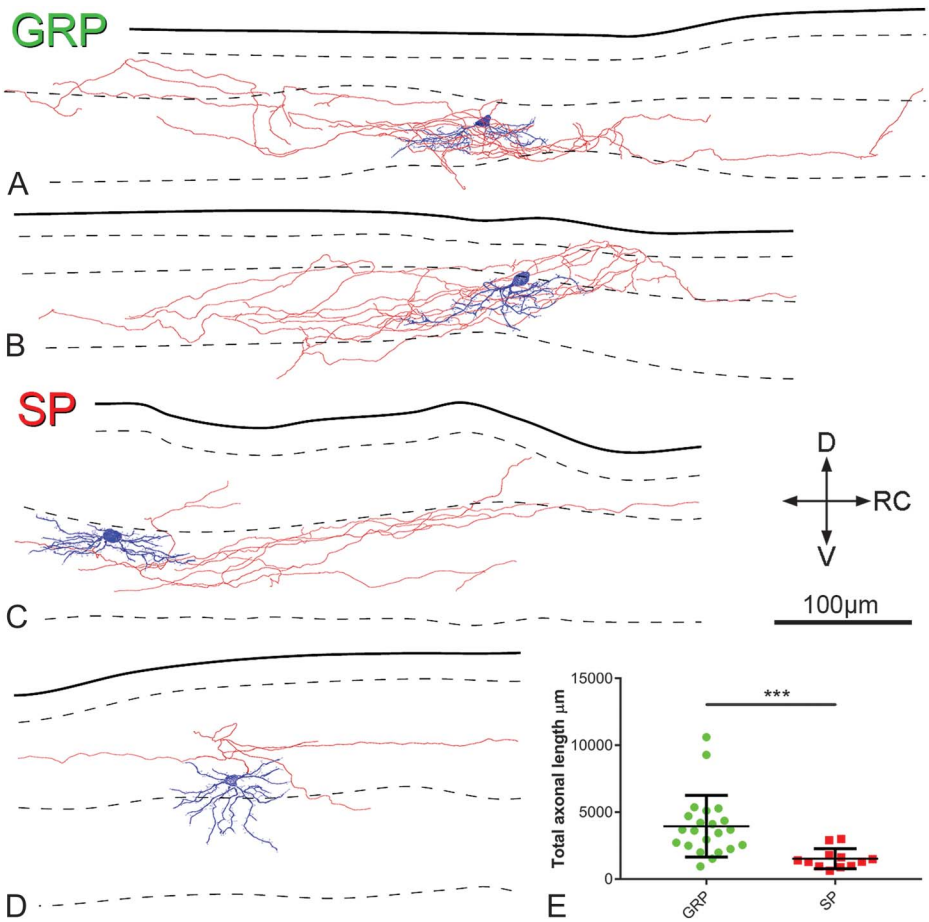

Figure 9. Morphology and laminar distribution of axons of GRP and SP cells. Cells were reconstructed after electrophysiological recordings, during which they were identified as described in the legend for Figure 4. (A–D) Typical examples of Neurolucida reconstructions of GRP cells (A and B) and SP cells (C and D). Cell bodies and dendrites are shown in blue and axons in red (axonal boutons are not shown). In each drawing, the solid line indicates the gray-white border, whereas dashed lines represent the boundaries between laminae I/IIo, IIo/IIi, and IIi/III. Note that the axons of the cells predominantly arborise in lamina II and rarely enter lamina I. Scale bar = 100 μm. The total measured axonal length in each population is shown (E) with the total length of axon being significantly greater in the GRP cells . *** Denotes significant difference ($P<0.001$, *t*-test). D, dorsal; GRP, gastrin-releasing peptide; RC, rostrocaudal; SP, substance P; V, ventral.

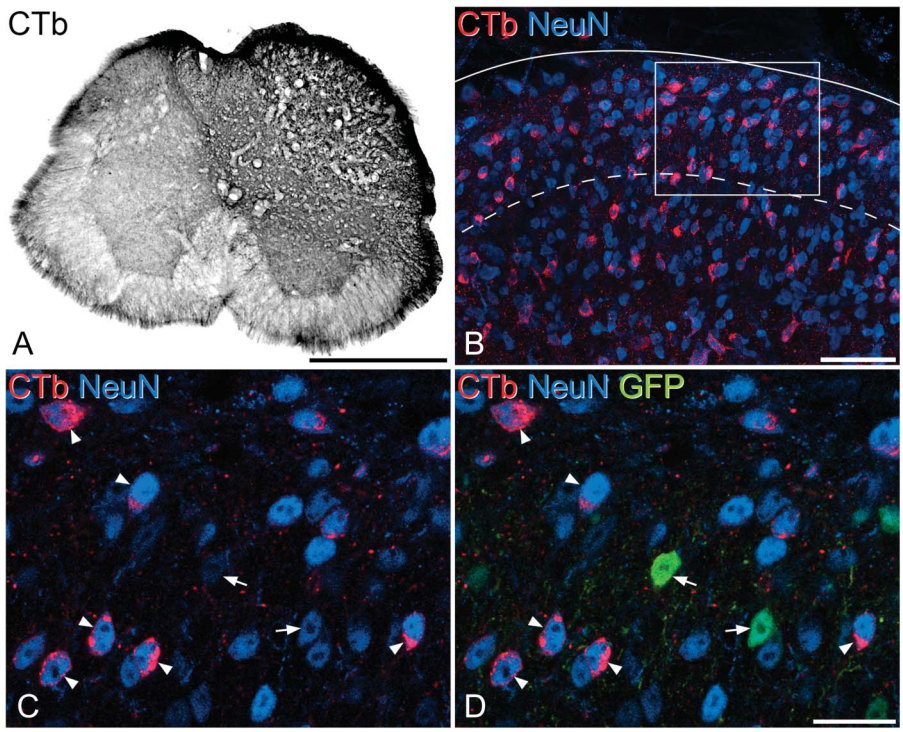

Figure 10. Retrograde labelling of L5 neurons from the T13 segment in a GRP::eGFP mouse. (A) The injection site in the T13 segment of one of the mice. The CTb reaction product fills the entire dorsal horn and part of the ventral horn on the right side, with limited spread onto the contralateral side. (B) A Projected confocal image (17 optical sections at 2-μm z-spacing) showing part of the ipsilateral dorsal horn from the L5 segment of the same animal. Numerous NeuN$^+$ (neuronal) profiles are visible (blue), and many of these are labelled with CTb (red) that has been retrogradely transported from the T13 injection site. The solid line indicates the dorsal edge of the dorsal horn and the dashed line the lamina II-III border. (C and D) A single confocal optical section showing a higher magnification view from the region in the box in (B). This field contains 2 GFP$^+$ (green) cells (arrows), which are not CTb-labelled, and these are surrounded by several GFP-negative CTb-labelled neurons, some of which are marked with arrowheads. Scale bars: (A) 500 μm; (B) 50 μm; and (C and D) 20 μm. CTb, cholera toxin B; GRP, gastrin-releasing peptide.

neuromodulators. Comparison with previous data suggests that they also differ in responses to noxious and pruritic stimuli, and their contribution to propriospinal projections.[23,25] These findings are summarised in **Figure 12**.

4.1. The function of gastrin-releasing peptide–expressing interneurons

It is well established that GRP-expressing neurons have a major role in itch.[46] Sun et al.[60] recently proposed that these cells respond weakly to pruritic stimuli and strongly to painful stimuli, but that when strongly activated, they suppress pain through feed-forward inhibition, forming a "leaky gate." We previously reported that GRP cells rarely show pERK or Fos following intradermal chloroquine,[6] and Sun et al. suggested that this was because of their weak activation by pruriceptors. However, we show here that these cells very seldom develop pERK after noxious stimuli. Interestingly, Sun et al.[60] report that capsaicin applied to the dorsal root ganglion generated mean firing rates of <1 Hz in GRP cells, and if this is similar to their response to natural noxious stimuli, it may be inadequate to phosphorylate ERK. It has been reported that GRP cells are innervated by various types of primary afferent, including TRPV1-

Table 4

The numbers and percentages of GRP-eGFP neurons in laminae I and II that were pERK after noxious or pruritic stimulation.

Stimulus	Total neurons	pERK$^+$ neurons	GRP-eGFP$^+$ neurons	GRP-eGFP$^+$ and pERK$^+$	% neurons pERK$^+$	% GRP-eGFP neurons pERK$^+$	χ^2 (1 df)	*P* (Mantel–Haenszel)
Histamine	438.7 (377-497)	145.3 (127-162)	58.7 (51-72)	2.3 (0-5)	33.4 (28.7-39.0)	4.2 (0-9.8)	78.6	<0.001
Pinch	421.7 (367-505)	157.7 (137-194)	44.3 (41-51)	1.3 (1-2)	37.3 (34.9-38.7)	3.1 (2.0-4.9)	73.7	<0.001
Noxious heat	572.3 (424-779)	133.3 (89-188)	82.3 (56-105)	6.3 (0-13)	23.0 (21.0-24.1)	6.5 (0-12.4)	39.8	<0.001
Capsaicin	459.0 (384-553)	122.7 (110-136)	53.3 (43-65)	2.7 (1-5)	27.0 (24.6-28.6)	5.0 (2.3-9.6)	42.8	<0.001

The table shows quantitative data from the region delineated by high levels of pERK, which were obtained from 3 mice in each case. *P* value shown is for the Mantel–Haenszel test for difference in proportions in pERK between GRP-expressing and non–GRP-expressing cells.
GRP, gastrin-releasing peptide; pERK, phosphorylated extracellular signal–regulated kinase.

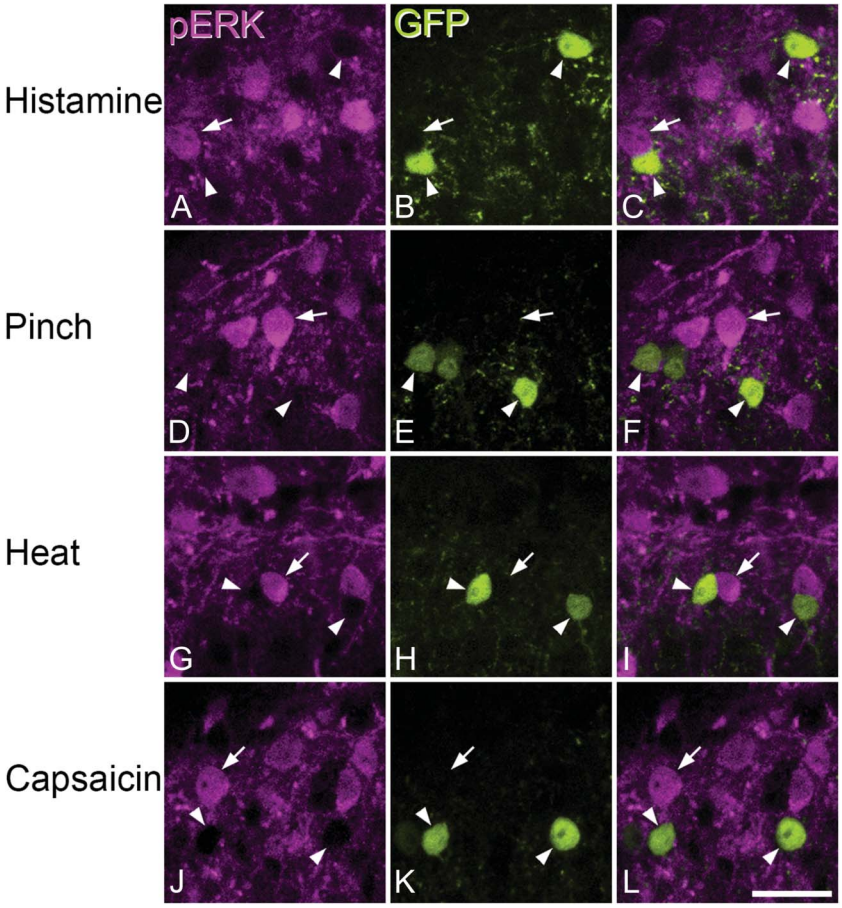

Figure 11. Phosphorylated extracellular signal–regulated kinase immunoreactivity in GRP::eGFP mice after noxious or pruritic stimulation. (A–C, D–F, G–I, and J–L) Representative fields from mice that were stimulated with histamine, pinch, noxious heat, or capsaicin, respectively. In each case, the same field from the superficial dorsal horn is shown immunostained for pERK (magenta), GFP (green), together with a merged image. Each stimulus resulted in numerous pERK$^+$ neurons, although GFP-labelled cells were rarely pERK-immunoreactive. Each set of images shows GFP$^+$ cells (some indicated with arrowheads), which are not immunostained for pERK, but are surrounded by pERK$^+$ neurons. In each case, one of the pERK$^+$ neurons is indicated with an arrow. Images are projections of 2 (A–C and J–L) or 3 (D–I) confocal optical sections at 2-μm z-spacing. Scale bar = 20 μm. GRP, gastrin-releasing peptide; pERK, phosphorylated extracellular signal–regulated kinase.

expressing nociceptors.[60] However, our finding that capsaicin increased mEPSC and sEPSC frequency in only 1/11 and 4/16 GRP neurons, respectively, suggests that TRPV1-expressing afferents seldom directly innervate GRP cells, although they do provide polysynaptic input to some of them. The potential involvement of GRP cells in nociceptive processing therefore remains to be established.

At first sight, our finding that GRP cells were inhibited by DAMGO is surprising because MOR agonists can cause itching.[63] However, it has been suggested that this is mediated by MOR1D-GRPR heterodimers on GRPR neurons.[39] Because these cells are believed to be located downstream of GRP cells in the spinal itch pathway, activation of the GRPR cells by morphine acting on these heterodimers would presumably override its inhibitory action on the GRP cells. The expression of MORs by GRP neurons suggests that endogenous release of MOR agonists (eg, endomorphin-2) from nociceptors will inhibit activity in the itch pathway, contributing to suppression of itch by noxious stimuli. Although KOR agonists are antipruritic, they are believed to act at the level of the GRPR cells,[30] consistent with the lack of response of GRP cells shown here. The finding that neither GRP nor SP cells responded to DOR agonist is consistent with the recent report that MOR and DOR are expressed by largely separate populations, with DOR-expressing cells being concentrated in lamina IIi.[68] It should be noted that in addition to their action on cell bodies and dendrites of dorsal horn neurons, opioid peptides can also act on axon terminals to modify synaptic transmission. Little is known about the role of monoaminergic systems in itch, although tricyclic antidepressants, which potentiate monoamine transmission, are used to treat pruritus.[37] The lack of effect of NA and 5-HT on GRP cells suggests that they act elsewhere in the itch pathway.

We found that there were consistently fewer GRP-eGFP cells in glabrous skin territory, and in situ hybridisation revealed that this was not due solely to lack of GRP-expressing neurons in this region. This variability in GFP expression presumably reflects transcriptional heterogeneity between GRP cells innervated from hairy and glabrous skin, and may be related to differences in itch sensation from these 2 skin types.[67] As the GRP cells are relatively numerous, they presumably correspond to one or more of the populations identified by Grudt and Perl.[22] Although many excitatory interneurons in lamina II show delayed/gap/reluctant firing,[29,49,73] this was seldom seen for GRP cells, which generally showed transient or single-spike firing. Because the GRP cells had dendritic trees that were moderately elongated along the RC axis, many of them are likely to correspond to the "transient central" population of Grudt and Perl. Interestingly, transient central cells have been implicated in a circuit linking low-threshold

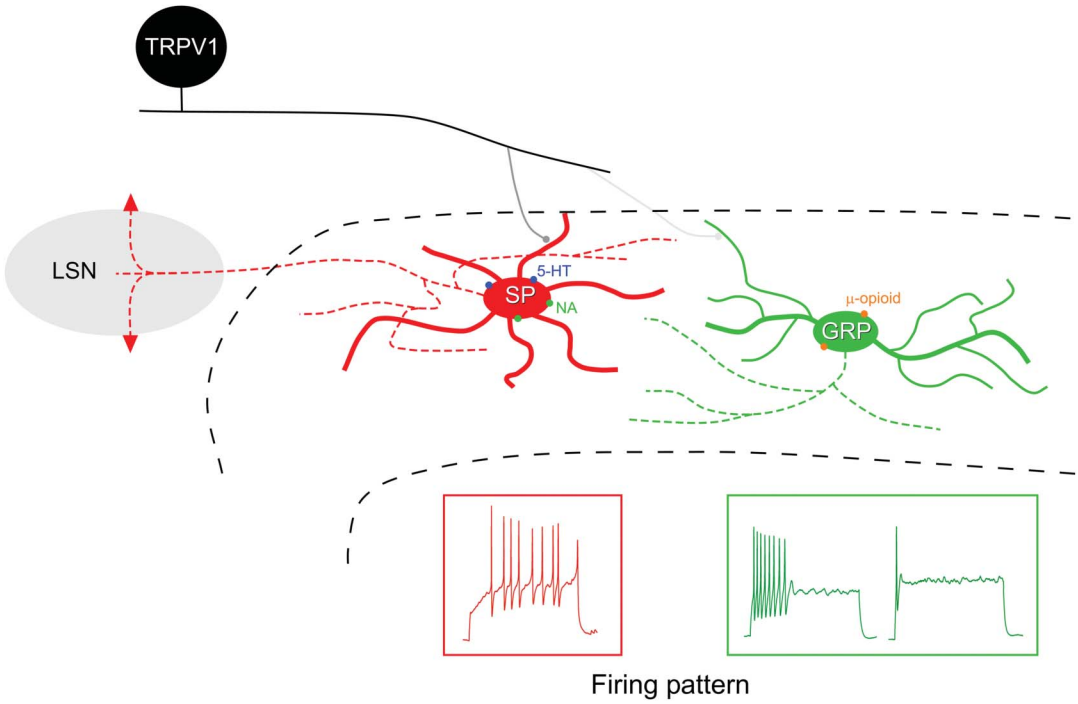

Figure 12. A diagram showing major differences that were detected between excitatory interneurons that express substance P (SP) and gastrin-releasing peptide (GRP). One cell of each type is represented on a transverse section of the dorsal horn, with dashed black lines indicating the borders of lamina II. The SP cells have more primary dendrites than the GRP cells, and typically show radial morphology, whereas the GRP cells were either central or unclassified cells. Note that these definitions are based on the somatodendritic morphology as seen in sagittal sections. Axons of both types (indicated with dashed lines of the corresponding colour) arborise locally in lamina II, whereas the SP cells also project to the lateral spinal nucleus (LSN), giving rise to propriospinal axons within this nucleus. Substance P cells generally responded (with outward current) to the monoamines noradrenaline (NA) and 5-hydroxytryptamine (5-HT), whereas the GRP cells responded with outward current to μ-opioid agonist. Around half of the SP cells showed an increase in mEPSC frequency in response to bath-applied capsaicin, indicating monosynaptic input from TRPV1-expressing primary afferents. However, this was only seen for 1 of 11 GRP cells tested, suggesting that these cells are seldom innervated directly by these afferents. The firing patterns in response to injected depolarising current pulses also differed, with most SP cells showing delayed firing, and GRP cells generally having transient or single-spike patterns. mEPSC, miniature excitatory postsynaptic current.

mechanoreceptive afferents to lamina I projection neurons, which is believed to contribute to tactile allodynia.[40,41] It will therefore be important to determine whether the cells in this putative circuit include GRP-expressing neurons, and how this relates to their proposed role in itch.

4.2. Substance P–expressing excitatory interneurons are radial cells

Unlike GRP cells, most SP neurons (79.2%) showed delayed firing, with a few having gap or reluctant patterns. As ~10% of the cells labelled with this strategy are inhibitory interneurons,[23] which seldom show these firing patterns, the proportion of excitatory SP interneurons with delayed/gap/reluctant firing is presumably even higher. Cluster analysis revealed a clear difference in dendritic morphology between SP and GRP cells. Substance P cells had significantly more primary dendrites, characteristic of radial cells. Alba-Delgado et al.[3] reported that some PKCγ-immunoreactive cells in lamina II of the medullary dorsal horn have radial morphology. However, unlike the radial cells described here and in previous studies,[22,73] PKCγ cells do not show delayed firing.[3,40] Among other differences, SP cells showed higher mEPSC frequencies than GRP cells, suggesting that they receive more excitatory synapses. Consistent with radial cells receiving both Aδ and C inputs,[22,71] 4 of 9 SP neurons showed a TRPV1-dependent, capsaicin-evoked increase in mEPSC frequency.

Little is known about the neuronal circuits engaged by radial cells. We previously reported that many excitatory SP neurons are activated by noxious or pruritic stimuli, and that many have long propriospinal axons targeting the LSN.[23,25] Interestingly, Grudt and Perl[22] reported that most radial cells had axons that ran rostrally and/or caudally in the dorsolateral fasciculus, consistent with our finding of propriospinal projections from these cells to the LSN. The SP cells may therefore contribute to the large cutaneous receptive fields, characteristic of LSN neurons in inflammatory pain states.[55] Conceivably, this circuit serves a protective role because extension of pain beyond the site of damage would limit use of an injured limb during recovery. The scarcity of GRP cells among propriospinal interneurons probably reflects the different behavioural requirement for itch, where spatial acuity is needed to remove the underlying cause by scratching or biting.

Most SP cells were inhibited by NA and 5-HT, and similar results have been found for radial cells in rats.[42,73] Inhibition of these cells from the brainstem may therefore contribute to the antinociceptive actions of descending monoaminergic pathways. Glycinergic neurons in deeper laminae of the dorsal horn provide another source of inhibition for radial cells,[71] and it has been proposed that reduction in glycinergic input to radial cells contributes to neuropathic pain.[33]

Together, these findings suggest that the excitatory SP interneurons correspond to the radial cells identified by Grudt and Perl,[22] and that they play an important role in pain mechanisms.

4.3. Excitatory interneuron populations

Two recent transcriptomic studies[27,53] have defined neurochemically distinct populations of dorsal horn excitatory neurons. Although both studies identified the SP, NKB, and neurotensin populations that we previously described,[25,66] only one recognised the GRP cells as a distinct population.[53] In that study, the GRP (but not SP) population was reported to express the MOR gene (OPMR1), consistent with our finding that GRP (but not SP) cells possess functional MORs. Haring et al.[27] did not detect a specific population of GRP-expressing cells, and reported considerable overlap between GRP and Tac1 mRNAs. However, our in situ hybridisation data clearly show that GRP-expressing cells in lamina II differ from those that express SP, suggesting that they are indeed a distinct neurochemical population.

Vertical cells constitute a well-defined class of excitatory interneurons, with cell bodies in lamina IIo and ventrally directed dendrites.[22,43,49,71–73] They are presynaptic to lamina I projection neurons[12,41] and have been implicated in transmitting low-threshold mechanoreceptive information to the projection cells, thus contributing to tactile allodynia.[40] The present results show that neither SP nor GRP populations include vertical cells, and because the neurotensin and NKB neurons are found in laminae IIi and III, these are also unlikely to include vertical cells. Finding the neurochemical signature of vertical cells is therefore a high priority. In this regard, we recently identified a cluster of dynorphin-expressing excitatory interneurons with vertical cell morphology; however, these are largely restricted to glabrous skin territory.[30] Two additional classes of excitatory interneuron identified in transcriptomic studies consist of cells that express neuropeptide FF or the neuromedin 2 receptor (NMUR2),[27,53] and in both cases, the cells are concentrated in lamina IIo.[11,27] It will therefore be important to test whether either of these populations corresponds to vertical cells, as this would allow for selective genetic targeting of these cells to investigate their role in spinal pain circuits. Because both SP and GRP populations have axons that arborise mainly in lamina II, vertical cells may also provide the route through which these cells can activate lamina I projection neurons. Defining the circuits that link the different populations of excitatory interneurons will therefore be of considerable importance.

Conflict of interest statement

The authors have no conflicts of interest to declare.

Acknowledgements

The authors are grateful to Robert Kerr and Christine Watt for expert technical help and to Drs Kieran Boyle, Mark Hoon, and Toshiharu Yasaka for helpful discussion. Financial support from the Wellcome Trust (grant 102645) and the Biotechnology and Biological Sciences Research Council (grant N006119/1) is gratefully acknowledged.

Supplemental video content

Video content associated with this article can be found online at http://links.lww.com/PAIN/A665.

Article history:
Received 26 May 2018
Received in revised form 19 July 2018
Accepted 23 August 2018
Available online 20 September 2018

References

[1] Abraira VE, Ginty DD. The sensory neurons of touch. Neuron 2013;79:618–39.
[2] Al-Khater KM, Kerr R, Todd AJ. A quantitative study of spinothalamic neurons in laminae I, III, and IV in lumbar and cervical segments of the rat spinal cord. J Comp Neurol 2008;511:1–18.
[3] Alba-Delgado C, El Khoueiry C, Peirs C, Dallel R, Artola A, Antri M. Subpopulations of PKCgamma interneurons within the medullary dorsal horn revealed by electrophysiologic and morphologic approach. PAIN 2015;156:1714–28.
[4] Atasoy D, Aponte Y, Su HH, Sternson SM. A FLEX switch targets Channelrhodopsin-2 to multiple cell types for imaging and long-range circuit mapping. J Neurosci 2008;28:7025–30.
[5] Balachandar A, Prescott SA. Origin of heterogeneous spiking patterns from continuously distributed ion channel densities: a computational study in spinal dorsal horn neurons. J Physiol 2018;596:1681–97.
[6] Bell AM, Gutierrez-Mecinas M, Polgar E, Todd AJ. Spinal neurons that contain gastrin-releasing peptide seldom express Fos or phosphorylate extracellular signal-regulated kinases in response to intradermal chloroquine. Mol Pain 2016;12:1744806916649602.
[7] Bice TN, Beal JA. Quantitative and neurogenic analysis of the total population and subpopulations of neurons defined by axon projection in the superficial dorsal horn of the rat lumbar spinal cord. J Comp Neurol 1997;388:550–64.
[8] Braz J, Solorzano C, Wang X, Basbaum AI. Transmitting pain and itch messages: a contemporary view of the spinal cord circuits that generate gate control. Neuron 2014;82:522–36.
[9] Cai D, Cohen KB, Luo T, Lichtman JW, Sanes JR. Improved tools for the Brainbow toolbox. Nat Methods 2013;10:540–7.
[10] Cameron D, Polgar E, Gutierrez-Mecinas M, Gomez-Lima M, Watanabe M, Todd AJ. The organisation of spinoparabrachial neurons in the mouse. PAIN 2015;156:2061–71.
[11] Chamessian A, Young M, Qadri Y, Berta T, Ji RR, Van de Ven T. Transcriptional profiling of somatostatin interneurons in the spinal dorsal horn. Sci Rep 2018;8:6809.
[12] Cordero-Erausquin M, Allard S, Dolique T, Bachand K, Ribeiro-da-Silva A, De Koninck Y. Dorsal horn neurons presynaptic to lamina I spinoparabrachial neurons revealed by transynaptic labeling. J Comp Neurol 2009;517:601–15.
[13] Demsar J, Curk T, Erjavec A, Gorup C, Hocevar T, Milutinovic M, Mozina M, Polajnar M, Toplak M, Staric A, Stajdohar M, Umek L, Zagar L, Zbontar J, Zitnik M, Zupan B. Orange: data mining toolbox in python. J Mach Learn Res 2013;14:2349–53.
[14] Dickie AC, McCormick B, Lukito V, Wilson KL, Torsney C. Inflammatory pain reduces C fiber activity-dependent slowing in a sex-dependent manner, amplifying nociceptive input to the spinal cord. J Neurosci 2017;37:6488–502.
[15] Dressler GR, Douglass EC. Pax-2 is a DNA-binding protein expressed in embryonic kidney and Wilms tumor. Proc Natl Acad Sci U S A 1992;89:1179–83.
[16] Duan B, Cheng L, Bourane S, Britz O, Padilla C, Garcia-Campmany L, Krashes M, Knowlton W, Velasquez T, Ren X, Ross SE, Lowell BB, Wang Y, Goulding M, Ma Q. Identification of spinal circuits transmitting and gating mechanical pain. Cell 2014;159:1417–32.
[17] Foster E, Wildner H, Tudeau L, Haueter S, Ralvenius WT, Jegen M, Johannssen H, Hosli L, Haenraets K, Ghanem A, Conzelmann KK, Bosl M, Zeilhofer HU. Targeted ablation, silencing, and activation establish glycinergic dorsal horn neurons as key components of a spinal gate for pain and itch. Neuron 2015;85:1289–304.
[18] Ganley RP, Iwagaki N, Del Rio P, Baseer N, Dickie AC, Boyle KA, Polgar E, Watanabe M, Abraira VE, Zimmerman A, Riddell JS, Todd AJ. Inhibitory interneurons that express GFP in the PrP-GFP mouse spinal cord are morphologically heterogeneous, innervated by several classes of primary afferent and include lamina I projection neurons among their postsynaptic targets. J Neurosci 2015;35:7626–42.
[19] Gong S, Zheng C, Doughty ML, Losos K, Didkovsky N, Schambra UB, Nowak NJ, Joyner A, Leblanc G, Hatten ME, Heintz N. A gene expression atlas of the central nervous system based on bacterial artificial chromosomes. Nature 2003;425:917–25.
[20] Graham BA, Brichta AM, Callister RJ. In vivo responses of mouse superficial dorsal horn neurones to both current injection and peripheral cutaneous stimulation. J Physiol 2004;561:749–63.

[21] Graham BA, Brichta AM, Schofield PR, Callister RJ. Altered potassium channel function in the superficial dorsal horn of the spastic mouse. J Physiol 2007;584:121–36.
[22] Grudt TJ, Perl ER. Correlations between neuronal morphology and electrophysiological features in the rodent superficial dorsal horn. J Physiol 2002;540:189–207.
[23] Gutierrez-Mecinas M, Bell AM, Marin A, Taylor R, Boyle KA, Furuta T, Watanabe M, Polgár E, Todd AJ. Preprotachykinin A is expressed by a distinct population of excitatory neurons in the mouse superficial spinal dorsal horn including cells that respond to noxious and pruritic stimuli. PAIN 2017;158:440–56.
[24] Gutierrez-Mecinas M, Furuta T, Watanabe M, Todd AJ. A quantitative study of neurochemically defined excitatory interneuron populations in laminae I-III of the mouse spinal cord. Mol Pain 2016;12: 1744806916629065.
[25] Gutierrez-Mecinas M, Polgár E, Bell AM, Herau M, Todd AJ. Substance P-expressing excitatory interneurons in the mouse superficial dorsal horn provide a propriospinal input to the lateral spinal nucleus. Brain Struct Funct 2018;223:2377–2392.
[26] Gutierrez-Mecinas M, Watanabe M, Todd AJ. Expression of gastrin-releasing peptide by excitatory interneurons in the mouse superficial dorsal horn. Mol Pain 2014;10:79.
[27] Haring M, Zeisel A, Hochgerner H, Rinwa P, Jakobsson JET, Lonnerberg P, La Manno G, Sharma N, Borgius L, Kiehn O, Lagerstrom MC, Linnarsson S, Ernfors P. Neuronal atlas of the dorsal horn defines its architecture and links sensory input to transcriptional cell types. Nat Neurosci 2018;21:869–880.
[28] Harris JA, Hirokawa KE, Sorensen SA, Gu H, Mills M, Ng LL, Bohn P, Mortrud M, Ouellette B, Kidney J, Smith KA, Dang C, Sunkin S, Bernard A, Oh SW, Madisen L, Zeng H. Anatomical characterization of Cre driver mice for neural circuit mapping and manipulation. Front Neural Circuits 2014;8:76.
[29] Heinke B, Ruscheweyh R, Forsthuber L, Wunderbaldinger G, Sandkuhler J. Physiological, neurochemical and morphological properties of a subgroup of GABAergic spinal lamina II neurones identified by expression of green fluorescent protein in mice. J Physiol 2004;560:249–66.
[30] Huang J, Polgar E, Solinski HJ, Mishra SK, Tseng PY, Iwagaki N, Boyle KA, Dickie AC, Kriegbaum MC, Wildner H, Zeilhofer HU, Watanabe M, Riddell JS, Todd AJ, Hoon MA. Circuit dissection of the role of somatostatin in itch and pain. Nat Neurosci 2018;21:707–16.
[31] Hughes DI, Scott DT, Todd AJ, Riddell JS. Lack of evidence for sprouting of Abeta afferents into the superficial laminas of the spinal cord dorsal horn after nerve section. J Neurosci 2003;23:9491–9.
[32] Hunt SP, Pini A, Evan G. Induction of c-fos-like protein in spinal cord neurons following sensory stimulation. Nature 1987;328:632–4.
[33] Imlach WL, Bhola RF, Mohammadi SA, Christie MJ. Glycinergic dysfunction in a subpopulation of dorsal horn interneurons in a rat model of neuropathic pain. Sci Rep 2016;6:37104.
[34] Iwagaki N, Ganley RP, Dickie AC, Polgár E, Hughes DI, Del Rio P, Revina Y, Watanabe M, Todd AJ, Riddell JS. A combined electrophysiological and morphological study of neuropeptide Y-expressing inhibitory interneurons in the spinal dorsal horn of the mouse. PAIN 2016;157: 598–612.
[35] Ji RR, Baba H, Brenner GJ, Woolf CJ. Nociceptive-specific activation of ERK in spinal neurons contributes to pain hypersensitivity. Nat Neurosci 1999;2:1114–19.
[36] Kim KK, Adelstein RS, Kawamoto S. Identification of neuronal nuclei (NeuN) as Fox-3, a new member of the Fox-1 gene family of splicing factors. J Biol Chem 2009;284:31052–61.
[37] Kouwenhoven TA, van de Kerkhof PCM, Kamsteeg M. Use of oral antidepressants in patients with chronic pruritus: a systematic review. J Am Acad Dermatol 2017;77:1068–73.e1067.
[38] Li L, Rutlin M, Abraira VE, Cassidy C, Kus L, Gong S, Jankowski MP, Luo W, Heintz N, Koerber HR, Woodbury CJ, Ginty DD. The functional organization of cutaneous low-threshold mechanosensory neurons. Cell 2011;147:1615–27.
[39] Liu XY, Liu ZC, Sun YG, Ross M, Kim S, Tsai FF, Li QF, Jeffry J, Kim JY, Loh HH, Chen ZF. Unidirectional cross-activation of GRPR by MOR1D uncouples itch and analgesia induced by opioids. Cell 2011;147:447–58.
[40] Lu Y, Dong H, Gao Y, Gong Y, Ren Y, Gu N, Zhou S, Xia N, Sun YY, Ji RR, Xiong L. A feed-forward spinal cord glycinergic neural circuit gates mechanical allodynia. J Clin Invest 2013;123:4050–62.
[41] Lu Y, Perl ER. Modular organization of excitatory circuits between neurons of the spinal superficial dorsal horn (laminae I and II). J Neurosci 2005;25:3900–7.
[42] Lu Y, Perl ER. Selective action of noradrenaline and serotonin on neurones of the spinal superficial dorsal horn in the rat. J Physiol 2007; 582:127–36.
[43] Maxwell DJ, Belle MD, Cheunsuang O, Stewart A, Morris R. Morphology of inhibitory and excitatory interneurons in superficial laminae of the rat dorsal horn. J Physiol 2007;584:521–33.
[44] McDonald JH. Handbook of biological statistics. Baltimore: Sparky House Publishing, 2014.
[45] Melzack R, Wall PD. Pain mechanisms: a new theory. Science 1965;150: 971–9.
[46] Mishra SK, Hoon MA. The cells and circuitry for itch responses in mice. Science 2013;340:968–71.
[47] Mullen RJ, Buck CR, Smith AM. NeuN, a neuronal specific nuclear protein in vertebrates. Development 1992;116:201–11.
[48] Polgár E, Gray S, Riddell JS, Todd AJ. Lack of evidence for significant neuronal loss in laminae I-III of the spinal dorsal horn of the rat in the chronic constriction injury model. PAIN 2004;111:144–50.
[49] Punnakkal P, von Schoultz C, Haenraets K, Wildner H, Zeilhofer HU. Morphological, biophysical and synaptic properties of glutamatergic neurons of the mouse spinal dorsal horn. J Physiol 2014;592:759–76.
[50] Roberson DP, Gudes S, Sprague JM, Patoski HA, Robson VK, Blasl F, Duan B, Oh SB, Bean BP, Ma Q, Binshtok AM, Woolf CJ. Activity-dependent silencing reveals functionally distinct itch-generating sensory neurons. Nat Neurosci 2013;16:910–18.
[51] Ruscheweyh R, Sandkuhler J. Lamina-specific membrane and discharge properties of rat spinal dorsal horn neurones in vitro. J Physiol 2002;541: 231–44.
[52] Sardella TC, Polgár E, Watanabe M, Todd AJ. A quantitative study of neuronal nitric oxide synthase expression in laminae I-III of the rat spinal dorsal horn. Neuroscience 2011;192:708–20.
[53] Sathyamurthy A, Johnson KR, Matson KJE, Dobrott CI, Li L, Ryba AR, Bergman TB, Kelly MC, Kelley MW, Levine AJ. Massively parallel single nucleus transcriptional profiling defines spinal cord neurons and their activity during behavior. Cell Rep 2018;22:2216–25.
[54] Seal RP, Wang X, Guan Y, Raja SN, Woodbury CJ, Basbaum AI, Edwards RH. Injury-induced mechanical hypersensitivity requires C-low threshold mechanoreceptors. Nature 2009;462:651–5.
[55] Sikandar S, West SJ, McMahon SB, Bennett DL, Dickenson AH. Sensory processing of deep tissue nociception in the rat spinal cord and thalamic ventrobasal complex. Physiol Rep 2017;5:e13323.
[56] Smith KM, Boyle KA, Madden JF, Dickinson SA, Jobling P, Callister RJ, Hughes DI, Graham BA. Functional heterogeneity of calretinin-expressing neurons in the mouse superficial dorsal horn: implications for spinal pain processing. J Physiol 2015;593:4319–39.
[57] Solorzano C, Villafuerte D, Meda K, Cevikbas F, Braz J, Sharif-Naeini R, Juarez-Salinas D, Llewellyn-Smith IJ, Guan Z, Basbaum AI. Primary afferent and spinal cord expression of gastrin-releasing peptide: message, protein, and antibody concerns. J Neurosci 2015;35:648–57.
[58] Spike RC, Puskar Z, Andrew D, Todd AJ. A quantitative and morphological study of projection neurons in lamina I of the rat lumbar spinal cord. Eur J Neurosci 2003;18:2433–48.
[59] Sterio DC. The unbiased estimation of number and sizes of arbitrary particles using the disector. J Microsc 1984;134:127–36.
[60] Sun S, Xu Q, Guo C, Guan Y, Liu Q, Dong X. Leaky gate model: intensity-dependent coding of pain and itch in the spinal cord. Neuron 2017;93:840–53.
[61] Sun YG, Chen ZF. A gastrin-releasing peptide receptor mediates the itch sensation in the spinal cord. Nature 2007;448:700–3.
[62] Sun YG, Zhao ZQ, Meng XL, Yin J, Liu XY, Chen ZF. Cellular basis of itch sensation. Science 2009;325:1531–4.
[63] Szarvas S, Harmon D, Murphy D. Neuraxial opioid-induced pruritus: a review. J Clin Anesth 2003;15:234–9.
[64] Ting JT, Daigle TL, Chen Q, Feng G. Acute brain slice methods for adult and aging animals: application of targeted patch clamp analysis and optogenetics. In: Martina M, Taverna S, editors. Patch-clamp methods and protocols. New York: Springer New York, 2014. p. 221–42.
[65] Todd AJ. Neuronal circuitry for pain processing in the dorsal horn. Nat Rev Neurosci 2010;11:823–36.
[66] Todd AJ. Identifying functional populations among the interneurons in laminae I-III of the spinal dorsal horn. Mol Pain 2017;13: 1744806917693003.
[67] Tuckett RP. Itch evoked by electrical stimulation of the skin. J Invest Dermatol 1982;79:368–73.
[68] Wang D, Tawfik VL, Corder G, Low SA, Francois A, Basbaum AI, Scherrer G. Functional divergence of delta and mu opioid receptor organization in CNS pain circuits. Neuron 2018;98:90–108.e105.
[69] Wang X, Zhang J, Eberhart D, Urban R, Meda K, Solorzano C, Yamanaka H, Rice D, Basbaum AI. Excitatory superficial dorsal horn interneurons are functionally heterogeneous and required for the full behavioral expression of pain and itch. Neuron 2013;78:312–24.
[70] Ward JL. Hierarchical grouping to optimize an objective function. J Am Stat Assoc 1963;58:236–44.

[71] Yasaka T, Kato G, Furue H, Rashid MH, Sonohata M, Tamae A, Murata Y, Masuko S, Yoshimura M. Cell-type-specific excitatory and inhibitory circuits involving primary afferents in the substantia gelatinosa of the rat spinal dorsal horn in vitro. J Physiol 2007;581: 603–18.
[72] Yasaka T, Tiong SY, Polgar E, Watanabe M, Kumamoto E, Riddell JS, Todd AJ. A putative relay circuit providing low-threshold mechanoreceptive input to lamina I projection neurons via vertical cells in lamina II of the rat dorsal horn. Mol Pain 2014;10:3.
[73] Yasaka T, Tiong SYX, Hughes DI, Riddell JS, Todd AJ. Populations of inhibitory and excitatory interneurons in lamina II of the adult rat spinal dorsal horn revealed by a combined electrophysiological and anatomical approach. PAIN 2010;151:475–88.
[74] Yoshida T, Fukaya M, Uchigashima M, Miura E, Kamiya H, Kano M, Watanabe M. Localization of diacylglycerol lipase-alpha around postsynaptic spine suggests close proximity between production site of an endocannabinoid, 2-arachidonoyl-glycerol, and presynaptic cannabinoid CB1 receptor. J Neurosci 2006;26:4740–51.

4 Paper III

Gutierrez-Mecinas, M., **Bell, A.M.,** Polgár, E., Watanabe, M., Todd, A.J., 2019. Expression of Neuropeptide FF Defines a Population of Excitatory Interneurons in the Superficial Dorsal Horn of the Mouse Spinal Cord that Respond to Noxious and Pruritic Stimuli. Neuroscience 416, 281–293.

CRediT statement

Conceptualization, A.J.T. and M.G.M.; Methodology, A.M.B., E.P., M.G.M. and A.J.T.; Formal analysis, A.M.B., M.G.M. and E.P.; Investigation, A.M.B., M.G.M. and E.P.; Resources, M.W.; Writing – Original Draft, A.J.T., A.M.B. and M.G.M.; Writing – Review & Editing, A.J.T., E.P., A.M.B. and M.G.M.; Visualization, A.J.T., A.M.B. and M.G.M.; Supervision, A.J.T.; Funding Acquisition, A.J.T.

Summary of practical involvement in components of study

In situ hybridisation experiments and analysis – A.M.B. primary role.
Antibody validation – A.M.B. primary role.
Immunohistochemical characterisation of Npff cells – M.G.M. primary role, A.M.B. secondary role.
Retrograde labelling of projection neurons – E.P. & A.J.T. primary role, A.M.B. no involvement.
Cellular responses by pERK immunohistochemistry – M.G.M. primary role, A.M.B. secondary role.

NEUROSCIENCE
RESEARCH ARTICLE
M. Gutierrez-Mecinas et al. / Neuroscience 416 (2019) 281–293

Expression of Neuropeptide FF Defines a Population of Excitatory Interneurons in the Superficial Dorsal Horn of the Mouse Spinal Cord that Respond to Noxious and Pruritic Stimuli

Maria Gutierrez-Mecinas, [a,1] **Andrew Bell,** [a,1] **Erika Polgár,** [a] **Masahiko Watanabe** [b] **and Andrew J. Todd** [a,*]

[a] *Institute of Neuroscience and Psychology, College of Medical, Veterinary and Life Sciences, University of Glasgow, Glasgow, G12 8QQ, UK*

[b] *Department of Anatomy, Hokkaido University School of Medicine, Sapporo 060-8638, Japan*

Abstract—The great majority of neurons in the superficial dorsal horn of the spinal cord are excitatory interneurons, and these are required for the normal perception of pain and itch. We have previously identified 5 largely non-overlapping populations among these cells, based on the expression of four different neuropeptides (cholecystokinin, neurotensin, neurokinin B and substance P) and of green fluorescent protein driven by the promoter for gastrin-releasing peptide (GRP) in a transgenic mouse line. Another peptide (neuropeptide FF, NPFF) has been identified among the excitatory neurons, and here we have used an antibody against the NPFF precursor (pro-NPFF) and a probe that recognises Npff mRNA to identify and characterise these cells. We show that they are all excitatory interneurons, and are separate from the five populations listed above, accounting for ~6% of the excitatory neurons in laminae I-II. By examining phosphorylation of extracellular signal-regulated kinases, we show that the NPFF cells can respond to different types of noxious and pruritic stimulus. Ablation of somatostatin-expressing dorsal horn neurons has been shown to result in a dramatic reduction in mechanical pain sensitivity, while somatostatin released from these neurons is thought to contribute to itch. Since the great majority of the NPFF cells co-expressed somatostatin, these cells may play a role in the perception of pain and itch.

Key words: NPFF; gastrin releasing peptide; neurokinin B; neurotensin; substance P; cholecystokinin.

INTRODUCTION

The superficial dorsal horn (laminae I-II) of the spinal cord receives excitatory synaptic input from primary sensory neurons that detect noxious, thermal and pruritic stimuli, and this information is conveyed to the brain *via* projection neurons belonging to the anterolateral tract (ALT) (Todd, 2010; Braz et al., 2014). Although the projection cells are concentrated in lamina I, they only account for ~1% of the neurons in the superficial dorsal horn (Abraira et al., 2017; Todd, 2017). The remaining nerve cells are defined as interneurons, and these have axons that remain within the spinal cord, where they contribute to local synaptic circuits (Peirs and Seal, 2016). Around 75% of the interneurons in laminae I-II are excitatory cells that use glutamate as their principal fast transmitter (Polgár et al., 2013). Behavioural assessment of mice in which excitatory interneurons in laminae I-II have been lost indicate that these cells are essential for the normal expression of pain and itch (Wang et al., 2013; Duan et al., 2014). However, the excitatory interneurons are heterogeneous in terms of their morphological, electrophysiological and neurochemical properties, and this has made it difficult to assign them to distinct functional populations (Todd, 2017).

We have identified 5 largely non-overlapping neurochemical populations among the excitatory interneurons in laminae I-II of the mouse spinal cord (Gutierrez-Mecinas et al., 2016, 2017, 2019). Cells belonging to 3 of these populations, which are defined by expression of neurotensin, neurokinin B (NKB, encoded by the Tac2 gene) and cholecystokinin (CCK), are concentrated in the inner part of lamina II, and extend into lamina III. These cells frequently co-express the γ isoform of protein kinase C (PKCγ). The other two populations consist of: (1) cells that express enhanced green

*Corresponding author at: Spinal Cord Group, Sir James Black Building, University of Glasgow, Glasgow, G12 8QQ, UK. Tel.: + 44 141 330 5868.
E-mail address: andrew.todd@glasgow.ac.uk (A. J. Todd).
[1] These authors contributed equally.
Abbreviations: ALT, anterolateral tract; CCK, cholecystokinin; CTb, cholera toxin B subunit; DAPI, 4′,6-diamidino-2-phenylindole; eGFP, enhanced green fluorescent protein; ERK, extracellular signal-regulated kinases; GRP, gastrin releasing peptide; LPb, lateral parabrachial area; LSN, lateral spinal nucleus; NKB, neurokinin B; NPFF, neuropeptide FF; pERK, phospho-ERK; PKCγ, protein kinase Cγ isoform.

https://doi.org/10.1016/j.neuroscience.2019.08.013
0306-4522/

fluorescent protein (eGFP) under control of the promoter for gastrin-releasing peptide (GRP) in a BAC transgenic mouse line (GRP-EGFP), and (2) cells that express the Tac1 gene, which codes for substance P (Dickie et al., 2019). The GRP-eGFP and substance P cells are located somewhat more dorsally than the other three populations, in the mid-part of lamina II. We have estimated that between them, these 5 populations account for around two-thirds of the excitatory interneurons in the superficial dorsal horn (Gutierrez-Mecinas et al., 2016, 2017, 2019). Our findings are generally consistent with the results of a recent transcriptomic study (Häring et al., 2018), which identified 15 clusters (named Glut1–15) among dorsal horn excitatory neurons. These included cells enriched with mRNAs for CCK (Glut1–3), neurotensin (Glut4), Tac2 (Glut5–7) and Tac1 (Glut10–11).

Another cluster identified by Häring et al. consisted of cells with mRNA for neuropeptide FF (NPFF; Glut9). Previous studies had identified NPFF-expressing cells in the superficial dorsal horn of rat spinal cord by using immunocytochemistry with anti-NPFF antibodies (Allard et al., 1991; Kivipelto and Panula, 1991). Both of these studies revealed a dense plexus of NPFF-immunoreactive axons in lamina I and the outer part of lamina II, which extended into the lateral spinal nucleus (LSN), together with scattered fibres in other regions including the intermediolateral cell column and the area around the central canal. Kivipelto and Panula (1991) also administered colchicine, which resulted in NPFF staining in cell bodies, and these were located throughout laminae I and II.

The aim of the present study was to identify and characterise NPFF-expressing cells in the mouse, by using a new antibody directed against the precursor protein pro-NPFF. In particular, our goal was to confirm that these were all excitatory interneurons and determine what proportion they accounted for, and to test the hypothesis that they formed a population that was distinct from those that we had previously identified. We also assessed their responses to different noxious and pruritic stimuli by testing for phosphorylation of extracellular signal-regulated kinases (ERK) (Ji et al., 1999).

EXPERIMENTAL PROCEDURES

Animals

All experiments were approved by the Ethical Review Process Applications Panel of the University of Glasgow, and were performed in accordance with the European Community directive 86/609/EC and the UK Animals (Scientific Procedures) Act 1986.

We used three genetically modified mouse lines during the course of this study. One was the BAC transgenic Tg(GRP-EGFP) in which enhanced green fluorescent protein (eGFP) is expressed under control of the GRP promoter (Gong et al., 2003; Gutierrez-Mecinas et al., 2014; Solorzano et al., 2015). We have recently shown that virtually all eGFP-positive cells in this line possess GRP mRNA, although the mRNA is found in many cells that lack eGFP (Dickie et al., 2019). We also used a line in which Cre recombinase (fused to the ligand binding domain of the oestrogen receptor) is inserted into the *Grpr* locus (GRPR-iCreERT2) (Mu et al., 2017), and this was crossed with the Ai9 reporter line, in which Cre-mediated excision of a STOP cassette drives expression of tdTomato. Both GRP-EGFP and $GRPR^{CreERT2}$; Ai9 mice were used for studies that assessed phosphorylated extracellular signal-regulated kinases (pERK) following noxious or pruritic stimuli. The use of $GRPR^{CreERT2}$; Ai9 mice for some of these experiments allowed us also to assess responses of GRPR-expressing neurons, and this will be reported in a separate study.

Four adult wild-type C57BL/6 mice of either sex (18–25 g) and 3 adult GRP-EGFP mice of either sex (20–31 g) were deeply anaesthetised (pentobarbitone, 20 mg i.p.) and perfused through the left cardiac ventricle with fixative containing 4% freshly depolymerised formaldehyde in phosphate buffer. Lumbar spinal cord segments were removed and post-fixed for 2 h, before being cut into transverse sections 60 μm thick with a vibrating blade microtome (Leica VT1200, Leica Microsystems, Milton Keynes, UK). These sections were used for stereological analysis of the proportion of neurons that were pro-NPFF-immunoreactive, and also to look for the presence of pro-NPFF in GRP-eGFP, somatostatin-immunoreactive and Pax2-immunoreactive cells.

In order to determine whether any of the pro-NPFF-immunoreactive cells were projection neurons, we used tissue from 3 male wild-type C57BL/6 mice (32–35 g) that had received injections of cholera toxin B subunit (CTb) targeted on the left lateral parabrachial area (LPb) as part of previously published study (Cameron et al., 2015). In all cases, the CTb injection filled the LPb on the left side. Transverse sections from the L2 segments of these mice, which had been fixed as described above, were used for this part of the study.

To look for evidence that pro-NPFF cells responded to noxious or pruritic stimuli, we performed immunostaining for pERK (Ji et al., 1999) on tissue from $GRPR^{CreERT2}$; Ai9 or GRP-EGFP mice. Twelve $GRPR^{CreERT2}$; Ai9 female mice (17–23 g) were used to investigate responses to pinch or intradermally injected pruritogens, and in all cases, this was carried out under urethane anaesthesia (40–60 mg urethane i.p.). For 3 of the mice, five skin folds on the left calf were pinched for 5 s each (Dickie et al., 2019), and after 5 min, the mice were perfused with fixative as described above. The remaining mice received intradermal injections of histamine (100 μg/10 μl PBS; 3 mice), chloroquine (100 μg/10 μl PBS; 3 mice) or vehicle (10 μl PBS; 3 mice) into the left calf, which had been shaved the day before. The success of the intradermal injections was verified by the presence of a small bleb in the skin (Roberson et al., 2013). We have previously shown that intradermal injections of vehicle result in pERK labelling if mice are allowed to survive for 5 mins after the stimulus, probably due to the noxious mechanical stimulus resulting from i.d. injection (Bell et al., 2016). However, if the mice survive 30 mins, pERK is seen in pruritogen-injected, but not vehicle-injected

Table 1. Antibodies used in this study.

Antibody	Species	Catalogue no	Dilution	Source
pro-NPFF	Guinea pig		0.83 μg/ml	M Watanabe
NeuN	Mouse	MAB377	1:500	Merck
eGFP	Chicken	ab13970	1:1000	Abcam
Pax2	Rabbit	HPA047704	1:200	Sigma
Somatostatin	Rabbit	T-4103	1:1000	Peninsula
CTb	Goat	703	1:1000	List Biological
pERK	Rabbit	9101	1:500	Cell Signalling Technology

animals, and this presumably reflects prolonged activation by the pruritogens. We therefore waited until 30 mins after the injections before intracardiac perfusion with fixative, which was carried out as described above. Tissue from 6 urethane-anaesthetised GRP-EGFP mice that had had the left hindlimb immersed in water at 52 °C for 15 s or had received a subcutaneous injection of capsaicin (10 μl, 0.25%) was also used. In these cases, the tissue was obtained from experiments that had formed part of a previously published study (Dickie et al., 2019), and injection of the vehicle for capsaicin had been shown to result in little or no pERK labelling. Capsaicin had initially been prepared at 1% by dissolving it in a mixture of 7% Tween 80 and 20% ethanol in saline. It was then diluted to 0.25% before injection.

Fluorescent *in situ* hybridisation was performed on lumbar spinal cord sections from 3 C57BL/6 mice (either sex, 18-20 g), tissue from which had been used in a previous study (Gutierrez-Mecinas et al., 2019).

Immunocytochemistry, confocal scanning and analysis

Multiple-labelling immunofluorescence reactions were performed as described previously (Gutierrez-Mecinas et al., 2017) on 60 μm thick transverse sections of spinal cord. The sources and concentrations of antibodies used are listed in Table 1. Sections were incubated for 3 days at 4 °C in primary antibodies diluted in PBS that contained 0.3 M NaCl, 0.3% Triton X-100 and 5% normal donkey serum, and then overnight in appropriate species-specific secondary antibodies (Jackson Immunoresearch, West Grove, PA) that were raised in donkey and conjugated to Alexa 488, Alexa 647, Rhodamine Red or biotin. All secondary antibodies were used at 1:500 (in the same diluent), apart from those conjugated to Rhodamine Red, which were diluted to 1:100. Biotinylated secondary antibodies were detected with Pacific Blue conjugated to avidin (1:1000; Life Technologies, Paisley, UK). Following the immunocytochemical reaction, sections were mounted in anti-fade medium and stored at −20 °C.

Sections from 3 wild-type mice were reacted with the following combinations of primary antibodies: (1) pro-NPFF and NeuN; (2) pro-NPFF, somatostatin and NeuN. Those reacted with the first combination were subsequently stained with the nuclear stain 4′6-diami dino-2-phenylindole (DAPI). Sections from 3 GRP-EGFP mice were reacted with the following combination: pro-NPFF, eGFP, Pax2 and NeuN. Sections from mice that had received injection of CTb into the LPb were reacted with antibodies against pro-NPFF, CTb and NeuN. Sections from mice that had undergone the various types of noxious or pruritic stimulation were reacted with antibodies against pro-NPFF, pERK and NeuN.

Sections were scanned with a Zeiss LSM 710 confocal microscope with Argon multi-line, 405 nm diode, 561 nm solid state and 633 nm HeNe lasers. Confocal image stacks were obtained through a 40 × oil immersion lens (numerical aperture 1.3) with the confocal aperture set to 1 Airy unit, and unless otherwise stated, the entire mediolateral width of laminae I-II was scanned to generate z-series of at least 20 μm (and in many cases the full thickness of the section), with a z-separation of 1 μm. Confocal scans were analysed with Neurolucida for Confocal software (MBF Bioscience, Williston, VT). The lamina II-III border was identified from the distribution of NeuN immunoreactivity, based on the relatively low neuronal packing density in lamina IIi. The lamina I-II border was assumed to be 20 μm from the dorsal edge of the dorsal horn (Ganley et al., 2015).

To determine the proportion of neurons in laminae I-II that are pro-NPFF-immunoreactive, we used a modification of the optical disector method (Polgár et al., 2004) on 2 sections each from 3 wild-type mice reacted with the first combination of antibodies. The reference and look-up sections were set 10 μm apart, and initially only the NeuN and DAPI channels were viewed. All intervening optical sections were examined, and neuronal

Table 2. RNAscope probes.

Probe	Protein/peptide	Channel numbers	Catalogue numbers	Z-pair number	Target region
Npff	Neuropeptide FF	2	479,901	9	47–433
Cck	CCK	1	402,271	12	23–679
Grp	Gastrin-releasing peptide	1	317,861	15	22–825
Nts	Neurotensin	3	420,441	20	2–1188
Tac1	Substance P	3	410,351	15	20–1034
Tac2	NKB	3	446,391	15	15–684
RNAscope multiplex positive control (Polr2a, Ppib, Ubc)	Polr2a: DNA-directed RNA polymerase II subunit RPB1; Ppib: Peptidyl-prolyl cis-trans isomerase B; Ubc: Polyubiquitin-C	1,2,3	320,881	20 15 n/a	2802–3678 98–856 34–860
RNAscope multiplex negative control (dapB)	dapB: 4-hydroxy-tetrahydrodipicolinate reductase (derived from B Subtilis)	1,2,3	320,871	10	414–862

nuclei (NeuN + /DAPI + structures) were selected if their bottom surface lay between the reference and look-up sections. These were plotted onto an outline drawing of the dorsal horn. The pro-NPFF channel was then switched on and the presence or absence of staining was determined for each of the selected neurons. To estimate the extent of co-localisation of NPFF and somatostatin, we scanned 2 sections that had been reacted with the 2nd antibody combination from each of 3 wild-type mice. The pro-NPFF and NeuN channels were viewed, and all pro-NPFF cells throughout the full thickness of the section were identified. The somatostatin channel was then switched on, and the presence or absence of somatostatin in each selected cell was noted. We searched for overlap between pro-NPFF and eGFP or Pax2 in two sections each from three GRP-EGFP mice. Again, all pro-NPFF-immunoreactive cells throughout the depth of the section were initially identified, and the presence or absence of eGFP and Pax2 was then determined. To test whether any of the pro-NPFF cells were projection neurons, we scanned and analysed between 4 and 7 sections from each of 3 mice that had received CTb injections into the LPb (Cameron et al., 2015). We identified all lamina I CTb + cells that were visible within each section and checked for the presence of pro-NPFF-immunoreactivity.

Analysis of ERK phosphorylation in pro-NPFF cells was performed as described previously (Bell et al., 2016; Gutierrez-Mecinas et al., 2017; Dickie et al., 2019). Sections that contained numerous pERK + cells were initially selected and scanned with the confocal microscope through the 40 × oil-immersion lens to generate z-stacks (1 μm z-separation) through the full thickness of the section so as to include the region of dorsal horn that contained pERK cells. The outline of the dorsal horn, together with the lamina II/III border, was plotted with Neurolucida, and the mediolateral extent of the region that contained a high density of pERK cells was delineated by drawing two parallel lines that were orthogonal to the laminar boundaries. The channels corresponding to NeuN and pro-NPFF were initially viewed, and all pro-NPFF + cells within this region were plotted onto the drawing. The pERK channel was then viewed, and the presence or absence of staining in each of the selected pro-NPFF cells was noted.

Fluorescent in situ hybridization histochemistry

Multiple-labelling fluorescent *in situ* hybridisation was performed with RNAscope probes and RNAscope fluorescent multiplex reagent kit 320,850 (ACD BioTechne; Newark, CA 94560). Fresh frozen lumbar spinal cord segments from 3 wild-type mice were embedded in OCT mounting medium and cut into 12 μm thick transverse sections with a cryostat (Leica CM1950; Leica; Milton Keynes, UK). These were mounted non-sequentially (such that sections on the same slide were at least 4 apart) onto SuperFrost Plus slides (48311–703; VWR; Lutterworth, UK) and air dried. Reactions were carried out according to the manufacturer's recommended protocol. The probes used in this study, and the proteins/peptides that they correspond to, are listed in Table 2. Sections from 3 mice were incubated in the following probe combinations: (1) Npff, Grp, Tac1; (2) Npff, Cck, Tac2; (3) Npff, Nts. Probes were revealed with Alexa 488 (Npff), Atto 550 (Grp, Cck) and Alexa 647 (Tac1, Tac2 and Nts). Sections were mounted with Prolong-Glass anti-fade medium with NucBlue (Hoechst 33342) (ThermoFisher Scientific, Paisley, UK). Positive and negative control probes were also tested on other sections (Table 2).

Sections were scanned with a Zeiss LSM 710 confocal microscope as above. Since the sections reacted with each probe combination were obtained from a 1 in 4 series, there was at least 36 μm separation between the scanned sections. Confocal image stacks were obtained through the 40 × oil immersion lens with the confocal aperture set to 1 Airy unit, and the entire mediolateral width of laminae I-II was scanned to generate a z-series of the full thickness of the section, with a z-separation of 2 μm. Confocal scans of 5 sections per animal were analysed with Neurolucida for Confocal software. Initially, only the channel corresponding to Npff mRNA was examined and all Npff positive NucBlue nuclei were identified. Then channels corresponding to other probes were viewed and any co-localisation noted. Cells were defined as positive for a particular mRNA if greater than 4 transcripts were present in the nucleus or immediate perinuclear area.

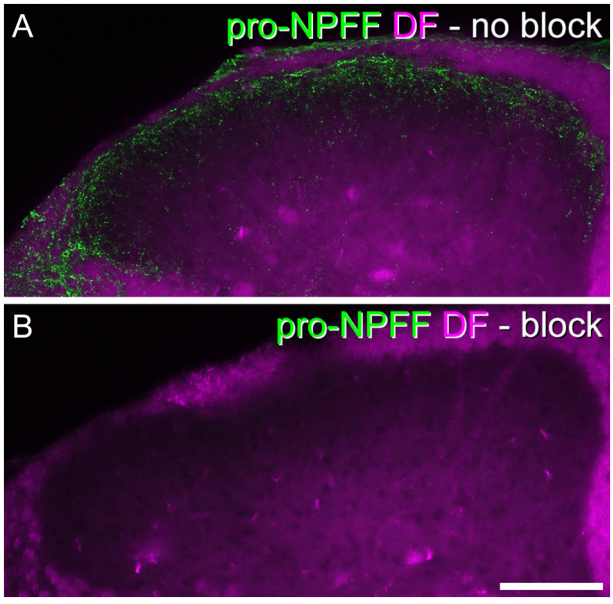

Fig. 1. Blocking of pro-NPFF immunostaining by pre-absorption with the antigen. A: transverse section from the L3 segment of a mouse, reacted with pro-NPFF antibody. Pro-NPFF-immunoreactivity (green) is superimposed on a dark-field image (magenta). B: A section reacted with pro-NPFF antibody that had been pre-absorbed overnight with 4.4 μg/ml of antigen, and scanned under identical conditions. The immunoreactivity has been completely abolished. Both images are maximum intensity projections of 11 optical sections at 2 μm z-spacing. Scale bar = 100 μm. (For interpretation of the references to colour in this figure legend, the reader is referred to the web version of this article.)

Characterization of antibodies

The sources and dilutions of primary antibodies used in the study are listed in Table 1. The pro-NPFF antibody was raised against a fusion protein consisting of glutathione S-transferase and amino acids 22–114 of the mouse pro-NPFF protein (NCBI, NM_018787). Staining was completely abolished by pre-incubating the antibody at its normal working concentration (0.83 μg/ml) with the antigen at 4.4 μg/ml (Fig. 1). The mouse monoclonal antibody NeuN reacts with a protein in cell nuclei extracted from mouse brain (Mullen et al., 1992), which has subsequently been identified as the splicing factor Fox-3 (Kim et al., 2009). This antibody apparently labels all neurons but no glial cells in the rat spinal dorsal horn (Todd et al., 1998). The eGFP antibody was raised against recombinant full-length eGFP, and its distribution matched that of native eGFP fluorescence. The Pax2 antibody was raised against amino acids 268–332 of the human protein, and it has been shown that this labels essentially all GABAergic neurons in adult rat dorsal horn (Larsson, 2017). The somatostatin antiserum is reported to show 100% cross-reactivity with somatostatin-28 and somatostatin-25, but none with substance P, neuropeptide Y, or vasoactive intestinal peptide (manufacturer's specification), and we have shown that staining with this antibody is abolished by pre-incubation with 10 μg/ml somatostatin (Proudlock et al., 1993). The CTb antibody was raised against the purified protein, and specificity is demonstrated by the lack of staining in regions that did not contain injected or transported tracer. The pERK antibody detects p44 and p42 MAP kinase (Erk1 and Erk2) when these are phosphorylated either individually or dually at Thr202 and Tyr204 of Erk1 or Thr185 and Tyr187 of Erk2. This antibody does not cross-react with the corresponding phosphorylated residues of JNK/SAPK or of p38 MAP kinase, or with non-phosphorylated Erk1/2 (manufacturer's specification). Specificity is demonstrated by the lack of staining in non-stimulated areas (*e.g.* in the contralateral dorsal horn).

RESULTS

Pro-NPFF-immunoreactivity in the dorsal horn

Immunoreactivity for pro-NPFF was highly concentrated in the superficial dorsal horn (laminae I-II) and the LSN, with a distribution very similar to that reported previously in the rat with antibodies against NPFF (Allard et al., 1991; Kivipelto and Panula, 1991) (Fig. 2). At high magnification, most immunoreactive profiles resembled axon terminals, but there were also labelled cell bodies, in which the immunoreactivity was present in the perikaryal cytoplasm (Fig. 2B and C). These pro-NPFF-immunoreactive cell bodies were present throughout laminae I-II, but were most numerous in the dorsal half of this region. They were not seen in the LSN.

In the quantitative analysis with the disector technique, we identified a mean of 392 (range 323–444) NeuN-positive cells in laminae I-II per mouse (n = 3 mice), and found that 4.74% (3.83–6.36%) of these were pro-NPFF-immunoreactive. To test the prediction that pro-NPFF cells were excitatory (Häring et al., 2018), we looked for the presence of Pax2. This was carried out on tissue from the GRP-EGFP mouse, which also allowed us to determine whether there was any co-expression of pro-NPFF and eGFP. We identified a mean of 55.6 pro-NPFF cells in this tissue (50–66, n = 3 mice), and found that none of these were either Pax2- or eGFP-immunoreactive (Fig. 3). Somatostatin is expressed by many excitatory interneurons in the superficial dorsal horn (Gutierrez-Mecinas et al., 2016), and we therefore looked for co-localisation of pro-NPFF- and somatostatin-immunoreactivity. We identified 62.7 (56–67) pro-NPFF-immunoreactive cells in sections from 3 wild-type mice, and found that 85.3% (81.5–89.3%) of these were also immunoreactive for somatostatin (Fig. 4). There was

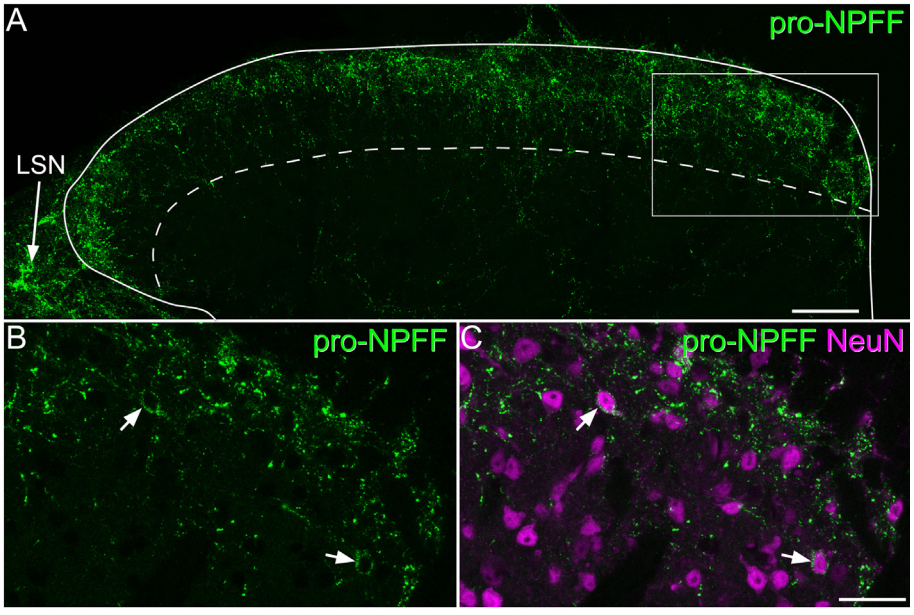

Fig. 2. Pro-NPFF-immunoreactivity in the dorsal horn and lateral spinal nucleus. A: transverse section through the L4 spinal segment of a mouse reacted with antibody against pro-NPFF (green). The dorsal horn outline is shown with a solid line and the lamina II-III border with a dashed line. There is a high density of immunoreactive axons in lamina I and the outer part of lamina II, with scattered profiles in deeper laminae. There is also a dense plexus in the lateral spinal nucleus (LSN) (arrow). The box indicates the area shown in B and C. B, C: a higher magnification view showing the relation of pro-NPFF (green) to NeuN (magenta). Two immunoreactive cell bodies are indicated with arrows. Note that the pro-NPFF immunostaining occupies the perikaryal cytoplasm, surrounding the nucleus (which is labelled strongly with the NeuN antibody). The images are maximum intensity projection of 23 optical sections (A) or 3 optical sections (B,C) at 1 μm z-separation. Scale bars: A = 50 μm; B, C = 25 μm. (For interpretation of the references to colour in this figure legend, the reader is referred to the web version of this article.)

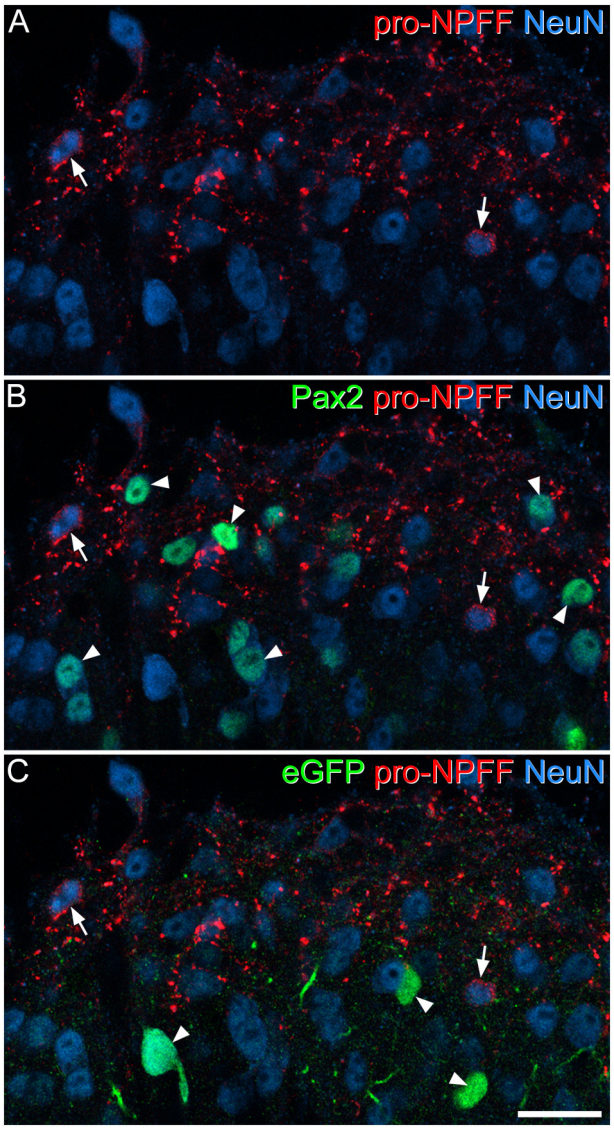

Fig. 3. Lack of co-localisation of pro-NPFF with either Pax2 or eGFP in the GRP-EGFP mouse. Part of the superficial dorsal horn of a GRP-EGFP mouse immunostained for pro-NPFF (red) and NeuN (blue), together with Pax2 and eGFP (both of which are shown in green, in B and C, respectively). A: Two pro-NPFF-immunoreactive cells are shown with arrows. These cells are negative for both Pax2 (B) and eGFP (C). Arrowheads in B and C show cells that are Pax2-immunoreactive (B) or eGFP-immunoreactive (C). Images are projections of 2 optical sections at 1 μm z-spacing. Scale bar = 20 μm. (For interpretation of the references to colour in this figure legend, the reader is referred to the web version of this article.)

also extensive co-localisation of pro-NPFF and somatostatin in axonal boutons.

Fluorescence in situ hybridization

The distribution of cells that contained Npff mRNA was the same as that of cells with pro-NPFF immunoreactivity. They were largely restricted to the superficial dorsal horn, and were most numerous in lamina I and the outer part of lamina II. In sections reacted with probes against Npff, Tac1 and Grp mRNAs, we identified 58.7 (51–65) Npff mRNA + cells in tissue from each of 3 mice. We found very limited overlap with Tac1, since only 4.6% (3.3–5.9%) of these cells were also Tac1 mRNA + (Fig. 5A, C, D). However, there was extensive overlap with the mRNA for Grp (Fig. 5A, B, D). Grp mRNA was found in 38% (28–47%) of Npff mRNA + cells, and this represented 6.3% (5.3–7.3%) of the Grp mRNA + cells in laminae I-II. In the sections reacted for Npff, Cck and Tac2 mRNAs, we identified 57 (53–62) Npff mRNA + cells from the 3 mice. None of these were positive for Tac2 mRNA, and only one was positive for Cck mRNA (corresponding to 0.6% of the Npff population) (Fig. 5E and F). In sections reacted for Npff and Nts mRNAs, we found 60.7 (56–68) Npff mRNA + cells in the 3 mice (Fig. 5G-I). Only two of these cells were Nts mRNA + (corresponding to 1% of the Npff population).

Lack of labelling of PNs

We identified a total of 111 CTb-labelled neurons in lamina I in the 3 animals that had received injections into the LPb (29–52 per mouse). None of the CTb-labelled cells were pro-NPFF-immunoreactive (Fig. 6).

pERK

The distribution of pERK-immunoreactivity in mice that had received noxious or pruritic stimuli was very similar to that described previously (Ji et al., 1999; Bell et al., 2016; Dickie et al., 2019). In each case, pERK-positive cells were only seen on the side ipsilateral to the stimulus, in the somatotopically appropriate region of the dorsal horn, and they were most numerous in the superficial laminae (I-II) (Fig. 7). Few, if any, pERK + cells were seen in mice that had received intradermal injection of vehicle. For each of the stimuli examined, we found that some pro-NPFF-immunoreactive cells were pERK-positive (Fig. 7, Table 3), although in many cases these cells showed relatively weak pERK immunoreactivity (Fig. 7C, F, O). For the noxious heat stimulus, and for both pruritogens (chloroquine, histamine), the proportion of pro-NPFF cells with pERK was around 30%, while for pinch and capsaicin injection the proportions were higher (around 50% and 60%, respectively; Table 3).

DISCUSSION

Our main findings are that the pro-NPFF antibody labels a population of excitatory interneurons in laminae I-II, that these cells account for nearly 5% of all neurons in this region, that they are distinct from cells belonging to other neurochemical populations that have recently been defined (Gutierrez-Mecinas et al., 2016, 2017, 2019), and that many of them respond to noxious and/or pruritic stimuli.

Technical considerations

The laminar pattern of staining with the pro-NPFF antibody closely matched that described previously for NPFF antibodies in rat spinal cord (Allard et al., 1991;

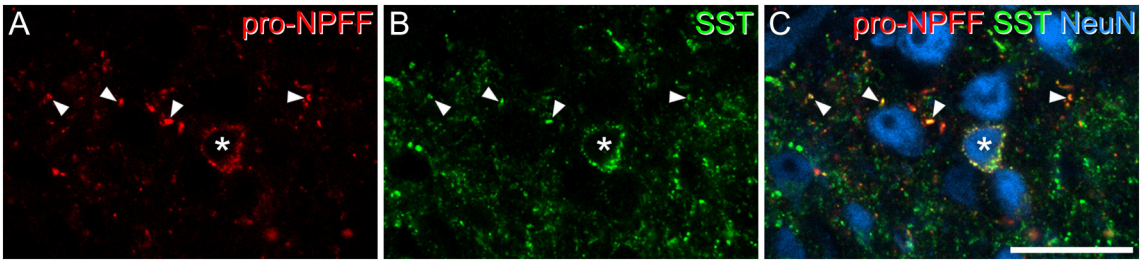

Fig. 4. Co-localisation of pro-NPFF and somatostatin in the superficial dorsal horn. A,B: Part of lamina II scanned to reveal pro-NPFF (red) and somatostatin (SST, green). C: the same field scanned to reveal both peptides, together with NeuN (blue). The asterisk shows a cell that contains both pro-NPFF and somatostatin in its perikaryal cytoplasm, and therefore expresses both peptides. Arrowheads point to varicosities that contain both types of peptide immunoreactivity, and presumably correspond to axon terminals. The image is from a single optical section. Scale bar = 20 μm. (For interpretation of the references to colour in this figure legend, the reader is referred to the web version of this article.)

Kivipelto and Panula, 1991), while the immunoreactive cell bodies showed a similar distribution to that seen with *in situ* hybridisation using NPFF probes. In addition, the lack of expression in Pax2-positive cells is consistent with the restriction of NPFF to excitatory neurons (Häring et al., 2018). Taken together with the finding that pre-absorption with the antigen blocked immunostaining, these observations suggest that this new antibody was indeed detecting NPFF-expressing neurons. Further confirmation of its specificity could be obtained in the future by testing the antibody on tissue from NPFF knock-out mice.

NPFF cells as a distinct population of excitatory interneurons

Earlier immunocytochemical and *in situ* hybridisation studies have shown a relatively high density of NPFF-expressing cells and processes in the superficial dorsal horn of the rodent spinal cord (Allard et al., 1991; Kivipelto and Panula, 1991; Lee et al., 1993; Panula et al., 1999; Vilim et al., 1999; Häring et al., 2018), with a distribution that closely matched that seen with the pro-NPFF antibody and the Npff mRNA probe in the present study. Häring et al. (2018) showed that these cells, which mainly represented their Glut9 cluster, co-expressed the mRNA for Slc17a6 (which codes for VGLUT2), indicating that these were excitatory neurons. This accords with our finding that pro-NPFF-expressing cells were invariably negative for Pax2-immunoreactivity, which is present in all inhibitory neurons in the dorsal horn (Cheng et al., 2004; Larsson, 2017).

None of the pro-NPFF-immunoreactive cells were retrogradely labelled with CTb that had been injected into the lateral parabrachial area, and since tracer injections into this region are thought to label virtually all projection neurons in lamina I (Todd, 2010; Cameron et al., 2015), it is likely that all of the NPFF cells are excitatory interneurons. We have previously reported that 76% of neurons in the mouse superficial dorsal horn are excitatory (Pax2-negative) (Polgár et al., 2013), and since we found pro-NPFF-immunoreactivity in 4.7% of lamina I-II neurons, we estimate that the NPFF-expressing cells account for around 6% of all excitatory neurons in this region. Our finding that the NPFF population showed virtually no overlap with those defined by expression of Cck, Nts or Tac2, and only minimal overlap with the Tac1 population is consistent with the findings of Haring et al., since these cells would correspond to those belonging to Glut1–3 (Cck), Glut4 (Nts), Glut5–7 (Tac2) and Glut10–11 (Tac1). We have also examined sections that had been immunostained for pro-NPFF together with various combinations of antibodies against neurotensin, preprotachykinin B (the precursor for NKB) and procholecystokinin (the precursor for CCK), and found no overlap of any of these with pro-NPFF (M Gutierrez-Mecinas and AJ Todd, unpublished data). With regard to GRP, there was an apparent discrepancy, since we found no overlap between pro-NPFF-immunoreactivity and eGFP expression in the GRP-EGFP mouse, but nearly 40% of the Npff mRNA + cells also contained Grp mRNA. By using multiple-label fluorescent *in situ* hybridisation we have found that although all Gfp mRNA + cells in this mouse line contain Grp mRNA, these only account for around 25% of the Grp mRNA + cells (AM Bell, unpublished observations). Interestingly, Häring et al. reported that Grp mRNA was widely distributed among several excitatory interneuron clusters (Glut5–12), whereas we have found that the GRP-eGFP-positive cells in lamina II form a relatively homogeneous population that shows very little overlap with neurons that express CCK, neurotensin, substance P or NKB (Gutierrez-Mecinas et al., 2016, 2019. Dickie et al., 2019). In addition, these cells show a unique somatotopic distribution, as they are far less frequent in regions that are innervated from glabrous skin (Dickie et al., 2019). This suggests that the GRP-eGFP cells represent a discrete functional population, even though Grp message is far more widely expressed.

We have previously estimated that the other neurochemical populations that we have identified (those that express neurokinin B, neurotensin, CCK, substance or GRP-eGFP) account for around two-thirds of the excitatory neurons in laminae I-II (Gutierrez-Mecinas et al., 2016, 2019; Dickie et al., 2019). With our finding that the NPFF population accounts for ~6% of excitatory neurons, this brings the total that can be assigned to one of these populations to ~75% of these cells (Fig. 8).

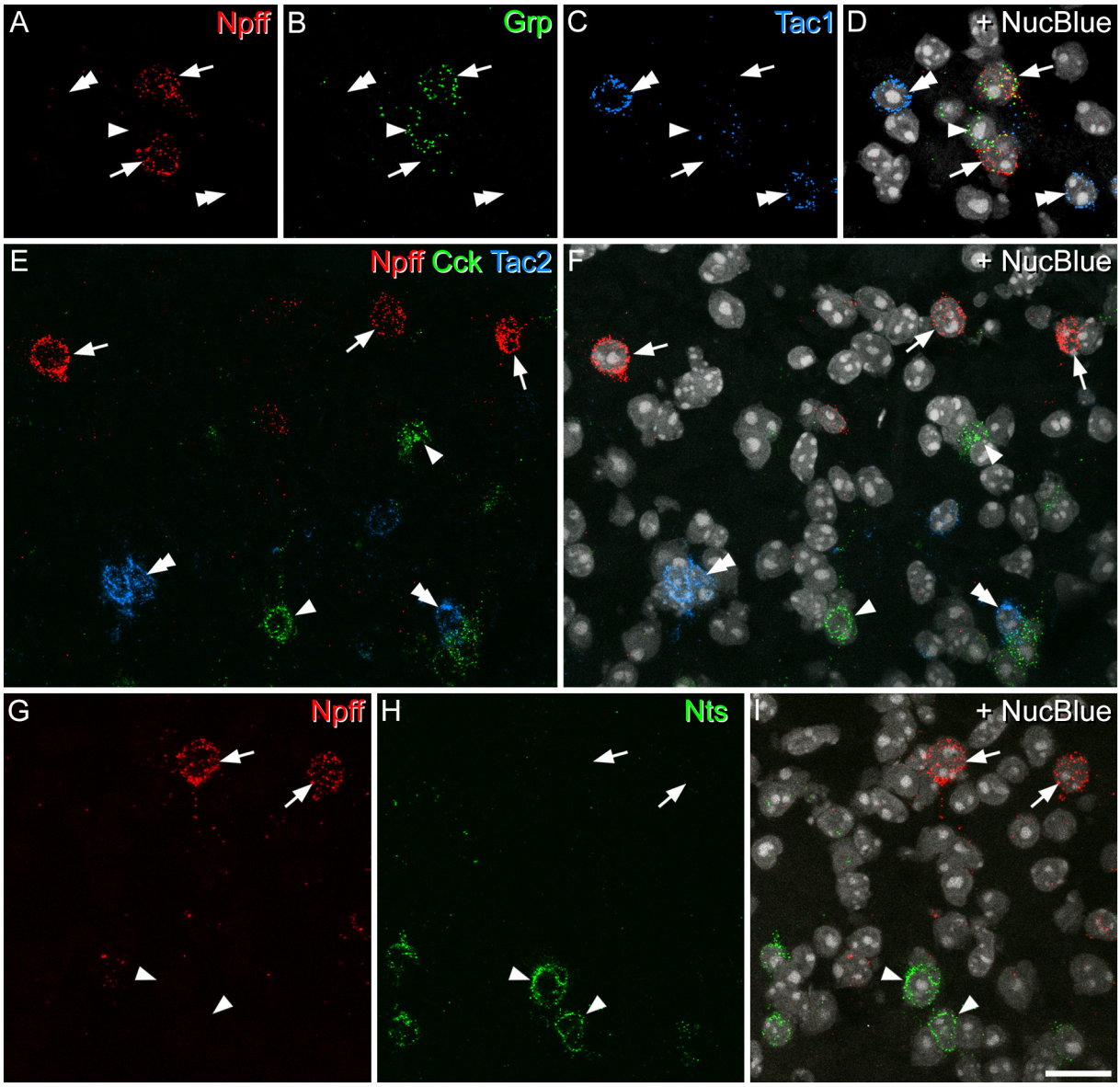

Fig. 5. Fluorescence *in situ* hybridisation for Npff and other neuropeptides. A-C show part of lamina II in a section reacted with probes for Npff (red), Grp (green) and Tac1 (blue) mRNAs. D is the same field, which has been scanned to reveal the nuclear counterstain NucBlue (grey). Two Npff mRNA + cells are indicated with arrows. These are both positive for Grp mRNA, but negative for Tac1 mRNA. Another cell with Grp mRNA only is shown with a single arrowhead, and two Tac1 mRNA + cells (which lack Npff and Grp mRNAs) are indicated with double arrowheads. E: part of laminae I and II scanned to reveal mRNAs for Npff (red), Cck (green) and Tac2 (blue). F: the same section also showing NucBlue (grey). Three Npff mRNA + cells are indicated with arrows, and these lack mRNAs for Cck or Tac2. Examples of cells with mRNA for Cck and Tac2 are shown with single and double arrowheads, respectively. G,H show part of laminae I and II scanned to reveal mRNAs for Npff (red) and Nts (green). I: The same field also showing NucBlue (grey). Two Npff mRNA + cells are indicated with arrows, and two Nts mRNA + cells with arrowheads. All images were projected from 2 optical sections at 2 μm z-separation. Scale bar = 20 μm. (For interpretation of the references to colour in this figure legend, the reader is referred to the web version of this article.)

The role of NPFF

Neuropeptide FF was initially isolated from bovine brainstem and characterised by Yang et al. (1985). The gene encoding the precursor protein pro-NPFF was subsequently identified and sequenced, and shown to code for both NPFF and an extended peptide known as neuropeptide AF (Perry et al., 1997). Initial studies demonstrated that intracerebroventricular injection of NPFF suppressed morphine analgesia (Yang et al., 1985). However, Gouarderes et al. (1993) reported that intrathecal NPFF caused a prolonged increase in both tail-flick latency and paw pressure threshold in rats, corresponding to an analgesic effect. In addition, NPFF enhanced the analgesic action of intrathecal morphine. A subsequent study suggested that the anti-nociceptive action of spinal NPFF involved both μ and δ opioid receptors, since it was reduced by co-administration of specific antagonists acting at both of these classes of opioid receptors, while

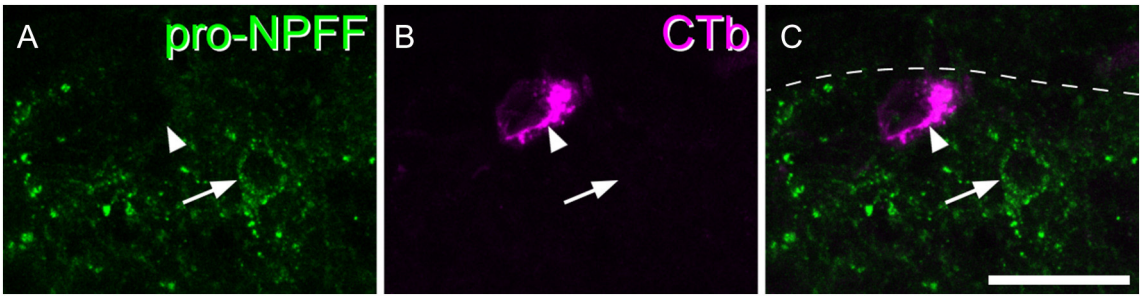

Fig. 6. Lack of pro-NPFF in lamina I projection neurons. A,B: part of lamina I from a mouse that had received an injection of cholera toxin B subunit (CTb) into the lateral parabrachial area on the contralateral side. A cell with pro-NPFF-immunoreactivity is indicated with an arrow, and a nearby CTb-labelled lamina I projection neuron with an arrowhead. C: merged image showing the two cells. The dashed line represents the dorsal border of lamina I. The image is a projection of 3 optical sections at 1 μm z-separation. Scale bar = 20 μm.

sub-effective doses of NPFF analogues enhanced the effect of both μ and δ opioid agonists administered intrathecally (Gouarderes et al., 1996).

Two G protein-coupled receptors for NPFF have been identified, and named NPFF-R1 and NPFF-R2 (Bonini et al., 2000; Elshourbagy et al., 2000; Hinuma et al., 2000). These both couple to G proteins of the Gi family (Ayachi and Simonin, 2014). NPFF-R2 is highly expressed in the spinal dorsal horn, as shown by both *in situ* hybridisation (Liu et al., 2001) and RT-PCR (Bonini et al., 2000; Yang and Iadarola, 2003), and the mRNA is also present in dorsal root ganglia (Bonini et al., 2000). This suggests that NPFF released from excitatory interneurons acts on NPFF-R2 expressed by both primary afferents and dorsal horn neurons (Yang et al., 2008). Primary afferents with mRNA for NPFF-R2 include those that express TRPM8 or MrgA3 (which are likely to be cold-sensitive and pruritoceptive, respectively) as well as peptidergic nociceptors (Zeisel et al., 2018). The antinociceptive action of NPFF is thought to involve opening of voltage-dependent potassium channels in primary afferent neurons (Mollereau et al., 2011). However, little is apparently known about the types of dorsal horn neuron that express the receptor. Binding sites for NPFF have also been identified in human spinal cord, with the highest levels in the superficial dorsal horn (Allard et al., 1994). This suggests that NPFF may also modulate nociceptive transmission in humans.

There is also evidence that expression of both NPFF and the NPFF-R2 are up-regulated in inflammatory, but not neuropathic, pain states (Kontinen et al., 1997; Vilim et al., 1999; Yang and Iadarola, 2003), and it has been suggested that this may contribute to the enhanced analgesic efficacy of morphine in inflammatory pain (Hylden et al., 1991; Yang et al., 2008).

Function of Npff cells

Häring et al. (2018) used expression of the immediate early gene Arc (which codes for activity-regulated cytoskeleton-associated protein) to assess activation of their neuronal populations in response to noxious heat and cold stimuli. They reported that cells belonging to the Glut9 cluster (which correspond to the NPFF-expressing excitatory interneurons) could upregulate Arc following both types of stimulus, with ~10% of these cells showing increased Arc mRNA after noxious heat. Our findings extend these observations, by showing that many NPFF cells were pERK-positive (and therefore activated), not only following noxious heat, but also after other noxious (pinch, capsaicin) and pruritic (histamine, chloroquine) stimuli. We have previously reported that among all neurons in laminae I-II, between 20 and 37% show pERK-immunoreactivity with the different stimuli that were used in this study (Table 3) (Bell et al., 2016; Dickie et al., 2019). Comparison with the results for the NPFF cells, suggests that for most of the stimuli the NPFF cells were at least as likely to show pERK as other neurons in this region, while in the case of pinch and capsaicin they appear to be more likely to be activated. Since each experiment involved only a single type of stimulus, we cannot determine whether there was convergence of different types of nociceptive, or of nociceptive and pruritoceptive inputs onto individual cells. The proportions that we identified as being pERK-positive are therefore likely to have underestimated the fraction of cells that respond to one or more of these stimuli.

Since the NPFF cells are glutamatergic interneurons, their main action is presumably through glutamatergic synapses with other dorsal horn cells. Part of the NPFF axonal plexus lies in lamina I, where it may target ALT projection cells. In addition, the NPFF axons that enter the LSN have been shown to form contacts with spinothalamic neurons in this region in the rat (Aarnisalo and Panula, 1998), although synaptic connections were not identified in that study. However, many of the NPFF axons remain in lamina II, where dendrites of projection neurons are relatively infrequent (Todd, 2010). It is therefore likely that they engage in complex synaptic circuits that transmit nociceptive and pruritoceptive information (Peirs and Seal, 2016; Huang et al., 2018). Cells in laminae IIi-III that express PKCγ are thought to form part of a polysynaptic pathway that can convey low-threshold mechanoreceptive inputs to nociceptive projection neurons in lamina I under conditions of disinhibition, and thus contribute to tactile allodynia (Lu et al., 2013). However, much less is known about the roles of excitatory interneurons in circuits that underlie acute mechanical or thermal pain, or those that are responsible for hyperalgesia in either inflammatory or neuropathic pain states.

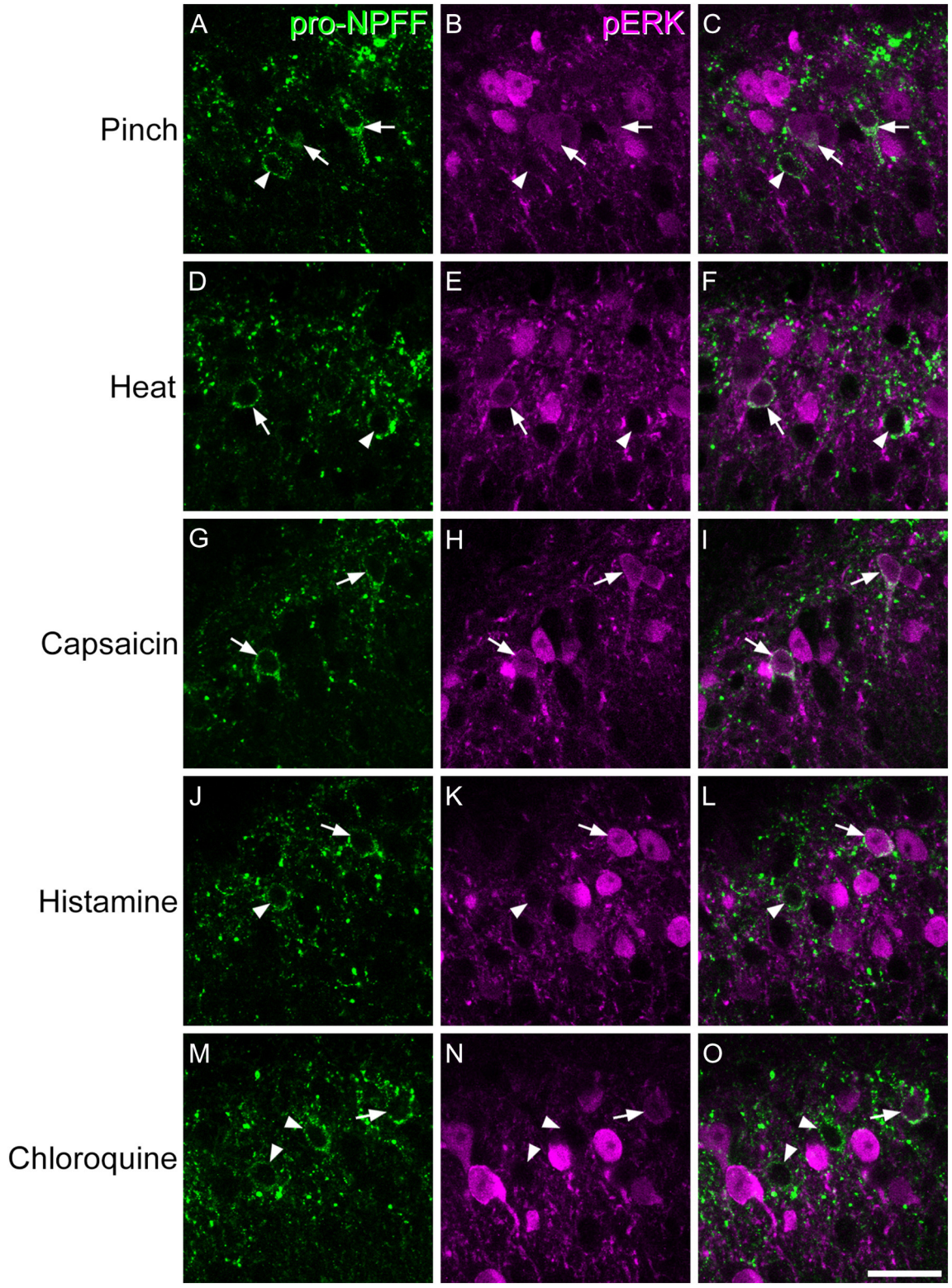

Fig. 7. Phosphorylation of extracellular signal-regulated kinases in NPFF-expressing neurons. Each row shows part of the superficial dorsal horn immunostained for pro-NPFF (green; A,D,G,J,M), pERK (magenta; B,E,H,K,N) together with a merged image (C,F,I,L,O), following pinch (A-C), noxious heat (D-F), intraplantar capsaicin (G-I), intradermal histamine (J-L) or intradermal chloroquine (M-O). Pro-NPFF cells that are pERK + are indicated with arrows, and those that lack pERK with arrowheads. Note that some of the pro-NPFF cells show relatively weak pERK immunoreactivity. Images are from single optical sections (G-I) or from maximum projections of 2 (A-C, J-L, M-O) or 3 (D-F) optical sections at 1 μm z-separation. Scale bar = 20 μm. (For interpretation of the references to colour in this figure legend, the reader is referred to the web version of this article.)

Table 3. NPFF cells that were pERK positive following noxious or pruritic stimuli.

Stimulus	NPFF$^+$ neurons	NPFF$^+$ and pERK$^+$	% NPFF neurons pERK$^+$	% of all neurons in laminae I-II with pERK
Pinch	82.3 (71–92)	41.6 (26–50)	49.8% (36.6–58.3%)	37%
Noxious heat	104.7 (102–110)	31.7 (27–39)	30.1% (26.5–35.5%)	23%
Capsaicin	90 (80–102)	55.7 (50–63)	62% (56.8–67.5%)	27%
Histamine	91 (76–109)	30 (28–34)	33.3% (31.5–36.8%)	33%
Chloroquine	114.3 (95–132)	37.7 (27–56)	32.2% (25.9–42.4%)	21%*

Column 2–4 show the number of NPFF cells identified within the zone that showed pERK, the number of NPFF/pERK double-labelled cells, and the proportion of NPFF cells with pERK, respectively. The 5th column shows the proportion of all neurons in laminae I-II that were found to be pERK-immunoreactive with equivalent stimuli in previous studies (Bell et al., 2016; Dickie et al., 2019). *Note that the proportion of laminae I-II neurons that were pERK + after chloroquine (21%) was estimated in experiments involving a lower dose of chloroquine (40 μg) than that used in the present study (100 μg) (Bell et al., 2016).

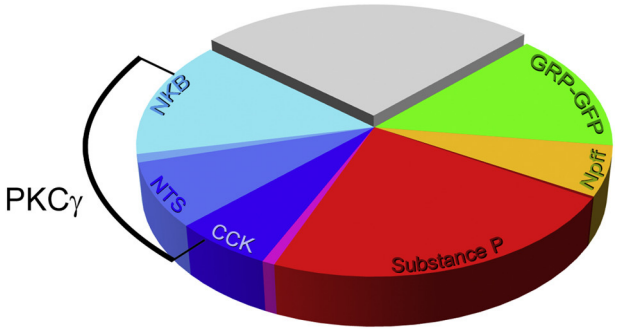

Fig. 8. Pie chart showing the relative sizes of different neurochemical populations among the excitatory interneurons in laminae I-II of the mouse dorsal horn. Note that the neurokinin B (NKB), neurotensin (NTS), cholecystokinin (CCK), substance P, NPFF and GRP-eGFP cells form largely non-overlapping populations, although there is some overlap between NKB/NTS and CCK/substance P populations. Protein kinase Cγ (PKCγ) is expressed by many of the NTS, and some of the NKB and CCK cells. The pie chart is based on quantitative data from the present study and from previous studies (Gutierrez-Mecinas et al., 2016, 2019; Dickie et al., 2019).

Interestingly, we found that the great majority of the NPFF cells were somatostatin-immunoreactive, and are therefore likely to have been affected in previous studies that manipulated the function of somatostatin-expressing dorsal horn neurons (Duan et al., 2014; Christensen et al., 2016). Since these studies implicated somatostatin cells in acute mechanical pain, as well as tactile allodynia in neuropathic and inflammatory pain states, our finding suggests that NPFF cells may contribute to these forms of pain. The somatostatin released by NPFF neurons that were activated by intradermal injection of pruritogens may be involved in itch, since somatostatin released from dorsal horn interneurons is thought to cause itch by a disinhibitory mechanism involving inhibitory interneurons that express the somatostatin 2a receptor (Huang et al., 2018). Assessing the roles of NPFF cells in spinal pain and itch mechanisms will require a method for selectively targeting them, presumably involving a genetically altered mouse line in which NPFF cells express a recombinase.

These results show that NPFF is expressed by a distinct population that accounts for around 6% of the excitatory interneurons in laminae I and II, and that these cells are frequently activated by noxious or pruritic stimuli.

ACKNOWLEDGEMENTS

We thank Mr. R. Kerr and Mrs. C. Watt for expert technical assistance and Dr. YanGang Sun for the generous gift of GRPR^{CreERT2} mice. Financial support from the Wellcome Trust (grant 102645), the Biotechnology and Biological Sciences Research Council (grant BB/N006119/1) and the Medical Research Council (grant MR/S002987/1) is gratefully acknowledged.

REFERENCES

Aarnisalo AA, Panula P (1998) Neuropeptide FF in the lateral spinal and lateral cervical nuclei: evidence of contacts on spinothalamic neurons. Exp Brain Res 119:159–165.

Abraira VE, Kuehn ED, Chirila AM, Springel MW, Toliver AA, Zimmerman AL, Orefice LL, Boyle KA, Bai L, Song BJ, Bashista KA, O'Neill TG, Zhuo J, Tsan C, Hoynoski J, Rutlin M, Kus L, Niederkofler V, Watanabe M, Dymecki SM, Nelson SB, Heintz N, Hughes DI, Ginty DD (2017) The cellular and synaptic architecture of the mechanosensory dorsal horn. Cell 168(295–310) e219.

Allard M, Theodosis DT, Rousselot P, Lombard MC, Simonnet G (1991) Characterization and localization of a putative morphine-modulating peptide, FLFQPQRFamide, in the rat spinal cord: biochemical and immunocytochemical studies. Neuroscience 40:81–92.

Allard M, Jordan D, Zajac JM, Ries C, Martin D, Monkouanga D, Kopp N, Simonnet G (1994) Autoradiographic localization of receptors for neuropeptide FF, FLFQPQRFamide, in human spinal sensory system. Brain Res 633:127–132.

Ayachi S, Simonin F (2014) Involvement of the mammalian RF-amide peptides and their receptors in the modulation of nociception in rodents. Front Endocrinol 5:158.

Bell AM, Gutierrez-Mecinas M, Polgar E, Todd AJ (2016) Spinal neurons that contain gastrin-releasing peptide seldom express Fos or phosphorylate extracellular signal-regulated kinases in response to intradermal chloroquine. Mol Pain 12:1744806916649602.

Bonini JA, Jones KA, Adham N, Forray C, Artymyshyn R, Durkin MM, Smith KE, Tamm JA, Boteju LW, Lakhlani PP, Raddatz R, Yao WJ, Ogozalek KL, Boyle N, Kouranova EV, Quan Y, Vaysse PJ, Wetzel JM, Branchek TA, Gerald C, Borowsky B (2000) Identification and characterization of two G protein-coupled receptors for neuropeptide FF. J Biol Chem 275:39324–39331.

Braz J, Solorzano C, Wang X, Basbaum AI (2014) Transmitting pain and itch messages: a contemporary view of the spinal cord circuits that generate gate control. Neuron 82:522–536.

Cameron D, Polgar E, Gutierrez-Mecinas M, Gomez-Lima M, Watanabe M, Todd AJ (2015) The organisation of spinoparabrachial neurons in the mouse. Pain 156:2061–2071.

Cheng L, Arata A, Mizuguchi R, Qian Y, Karunaratne A, Gray PA, Arata S, Shirasawa S, Bouchard M, Luo P, Chen CL, Busslinger M, Goulding M, Onimaru H, Ma Q (2004) Tlx3 and Tlx1 are post-mitotic selector genes determining glutamatergic over GABAergic cell fates. Nat Neurosci 7:510–517.

Christensen AJ, Iyer SM, Francois A, Vyas S, Ramakrishnan C, Vesuna S, Deisseroth K, Scherrer G, Delp SL (2016) In vivo

interrogation of spinal mechanosensory circuits. Cell Rep 17:1699–1710.
Dickie AC, Bell AM, Iwagaki N, Polgar E, Gutierrez-Mecinas M, Kelly R, Lyon H, Turnbull K, West SJ, Etlin A, Braz J, Watanabe M, Bennett DLH, Basbaum AI, Riddell JS, Todd AJ (2019) Morphological and functional properties distinguish the substance P and gastrin-releasing peptide subsets of excitatory interneuron in the spinal cord dorsal horn. Pain 160:442–462.
Duan B, Cheng L, Bourane S, Britz O, Padilla C, Garcia-Campmany L, Krashes M, Knowlton W, Velasquez T, Ren X, Ross SE, Lowell BB, Wang Y, Goulding M, Ma Q (2014) Identification of spinal circuits transmitting and gating mechanical pain. Cell 159:1417–1432.
Elshourbagy NA, Ames RS, Fitzgerald LR, Foley JJ, Chambers JK, Szekeres PG, Evans NA, Schmidt DB, Buckley PT, Dytko GM, Murdock PR, Milligan G, Groarke DA, Tan KB, Shabon U, Nuthulaganti P, Wang DY, Wilson S, Bergsma DJ, Sarau HM (2000) Receptor for the pain modulatory neuropeptides FF and AF is an orphan G protein-coupled receptor. J Biol Chem 275:25965–25971.
Ganley RP, Iwagaki N, Del Rio P, Baseer N, Dickie AC, Boyle KA, Polgar E, Watanabe M, Abraira VE, Zimmerman A, Riddell JS, Todd AJ (2015) Inhibitory interneurons that express GFP in the PrP-GFP mouse spinal cord are morphologically heterogeneous, innervated by several classes of primary afferent and include lamina I projection neurons among their postsynaptic targets. J Neurosci 35:7626–7642.
Gong S, Zheng C, Doughty ML, Losos K, Didkovsky N, Schambra UB, Nowak NJ, Joyner A, Leblanc G, Hatten ME, Heintz N (2003) A gene expression atlas of the central nervous system based on bacterial artificial chromosomes. Nature 425:917–925.
Gouarderes C, Sutak M, Zajac JM, Jhamandas K (1993) Antinociceptive effects of intrathecally administered F8Famide and FMRFamide in the rat. Eur J Pharmacol 237:73–81.
Gouarderes C, Jhamandas K, Sutak M, Zajac JM (1996) Role of opioid receptors in the spinal antinociceptive effects of neuropeptide FF analogues. Br J Pharmacol 117:493–501.
Gutierrez-Mecinas M, Watanabe M, Todd AJ (2014) Expression of gastrin-releasing peptide by excitatory interneurons in the mouse superficial dorsal horn. Mol Pain 10:79.
Gutierrez-Mecinas M, Furuta T, Watanabe M, Todd AJ (2016) A quantitative study of neurochemically defined excitatory interneuron populations in laminae I-III of the mouse spinal cord. Mol Pain 12:1744806916629065.
Gutierrez-Mecinas M, Bell AM, Marin A, Taylor R, Boyle KA, Furuta T, Watanabe M, Polgár E, Todd AJ (2017) Preprotachykinin a is expressed by a distinct population of excitatory neurons in the mouse superficial spinal dorsal horn including cells that respond to noxious and pruritic stimuli. Pain 158:440–456.
Gutierrez-Mecinas M, Bell AM, Shepherd F, Polgar E, Watanabe M, Furuta T, Todd AJ (2019) Expression of cholecystokinin by neurons in mouse spinal dorsal horn. J Comp Neurol *in press*.
Häring M, Zeisel A, Hochgerner H, Rinwa P, Jakobsson JET, Lonnerberg P, La Manno G, Sharma N, Borgius L, Kiehn O, Lagerstrom MC, Linnarsson S, Ernfors P (2018) Neuronal atlas of the dorsal horn defines its architecture and links sensory input to transcriptional cell types. Nat Neurosci 21:869–880.
Hinuma S, Shintani Y, Fukusumi S, Iijima N, Matsumoto Y, Hosoya M, Fujii R, Watanabe T, Kikuchi K, Terao Y, Yano T, Yamamoto T, Kawamata Y, Habata Y, Asada M, Kitada C, Kurokawa T, Onda H, Nishimura O, Tanaka M, Ibata Y, Fujino M (2000) New neuropeptides containing carboxy-terminal RFamide and their receptor in mammals. Nat Cell Biol 2:703–708.
Huang J, Polgar E, Solinski HJ, Mishra SK, Tseng PY, Iwagaki N, Boyle KA, Dickie AC, Kriegbaum MC, Wildner H, Zeilhofer HU, Watanabe M, Riddell JS, Todd AJ, Hoon MA (2018) Circuit dissection of the role of somatostatin in itch and pain. Nat Neurosci 21:707–716.
Hylden JL, Thomas DA, Iadarola MJ, Nahin RL, Dubner R (1991) Spinal opioid analgesic effects are enhanced in a model of unilateral inflammation/hyperalgesia: possible involvement of noradrenergic mechanisms. Eur J Pharmacol 194:135–143.
Ji RR, Baba H, Brenner GJ, Woolf CJ (1999) Nociceptive-specific activation of ERK in spinal neurons contributes to pain hypersensitivity. Nat Neurosci 2:1114–1119.
Kim KK, Adelstein RS, Kawamoto S (2009) Identification of neuronal nuclei (NeuN) as Fox-3, a new member of the Fox-1 gene family of splicing factors. J Biol Chem 284:31052–31061.
Kivipelto L, Panula P (1991) Origin and distribution of neuropeptide-FF-like immunoreactivity in the spinal cord of rats. J Comp Neurol 307:107–119.
Kontinen VK, Aarnisalo AA, Idanpaan-Heikkila JJ, Panula P, Kalso E (1997) Neuropeptide FF in the rat spinal cord during carrageenan inflammation. Peptides 18:287–292.
Larsson M (2017) Pax2 is persistently expressed by GABAergic neurons throughout the adult rat dorsal horn. Neurosci Lett 638:96–101.
Lee CH, Wasowicz K, Brown R, Majane EA, Yang HT, Panula P (1993) Distribution and characterization of neuropeptide FF-like immunoreactivity in the rat nervous system with a monoclonal antibody. Eur J Neurosci 5:1339–1348.
Liu Q, Guan XM, Martin WJ, McDonald TP, Clements MK, Jiang Q, Zeng Z, Jacobson M, Williams Jr DL, Yu H, Bomford D, Figueroa D, Mallee J, Wang R, Evans J, Gould R, Austin CP (2001) Identification and characterization of novel mammalian neuropeptide FF-like peptides that attenuate morphine-induced antinociception. J Biol Chem 276:36961–36969.
Lu Y, Dong H, Gao Y, Gong Y, Ren Y, Gu N, Zhou S, Xia N, Sun Y-Y, Ji R-R, Xiong L (2013) A feed-forward spinal cord glycinergic neural circuit gates mechanical allodynia. J Clin Invest 123:4050–4062.
Mollereau C, Roumy M, Zajac J-M (2011) Neuropeptide FF receptor modulates potassium currents in a dorsal root ganglion cell line. Pharmacol Rep 63:1061–1065.
Mu D, Deng J, Liu KF, Wu ZY, Shi YF, Guo WM, Mao QQ, Liu XJ, Li H, Sun YG (2017) A central neural circuit for itch sensation. Science 357:695–699.
Mullen RJ, Buck CR, Smith AM (1992) NeuN, a neuronal specific nuclear protein in vertebrates. Development 116:201–211.
Panula P, Kalso E, Nieminen M, Kontinen VK, Brandt A, Pertovaara A (1999) Neuropeptide FF and modulation of pain. Brain Res 848:191–196.
Peirs C, Seal RP (2016) Neural circuits for pain: recent advances and current views. Science 354:578–584.
Perry SJ, Yi-Kung Huang E, Cronk D, Bagust J, Sharma R, Walker RJ, Wilson S, Burke JF (1997) A human gene encoding morphine modulating peptides related to NPFF and FMRFamide. FEBS Lett 409:426–430.
Polgár E, Gray S, Riddell JS, Todd AJ (2004) Lack of evidence for significant neuronal loss in laminae I-III of the spinal dorsal horn of the rat in the chronic constriction injury model. Pain 111:144–150.
Polgár E, Durrieux C, Hughes DI, Todd AJ (2013) A quantitative study of inhibitory interneurons in laminae I-III of the mouse spinal dorsal horn. PloS One 8 e78309.
Proudlock F, Spike RC, Todd AJ (1993) Immunocytochemical study of somatostatin, neurotensin, GABA, and glycine in rat spinal dorsal horn. J Comp Neurol 327:289–297.
Roberson DP, Gudes S, Sprague JM, Patoski HA, Robson VK, Blasl F, Duan B, Oh SB, Bean BP, Ma Q, Binshtok AM, Woolf CJ (2013) Activity-dependent silencing reveals functionally distinct itch-generating sensory neurons. Nat Neurosci 16:910–918.
Solorzano C, Villafuerte D, Meda K, Cevikbas F, Braz J, Sharif-Naeini R, Juarez-Salinas D, Llewellyn-Smith IJ, Guan Z, Basbaum AI (2015) Primary afferent and spinal cord expression of gastrin-releasing peptide: message, protein, and antibody concerns. J Neurosci 35:648–657.
Todd AJ (2010) Neuronal circuitry for pain processing in the dorsal horn. Nat Rev Neurosci 11:823–836.
Todd AJ (2017) Identifying functional populations among the interneurons in laminae I-III of the spinal dorsal horn. Mol Pain 13:1744806917693003.

Todd AJ, Spike RC, Polgar E (1998) A quantitative study of neurons which express neurokinin-1 or somatostatin sst2a receptor in rat spinal dorsal horn. Neuroscience 85:459–473.

Vilim FS, Aarnisalo AA, Nieminen ML, Lintunen M, Karlstedt K, Kontinen VK, Kalso E, States B, Panula P, Ziff E (1999) Gene for pain modulatory neuropeptide NPFF: induction in spinal cord by noxious stimuli. Mol Pharmacol 55:804–811.

Wang X, Zhang J, Eberhart D, Urban R, Meda K, Solorzano C, Yamanaka H, Rice D, Basbaum AI (2013) Excitatory superficial dorsal horn interneurons are functionally heterogeneous and required for the full behavioral expression of pain and itch. Neuron 78:312–324.

Yang HY, Iadarola MJ (2003) Activation of spinal neuropeptide FF and the neuropeptide FF receptor 2 during inflammatory hyperalgesia in rats. Neuroscience 118:179–187.

Yang HY, Fratta W, Majane EA, Costa E (1985) Isolation, sequencing, synthesis, and pharmacological characterization of two brain neuropeptides that modulate the action of morphine. Proc Natl Acad Sci U S A 82:7757–7761.

Yang HY, Tao T, Iadarola MJ (2008) Modulatory role of neuropeptide FF system in nociception and opiate analgesia. Neuropeptides 42:1–18.

Zeisel A, Hochgerner H, Lonnerberg P, Johnsson A, Memic F, van der Zwan J, Haring M, Braun E, Borm LE, La Manno G, Codeluppi S, Furlan A, Lee K, Skene N, Harris KD, Hjerling-Leffler J, Arenas E, Ernfors P, Marklund U, Linnarsson S (2018) Molecular architecture of the mouse nervous system. Cell 174(999–1014) e1022.

(Received 5 May 2019, Accepted 6 August 2019)
(Available online 14 August 2019)

5 Paper IV

Bell, A.M., Gutierrez-Mecinas, M., Stevenson, A., Casas-Benito, A., Wildner, H., West, S.J., Watanabe, M., Todd, A.J., 2020. Expression of green fluorescent protein defines a specific population of lamina II excitatory interneurons in the GRP::eGFP mouse. Scientific Reports 10, 13176.

CRediT statement

Conceptualization, A.M.B. and A.J.T., Methodology, A.M.B. and A.J.T.; Formal analysis, A.M.B., A.S. and A.C.B.; Investigation, A.M.B., A.S., A.C.B. and M.G.M.; Resources, H.W., S.J.W. and M.W.; Writing – Original Draft, A.M.B. and A.J.T., Writing – Review & Editing, A.M.B., A.J.T., H.W. and M.G.M.; Visualization, A.M.B. and A.J.T.; Supervision, A.M.B. and A.J.T.; Funding Acquisition, A.J.T.

Summary of practical involvement in components of study

All experiments and analysis with exception of those below– A.M.B primary role.
Characterisation of SST+ afferents – A.S. supervised by A.M.B.
Quantification of MrgprD inputs – A.C.B supervised by A.M.B. and M.G.M.

SCIENTIFIC REPORTS
nature research

Check for updates

OPEN

Expression of green fluorescent protein defines a specific population of lamina II excitatory interneurons in the GRP::eGFP mouse

Andrew M. Bell[1]✉, Maria Gutierrez-Mecinas[1], Anna Stevenson[1], Adrian Casas-Benito[1], Hendrik Wildner[2,3], Steven J. West[4], Masahiko Watanabe[5] & Andrew J. Todd[1]✉

Dorsal horn excitatory interneurons that express gastrin-releasing peptide (GRP) are part of the circuit for pruritogen-evoked itch. They have been extensively studied in a transgenic line in which enhanced green fluorescent protein (eGFP) is expressed under control of the *Grp* gene. The GRP-eGFP cells are separate from several other neurochemically-defined excitatory interneuron populations, and correspond to a class previously defined as transient central cells. However, mRNA for GRP is widely distributed among excitatory interneurons in superficial dorsal horn. Here we show that although *Grp* mRNA is present in several transcriptomically-defined populations, eGFP is restricted to a discrete subset of cells in the GRP::eGFP mouse, some of which express the neuromedin receptor 2 and likely belong to a cluster defined as Glut8. We show that these cells receive much of their excitatory synaptic input from MrgA3/MrgD-expressing nociceptive/pruritoceptive afferents and C-low threshold mechanoreceptors. Although the cells were not innervated by pruritoceptors expressing brain natriuretic peptide (BNP) most of them contained mRNA for NPR1, the receptor for BNP. In contrast, these cells received only ~ 10% of their excitatory input from other interneurons. These findings demonstrate that the GRP-eGFP cells constitute a discrete population of excitatory interneurons with a characteristic pattern of synaptic input.

Neuronal circuits in the spinal dorsal horn process somatosensory information, which is then transmitted to the brain by projection cells. The vast majority of dorsal horn neurons are interneurons, and these can be assigned to two main classes: excitatory and inhibitory cells[1,2]. Nociceptive and pruritoceptive primary afferents terminate in the superficial dorsal horn (SDH; laminae I-II), and ~ 75% of neurons in this region are excitatory interneurons[2]. Recent studies have shown that these cells can be assigned to several largely non-overlapping populations, based on the expression of different neuropeptides[3–6], and these are thought to have distinct roles in pain and itch.

There is compelling evidence that gastrin-releasing peptide (GRP) and its receptor (GRPR) play a key role in itch. Intrathecal administration of GRP evokes scratching, while GRPR antagonists reduce scratching in response to pruritogens[7–11]. In addition, mice lacking GRPR, or those in which GRPR-expressing dorsal horn neurons are ablated, show reduced responses in several itch models[7,8,12,13]. Excitatory interneurons within the SDH provide a source of GRP[7,14–16], and several studies have investigated the role of these cells by using BAC transgenic mouse lines from the GENSAT project[17] in which either enhanced green fluorescent protein (eGFP)[7,14,15,18–20] or Cre recombinase[18–21] is expressed under control of the *Grp* promoter (GRP::eGFP and GRP::Cre, respectively). We have reported that the eGFP-positive cells in the GRP::eGFP line are all excitatory, accounting for ~ 15% of the

[1]Spinal Cord Group, Institute of Neuroscience and Psychology, College of Medical, Veterinary and Life Sciences, University of Glasgow, Sir James Black Building, Glasgow G12 8QQ, UK. [2]Institute of Pharmacology and Toxicology, University of Zurich, Zürich, Switzerland. [3]Institute of Pharmaceutical Sciences, Swiss Federal Institute of Technology (ETH) Zürich, Zürich, Switzerland. [4]The Nuffield Department of Clinical Neurosciences, University of Oxford, John Radcliffe Hospital, Oxford OX3 9DU, UK. [5]Department of Anatomy, Hokkaido University School of Medicine, Sapporo 060-8638, Japan. ✉email: andrew.bell@glasgow.ac.uk; andrew.todd@glasgow.ac.uk

excitatory interneurons in laminae I-II[4,14], and that they are largely separate from populations defined by the expression of five other peptides: cholecystokinin (CCK), neurotensin, neurokinin B (NKB), neuropeptide FF (NPFF) and substance P (SP)[3,4,22,23]. Between them, these 6 populations account for ~ 75% of SDH excitatory interneurons, and each of the other populations maps onto clusters that were identified by Häring et al.[5] in a recent transcriptomic study. Specifically, cells in laminae I-II that express these other peptides correspond to the Glut2 (CCK), Glut4 (neurotensin), Glut5-7 (NKB), Glut9 (NPFF) and Glut10-11 (SP) populations defined by Häring et al.

However, Häring et al.[5] reported that *Grp* mRNA was widely distributed across several of the excitatory interneuron clusters that they identified (Glut5-12), suggesting that the *Grp* message may be expressed by many cells that lack eGFP in this transgenic line. In fact, studies of the GRP-eGFP cells[3,19,20] have shown that they form a relatively homogeneous population in terms of morphological, electrophysiological and pharmacological properties, and correspond to a class previously defined as transient central cells[24–26].

The initial aim of this study was therefore to compare the distribution of mRNAs for GRP and eGFP in the GRP::eGFP mouse, and determine whether the eGFP cells correspond to any of the transcriptomic populations identified by Häring et al.[5]. We also used anatomical methods, based on detection of the postsynaptic protein Homer[27,28], to quantify their excitatory synaptic input from different sources. Recent studies[18,19] have shown that GRP-eGFP cells are "secondary pruritoceptors"[7], innervated by pruritoceptive afferents that express the mas-related G protein-coupled receptor A3 (MrgA3)[29], although it is not known what proportion of their excitatory synaptic input this accounts for. Huang et al[9] identified another population of pruritoceptors, which express somatostatin (SST) and brain natriuretic peptide (BNP; also known as natriuretic polypeptide B, NPPB), and these could activate the GRP-eGFP cells either synaptically, or through the action of BNP on its receptor, natriuretic peptide receptor 1 (NPR1)[7]. It has been suggested that GRP-eGFP cells also respond to noxious stimuli[18], and these cells may therefore be innervated by nociceptive afferents. In addition, they overlap with the plexus of C low-threshold mechanoreceptors (C-LTMRs), which express vesicular glutamate transporter 3 (VGLUT3)[3,30]. We therefore quantified excitatory synaptic input from different sources to the GRP-eGFP cells, as well as testing them for the presence of *NPR1*.

Results

eGFP expression in the GRP::eGFP mouse is restricted to a molecularly distinct subset of excitatory interneurons. To test whether *Grp* message is as widely distributed among SDH neurons as reported by Häring et al.[5], we initially performed multiple-labelling fluorescent in situ hybridisation with RNAscope and determined the proportion of excitatory neurons in laminae I-II that had mRNA for GRP. We also investigated the relationship of GRP cells to those that express SST, because this peptide is present in the majority of excitatory interneurons in this region[4,5]. To do this, we analysed sections from three wild-type C57BL/6 mice that had been reacted with probes for *Grp*, *Slc17a6* (the gene coding for vesicular glutamate transporter 2, VGLUT2, which is thought to be expressed by all excitatory interneurons in this region[31]) and *SST*. We identified between 360 and 412 (mean 386) excitatory (*Slc17a6* +) cells in laminae I-II from each animal and found that 37% (range 35–38%) of these were labelled for *Grp* mRNA and 66% (63–69%) for *SST* mRNA. The great majority (83%, range 80–85%) of the *Grp* + cells were also positive for *SST*, and these accounted for 47% (43–50%) of all *SST* + cells (Fig. 1). Although Fatima et al.[32] recently estimated that only 16% of GRP cells expressed SST and that 5% of SST cells were GRP +, their identification of SST cells was based on a genetic strategy rather than direct observation of the mRNA, and this presumably accounts for the difference between these values. The finding that 66% of VGLUT2 + neurons contain mRNA for SST is consistent with our previous estimate that 59% of excitatory SDH neurons are SST-immunoreactive[4]. Taken together, these results are in agreement with those of Häring et al.[5], and show that GRP and SST overlap extensively in laminae I-II, and are both widely expressed among the excitatory interneurons in this region.

We next revealed the mRNAs for both GRP and eGFP in sections from three GRP::eGFP mice and found that while all eGFP-positive cells were also labelled with the *Grp* probe, they only accounted for 23.3% (20.1–26.2%) of the *Grp* + cells in laminae I-II (Table 1, Fig. 2). Albisetti et al.[20] recently examined the GRP::Cre line and showed that only 25% of cells with *Grp* mRNA expressed Cre. Sun et al.[18] had previously crossed the GRP::eGFP and GRP::Cre lines and shown that 90% of the Cre + cells had eGFP, while 64% of eGFP cells were Cre-positive, indicating that the two lines capture a largely overlapping population. Collectively, these findings indicate that while the cells that are labelled in these two BAC transgenic lines are all GRP-expressing, they only account for a minority of the GRP cells.

Since GRP is highly expressed among the Glut5-12 clusters of Häring et al.[5], we then compared the distribution of both *Grp* and *eGFP* mRNAs with those of other markers that can be used to reveal these populations. This analysis was again performed in laminae I-II in 3 GRP::eGFP mice and results are shown in Table 1 and Fig. 2. The tachykinin peptides SP and NKB are encoded by *Tac1* and *Tac2* and are expressed by the Glut5-7 and Glut10-11 clusters, respectively, while the neuromedin receptor 2 (Nmur2) is expressed in the Glut8 cluster[5]. In the case of *Tac2* mRNA we found, as reported by Häring et al.[5], that there were two populations: those with high and low levels (corresponding to Glut5-6 and Glut7, respectively), and we therefore analysed these separately. For both of the tachykinin peptides, we found a moderate degree of overlap with *Grp* mRNA, such that ~ 10% and 25% of cells with *Grp* mRNA also contained *Tac1* or *Tac2* mRNA (respectively), while around 15% of *Tac1* and 50% of *Tac2* cells had *Grp* mRNA. However, there was minimal overlap of tachykinin and eGFP expression, since only < 1% of *Tac1* mRNA cells and < 2% of *Tac2* mRNA cells were positive for eGFP. In contrast, *Nmur2* mRNA showed a moderate degree of overlap with both *Grp* and *eGFP* mRNA. Specifically, 30% of *Grp* + cells and 26% of *eGFP* + cells contained *Nmur2* mRNA, and these corresponded to 69% and 14% of the Nmur2 population, respectively. We have previously shown that *Npff* mRNA overlaps with *Grp* mRNA, but that GRP-eGFP cells are

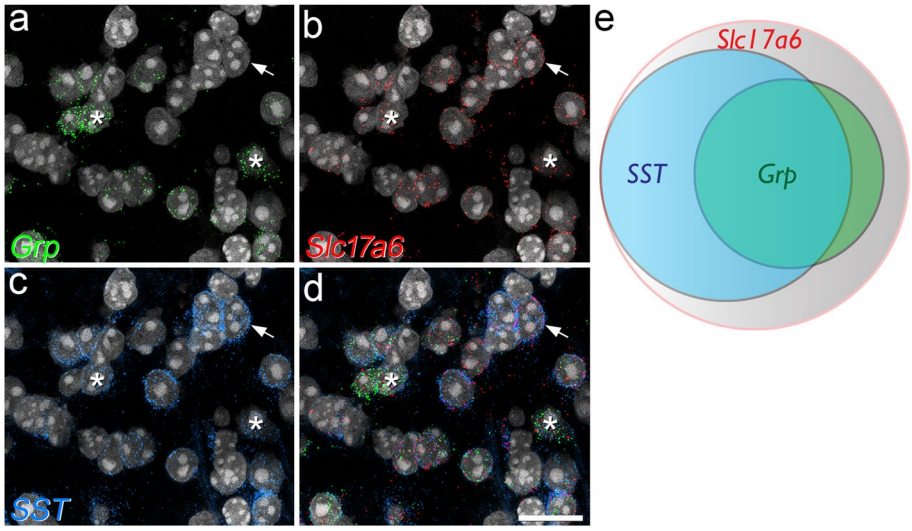

Figure 1. Co-localisation of mRNAs for VGLUT2, somatostatin and GRP revealed by fluorescent in situ hybridisation. (**a**–**c**) Part of lamina II in a section reacted with probes for *Grp* (green), *Slc17a6* (the gene that encodes VGLUT2, red) and *SST* (blue). In each case nuclei, which were stained with NucBlue, are shown in grey. (**d**) A merged image of the same field. This region contains several cells that are positive for each probe. Asterisks show two cells that are positive for all 3 probes, and the arrow points to a cell that has mRNAs for VGLUT2 and SST, but not for GRP. (**e**) Venn diagram showing the proportions of VGLUT2 cells that are positive for *SST* and/or *Grp* mRNAs. Images in (**a**–**d**) are projections of confocal optical sections (1 µm z-separation) taken through the full thickness of the section. Scale bar for (**a**–**d**): 20 µm.

Other mRNA	No. *Grp* + cells	No. *eGFP* + cells	% *Grp* + with *eGFP*[a]	No. *Tac1* +, *Tac2* + or *Nmur2* + (Other) cells	No. Other cells with *Grp*	% Other cells with *Grp*	No. Other cells with *eGFP*	% Other cells with *eGFP*	% *Grp* + with other marker	% *eGFP* + with other marker
Tac1	253.6 (185–305)	57.6 (49–69)	23.3% (18.0–26.5)	170.3 (136–208)	28 (15–39)	15.9 (11.0–18.8)	1.3 (0–2)	0.7 (0–1.2)	10.7 (8.1–12.8)	2.2 (0–3.6)
Tac2 High	296.3 (237–356)	69.6 (64–80)	23.8 (22.0–27.0)	73.3 (46–99)	40 (25–58)	54.1 (49.3–58.6)	1.0 (0–2)	1.2 (0–2.7)	13.1 (10.5–16.3)	0.3 (0–0.7)
Tac2 Low				77.3 (58–88)	36 (27–50)	47.2 (31.4–56.8)	1.3 (1–2)	1.7 (1.1–2.3)	12.1 (9.2–14.0)	0.5 (0.3–0.7)
Nmur2	201.6 (165–237)	46.3 (41–55)	23.1% (21.2–24.8)	87.3 (78–105)	60.3 (54–72)	69.1 (68.8–69.6)	12 (8–15)	13.7 (10.3–16.5)	30.1 (26.6–33.3)	25.9 (18.6–31.7)

Table 1. Quantitative in situ hybridisation data. Data are presented from 3 animals in each case and are shown as mean (range). [a]The corresponding percentage given in the "Results" section was obtained by pooling data from each individual animal, giving a mean of 23.3% with a range of 20.1–26.2%.

not NPFF-immunoreactive[22], indicating that although *Grp* message is present in cells in the Glut9 cluster, GRP-eGFP cells are excluded from this cluster (Fig. 2m). Taken together, these results show that eGFP expression is restricted to a distinct subset of GRP cells.

Pruritoceptive input to GRP-eGFP cells. Two major classes of primary afferent have been identified as potential pruritoceptors: those defined by expression of MrgA3[29] and SST/BNP[9], and these correspond, respectively, to the NP2 and NP3 classes defined by Usoskin et al.[33]. We therefore quantified synaptic input to GRP-eGFP cells from these two populations.

Input from MrgA3 afferents was analysed in tissue from 2 GRP::eGFP;MrgA3::Cre;Ai14 mice, in which these afferents express tdTomato[29], and sections were stained to reveal tdTomato, eGFP and Homer. As noted by Albisetti et al.[20], we found a high degree of overlap between the plexus of MrgA3 afferents and the dendritic trees of the GRP-eGFP neurons in lamina II, and we observed numerous contacts between these profiles (Fig. 3). We found that tdTomato-positive boutons were in contact with ~ 25% of the Homer puncta on the dendritic trees of the GRP-eGFP cells (Figs. 3, 4), and these accounted for 29.4% (22.9–36%) of the Homer puncta that were contacted by MrgA3 boutons. However, only 9.1% (8.4–9.8%) of all Homer puncta within the band of GRP-eGFP dendrites were associated with an eGFP-labelled profile. This corresponds to a threefold enrichment on GRP-eGFP cell dendrites, and shows that MrgA3 boutons preferentially target the GRP-eGFP cells.

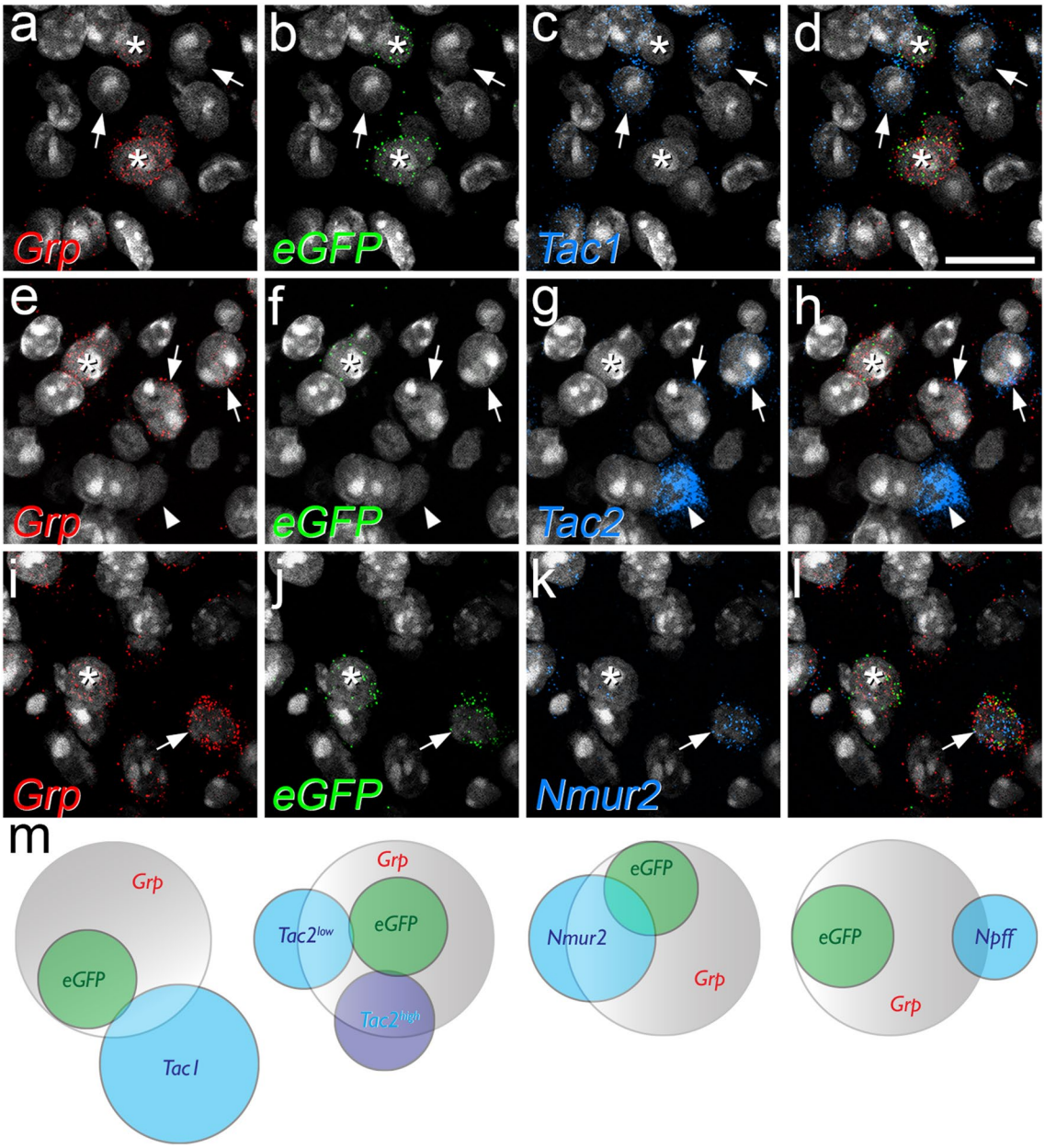

Figure 2. The relationship between mRNAs for GRP, eGFP and other neurochemical markers in the GRP::eGFP mouse. (**a**–**d**), (**e**–**h**) and (**i**–**l**) show parts of lamina II in sections reacted with probes directed against the mRNA for GRP (**a**, **e**, **i**), eGFP (**b**, **f**, **j**) and either Tac1 (**c**), Tac2 (**g**) or Nmur2 (**k**). Merged images are also shown (**d**, **h**, **l**). In each case the probe for GRP is shown in red, that for eGFP in green and that for the other marker in blue. In all of these images counterstaining for NucBlue is shown in grey. (**a**–**d**) This field shows 2 cells that are positive for both *Grp* and *eGFP*, but negative for *Tac1* (asterisks), as well as several *Tac1*-positive cells that lack mRNA for GRP and eGFP (two shown with arrows). (**e**–**h**) The cell marked with an asterisk is positive for both *Grp* and *eGFP*, but negative for *Tac2*, while that shown with the arrowhead is strongly positive for *Tac2* (*Tac2*^{high}) but negative for *Grp* and *eGFP*. Two other cells (arrows) show low levels of *Tac2* (*Tac2*^{low}) and are positive for *Grp* but negative for *eGFP*. (**i**–**l**) This field shows two *Grp*-positive/*eGFP*-positive cells one of which (arrow) is positive for *Nmur2* (arrow) and one of which lacks *Nmur2* mRNA (asterisk). (**m**) Venn diagrams illustrating the extent of overlap between these different populations. The data for *Npff* is obtained from a previous study[22] in which we reported that there was some overlap between mRNAs for GRP and NPFF, but that cells immunoreactive for pro-NPFF were never eGFP-positive in the GRP::eGFP mouse. This is shown here to allow comparison with the results for other neurochemical markers. Images in (**a**–**l**) are projections of confocal optical sections (1 µm z-separation) taken through the full thickness of the section. Scale bar (for **a**–**l**) = 20 µm.

To look for evidence of input from SST-expressing primary afferents, we needed to distinguish these from

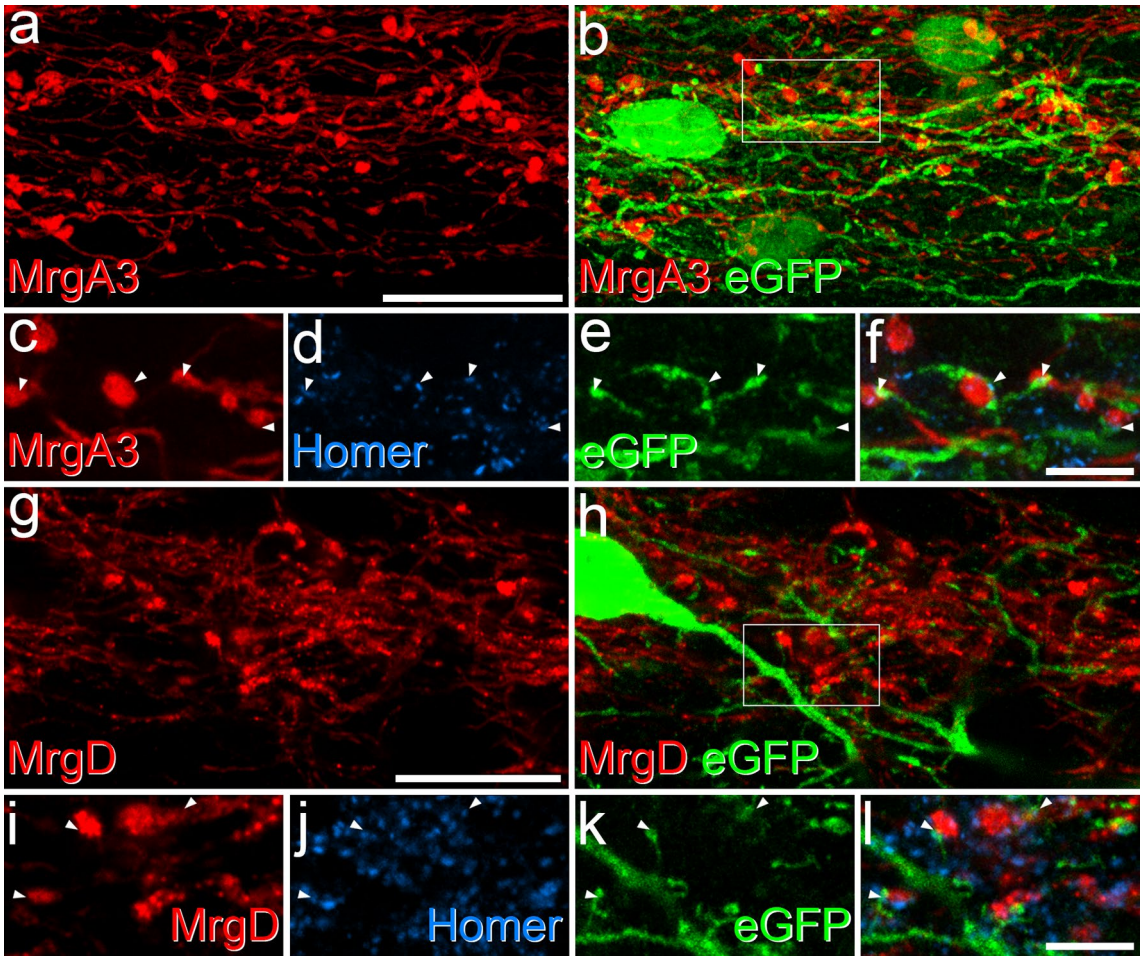

Figure 3. Synaptic input to GRP-eGFP cells from two classes of non-peptidergic C afferent. (**a**–**f**) Part of lamina II shown in a sagittal section from a GRP::eGFP;MrgA3::Cre;Ai14 mouse scanned to reveal tdTomato (red), which labels MrgA3 afferents, eGFP (green) and Homer (blue). (**a**) and (**b**) show a projected confocal image taken from 61 optical sections at 0.2 µm z-separation. Numerous contacts between tdTomato-positive boutons and the dendrites of the GRP-eGFP cells can be seen. The box in (**b**) indicates the region illustrated at higher magnification in (**c**–**f**). (**c**–**f**) a single optical section shows several appositions between tdTomato-labelled boutons and eGFP-labelled dendrites at which a Homer punctum is present (four indicated with arrowheads). (**g**–**l**) Part of lamina II in a sagittal section from a GRP::eGFP;MrgD^{CreERT2};Ai9 mouse scanned for tdTomato (red), which labels MrgD afferents, eGFP (green) and Homer (blue). (**g**) and (**h**) show a projected confocal image from 21 optical sections at 0.2 µm z-spacing. Again, contacts between tdTomato-positive boutons and dendrites of GRP-eGFP cells are visible. (**i**–**l**) A higher magnification view taken from a projection of 5 z-sections corresponding to the region shown in the box in (**h**), showing 3 contacts at which a Homer punctum is present (arrowheads). Scale bars: (**a**,**b**) and (**g**,**h**) = 20 µm, (**c**–**f**) and (**i**–**l**) = 5 µm.

boutons belonging to SST-expressing interneurons[4]. To do this, we used an antibody against prostatic acid phosphatase (PAP), which is expressed by the majority of non-peptidergic afferents[33,34]. We first validated this approach by reacting sections from mice in which eGFP is expressed under control of the promoter for Advillin (Avil::eGFP), and is therefore restricted to primary afferents[35]. This analysis showed that virtually all (99%) of the SST primary afferents, defined by co-localisation of SST and eGFP, were PAP-immunoreactive, and that these were restricted to the middle and outer parts of lamina II (Fig. 5a–e). We therefore immunoreacted sections from GRP::eGFP mice to reveal SST, PAP, eGFP and Homer. We found that SST + /PAP + boutons seldom contacted eGFP dendrites, accounting for only 4.1% (2.4–4.7%) of the Homer puncta associated with these boutons (Fig. 5f). Since these apparently make up a very small part of the excitatory synaptic input to the GRP-eGFP cells, we did not quantify the input from SST afferents to individual GRP-eGFP cells.

To test whether GRP-eGFP cells possessed the receptor for BNP, and could therefore respond to peptidergic (rather than synaptic) signalling from the SST/BNP afferents, we performed fluorescent in situ hybridisation with probe directed against *NPR1* mRNA. Labelling was present over certain cells in the SDH (Fig. 5g–j), and we found that 77% of eGFP cells were *NPR1*-positive, whereas the proportion was only 32% for those GRP cells that lacked *eGFP* mRNA. These proportions were significantly different (Mantel–Haenszel common odds ratio estimate for *NPR1* expression in eGFP + cells vs eGFP− cells = 8.2; 95% CI 5.9–11.2, $p < 0.0001$), showing that

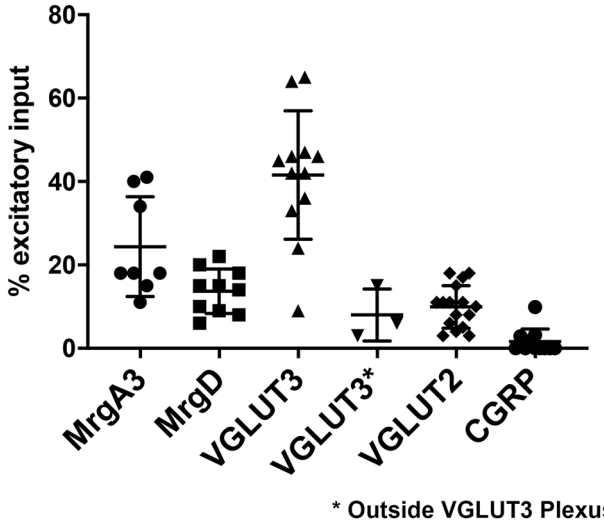

Figure 4. The contribution of different types of glutamateric input to GRP-eGFP cells. Scatter plot showing the percentage of Homer puncta on these cells that were in contact with axons defined by the expression of different markers. For VGLUT3, we tested GRP-eGFP cells that had dendritic trees both within and outside the VGLUT3 plexus, and the latter are shown separately (VGLUT3*). The numbers of cells tested for each axonal population are shown in table S4. Each symbol represents an individual cell, and the mean and standard deviation are shown.

GRP-eGFP cells are more likely to express *NPR1* than other GRP cells (Table S1). However, *NPR1* expression was not exclusive to GRP cells, as *Grp* mRNA was only detected in 57% of *NPR1* + cells (Table S1).

Other excitatory synaptic inputs to GRP-eGFP cells. Primary afferents that express MrgD correspond to the NP1 class of Usoskin et al.[33], and their central projections overlap extensively with the dendritic trees of the GRP-eGFP cells. We therefore analysed input from MrgD afferents to GRP-eGFP cells in 2 GRP::eGFP;MrgD^{CreERT2};Ai9 mice (in which tdTomato is expressed by MrgD afferents[36]), using the same approach as that described above. We found that the dendrites of the GRP-eGFP cells were co-extensive with the plexus of MrgD afferents (Fig. 3g,h), and numerous Homer-associated contacts were seen. These represented ~ 14% of the Homer puncta on the dendritic trees of the GRP-eGFP cells (Figs. 3, 4), while GRP-eGFP dendrites accounted for 14% (12.9–15.1%) of the Homer puncta that were in contact with MrgD boutons.

Sun et al.[18] used monosynaptic rabies tracing to identify inputs to GRP-Cre cells in the GRP::Cre line, and reported that these cells were innervated by CGRP-expressing primary afferents. We therefore analysed synaptic input to GRP-eGFP cells from CGRP-immunoreactive boutons. There was little spatial overlap between the GRP-eGFP cells and the CGRP plexus (Fig. 6a–c), and CGRP boutons were present at only 1.6% of the Homer puncta on the GRP-eGFP cells (Fig. 4). Within the GRP-eGFP plexus, GFP-labelled profiles were associated with 4.5% (3.5–5%) of the Homer puncta adjacent to CGRP boutons. This suggests that CGRP-immunoreactive boutons provide a very limited synaptic input to GRP-eGFP cells.

In a previous study, we noted that GRP-eGFP cells were largely restricted to regions of the dorsal horn that were innervated by hairy skin[3]. This was demonstrated by revealing C-LTMRs (which are also restricted to hairy skin) with an antibody against VGLUT3[30]. During the course of that study we found frequent contacts between VGLUT3-immunoreactive boutons and GRP-eGFP cells, although only those GRP-eGFP cells in the ventral half of the eGFP band overlapped the VGLUT3 plexus (see Fig. 1 of Dickie et al.[30]). We therefore quantified the synaptic input from VGLUT3 boutons to eGFP cells that were either within this plexus or dorsal to it. We found that for GRP-eGFP cells within the VGLUT3 plexus, 42% of their Homer puncta were associated with VGLUT3 boutons (Figs. 4, 7). Unsurprisingly, the input was far less dense for eGFP cells located dorsal to the VGLUT3 plexus, for which only 8% of Homer puncta were adjacent to a VGLUT3 bouton (Fig. 4). Conversely, GRP-eGFP dendrites were identified at between 8.8 and 23.2% (mean 14.6%) of the Homer puncta that were adjacent to VGLUT3 boutons. As this was apparently the first indication that C-LTMRs provide synaptic input to GRP-eGFP cells, we used a combined confocal/electron microscopy approach[37] to confirm that the appositions corresponded to synapses. We identified 8 Homer-associated VGLUT3 contacts onto a single GRP-eGFP cell from each of two GRP::eGFP mice with the electron microscope. We found that, as reported recently[38], the VGLUT3 boutons corresponded to central axons of synaptic glomeruli, which were presynaptic to several dendritic profiles and were postsynaptic to profiles that resembled peripheral axons (Fig. 7k–m). We were able to confirm the presence of asymmetrical synapses onto the GRP-eGFP dendrites at 15 of the 16 contacts identified.

Finally, we investigated synaptic input to the GRP-eGFP cells from VGLUT2-immunoreactive boutons. Although many unmyelinated primary afferents express VGLUT2[39], the level of immunoreactivity in their central terminals is typically very low, and the majority of boutons with strong VGLUT2 immunoreactivity are thought

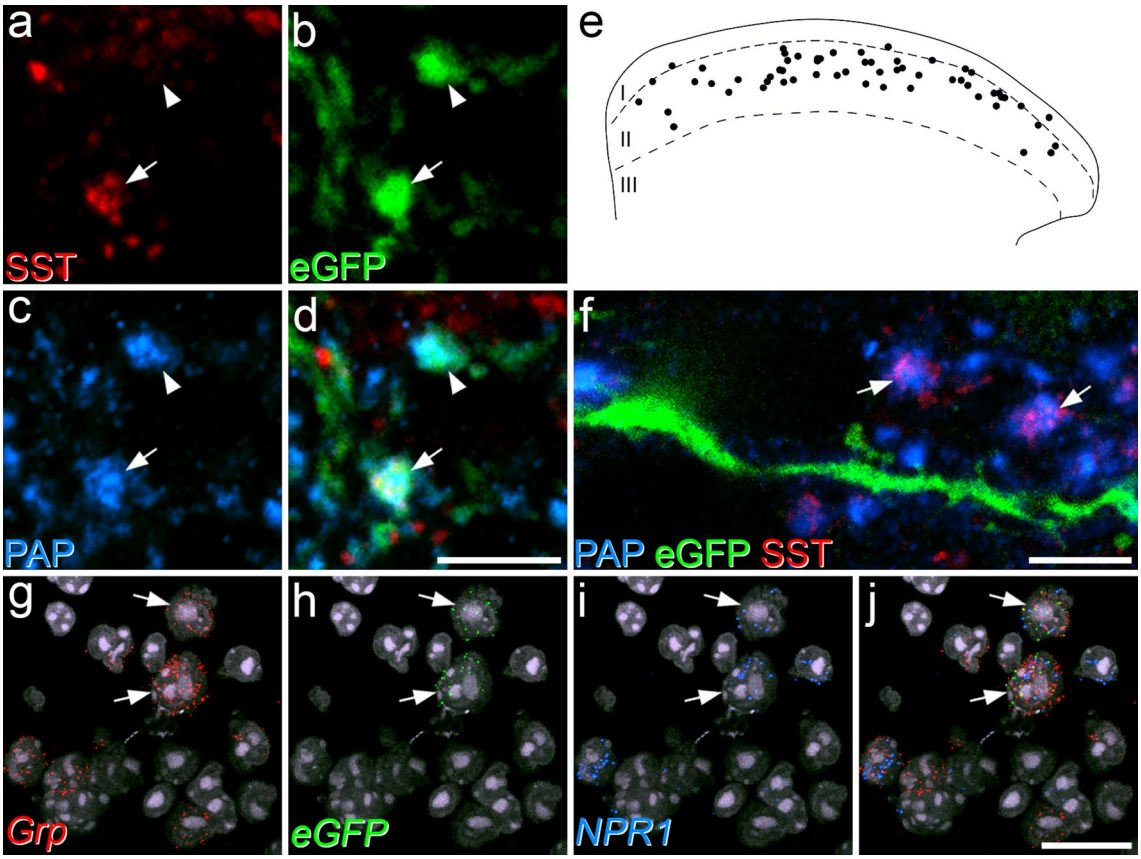

Figure 5. Somatostatin afferents as a potential source of input to GRP-eGFP cells. (**a**–**d**) Somatostatin-expressing primary afferents were initially revealed in tissue from the Avil::eGFP mouse, by immunostaining for somatostatin (SST, red), eGFP (green) and prostatic acid phosphatase (PAP, blue). These images are from a single confocal optical section through lamina IIo and show two eGFP + boutons, both of which are also PAP-immunoreactive. One of these (arrow) is SST-positive, indicating that it originates from a SST-expressing primary afferent, while the other (arrowhead) lacks SST. (**e**) The distribution of SST-afferents revealed by coexpression of PAP and SST seen in a single 60 µm thick section. Note that these are largely restricted to lamina IIo. (**f**) Part of a sagittal section through lamina II from a GRP::eGFP mouse, immunostained to reveal PAP (blue), eGFP (green) and SST (red). The image is projected from 13 optical sections at 0.2 µm z-separation. Two large SST afferent boutons, identified by the presence of SST and PAP are close to the dendrite of a GRP-eGFP cell, but are not in direct contact. (**g**–**j**) Fluorescent in situ hybridisation on a section from a GRP::eGFP mouse shows two cells (arrows) that are labelled with probes against both *Grp* and *eGFP* mRNAs, and both of which are also *NPR1*-positive. Images in (**g**–**j**) are projections of confocal images (1 µm z-separation) taken through the full thickness of the section. Scale bars: (**a**–**d**) = 5 µm, (**f**) = 5 µm, (**g**–**j**) = 20 µm.

to originate from local excitatory interneurons[14,31]. We examined sections from 5 GRP::eGFP mice that had been reacted to reveal VGLUT2, Homer and eGFP and analysed the input to 16 GRP-eGFP cells (2–4 cells per mouse). Although all of the cells received contacts from boutons with strong VGLUT2 immunoreactivity at some of their Homer puncta, these only accounted for ~ 10% of the puncta on these cells (Figs. 4, 6). This suggests that excitatory interneurons provide only a relatively small part of the excitatory synaptic input to the GRP-eGFP cells.

Discussion

Our main findings are: (1) that although *Grp* mRNA is widely expressed among different populations of excitatory interneurons, eGFP expression in the GRP::eGFP mouse is restricted to a specific subset, with some of these cells co-expressing *Nmur2*; (2) that GRP-eGFP cells receive many excitatory synapses from primary afferents that express MrgA3, MrgD or (for those cells in lamina IIi) VGLUT3, but few from those that express CGRP or SST; (3) that most of these cells express the receptor for BNP; and (4) that they receive few synapses from boutons with strong VGLUT2-immunoreactivity, which are likely to originate from local excitatory interneurons.

Recent neurochemical[2–4,22] and transcriptomic[5,6,40] studies have revealed several distinct populations among the excitatory interneurons in the SDH. For example, we have identified largely non-overlapping classes that express CCK, neurotensin, NKB, NPFF and SP, and found that these were different from the GRP-eGFP cells[22]. However, this finding was apparently at odds with that of Häring et al., who reported that *Grp* mRNA was widely expressed, including by cells in clusters defined by the expression of three of these peptides (NKB, NPFF and SP). The present findings help to resolve this discrepancy, by showing that the *Grp* mRNA+ cells that co-express these neuropeptides are those that lack eGFP in the GRP::eGFP line, and that the GRP-eGFP cells therefore

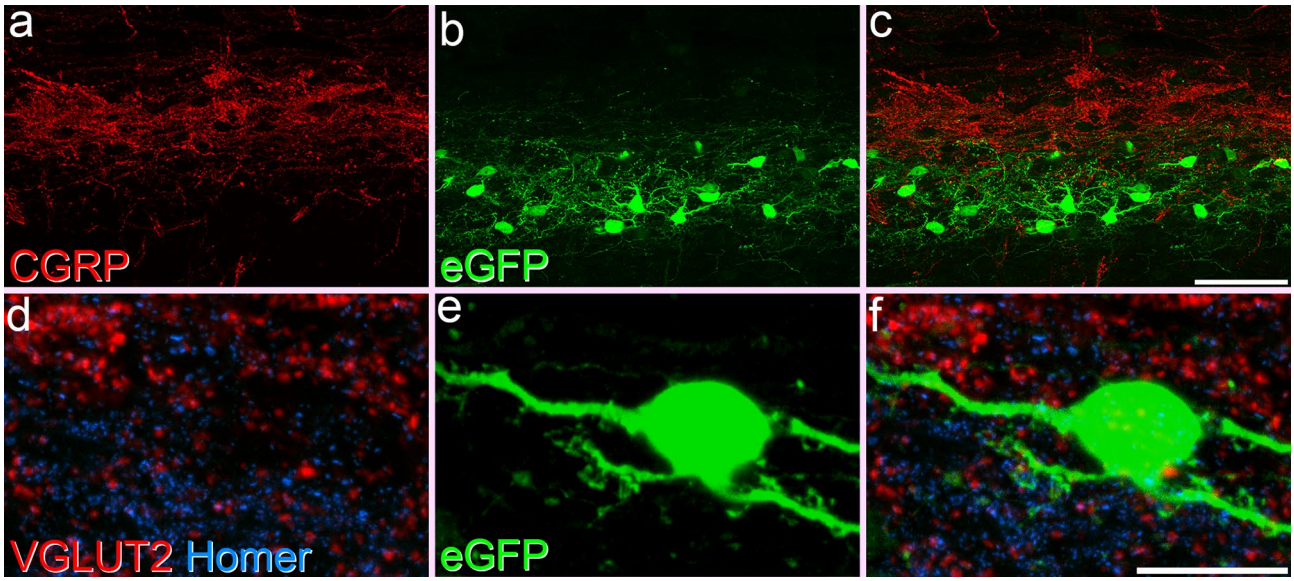

Figure 6. Limited input to GRP-eGFP cells from peptidergic nociceptors and boutons with strong VGLUT2-immunoreactivity. (**a**–**c**) Part of laminae I and II in a sagittal section from a GRP::eGFP mouse to show the relationship between the plexus of CGRP-immunoreactive axons (red), which are mainly located in lamina I and IIo, and the band of GRP-eGFP cells and dendrites (green). Although there is some overlap, the great majority of CGRP boutons are located dorsal to the GRP-eGFP band. The images were obtained from 51 optical sections at 0.2 µm z-spacing. (**d**,**e**) Part of lamina II in a section from a GRP::eGFP mouse stained to show VGLUT2 (red), Homer (blue) and eGFP (green) in a projection of 11 optical sections at 0.2 µm z-separation. Although there are many VGLUT2-immunoreactive boutons in this field, they are seldom associated with Homer puncta on the GRP-eGFP cell. Scale bars: (**a**–**c**) = 50 µm, (**d**–**f**) = 20 µm.

represent a highly specific population that shows virtually no overlap with any of these neuropeptide populations. As noted above, GRP itself is expressed among several transcriptomic clusters (Glut5-12)[5], but for the GRP-eGFP cells, we can rule out those that express NKB (Glut5-7), NPFF (Glut9) and SP (Glut10-11). This leaves two remaining clusters: Glut8 and Glut12. Glut12 is characterised by expression of GRPR[5], and we have found no overlap between GRP::eGFP cells and those that are Cre-positive in a $GRPR^{CreERT2}$ mouse line[41] (MG-M and AJT, unpublished data), consistent with the report by Albisetti et al.[20] that there is no overlap between mRNAs for GRP and GRPR. Our finding that ~ 25% of the eGFP + cells contained *Nmur2* mRNA suggests that at least some of them belong to the Glut8 cluster[5]. The proportion belonging to Glut8 may be considerably higher than 25%, because not all cells in this cluster apparently express Nmur2[5]. Interestingly, we had previously reported that GRP-eGFP cells were largely absent from the medial part of the dorsal horn (glabrous skin territory) in the L4-5 segments[3]. Although Häring et al.[5] do not indicate which lumbar segments were used to analyse the distribution of the different clusters in their Fig. 5, the Glut8 cells are far more numerous in the lateral half of the dorsal horn, suggesting that these cells may also be at least partially excluded from regions innervated by glabrous skin.

Unlike Häring et al., Sathyamurthy et al.[6] identify a population of excitatory interneurons based on *Grp* mRNA expression, which they define as DE1. However, these cells do not appear to express Nmur2, and given the widespread distribution of *Grp* mRNA that we observed in other well-defined neuropeptide populations, it is difficult to interpret this finding.

Since our results show that eGFP is expressed in a distinct subset of GRP neurons, this raises the question as to why this should occur. There are various reasons why BAC transgenic mice may show unexpectedly restricted expression patterns. The region of chromatin where the BAC has integrated may be silenced in certain neurons. Alternatively, fragmentation of the BAC may have occurred, resulting in loss of some regulatory elements, and there may be certain regulatory elements at a large distance from the transcription start site that were not included in the BAC. In either of these cases, expression of the transgene may be restricted to a specific subset of the expected population.

Our results provide novel information concerning the excitatory synaptic input to the GRP-eGFP cells. Albisetti et al.[20] and Pagani et al.[19] had already demonstrated that MrgA3-expressing pruritoceptive afferents innervate these cells. Here we show that they provide around a quarter of their excitatory synaptic input, and that this represents a selective targeting of the GPR-eGFP population by these afferents. In contrast, another major population of pruritoceptors, those that express SST and BNP provide little synaptic input to the GRP-eGFP cells, but are presumably able to influence them via the action of BNP on NPR1[7], since mRNA for the receptor was present in ~ 80% of these cells. Some cells in the Glut8 population express the mRNA for NPR3[5], and BNP might therefore also interact with this receptor on the GRP-eGFP cells. The post-synaptic targets of the SST/BNP afferents are as yet unknown, but the SST that they release (together with that from SST-expressing excitatory interneurons) is thought to contribute to itch via a disinhibitory mechanism involving Sst_{2a} receptors on dynorphin-expressing inhibitory interneurons[9].

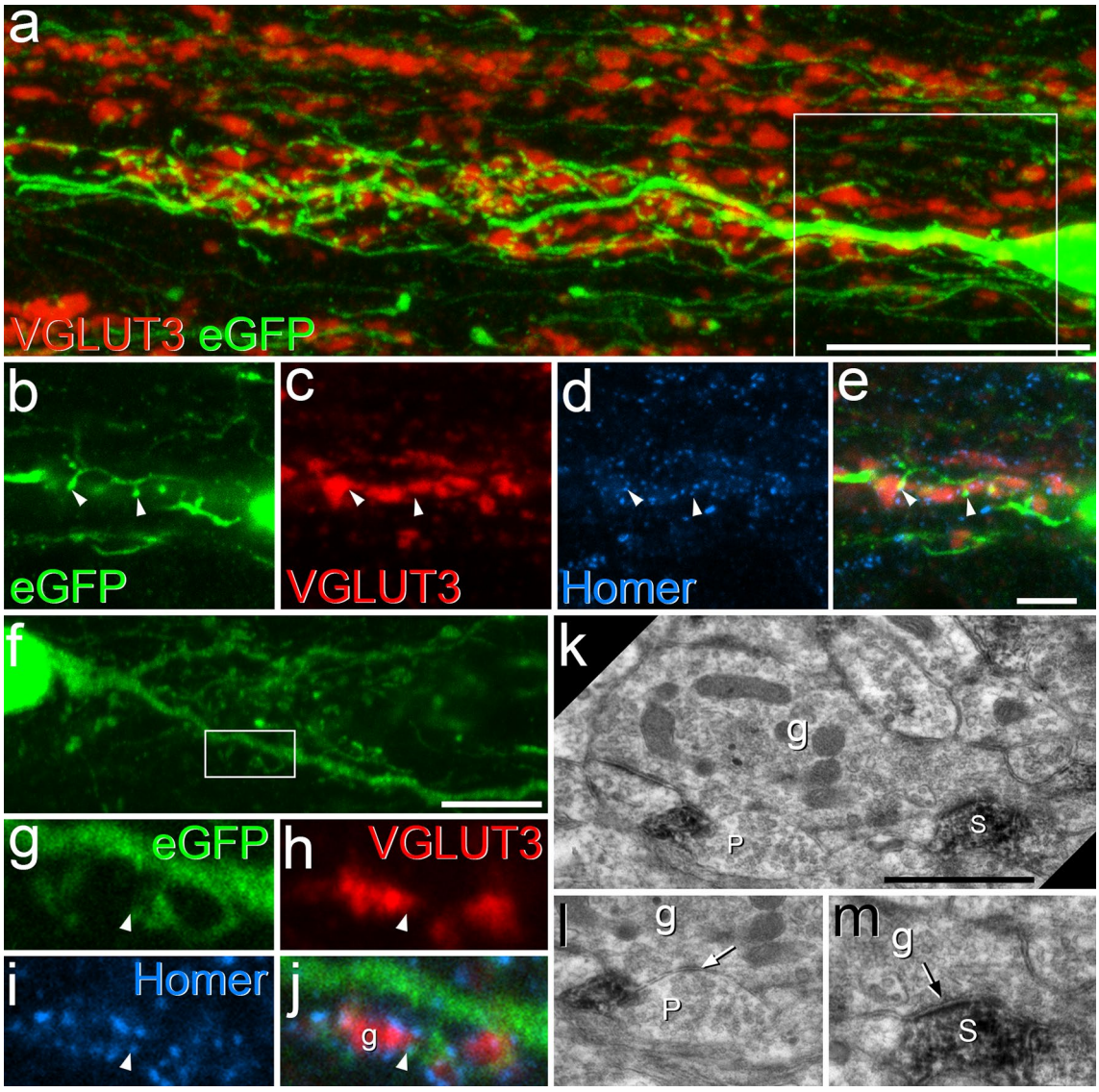

Figure 7. Synaptic input to GRP-eGFP cells from C-low threshold mechanoreceptors (C-LTMRs). (**a**) A sagittal section from a GRP::eGFP mouse that had been immunostained to reveal VGLUT3 (red) and eGFP (green) (24 optical sections at 0.2 µm z-spacing). Part of the cell body and dendritic tree of a GRP-eGFP can be seen lying within the plexus of VGLUT3-immunoreactive profiles, which correspond to C-LTMRs. (**b**–**e**) A detail from the same field in a projection of 6 optical sections (corresponding to the box in **a**), with staining for Homer (blue) also included. Two contacts between VGLUT3 boutons and GRP-eGFP dendritic spines at which Homer is present are indicated with arrowheads. (**f**–**m**) Combined confocal and electron microscopy to reveal synapses. (**f**) Part of the soma and dendrites of a GRP-eGFP cell in a projection of 36 optical sections at 0.2 µm z-spacing. (**g**–**j**) A higher magnification view (single optical section) of the boxed region in (**f**), scanned to reveal eGFP (green), VGLUT3 (red) and Homer (blue). The arrowhead points to a Homer punctum associated with an eGFP-labelled dendritic spine that is in contact with a large VGLUT3-positive bouton. (**k**–**m**) Electron microscopic images that correspond to part of the field shown in (**g**–**j**). The VGLUT3-positive bouton is shown to correspond to the central bouton of a synaptic glomerulus (g), and this forms a synapse on the eGFP-labelled dendritic spine (S), indicated with an arrow in (**m**). The VGLUT3 bouton is in synaptic contact with several other profiles, including a peripheral bouton (P) shown in (**l**) that is presynaptic to it at an axoaxonic synapse (arrow). Note that the images shown in (**l**) and (**m**) were taken after tilting the specimen in the electron beam to show synaptic specialisations more clearly. Scale bars: (**a**) = 20 µm, (**b**–**e**) = 5 µm, (**f**) = 10 µm, (**k**) = 1 µm.

We also provide evidence that the GRP-eGFP cells receive ~ 15% of their excitatory input from MrgD-expressing afferents. Although these are thought to function as mechanical nociceptors[42], MrgD is the receptor for the pruritogen β-alanine[32,43,44]. Interestingly, it has recently been reported the MrgA3 afferents, which have a well-established role in chloroquine-evoked itch[29], can also function as nociceptors engaging central opioid-responsive circuits[45]. Together, these findings are consistent with the involvement of the GRP-eGFP cells in both pruritoceptive and nociceptive transmission[18]. We have previously reported that the great majority of the GRP-eGFP cells

show outward currents during the application of DAMGO, indicating that they possess μ-opioid receptors[3], and this provides further support for the suggestion that GRP-eGFP cells engage nociceptive circuits. The finding that some of these cells express the mRNA for Nmur2 is also of interest, since mice lacking this receptor show reduced pain behaviours[46,47]. However, despite the synaptic input that the GRP-eGFP cells receive from nociceptive and pruritoceptive afferents, we have found that these cells seldom show phosphorylated extracellular signal-regulated kinases in response to either noxious or pruritic stimuli[3]. It will therefore be important in future studies to assess their responses to stimuli applied to their receptive fields.

Our findings indicate that GRP-eGFP cells in lamina IIi receive numerous synapses from VGLUT3-immunoreactive profiles, which originate from C-LTMRs. It has been suggested that these afferents may contribute to mechanically-evoked itch in humans[48], although there is apparently little evidence for such a role in rodents. Alternatively, the circuit involving C-LTMRs and GRP-eGFP cells may contribute to the phenomenon of "affective touch", which is thought to be the main function for these afferents[49].

Sun et al.[18] reported that 64% of the dorsal root ganglion neurons trans-synaptically labelled from the GRP::Cre line were CGRP-immunoreactive, suggesting a strong input to these cells from peptidergic nociceptors. However, peptidergic nociceptors have high levels of TRPV1 and we had previously found that the GRP-eGFP cells rarely showed increased miniature EPSC frequency during application of the TRPV1 agonist capsaicin[3], suggesting that they were seldom innervated by this class of afferent. Consistent with this, we found that CGRP-immunoreactive boutons provided a very small proportion of the input to the GRP-eGFP cells. The most likely explanation for this discrepancy is that some cells with CGRP in their cell bodies do not have detectable levels of the peptide in their central terminals, and these are known to include the MrgA3 afferents[29].

One unexpected finding was the low proportion (~ 10%) of Homer puncta on the GRP-eGFP cells that were associated with boutons showing strong VGLUT2-immunoreactivity, most of which are thought to originate from local excitatory interneurons[14,31]. Together with the relatively high proportions of Homer puncta that were associated with defined primary afferent populations, this suggests that these cells receive the great majority of their excitatory synaptic input from primary afferents, rather than from other excitatory interneurons. We have recently examined the input to a different interneuron population, cells that express SP, and found that for these cells boutons with strong VGLUT2 immunoreactivity contact nearly half of the Homer puncta[50], suggesting that the pattern of input to different types of interneurons varies considerably. Interestingly, we found that in slice preparations GRP-eGFP cells had exceptionally low spontaneous EPSC frequencies (mean 0.02 Hz, compared to ~ 3 Hz for SP cells)[3]. Primary afferents were transected during the slice preparation, and since it is known that axotomy can reduce the capacity for vesicle release from boutons[51], this may have contributed to the low spontaneous EPSC frequency. Alternatively, these afferents may have a naturally low release probability.

Although it is not possible to determine what proportion of excitatory synaptic input is accounted for by the different sources examined here, it is unlikely that we have been able to identify all of the input to the GRP-eGFP cells. The remainder may include contributions from other classes of primary afferent (e.g. myelinated LTMRs[21], thermoreceptors or those that express MrgB4[52]) as well as from descending sources such as the corticospinal tract[27].

Overall, our findings suggest that although the GRP-eGFP cells are a source of GRP in the dorsal horn, the peptide can also be released from other excitatory interneurons that are not captured in this line. Our understanding of the distribution of GRP within the dorsal horn has been limited by the cross-reaction of at least some GRP antibodies with other peptides, in particular SP[14,53], which results in false-positive labelling of many peptidergic nociceptors in immunohistochemical studies (although see reference[54]). However, we reported that GRP immunoreactivity could also be detected in ~ 30% of boutons with strong VGLUT2 in laminae I-IIo, most of which are likely to have originated from excitatory interneurons[14]. We also showed that in the GRP::eGFP mouse, around 75% of eGFP-labelled boutons had detectable GRP-immunoreactivity but that these accounted for only 40% of the boutons that were both VGLUT2- and GRP-immunoreactive. This would be consistent with the presence of GRP in some GFP-negative excitatory interneurons, although some of this staining may have resulted from cross-reaction with SP in boutons of SP-expressing interneurons.

Anatomical and electrophysiological evidence has indicated that the GRP-eGFP cells target another population of excitatory interneurons, which are defined by the expression of GRPR[19]. Activation of the GRPR-expressing cells depended on both a glutamatergic synaptic mechanism, and simultaneous action of GRP on the GRPR, and this connection is thought to be part of the spinal cord circuit for itch, conveying information from pruritoceptors via these two classes of interneuron (secondary and tertiary pruritoceptors) to anterolateral tract (ALT) projection neurons in lamina I[7,9]. However, a recent study[55] identified GRPR neurons as vertical cells, and this is consistent with our observations from a $GRPR^{CreERT2}$ mouse line[41] (MG-M, EP, AMB, AJT, unpublished data). Two independent groups have shown that GRP-eGFP cells correspond to a population identified by Grudt and Perl[24] as transient central cells[3,19,20]. Interestingly, paired recording studies in spinal cord slices had previously shown that transient central cells were presynaptic to vertical cells[26], but this was thought to be part of a circuit that could convey low-threshold mechanoreceptive information to lamina I ALT cells, which, when disinhibited led to tactile allodynia[25]. This raises the question of whether the transient central to vertical cell circuit contributes to tactile allodynia, itch or both. In addition, the present results suggest that this connection may be involved in transmitting information from C-LTMRs to lamina I ALT cells, consistent with the finding that affective touch is lost following anterolateral cordotomy, in which the ALT is disrupted[49].

Methods

Animals. All experiments were approved by the Ethical Review Process Applications Panel of the University of Glasgow, and were performed in accordance with the European Community directive 86/609/EC and the UK Animals (Scientific Procedures) Act 1986.

Fluorescent in situ hybridisation. Multiple-labelling fluorescent in situ hybridisation was carried out with RNAscope probes and RNAscope fluorescent multiplex reagent kit 320,850 (ACD BioTechne; Newark, CA 94560). Fresh frozen lumbar spinal cords from 3 wild-type C57BL/6 mice (either sex, 18–20 g) and 3 GRP::eGFP mice (GENSAT) (either sex, 20–24 g) were embedded in OCT medium and cut into 12 µm thick transverse sections with a cryostat (Leica CM1950; Leica, Milton Keynes, UK). Sections were mounted non-sequentially (such that sections on the same slide were at least 4 apart) onto SuperFrost Plus slides (48311-703; VWR; Lutterworth, UK) and air dried. Reactions were performed according to the manufacturer's recommended protocol. The probes used in this study, and the proteins/peptides that they correspond to, are listed in Table S2. Five different probe combinations were used. The first consisted of *Grp* (channel 1), *Slc17a6* (channel 2) and *Sst* (channel 3). For the other four, the probes for channel 1 and channel 2 were *Grp* and *eGFP*, respectively, while the 3rd channel probe was *Tac1*, *Tac2*, *Nmur2* or *NPR1*. Positive and negative control probes were also tested on other sections as described previously[23]. Sections were mounted with Prolong-Glass anti-fade medium with NucBlue (Hoechst 33342) (ThermoFisher Scientific, Paisley, UK) and scanned with a Zeiss LSM 710 confocal microscope through the 40 × oil-immersion lens (numerical aperture 1.3) with the confocal aperture set to 1 Airy unit. Sections were selected prior to viewing in situ hybridization fluorescence, to avoid bias and for each section the full thickness was acquired with a 1 µm z-step, using tile scanning to include the whole of laminae I and II.

Analysis of the relationship between *Sst*, *Grp* and *Slc17a6* was conducted on a single representative optical section from the centre of the image stack using the cell detection and subcellular objects features of Qupath software (Qupath, University of Edinburgh, Edinburgh, UK). Recognition and segmentation of individual nuclei was performed based on NucBlue staining and an additional 2 µm perimeter was added to each nucleus to allow detection of perinuclear transcripts. This additional perimeter was omitted where cells were directly adjacent to each other. Any areas with poor nuclear segmentation were excluded manually from the analysis following examination of each segmented section. Single RNA transcripts for each target gene appeared as individual puncta and detection thresholds were adjusted manually until the mark-up accurately reflected the transcript distribution. Cells were defined as positive for expression of a given gene if they contained greater than four transcripts. Where *eGFP* distribution was analysed, this was performed manually using Neurolucida for Confocal software (MBF Bioscience, Williston, VT, USA) as transcripts were less numerous than in the experiments described above. The entire z-stack was examined, and transcripts belonging to a cell were judged as those distributed either within the nucleus or immediately adjacent to it. Cells were categorised in such a way (using the hide marker feature) that positivity for eGFP and the other marker (i.e. *Nmur2, Tac1, Tac2, Npr1*) were allocated blindly to prior assessments.

Immunohistochemistry. Tissue for immunohistochemistry came from 9 GRP::eGFP mice (either sex, 18–30 g) and 2 male GRP::eGFP;MrgD^{CreERT2};Ai9 mice (24, 29 g). The GRP::eGFP;MrgD^{CreERT2};Ai9 mice had received i.p. injections of 2 mg tamoxifen at least 10 days before perfusion fixation. The animals were deeply anaesthetised and perfused with fixative, containing 4% freshly depolymerised formaldehyde. Lumbar spinal cord segments were removed and stored in the same fixative for 2 h at 4 °C. In addition, we obtained fixed tissue from 2 GRP::eGFP;MrgA3::Cre;Ai14 mice[19,20] and from 4 Tg-Avil (GENSAT) mice[35].

Multiple-labelling immunofluorescence reactions were performed as described previously[22,56] on 60 µm thick parasagittal or transverse sections cut from this tissue with a vibrating blade microtome (Leica VT1200 or VT1000). The sources and concentrations of antibodies are listed in Table S3. Sections were incubated for 3 days at 4 °C in primary antibodies diluted in PBS that contained 0.3 M NaCl, 0.3% Triton X-100 and 5% normal donkey serum, and then overnight in appropriate species-specific secondary antibodies (Jackson Immunoresearch, West Grove, PA, USA), which were raised in donkey and conjugated to Alexa488, Alexa647, Rhodamine Red, Pacific Blue or biotin. All secondary antibodies were diluted 1:500 (in the same diluent), apart from those conjugated to Rhodamine Red or Pacific Blue, which were diluted 1:100 and 1:200, respectively. Biotinylated secondary antibodies were revealed either with Pacific Blue conjugated to avidin (1:1,000; Life Technologies, Paisley, UK) or with a tyramide signal amplification (TSA) method (TSA kit tetramethylrhodamine NEL702001, Perkin Elmer Life Sciences, Boston, MA, USA). The TSA reaction was used to detect the VGLUT3 antibody. Following the immunoreaction, sections were mounted in anti-fade medium and stored at – 20 °C. They were scanned with a Zeiss LSM710 confocal microscope equipped with Argon multi-line, 405 nm diode, 561 nm solid state and 633 nm HeNe lasers. Confocal image stacks were obtained through a 63 × oil immersion lens (numerical aperture 1.4) with the confocal aperture set to 1 Airy unit or less. All analyses were performed with Neurolucida for Confocal software (MBF Bioscience, Williston, VT, USA).

Transverse sections from the Tg-Avil mice were reacted to reveal eGFP (guinea-pig antibody), PAP and SST, and confocal image stacks including the entire medio-lateral extent of the dorsal horn were acquired at a z-separation of 0.3 µm. Scans were initially viewed such that only the eGFP and SST channels were visible, and SST + /eGFP + boutons were sampled based on a grid system, as described previously[14]. Between 94 and 159 (mean 140) boutons per animal were selected and the presence or absence of PAP was then determined. For one of the animals, the locations of these boutons seen in a single section was plotted onto an outline of the dorsal horn.

Tissue from the GRP::eGFP;MrgA3::Cre;Ai14 and GRP::eGFP;MrgD^{CreERT2};Ai9 mice was cut into sagittal sections, which were reacted with antibodies against eGFP (guinea-pig antibody), Homer and mCherry.

Sections were initially viewed to allow identification of suitable GRP-eGFP cells, and 4 of these were selected from each animal, before the relationship to labelled primary afferents was visualised. As we have previously shown that GRP-eGFP cells were largely absent from the medial part of the dorsal horn (glabrous skin territory) in the L4-5 segments[3], these areas were avoided when selecting cells to be traced. Confocal z-scans (0.2 µm separation) were obtained to include as much of the dendritic tree of each cell as could be identified within the section. The dendritic trees were reconstructed for as far as these could be followed in the confocal scans, and

the locations of Homer puncta in the dendritic spines and shafts were plotted onto these reconstructions. Only when this was completed was the channel corresponding to tdTomato revealed, and the presence or absence of a tdTomato profile adjacent to each Homer punctum was recorded. In this way, we determined the proportion of Homer puncta on each cell that were in contact with a labelled primary afferent bouton. Details of the numbers of Homer puncta and the lengths of reconstructed dendrites are given in Table S4. To determine the proportion of synaptic output from each afferent type that was accounted for by GRP-eGFP cells, we used an unbiased grid sampling strategy to select Homer puncta that were associated with tdTomato+ boutons and subsequently determined whether these were in contact with an eGFP profile. In order to determine the proportion of excitatory synapses in the GRP-eGFP dendritic band that were associated with GRP-eGFP cells, we viewed only the Homer channel and sampled between 400 and 430 immunoreactive puncta per animal, before revealing the eGFP channel and noting whether these were within an eGFP profile.

To analyse input from other primary afferent classes, tissue from GRP::eGFP or GRP::eGFP;MrgA3::Cre;Ai14 mice was cut into sagittal sections. These were immunoreacted to detect the following presynaptic bouton markers: (i) SST/PAP, (ii) CGRP, and (iii) VGLUT3. The combinations of antibodies used were as follows: (i) SST, PAP, Homer, GFP (guinea pig-antibody); (ii) CGRP, Homer, GFP (guinea pig-antibody); and (iii) VGLUT3, Homer, GFP (rabbit antibody). In order to investigate synaptic input from putative excitatory interneurons, we used antibody against VGLUT2 on sections from 5 different mice. In three of these cases, chicken anti-VGLUT2 was added to combinations (ii) or (iii) above, while tissue from two further GRP::eGFP mice was reacted with guinea-pig anti-VGLUT2, together with rabbit anti-GFP and Homer antibody. Confocal scanning and cell reconstruction were performed as described above. Once this was completed, the channel corresponding to the axonal marker in question was revealed and the presence or absence of an immunoreactive bouton adjacent to each Homer punctum recorded. Details of the numbers of Homer puncta and the lengths of reconstructed dendrites are given in Table S4. To determine the proportion of synaptic output from each afferent type that was associated with GRP-eGFP cells, we again used an unbiased grid sampling strategy to select Homer puncta that were associated with primary afferent boutons and subsequently determined whether these were in an eGFP profile.

Combined confocal and electron microscopy. To confirm that synapses were present at contacts between VGLUT3-immunoreactive boutons and dendrites of GRP-eGFP neurons, we used a combined confocal and electron microscopic method[37]. Sagittal sections from lumbar spinal cord of two GRP::eGFP mice (either sex, 24–28 g) that had been fixed by perfusion with a solution containing glutaraldehyde (0.2%) and formaldehyde (4%) were processed for immunostaining with antibodies against eGFP (rabbit-antibody), Homer and VGLUT3. The immunoreaction was performed as described above, except that the sections were treated for 30 min with 1% sodium borohydride (to minimise non-specific staining resulting from glutaraldehyde fixation) and antibodies were diluted in PBS that did not contain detergent. The secondary antibody mixture included fluorescent secondary antibodies to reveal eGFP, Homer and VGLUT3, together with a biotinylated antibody to reveal eGFP. Following this step, sections were incubated in avidin-HRP (Sigma-Aldrich, Gillinhgam, UK; E2886, 1:1,000) and mounted in anti-fade medium. One eGFP-immunoreactive cell was identified from each animal and scanned with the confocal microscope to reveal contacts from VGLUT3 containing boutons. The section containing the cell was then removed from the slide, reacted with diaminobenzidine to reveal the HRP-labelled (GFP-immunoreactive) profiles, osmicated (1% OsO_4 for 20 min) and flat-embedded in Durcupan resin, as described previously[37]. A series of ~ 100 ultrathin sections (silver interference colour, ~ 70 nm thickness) was cut through part of the cell with a diamond knife. The sections were collected in serial order on Formvar-coated slot grids, stained with uranyl acetate and lead citrate, and viewed with a Philips CM100 electron microscope (EM), equipped with a digital camera. The regions of dendrite that appeared in the ultrathin sections were identified based on their location in relation to landmarks (e.g. capillaries) that could be recognised in the confocal image stacks.

Data availability

The datasets generated and analysed during the current study are available from the corresponding authors on reasonable request.

Received: 28 March 2020; Accepted: 15 July 2020
Published online: 06 August 2020

References

1. Abraira, V. E. & Ginty, D. D. The sensory neurons of touch. *Neuron* **79**, 618–639 (2013).
2. Todd, A. J. Identifying functional populations among the interneurons in laminae I-III of the spinal dorsal horn. *Molecular pain* **13**, 1744806917693003 (2017).
3. Dickie, A. C. *et al.* Morphological and functional properties distinguish the substance P and gastrin-releasing peptide subsets of excitatory interneuron in the spinal cord dorsal horn. *Pain* **160**, 442–462 (2019).
4. Gutierrez-Mecinas, M., Furuta, T., Watanabe, M. & Todd, A. J. A quantitative study of neurochemically defined excitatory interneuron populations in laminae I-III of the mouse spinal cord. *Mol. Pain* **12**, 1744806916629065 (2016).
5. Häring, M. *et al.* Neuronal atlas of the dorsal horn defines its architecture and links sensory input to transcriptional cell types. *Nat. Neurosci.* **21**, 869–880 (2018).
6. Sathyamurthy, A. *et al.* Massively parallel single nucleus transcriptional profiling defines spinal cord neurons and their activity during behavior. *Cell Rep.* **22**, 2216–2225 (2018).
7. Mishra, S. K. & Hoon, M. A. The cells and circuitry for itch responses in mice. *Science* **340**, 968–971 (2013).
8. Sun, Y. G. & Chen, Z. F. A gastrin-releasing peptide receptor mediates the itch sensation in the spinal cord. *Nature* **448**, 700–703 (2007).
9. Huang, J. *et al.* Circuit dissection of the role of somatostatin in itch and pain. *Nat. Neurosci.* **21**, 707–716 (2018).

10. Sukhtankar, D. D. & Ko, M. C. Physiological function of gastrin-releasing peptide and neuromedin B receptors in regulating itch scratching behavior in the spinal cord of mice. *PLoS ONE* **8**, e67422 (2013).
11. Pereira, P. J. *et al.* GRPR/PI3Kgamma: Partners in Central Transmission of Itch. *J. Neurosci.* **35**, 16272–16281 (2015).
12. Sun, Y. G. *et al.* Cellular basis of itch sensation. *Science* **325**, 1531–1534 (2009).
13. Akiyama, T. *et al.* A central role for spinal dorsal horn neurons that express neurokinin-1 receptors in chronic itch. *Pain* **156**, 1240–1246 (2015).
14. Gutierrez-Mecinas, M., Watanabe, M. & Todd, A. J. Expression of gastrin-releasing peptide by excitatory interneurons in the mouse superficial dorsal horn. *Mol. Pain* **10**, 79 (2014).
15. Solorzano, C. *et al.* Primary afferent and spinal cord expression of gastrin-releasing peptide: message, protein, and antibody concerns. *J. Neurosci.* **35**, 648–657 (2015).
16. Fleming, M. S. *et al.* The majority of dorsal spinal cord gastrin releasing peptide is synthesized locally whereas neuromedin B is highly expressed in pain- and itch-sensing somatosensory neurons. *Mol. Pain* **8**, 52 (2012).
17. Heintz, N. BAC to the future: the use of BAC transgenic mice for neuroscience research. *Nat. Rev. Neurosci.* **2**, 861–870 (2001).
18. Sun, S. *et al.* Leaky Gate Model: intensity-dependent coding of pain and itch in the spinal cord. *Neuron* **93**, 840–853 (2017).
19. Pagani, M. *et al.* How gastrin-releasing peptide opens the spinal gate for itch. *Neuron* **103**, 102–117 (2019).
20. Albisetti, G. W. *et al.* Dorsal horn gastrin-releasing peptide expressing neurons transmit spinal itch but not pain signals. *J. Neurosci.* **39**, 2238–2250 (2019).
21. Albisetti, G. W. *et al.* Identification of two classes of somatosensory neurons that display resistance to retrograde infection by rabies virus. *J. Neurosci.* **37**, 10358–10371 (2017).
22. Gutierrez-Mecinas, M., Bell, A., Polgar, E., Watanabe, M. & Todd, A. J. Expression of neuropeptide FF defines a population of excitatory interneurons in the superficial dorsal horn of the mouse spinal cord that respond to noxious and pruritic stimuli. *Neuroscience* **416**, 281–293 (2019).
23. Gutierrez-Mecinas, M. *et al.* Expression of cholecystokinin by neurons in mouse spinal dorsal horn. *J. Comp. Neurol.* **527**, 1857–1871 (2019).
24. Grudt, T. J. & Perl, E. R. Correlations between neuronal morphology and electrophysiological features in the rodent superficial dorsal horn. *J. Physiol.* **540**, 189–207 (2002).
25. Lu, Y. *et al.* A feed-forward spinal cord glycinergic neural circuit gates mechanical allodynia. *J. Clin. Invest.* **123**, 4050–4062 (2013).
26. Lu, Y. & Perl, E. R. Modular organization of excitatory circuits between neurons of the spinal superficial dorsal horn (laminae I and II). *J. Neurosci.* **25**, 3900–3907 (2005).
27. Abraira, V. E. *et al.* The cellular and synaptic architecture of the mechanosensory dorsal horn. *Cell* **168**, 295–310 (2017).
28. Gutierrez-Mecinas, M. *et al.* Immunostaining for Homer reveals the majority of excitatory synapses in laminae I-III of the mouse spinal dorsal horn. *Neuroscience* **329**, 171–181 (2016).
29. Han, L. *et al.* A subpopulation of nociceptors specifically linked to itch. *Nat. Neurosci.* **16**, 174–182 (2013).
30. Seal, R. P. *et al.* Injury-induced mechanical hypersensitivity requires C-low threshold mechanoreceptors. *Nature* **462**, 651–655 (2009).
31. Todd, A. J. *et al.* The expression of vesicular glutamate transporters VGLUT1 and VGLUT2 in neurochemically defined axonal populations in the rat spinal cord with emphasis on the dorsal horn. *Eur. J. Neurosci.* **17**, 13–27 (2003).
32. Fatima, M. *et al.* Spinal somatostatin-positive interneurons transmit chemical itch. *Pain* **160**, 1166–1174 (2019).
33. Usoskin, D. *et al.* Unbiased classification of sensory neuron types by large-scale single-cell RNA sequencing. *Nat. Neurosci.* **18**, 145–153 (2015).
34. Taylor-Blake, B. & Zylka, M. J. Prostatic acid phosphatase is expressed in peptidergic and nonpeptidergic nociceptive neurons of mice and rats. *PLoS ONE* **5**, e8674 (2010).
35. Sikandar, S., West, S. J., McMahon, S. B., Bennett, D. L. & Dickenson, A. H. Sensory processing of deep tissue nociception in the rat spinal cord and thalamic ventrobasal complex. *Physiol. Rep.* **5**, e13323 (2017).
36. Olson, W. *et al.* Sparse genetic tracing reveals regionally specific functional organization of mammalian nociceptors. *Elife* **6**, 1 (2017).
37. Todd, A. J. *et al.* Projection neurons in lamina I of rat spinal cord with the neurokinin 1 receptor are selectively innervated by substance P-containing afferents and respond to noxious stimulation. *J. Neurosci.* **22**, 4103–4113 (2002).
38. Larsson, M. & Broman, J. Synaptic organization of VGLUT3 expressing low-threshold mechanosensitive c fiber terminals in the rodent spinal cord. *eNeuro* **6**, 1. https://doi.org/10.1523/ENEURO.0007-19.2019 (2019).
39. Brumovsky, P., Watanabe, M. & Hokfelt, T. Expression of the vesicular glutamate transporters-1 and -2 in adult mouse dorsal root ganglia and spinal cord and their regulation by nerve injury. *Neuroscience* **147**, 469–490 (2007).
40. Zeisel, A. *et al.* Molecular architecture of the mouse nervous system. *Cell* **174**, 999–1014 (2018).
41. Mu, D. *et al.* A central neural circuit for itch sensation. *Science* **357**, 695–699 (2017).
42. Cavanaugh, D. J. *et al.* Distinct subsets of unmyelinated primary sensory fibers mediate behavioral responses to noxious thermal and mechanical stimuli. *Proc. Natl. Acad. Sci. USA* **106**, 9075–9080 (2009).
43. Liu, Q. *et al.* Mechanisms of itch evoked by beta-alanine. *J. Neurosci.* **32**, 14532–14537 (2012).
44. Qu, L. *et al.* Enhanced excitability of MRGPRA3- and MRGPRD-positive nociceptors in a model of inflammatory itch and pain. *Brain* **137**, 1039–1050 (2014).
45. Sharif, B., Ase, A. R., Ribeiro-da-Silva, A. & Seguela, P. Differential coding of itch and pain by a subpopulation of primary afferent neurons. *Neuron* **106**, 1–12 (2020).
46. Zeng, H. *et al.* Neuromedin U receptor 2-deficient mice display differential responses in sensory perception, stress, and feeding. *Mol Cell Biol* **26**, 9352–9363 (2006).
47. Torres, R. *et al.* Mice genetically deficient in neuromedin U receptor 2, but not neuromedin U receptor 1, have impaired nociceptive responses. *Pain* **130**, 267–278 (2007).
48. Fukuoka, M., Miyachi, Y. & Ikoma, A. Mechanically evoked itch in humans. *Pain* **154**, 897–904 (2013).
49. McGlone, F., Wessberg, J. & Olausson, H. Discriminative and affective touch: sensing and feeling. *Neuron* **82**, 737–755 (2014).
50. Polgár, E. *et al.* Substance P-expressing neurons in the superficial dorsal horn of the mouse spinal cord: insights into their functions and their roles in synaptic circuits. Neuroscience (In Press). (2020).
51. Staley, K. J. & Mody, I. Integrity of perforant path fibers and the frequency of action potential independent excitatory and inhibitory synaptic events in dentate gyrus granule cells. *Synapse* **9**, 219–224 (1991).
52. Liu, Q. *et al.* Molecular genetic visualization of a rare subset of unmyelinated sensory neurons that may detect gentle touch. *Nat. Neurosci.* **10**, 946–948 (2007).
53. Goswami, S. C. *et al.* Itch-associated peptides: RNA-Seq and bioinformatic analysis of natriuretic precursor peptide B and gastrin releasing peptide in dorsal root and trigeminal ganglia, and the spinal cord. *Mol. Pain* **10**, 44 (2014).
54. Barry, D. M. *et al.* Exploration of sensory and spinal neurons expressing gastrin-releasing peptide in itch and pain related behaviors. *Nat. Commun.* **11**, 1397 (2020).
55. Koga, K. *et al.* Sensitization of spinal itch transmission neurons in a mouse model of chronic itch requires an astrocytic factor. *J. Allergy Clin. Immunol.* **145**, 183–191 (2020).
56. Gutierrez-Mecinas, M. *et al.* Preprotachykinin A is expressed by a distinct population of excitatory neurons in the mouse superficial spinal dorsal horn including cells that respond to noxious and pruritic stimuli. *Pain* **158**, 440–456 (2017).

Acknowledgements
We thank Mr. R. Kerr and Mrs. C. Watt for expert technical assistance. Financial support from the Wellcome Trust (Grant 102645) and the Medical Research Council (Grant MR/S002987/1) is gratefully acknowledged.

Author contributions
A.M.B. and A.J.T. conceived the project, designed experiments, prepared the figures and wrote the manuscript; A.M.B., M.G.-M., A.S. and A.C.-B. performed immunohistochemistry, confocal scanning and analysis; A.M.B. performed in situ hybridisation, confocal scanning and analysis; H.W. and S.J.W. provided spinal cord tissue; M.W. provided reagents; all authors reviewed and approved the manuscript.

Competing interests
The authors declare no competing interests.

Additional information
Supplementary information is available for this paper at https://doi.org/10.1038/s41598-020-69711-7.

Correspondence and requests for materials should be addressed to A.M.B. or A.J.T.

Reprints and permissions information is available at www.nature.com/reprints.

Publisher's note Springer Nature remains neutral with regard to jurisdictional claims in published maps and institutional affiliations.

Expression of green fluorescent protein defines a specific population of lamina II excitatory interneurons in the GRP::eGFP mouse

Andrew M. Bell*[1], Maria Gutierrez-Mecinas[1], Anna Stevenson[1], Adrian Casas-Benito[1], Hendrik Wildner[2], Steven J. West[3], Masahiko Watanabe[4], Andrew J. Todd*[1]

[1]Institute of Neuroscience and Psychology, College of Medical, Veterinary and Life Sciences, University of Glasgow, Glasgow, G12 8QQ, UK; [2]Institute of Pharmacology and Toxicology, University of Zurich; and Institute of Pharmaceutical Sciences, Swiss Federal Institute of Technology (ETH) Zürich, Zürich, Switzerland; [3]The Nuffield Department of Clinical Neurosciences, University of Oxford, John Radcliffe Hospital, Oxford, OX3 9DU, UK; [4]Department of Anatomy, Hokkaido University School of Medicine, Sapporo 060-8638, Japan

Supplementary Tables 1-4

Table S1 Results of in situ hybridisation experiments with probes against mRNAs for *Grp*, *eGFP* and *NPR1*.

	Number of *Grp*+ *eGFP*+ cells	Number of *Grp*+ *eGFP*+ With *NPR1*	% *Grp*+ *eGFP*+ with *NPR1*	Number of *Grp*+ *eGFP*- cells	Number of *Grp*+ *eGFP*- With *NPR1*	% *Grp*+ *eGFP*- with *NPR1*	Total Number *NPR1*+ cells	% *NPR1* that are *Grp*+ *eGFP*+	% *NPR1* that are *Grp*+ *eGFP*-	% *NPR1* that are G*rp*+
Mean	86.6	66.3	76.5%	260.6	82.2	32.2	260	25.6	31.8	57.3
Range	72-94	55-73	75.5-77.7	186-324	65-90	27.8-34.9	239-298	23.0-29.2	27.2-37.9	50.2-67.1

Results are from 3 animals, in which transverse sections including the whole superficial dorsal horn were analysed.

Table S2 RNAscope probes used in this study

Probe	**Protein/peptide**	**Channel numbers**	**Catalogue numbers**	**Z-pair number**	**Target region**
Slc17a6	VGLUT2	2	319171	20	1986-2998
SST	Somatostatin	1,3	404631	6	18 - 407
Grp	Gastrin-releasing peptide	1	317861	15	22 – 825
eGFP	enhanced green fluorescent protein	2	400281	13	628 - 1352
Tac1	Substance P	3	410351	15	20 - 1034
Tac2	NKB	3	446391	15	15 - 684
Npff	Neuropeptide FF	2	479901	9	47 - 433
Nmur2	Neuromedin U receptor 2	3	314111	20	69 - 1085
NPR1	Natriuretic peptide receptor 1	3	484531	20	941 - 1882
RNAscope multiplex positive control (*Polr2a*, *Ppib*, *Ubc*)	Polr2a: DNA-directed RNA polymerase II subunit RPB1; Ppib: Peptidyl-prolyl cis-trans isomerase B; Ubc: Polyubiquitin-C	1,2,3	320881	20 15 n/a	2802 – 3678 98 – 856 34 - 860
RNAscope multiplex negative control (*dapB*)	dapB: 4-hydroxy-tetrahydrodipicolinate reductase (derived from B Subtilis)	1,2,3	320871	10	414 - 862

Table S3 Antibodies used in this study

Antibody	**Species**	**Dilution**	**Source**	**Catalogue #**
eGFP	Rabbit	1:5K	M Watanabe	
eGFP	Guinea Pig	1:1K	M Watanabe	
mCherry†	Rat	1:1K	Invitrogen	M11217
Homer	Goat	1:1K	M Watanabe	
PAP	Chicken	1:1K	Aves	PAP
SST	Rabbit	1:1K	Peninsula	T-4103
CGRP	Rabbit	1:10K	Enzo	BML-CA1134
VGLUT2	Chicken	1:500	Synaptic systems	135416
VGLUT2	Guinea Pig	1:5K	MilliporeSigma	AB2251-I
VGLUT3	Guinea Pig	1:20K* or 1:100#	M Watanabe	

* Used with the tyramide signal-amplification method for confocal microscopy
# Used without amplification in tissue for combined confocal and electron microscopy
†This antibody recognizes TdTomato

Table S4. Quantitative data for Homer-based analyses

		Analysis of input to individual cells			Analysis of output from different types of bouton
Bouton type	Number of animals	Total cells (cells per animal)	Dendritic length µm	Homer puncta per cell	Number of Homer puncta analysed
MrgA3	2	8 (4)	406.7 (224-793)	107.1 (64-159)	161 (154 - 170)
MrgD	2	8 (4)	428.1 (248 - 629)	81.75 (43 - 152)	401 (392 - 410)
SST+/PAP+	3	N/A	N/A	N/A	129 (104 - 141)
VGLUT3 - Majority of cell within plexus	4	12 (3)	483.8 (249-755)	86.75 (41-126)	105 (100 - 113)
VGLUT3 - Majority of cell outside plexus	3	3 (1)	379.6 (308-452)	80 (58 - 121)	N/A
CGRP	3	12 (4)	508.6 (182-1167)	115.9 (59-206)	121 (154 - 170)
VGLUT2	5	16 (3.2)	484.3 (290 - 1167)	95.6 (45 - 206)	N/A

N/A: not analysed

6 General Discussion

The underlying hypothesis of this work is that EGFP-expressing cells in the GRP-EGFP mouse represent a distinct functional population of excitatory interneurons. The major findings of each study and those that support this are outlined below.

Paper I

Since GRP-EGFP cells have been proposed as secondary pruritoceptors, we hypothesised that they would be activated following intradermal injection of the pruritogen chloroquine. Using both Fos expression and phosphorylation of ERK as markers of neuronal activation we found that around 20% of all neurons in laminae I-IIo in a somatotopically appropriate area showed these markers. However, GRP-EGFP cells were seldom positive for Fos or pERK; showing these markers in 7% and 3% of cells respectively. We conclude that despite frequently being intermingled with activated neurons GRP-EGFP cells were significantly less likely to show Fos or pERK following chloroquine injection than other neurons.

Paper II

In order to provide evidence that GRP-EGFP cells represent a distinct functional population, in this study we compared a number of their characteristics with those of a separate population of excitatory interneurons in lamina II; those expressing substance P. Substance P-expressing cells were identified using a $Tac1^{Cre}$ mouse line and these populations were shown to be largely non-overlapping using both immunocytochemical and *in situ* hybridisation based analyses.

One of the primary aims of this study was to reconstruct the somatodendritic and axonal morphology of GRP-EGFP cells and compare this to that of the SP-expressing cells. Although we found that GRP-EGFP cells were morphologically heterogeneous, at least some of these cells could be classified as central. This was in marked contrast to the SP-expressing cells, which generally showed radial like morphology. Hierarchical cluster analysis using morphometric parameters was able to separate these two classes into two clear clusters further confirming the initial qualitative assessment. Significant differences between the two

populations were also found in terms of their propriospinal connections. Gutierrez-Mecinas et al. (2018) had previously shown that SP-expressing cells have long propriospinal axonal projections. We hypothesised that this may be the case with GRP-EGFP cells as during the course of our experiments we often found their axons left the tissue slice in which cells were located. However, using CTb retrograde tracing, we established that GRP-EGFP cells are significantly underrepresented among the superficial dorsal horn neurons that have long ascending propriospinal axons extending greater than 5 segments.

The two populations of cells were also shown to be different in terms of their activity-dependent marker immunoreactivity following noxious and pruritic stimuli. Again, we had previously shown that SP-expressing cells were commonly activated following noxious and pruritic stimuli using Fos expression as an activity dependent marker (Gutierrez-Mecinas et al., 2017). Conversely, in the study presented here we found that GRP-EGFP cells were significantly underrepresented amongst cells phosphorylating ERK following noxious heat, capsaicin and mechanical stimulation and the intradermal injection of histamine. This is despite a similar percentage of activated cells (those positive for Fos or pERK) in both the studies.

Finally, we showed that several electrophysiological properties were significantly different between the two cell populations. The majority of GRP-EGFP cells showed transient or single spike firing patterns, whereas SP-expressing cells mainly showed delayed firing. Differences were also documented in their pattern of inputs, with GRP-EGFP cells seldom receiving input from primary afferents expressing TRPV1 in contrast to SP-expressing cells which frequently did. The responses to neuromodulators were also notably different between the two populations, with GRP-EGFP cells consistently showing outward currents in response to MOR agonists while SP cells did not. The converse was true of responses to noradrenaline and 5-HT, where SP cells demonstrated outward currents following application but GRP-EGFP cells did not.

In summary, we find a number of anatomical and physiological features which are not only highly consistent within the GRP-EGFP population but are also markedly different from the properties of SP-expressing cells. This suggests that in this instance, two defined populations of interneurons appear functionally different.

Paper III

Transcriptomic studies have suggested the presence of additional classes of excitatory interneurons in the dorsal horn, and one of these classes is defined by the expression of NPFF. In this study we validated a new antibody against pro-NPFF in order to reveal these cells. The distribution of pro-NPFF immunoreactivity was concentrated in the superficial dorsal horn and was observed in both axon terminals and perikaryal cytoplasm. The distribution of cells was very similar to that seen with previous *in situ* hybridisation and immunocytochemical studies. These cells represented 5% of SDH neurons and were universally excitatory as defined by the absence of Pax2 staining. Furthermore, 85% of them co-expressed somatostatin. In order to establish whether the Npff population overlapped with any of the previous established populations we performed *in situ* hybridisation for *Npff* against *Tac1*, *Tac2*, *Cck*, *Nts* and *Grp*. There was negligible overlap with *Tac2, Cck* and *Nts* and only 4% of the cells were *Tac1*. However, there was significant overlap between cells expressing *Grp* and those expressing *Npff*. Around 38% of the *Npff* cells were positive for *Grp* mRNA, which represented 6% of the *Grp*+ population. This was somewhat unexpected as GRP-EGFP cells have been proposed as a homogeneous functional population of cells. Further immunocytochemistry in this paper demonstrated a complete lack of overlap between pro-NPFF-expressing cells and those which were EGFP positive in the GRP-EGFP mouse. This is evidence of a significant discrepancy between *Grp* expression and EGFP expression in that mouse line, and this is investigated further in paper IV.

The proportions of NPFF cells which responded to noxious and pruritic stimuli were also tested in this paper with around 50% phosphorylating ERK in response to pinch, 60% to capsaicin, and 30% each to heat, histamine & chloroquine. Altogether the results of this paper suggest that NPFF is expressed by a distinct population of SDH excitatory interneurons, which are likely to be involved in pain and itch transmission.

Paper IV

In this study we initially tested whether *Grp* expression was as widespread as suggested by transcriptomic studies. Using multiplex *in situ* hybridisation with probes against *Slc17a6*

(VGLUT2), *Grp* and *Sst*, we found that *Grp* was expressed in 37% of all SDH excitatory interneurons. We also found that 66% of all superficial dorsal horn excitatory neurons were somatostatin-expressing, and around half of the cells in this population were positive for *Grp* mRNA. This shows that *Grp*-expressing cells were significantly more numerous than previously suggested by studies using the GRP-EGFP mouse. Subsequently, using probes against *Grp* and *Egfp* in tissue from the GRP-EGFP mouse, we found that only 23% of cells that expressed *Grp* also expressed *Egfp*. Again, using multiplex *in situ* hybridisation we looked to determine whether the subset that expressed *Egfp* belonged to a specific class of neurons. The finding that *Grp* mRNA overlapped to a significant degree with *Tac1, Tac2* and *Npff* mRNAs but that *Egfp* mRNA do not, suggests that EGFP expression in the GRP-EGFP mouse is restricted to a discrete subset of cells that excludes these other populations. We also found a moderate degree of overlap between cells with mRNA for *Grp* with cells expressing *Nmur2* and this suggests that at least some of the GRP-EGFP cells may belong to the Glut8 population of Häring et al. (2018).

The excitatory synaptic input to GRP-EGFP cells was then analysed using neuronal reconstructions and the excitatory post-synaptic marker Homer. We observed a high level of input from MrgprA3-expressing pruritoceptors accounting for ~25% of the excitatory synapses onto the cells. Additionally, this input was selective as EGFP dendritic profiles were only apposed to ~9% of Homer profiles in lamina II, but around 30% of MrgprA3 bouton associated Homer profiles were apposed to GRP-EGFP dendrites. Subsequently, in order to determine what proportion of synapses arose from the somatostatin-expressing pruritoceptive primary afferent population (NP3), we first had to develop an approach for identifying the central terminals of these fibres. Using an Avil-GFP mouse to identify primary afferents we stained for GFP, PAP and SST and found that SST expressing primary afferent boutons (GFP+) universally expressed PAP. This meant that co-expression of SST and PAP could be used to identify these afferents in tissue from other mouse lines. Using this technique, we found there was no significant synaptic input to GRP-EGFP cells from somatostatin-expressing pruritoceptors. However, these pruritoceptors release the peptide BNP and we were able to confirm expression of mRNA for its receptor (NPR1) in 77% of GRP-EGFP cells. While expression of this receptor was not exclusive to GRP-EGFP cells this finding confirms previous results and suggests that that SST+/BNP primary afferents signal to GRP-EGFP cells via peptidergic rather than glutamatergic mechanisms.

We also determined the number of synapses arising from other primary afferent classes and found a moderate input from MrgprD-expressing non-peptidergic C-fibres but very sparse synaptic contacts arising from GCRP-immunoreactive peptidergic nociceptors. Unexpectedly we found that a very high proportion of synaptic input originated from VGLUT3-expressing C-LTMRs in the more ventral GRP-EGFP cells and these findings were verified with electron microscopy. Finally, we quantified the level of synaptic input from other local excitatory neurons using the presence of strong VGLUT2 immunoreactivity to identify their axonal boutons. The GRP-EGFP cells rarely received synapses from other local interneurons with these representing ~10% of total excitatory input. This finding is in stark contrast to those in a recent study where SP-expressing cells were found to receive approximately 50% of their excitatory synaptic inputs via this route (Polgár et al., 2020).

In summary, this paper shows that GRP-EGFP cells represent a discrete subset of those cells expressing *Grp* in the superficial dorsal horn. They demonstrate characteristic patterns of connectivity with evidence of selective input from pruritoceptors via both synaptic and peptidergic signalling. The pattern of synaptic input to GRP-EGFP cells is also clearly different from that of SP-expressing interneurons, at least with respect to connections from other local excitatory neurons, and this has functional implications for these cells.

In the light of these findings, it is appropriate to reassess the overall aims of this project beyond what is already discussed in the presented papers. These aims were; i) to establish the morphology of GRP-EGFP cells, ii) to determine the responses of these cells to noxious and pruritic stimuli, iii) To determine the pattern of synaptic inputs to these cells and, iv & v) reconcile the conflicting transcriptomic vs transgenic evidence identifying the cells that express GRP in the dorsal horn.

6.1 GRP-EGFP cells as Transient Central Cells

Several of the GRP-EGFP cells reconstructed as part of these studies were recognised as having central type morphology. This has recently been independently confirmed in a separate study with the GRP-Cre mouse (Albisetti et al., 2019). Many excitatory interneurons display delayed, gap or reluctant firing patterns (Yasaka et al., 2010), therefore the

electrophysiological finding that many of these cells display transient firing patterns also indicates that they constitute a potentially distinct population. Together these findings suggest that this population may correspond to the transient central cell population, which has been previously identified as a component of a circuit for tactile allodynia (Lu et al., 2013). This is further supported by the finding that the axonal arbors of these cells rarely enter lamina I, indicating that (as proposed in Lu et al.) they are not directly pre-synaptic to lamina I projection neurons. The finding that GRP-EGFP cells are clearly distinguishable from SP-expressing cells both qualitatively and based on detailed morphometric clustering also supports the utility of neuronal morphology as a functional classifier.

However, the GRP-EGFP cells still represent a heterogeneous group of neurons and this is seen clearly in the cluster dendrogram (Figure 8f) in Paper II. In this visualisation, the degree of heterogeneity is represented by the branching in the tree. The SP-expressing cell cluster branches late and forms a compact tree, indicating that this population is relatively homogeneous. However, the GRP-EGFP cells belong to a cluster that branches early and extensively suggesting significant heterogeneity. Based on this finding, it is arguably the consistency in morphology amongst the SP cells that results in the significant differences between the clusters rather than any consistent feature of the GRP-EGFP cells. We had hoped that using detailed morphometric analysis might offer some insights into heterogeneity that could not be captured using the existing Grudt and Perl (2002) classification scheme. In particular it might have been possible that despite marked heterogeneity, the GRP-EGFP cells could be separated into subgroups based on their morphology. However, again looking at the extensive branching in the dendrogram it is unlikely that there are clear morphological subgroups among the GRP-EGFP neurons.

What then does the morphology of a neuron dictate about its function? Ultimately the shape of the dendritic arbor is related to the type and number of synaptic inputs that cell will receive and this will define the receptive field to some degree (Parekh and Ascoli, 2013). Axonal distribution affects downstream circuits, and the lack of long propriospinal axons suggests that the GRP-EGFP cells do not broadly engage other neurons across segments and dermatomes. However, even in well-defined and distinctive neural populations, such as cortical pyramidal cells, the functional implications of a clearly organised synaptic architecture are still not fully understood (Spruston, 2008). Beyond the relationship of morphology to inputs and outputs, it

has been shown that dendritic geometry is responsible for firing properties in the neocortex (Mainen and Sejnowski, 1996). Furthermore, Abraira et al. (2017) demonstrate that detailed morphometric analysis of neurons in lamina III of the dorsal horn can be used to train linear classifiers that recognise neuronal subtypes with >80% accuracy. This approach was not used here as we only investigated 2 subtypes that were easily distinguished. However, as more digital reconstructions of dorsal horn neurons become available in open-source libraries it may be possible that a 'big data' approach will allow us to refine morphological subtypes and their links to function (Polavaram et al., 2014; Ascoli, 2015).

6.2 GRP-EGFP cells Seldom show Fos or pERK following Noxious or Pruritic Stimuli

Here we show a consistent failure of GRP-EGFP cells to respond to noxious or pruritic stimuli by phosphorylating ERK, and also expressing Fos in the case of chloroquine stimulation. This is particularly surprising in light of the proposed role of GRP-EGFP cells as secondary pruritoceptors. Itch transmission between GRP+ and GRPR+ cells in the dorsal horn has been shown to be dependent on peptide transmission alongside fast aminoacid transmitters (Akiyama et al., 2014; Pagani et al., 2019). It may be that the release of peptides and any consequently slower peptidergic signalling may be equally important at the first synapse in itch pathways. The finding of numerous neuropeptides associated with itch that are enriched in pruritoceptors is consistent with this. The NP3 class has been shown to release somatostatin and BNP (Huang et al., 2018), while neurons of the NP2 class contain NMB and other potentially important peptides of which the functional significance is as yet unknown (Xing et al., 2020). As such, itch transmission may be predominantly slow and peptidergic and hence does not drive the degree of action potential firing necessary to drive the intracellular phosphorylation of ERK and consequent downstream processes.

However, this hypothesis is not consistent with the general belief that neuropeptide release tends to require higher firing rates than those required for the release of small-molecule transmitters (Nusbaum et al., 2017). This may not be the case in all neurons however (Nusbaum et al., 2017), and firing rates in primary afferents have been shown to be lower following pruritoceptive compared to nociceptive stimuli (Ma et al., 2012). There is some evidence that distinctive patterns of firing are also seen in GRP-EGFP neurons following pruritoceptive stimuli. Sun et al. (2017), showed that action potential firing in GRP cells was

of a relatively low frequency (~1 Hz) following application of pruritogens to the DRG. Additionally, Pagani et al. (2019) reported that optogenetic stimulation of NP2 pruritoceptors induced bursts of firing in GRP-EGFP cells, but that these short bursts occurred with a low frequency (0.5 Hz). Activity-dependent markers such as pERK and Fos are proposed as markers of nociceptive activation in dorsal horn neurons (Coggeshall, 2005). However, one must question the sensitivity of these markers as indicators of activation. Motor neurons or neurons in circuits conveying touch, for example, clearly fire action potentials yet do not express Fos during movement or low threshold stimulation. It is therefore possible that the distinctive patterns of neuronal activity in GRP-EGFP cell following itch inducing stimuli may have significant behavioural implications, and yet the cells may fail to show pERK or Fos. Given the proposed role in pain suggested by Sun et al. (2017) and our finding that GRP-EGFP cells are innervated by NP1 mechano-nociceptive primary afferents, it is also surprising that these cells also do not appear to respond to noxious stimuli. However, the same considerations surrounding the sensitivity of activity-dependent markers in all neuronal classes apply to this finding. It would be of significant interest to perform patch-clamp electrophysiology on these cells while applying natural stimuli to better understand their patterns of activity. This would be possible using the novel semi-intact electrophysiology technique (Hachisuka et al., 2016).

In the majority of these experiments we used pERK as an activity dependent marker rather than Fos expression. However, our pERK based analyses resulted in a similar number of activated cells as in other separate Fos-based experiments and it is unlikely that the choice of pERK as an activity dependent marker resulted in a failure to detect activation. The expression of Fos occurs downstream of ERK phosphorylation and both are appropriate as markers of neural activation (Gao and Ji, 2009). It is therefore still unclear exactly why the GRP-EGFP cells failed to respond to noxious and pruritic stimuli. As the finding was consistent across the population it may indicate a specific functional property of these cells related to their neuronal activity and the gene expression program that this induces. Different neurochemical classes of neurons in the brain have been shown to have different gene expression responses to stimuli (Yap and Greenberg, 2018), and this could relate to the duration and pattern of neuronal activity (Tyssowski et al., 2018). Although activation of the MAPK/ERK pathway is thought to be a common factor in neuronal activity induced intracellular changes (Tyssowski et al., 2018).

6.3 GRP-EGFP cells have a Characteristic Pattern of Excitatory Synaptic Inputs

Previous studies have demonstrated direct synaptic connections between MrgprA3-expressing pruritoceptors and GRP-EGFP cells using rabies tracing and electrophysiology (Sun et al., 2017; Albisetti et al., 2019; Pagani et al., 2019). Here we extend those findings by quantifying excitatory synaptic input and showing a selective innervation of this cell type by MrgprA3 fibres. The selective nature and high proportion of this input is highly supportive of a role of GRP-EGFP cells in itch, although recent studies have questioned the itch-selectivity of MrgprA3 neurons (Sharif et al., 2020). We also showed that another class of pruritoceptor, those expressing SST/BNP, do not frequently synapse with GRP-EGFP cells. Instead there is the potential for peptidergic signalling, as GRP-EGFP cells possess mRNA for NPRA, the receptor for BNP. The co-expression of NPRA and GRP in dorsal horn neurons has previously been reported (Mishra and Hoon, 2013), and these authors showed a perfect match between NPRA and GRP-EGFP. However, this finding may have been due to cross reaction of antibodies or bleed-through of fluorophores. We extend these findings using a highly sensitive and specific multiplex *in situ* hybridisation technique which suggests that although the receptor for BNP is enriched in GRP-EGFP cells it is not exclusively expressed in either these cells or the broader population that express *Grp*.

Rabies tracing studies require the use of Cre-expressing mice so that the appropriate starter population can be targeted. Rabies-based studies investigating the inputs to GRP-expressing cells in the dorsal horn have used the GENSAT GRP-Cre mouse line (Albisetti et al., 2017; Sun et al., 2017). This line is closely related to the GRP-EGFP mouse and the populations the two mice reveal are largely overlapping (Sun et al., 2017). These rabies tracing studies offer conflicting findings, particularly relating to the degree of peptidergic and low-threshold inputs to the cells (Albisetti et al., 2017; Sun et al., 2017). Our investigations used the GRP-EGFP transgenic line and there may be differences between these lines in terms of how faithfully they report *Grp* expression which affect the translatability of findings between mice. However, in the GRP-EGFP mouse we find a low proportion of input from CGRP-expressing peptidergic nociceptors, which is consistent with electrophysiological findings in paper II suggesting that these cells do not receive inputs from TRPV1 expressing afferents. It is notable that MrgprA3 fibres do express both CGRP and TRPV1, but this is still consistent

with our results as; a) they only express detectable levels of CGRP in the DRG and not their central terminals (Han et al., 2013), and b) their expression of TRPV1 is low compared to other classes of afferent, and agonists would have been unlikely to have a significant effect (Zeisel et al., 2018).

The finding that VGLUT3-expressing C-LTMRs innervate the ventral GRP-EGFP cells was unexpected. This may represent a novel mechanism for low threshold mechanical information to access itch pathways in the central nervous system and the behavioural implications of this connectivity require further investigation. It may be that this represents an as yet undocumented component of the mechanical itch pathway (Acton et al., 2019; Pan et al., 2019) but this proposal does not agree with the recent finding that optogenetic activation of C-LTMRs inhibits itch (Sakai et al., 2020). We confirmed our C-LTMR confocal findings using a combined confocal and electron microscopy technique. Our confirmation of Homer puncta as synapses provides further support for the validity of Homer-based techniques for the quantitative analysis of neuronal synaptic connectivity. Altogether the findings relating to synaptic input demonstrate characteristic patterns of connectivity that differ between the GRP-EGFP and SP-expressing populations and this presumably has functional implications for these cells in terms of their receptive field properties.

6.4 GRP-EGFP cells represent a Discrete Subset of those cells Expressing GRP in the Dorsal Horn

Early studies with the GRP-EGFP mouse suggested a strong correspondence between EGFP and GRP with 93% of EGFP-positive cells positive for *Grp* mRNA and 68% of GRP-positive cells being EGFP immunoreactive (Solorzano et al., 2015). These authors suggested that the 68% figure was a low estimate as protease treatment prior to *in situ* hybridisation may have reduced the numbers of EGFP-immunoreactive cells. However, a number of our earlier findings suggested that EGFP expression might define a smaller population than all those cells expressing *Grp* mRNA. Firstly, the relative absence of EGFP staining in regions of the dorsal horn receiving input from glabrous skin despite the presence of *Grp* mRNA suggests failure of the reporter to express in some cells. Secondly in our initial combined *in situ* and immunocytochemistry experiments in paper II (Figure 2c) we only documented 50% of GRP-expressing cells as immunoreactive for EGFP (although this could also have been due to

protease treatment). We confirm these findings and better quantify the discrepancy using a more sensitive multiplex *in situ* technique in paper IV and find that only 25% of those cells expressing *Grp* mRNA are also EGFP positive. This is indicative of EGFP expression revealing a sub-population of these neurons. It is likely that this issue also affects the GRP-Cre mouse line as Albisetti et al. (2019) report that only 25% of *Grp* mRNA neurons are positive for reporter mRNA. It is probable that the subset of cells revealed is much the same in both mouse lines, as they have been shown to reveal largely overlapping populations (Sun et al., 2017).

This population of cells appears to be a distinct subset of *Grp*-expressing neurons as our results exclude EGFP-expressing cells from several well-defined populations that also include cells that express *Grp* mRNA. We have also attempted to reconcile the identity of this class with the clusters of Häring et al. (2018). Although we do see some of the cells expressing *Nmur2*, and hence possibly belonging to Glut8, this approach is not perfect. Nmur2 expression extends beyond just the Glut8 population and also does not reveal all the cells within this population. This issue with identity is indicative of the nature of transcriptomic definitions of cell types, where it is unlikely that one marker will define a population; instead a combination of marker genes is more likely to be required. Therefore, to truly reconcile our findings with those of Häring et al. it would be most appropriate to use a highly multiplexed *in situ* approach and include other markers such as *Reln*, which is also highly expressed in Glut8 cells. Further studies using a cell sorting and RNA-sequencing approach would also be appropriate as these could further define the cells and offer insights into their function by defining their pain and itch gene complement more broadly (Chamessian et al., 2018).

6.5 The Role of GRP-EGFP cells

In this thesis I present a number of lines of evidence which indicate that GRP-EGFP cells represent a homogeneous population of cells that correspond to a distinct functional class. Our findings, and those of others, offer insights into the functional role of this cell population. Given their characteristic connectivity and the behavioural phenotypes shown after chemogenetic manipulation or ablation of these cells, it seems highly likely that they act as secondary pruritoceptors. What is also evident however is that GRP-EGFP neurons do not represent the only source of GRP in the dorsal horn, with *Grp* mRNA present in a number of

other classes of neurons. Given the importance of GRP in itch signalling, the relative importance of GRP release from these other cells is worthy of further investigation. This could be investigated by generating a conditional knockout of the *Grp* gene in the GRP-Cre mouse, thereby limiting GRP release to only those cells not revealed in this line. Responses to pruritogens could then be determined which would indicate the relative importance of GRP from other sources. It may be the case however, that the failure to express EGFP we describe in the GRP-EGFP mouse is a consequence of a functional specialisation of this sub-class of *Grp* positive cells and that is reflected in chromatin accessibility. As such, it may even be that the GRP-EGFP population happens to be the subset of *Grp*-expressing cells that is the most important for itch transmission. At best this would be serendipitous. However, the finding that NPRA is enriched in this cell type would appear to support this. Furthermore, despite anatomical evidence of involvement of these cells in nociceptive and affective touch pathways, the functional relevance of this is still to be established.

7 References

Abraira, V.E., Ginty, D.D., 2013. The sensory neurons of touch. Neuron 79, 618–639. https://doi.org/10.1016/j.neuron.2013.07.051

Abraira, V.E., Kuehn, E.D., Chirila, A.M., Springel, M.W., Toliver, A.A., Zimmerman, A.L., Orefice, L.L., Boyle, K.A., Bai, L., Song, B.J., Bashista, K.A., O'Neill, T.G., Zhuo, J., Tsan, C., Hoynoski, J., Rutlin, M., Kus, L., Niederkofler, V., Watanabe, M., Dymecki, S.M., Nelson, S.B., Heintz, N., Hughes, D.I., Ginty, D.D., 2017. The Cellular and Synaptic Architecture of the Mechanosensory Dorsal Horn. Cell 168, 295-310.e19. https://doi.org/10.1016/j.cell.2016.12.010

Acton, D., Ren, X., Di Costanzo, S., Dalet, A., Bourane, S., Bertocchi, I., Eva, C., Goulding, M., 2019. Spinal Neuropeptide Y1 Receptor-Expressing Neurons Form an Essential Excitatory Pathway for Mechanical Itch. Cell Rep. 28, 625-639.e6. https://doi.org/10.1016/j.celrep.2019.06.033

Akiyama, T., Carstens, E., 2013. Neural processing of itch. Neuroscience 250, 697–714. https://doi.org/10.1016/j.neuroscience.2013.07.035

Akiyama, T., Tominaga, M., Takamori, K., Carstens, M.I., Carstens, E., 2014. Roles of glutamate, substance P, and gastrin-releasing peptide as spinal neurotransmitters of histaminergic and nonhistaminergic itch. Pain 155, 80–92. https://doi.org/10.1016/j.pain.2013.09.011

Alba-Delgado, C., El Khoueiry, C., Peirs, C., Dallel, R., Artola, A., Antri, M., 2015. Subpopulations of PKCγ interneurons within the medullary dorsal horn revealed by electrophysiologic and morphologic approach. Pain 156, 1714–1728. https://doi.org/10.1097/j.pain.0000000000000221

Albisetti, G.W., Ghanem, A., Foster, E., Conzelmann, K.-K., Zeilhofer, H.U., Wildner, H., 2017. Identification of Two Classes of Somatosensory Neurons That Display Resistance to Retrograde Infection by Rabies Virus. J. Neurosci. 37, 10358–10371. https://doi.org/10.1523/JNEUROSCI.1277-17.2017

Albisetti, G.W., Pagani, M., Platonova, E., Hösli, L., Johannssen, H.C., Fritschy, J.-M., Wildner, H., Zeilhofer, H.U., 2019. Dorsal Horn Gastrin-Releasing Peptide Expressing Neurons Transmit Spinal Itch But Not Pain Signals. J. Neurosci. 39, 2238–2250. https://doi.org/10.1523/JNEUROSCI.2559-18.2019

Arcourt, A., Gorham, L., Dhandapani, R., Prato, V., Taberner, F.J., Wende, H., Gangadharan, V., Birchmeier, C., Heppenstall, P.A., Lechner, S.G., 2017. Touch Receptor-Derived Sensory Information Alleviates Acute Pain Signaling and Fine-Tunes Nociceptive Reflex Coordination. Neuron 93, 179–193. https://doi.org/10.1016/j.neuron.2016.11.027

Aresh, B., Freitag, F.B., Perry, S., Blümel, E., Lau, J., Franck, M.C.M., Lagerström, M.C., 2017. Spinal cord interneurons expressing the gastrin-releasing peptide receptor convey itch through VGLUT2-mediated signaling. Pain 158, 945–961. https://doi.org/10.1097/j.pain.0000000000000861

Ascoli, G.A., 2015. Sharing Neuron Data: Carrots, Sticks, and Digital Records. PLoS Biol 13, e1002275. https://doi.org/10.1371/journal.pbio.1002275

Balachandar, A., Prescott, S.A., 2018. Origin of heterogeneous spiking patterns from continuously distributed ion channel densities: a computational study in spinal dorsal horn neurons. J. Physiol. 596, 1681–1697. https://doi.org/10.1113/JP275240

Bardoni, R., Shen, K.-F., Li, H., Jeffry, J., Barry, D.M., Comitato, A., Li, Y.-Q., Chen, Z.-F., 2019. Pain Inhibits GRPR Neurons via GABAergic Signaling in the Spinal Cord. Sci. Rep. 9, 15804. https://doi.org/10.1038/s41598-019-52316-0

Barry, D.M., Li, H., Liu, X.-Y., Shen, K.-F., Liu, X.-T., Wu, Z.-Y., Munanairi, A., Chen, X.-J., Yin, J., Sun, Y.-G., Li, Y.-Q., Chen, Z.-F., 2016. Critical evaluation of the expression of gastrin-releasing peptide in dorsal root ganglia and spinal cord. Mol. Pain 12, 1744806916643724. https://doi.org/10.1177/1744806916643724

Barry, D.M., Liu, X.-T., Liu, B., Liu, X.-Y., Gao, F., Zeng, X., Liu, J., Yang, Q., Wilhelm, S., Yin, J., Tao, A., Chen, Z.-F., 2020. Exploration of sensory and spinal neurons expressing gastrin-releasing peptide in itch and pain related behaviors. Nat. Commun. 11, 1397. https://doi.org/10.1038/s41467-020-15230-y

Bautista, D.M., Siemens, J., Glazer, J.M., Tsuruda, P.R., Basbaum, A.I., Stucky, C.L., Jordt, S.-E., Julius, D., 2007. The menthol receptor TRPM8 is the principal detector of environmental cold. Nature 448, 204–208. https://doi.org/10.1038/nature05910

Bennett, D.L.H., Michael, G.J., Ramachandran, N., Munson, J.B., Averill, S., Yan, Q., McMahon, S.B., Priestley, J.V., 1998. A Distinct Subgroup of Small DRG Cells Express GDNF Receptor Components and GDNF Is Protective for These Neurons after Nerve Injury. J. Neurosci. 18, 3059–3072.

Bice, T.N., Beal, J.A., 1997. Quantitative and neurogenic analysis of the total population and subpopulations of neurons defined by axon projection in the superficial dorsal horn of

the rat lumbar spinal cord. J. Comp. Neurol. 388, 550–564. https://doi.org/10.1002/(sici)1096-9861(19971201)388:4<550::aid-cne4>3.0.co;2-1

Boada, M.D., Woodbury, C.J., 2008. Myelinated Skin Sensory Neurons Project Extensively throughout Adult Mouse Substantia Gelatinosa. J. Neurosci. 28, 2006–2014. https://doi.org/10.1523/JNEUROSCI.5609-07.2008

Bourane, S., Duan, B., Koch, S.C., Dalet, A., Britz, O., Garcia-Campmany, L., Kim, E., Cheng, L., Ghosh, A., Ma, Q., Goulding, M., 2015. Gate control of mechanical itch by a subpopulation of spinal cord interneurons. Science 350, 550–554. https://doi.org/10.1126/science.aac8653

Boyle, K.A., Gradwell, M.A., Yasaka, T., Dickie, A.C., Polgár, E., Ganley, R.P., Orr, D.P.H., Watanabe, M., Abraira, V.E., Kuehn, E.D., Zimmerman, A.L., Ginty, D.D., Callister, R.J., Graham, B.A., Hughes, D.I., 2019. Defining a Spinal Microcircuit that Gates Myelinated Afferent Input: Implications for Tactile Allodynia. Cell Rep. 28, 526-540.e6. https://doi.org/10.1016/j.celrep.2019.06.040

Boyle, K.A., Gutierrez-Mecinas, M., Polgár, E., Mooney, N., O'Connor, E., Furuta, T., Watanabe, M., Todd, A.J., 2017. A quantitative study of neurochemically defined populations of inhibitory interneurons in the superficial dorsal horn of the mouse spinal cord. Neuroscience 363, 120–133. https://doi.org/10.1016/j.neuroscience.2017.08.044

Branda, C.S., Dymecki, S.M., 2004. Talking about a Revolution: The Impact of Site-Specific Recombinases on Genetic Analyses in Mice. Dev. Cell 6, 7–28. https://doi.org/10.1016/S1534-5807(03)00399-X

Brewer, C.L., Styczynski, L.M., Serafin, E.K., Baccei, M.L., 2020. Postnatal maturation of spinal dynorphin circuits and their role in somatosensation. Pain 161, 1906–1924. https://doi.org/10.1097/j.pain.0000000000001884

Bröhl, D., Strehle, M., Wende, H., Hori, K., Bormuth, I., Nave, K.-A., Müller, T., Birchmeier, C., 2008. A transcriptional network coordinately determines transmitter and peptidergic fate in the dorsal spinal cord. Dev. Biol. 322, 381–393. https://doi.org/10.1016/j.ydbio.2008.08.002

Browne, T.J., Gradwell, M.A., Iredale, J.A., Madden, J.F., Hughes, D.I., Callister, R.J., Dayas, C.V., Graham, B.A., 2020. Transgenic cross-referencing of inhibitory and excitatory interneuron populations to dissect neuronal heterogeneity in the dorsal horn. Front. Mol. Neurosci. 13. https://doi.org/10.3389/fnmol.2020.00032

Callaway, E.M., Luo, L., 2015. Monosynaptic Circuit Tracing with Glycoprotein-Deleted Rabies Viruses. J. Neurosci. 35, 8979–8985. https://doi.org/10.1523/JNEUROSCI.0409-15.2015

Cavanaugh, D.J., Lee, H., Lo, L., Shields, S.D., Zylka, M.J., Basbaum, A.I., Anderson, D.J., 2009. Distinct subsets of unmyelinated primary sensory fibers mediate behavioral responses to noxious thermal and mechanical stimuli. Proc. Natl. Acad. Sci. U. S. A. 106, 9075–9080. https://doi.org/10.1073/pnas.0901507106

Chamessian, A., Young, M., Qadri, Y., Berta, T., Ji, R.-R., Ven, T.V. de, 2018. Transcriptional Profiling of Somatostatin Interneurons in the Spinal Dorsal Horn. Sci. Rep. 8, 6809. https://doi.org/10.1038/s41598-018-25110-7

Chen, X.-J., Sun, Y.-G., 2020. Central circuit mechanisms of itch. Nat. Commun. 11, 3052. https://doi.org/10.1038/s41467-020-16859-5

Chisholm, K.I., Khovanov, N., Lopes, D.M., La Russa, F., McMahon, S.B., 2018. Large Scale In Vivo Recording of Sensory Neuron Activity with GCaMP6. eNeuro 5. https://doi.org/10.1523/ENEURO.0417-17.2018

Christensen, A.J., Iyer, S.M., François, A., Vyas, S., Ramakrishnan, C., Vesuna, S., Deisseroth, K., Scherrer, G., Delp, S.L., 2016. In Vivo Interrogation of Spinal Mechanosensory Circuits. Cell Rep. 17, 1699–1710. https://doi.org/10.1016/j.celrep.2016.10.010

Coggeshall, R.E., 2005. Fos, nociception and the dorsal horn. Prog. Neurobiol. 77, 299–352. https://doi.org/10.1016/j.pneurobio.2005.11.002

Cordero-Erausquin, M., Allard, S., Dolique, T., Bachand, K., Ribeiro-da-Silva, A., De Koninck, Y., 2009. Dorsal horn neurons presynaptic to lamina I spinoparabrachial neurons revealed by transynaptic labeling. J. Comp. Neurol. 517, 601–615. https://doi.org/10.1002/cne.22179

Crow, M., Denk, F., 2019. RNA-seq data in pain research–an illustrated guide. Pain 160, 1502–1504. https://doi.org/10.1097/j.pain.0000000000001562

Cuello, A.C., Jessell, T.M., Kanazawa, I., Iversen, L.L., 1977. Substance P: localization in synaptic vesicles in rat central nervous system. J. Neurochem. 29, 747–751. https://doi.org/10.1111/j.1471-4159.1977.tb07795.x

Del Barrio, M.G., Bourane, S., Grossmann, K., Schüle, R., Britsch, S., O'Leary, D.D.M., Goulding, M., 2013. A transcription factor code defines nine sensory interneuron

subtypes in the mechanosensory area of the spinal cord. PloS One 8, e77928. https://doi.org/10.1371/journal.pone.0077928

Delile, J., Rayon, T., Melchionda, M., Edwards, A., Briscoe, J., Sagner, A., 2019. Single cell transcriptomics reveals spatial and temporal dynamics of gene expression in the developing mouse spinal cord. Development 146. https://doi.org/10.1242/dev.173807

Denk, F., 2017. Don't let useful data go to waste. Nat. News 543, 7. https://doi.org/10.1038/543007a

Denk, F., Bennett, D.L., McMahon, S.B., 2017. Nerve Growth Factor and Pain Mechanisms. Annu. Rev. Neurosci. 40, 307–325. https://doi.org/10.1146/annurev-neuro-072116-031121

Dickie, A.C., Bell, A.M., Iwagaki, N., Polgár, E., Gutierrez-Mecinas, M., Kelly, R., Lyon, H., Turnbull, K., West, S.J., Etlin, A., Braz, J., Watanabe, M., Bennett, D.L.H., Basbaum, A.I., Riddell, J.S., Todd, A.J., 2019. Morphological and functional properties distinguish the substance P and gastrin-releasing peptide subsets of excitatory interneuron in the spinal cord dorsal horn. Pain 160, 442–462. https://doi.org/10.1097/j.pain.0000000000001406

Djouhri, L., Lawson, S.N., 2004. Abeta-fiber nociceptive primary afferent neurons: a review of incidence and properties in relation to other afferent A-fiber neurons in mammals. Brain Res. Brain Res. Rev. 46, 131–145. https://doi.org/10.1016/j.brainresrev.2004.07.015

Dong, X., Han, S., Zylka, M.J., Simon, M.I., Anderson, D.J., 2001. A Diverse Family of GPCRs Expressed in Specific Subsets of Nociceptive Sensory Neurons. Cell 106, 619–632. https://doi.org/10.1016/S0092-8674(01)00483-4

Dong, Xintong, Dong, Xinzhong, 2018. Peripheral and Central Mechanisms of Itch. Neuron 98, 482–494. https://doi.org/10.1016/j.neuron.2018.03.023

Duan, B., Cheng, L., Bourane, S., Britz, O., Padilla, C., Garcia-Campmany, L., Krashes, M., Knowlton, W., Velasquez, T., Ren, X., Ross, S.E., Lowell, B.B., Wang, Y., Goulding, M., Ma, Q., 2014. Identification of Spinal Circuits Transmitting and Gating Mechanical Pain. Cell 159, 1417–1432. https://doi.org/10.1016/j.cell.2014.11.003

Dubin, A.E., Patapoutian, A., 2010. Nociceptors: the sensors of the pain pathway. J. Clin. Invest. 120, 3760–3772. https://doi.org/10.1172/JCI42843

Emery, E.C., Ernfors, P., 2020. Dorsal Root Ganglion Neuron Types and Their Functional Specialization, in: Wood, J. (Ed.), The Oxford Handbook of the Neurobiology of Pain. Oxford Handbooks. https://doi.org/10.1093/oxfordhb/9780190860509.013.4

Emery, E.C., Luiz, A.P., Sikandar, S., Magnúsdóttir, R., Dong, X., Wood, J.N., 2016. In vivo characterization of distinct modality-specific subsets of somatosensory neurons using GCaMP. Sci. Adv. 2, e1600990. https://doi.org/10.1126/sciadv.1600990

Erspamer, V., 1988. Discovery, Isolation, and Characterization of Bombesin-like Peptides. Ann. N. Y. Acad. Sci. 547, 3–9. https://doi.org/10.1111/j.1749-6632.1988.tb23870.x

Fatima, M., Ren, X., Pan, H., Slade, H., Asmar, A., Xiong, C., Shi, A., Xiong, A., Wang, L., Duan, B., 2019. Spinal somatostatin-positive interneurons transmit chemical itch. Pain 160, 1166–1174. https://doi.org/10.1097/j.pain.0000000000001499

Feil, R., Wagner, J., Metzger, D., Chambon, P., 1997. Regulation of Cre recombinase activity by mutated estrogen receptor ligand-binding domains. Biochem. Biophys. Res. Commun. 237, 752–757. https://doi.org/10.1006/bbrc.1997.7124

Feng, L., Kwon, O., Lee, B., Oh, W.C., Kim, J., 2014. Using mammalian GFP reconstitution across synaptic partners (mGRASP) to map synaptic connectivity in the mouse brain. Nat. Protoc. 9, 2425–2437. https://doi.org/10.1038/nprot.2014.166

Fleming, M.S., Ramos, D., Han, S.B., Zhao, J., Son, Y.-J., Luo, W., 2012. The majority of dorsal spinal cord gastrin releasing peptide is synthesized locally whereas neuromedin B is highly expressed in pain- and itch-sensing somatosensory neurons. Mol. Pain 8, 52. https://doi.org/10.1186/1744-8069-8-52

Foster, E., Wildner, H., Tudeau, L., Haueter, S., Ralvenius, W.T., Jegen, M., Johannssen, H., Hösli, L., Haenraets, K., Ghanem, A., Conzelmann, K.-K., Bösl, M., Zeilhofer, H.U., 2015. Targeted Ablation, Silencing, and Activation Establish Glycinergic Dorsal Horn Neurons as Key Components of a Spinal Gate for Pain and Itch. Neuron 85, 1289–1304. https://doi.org/10.1016/j.neuron.2015.02.028

Franck, M.C.M., Stenqvist, A., Li, L., Hao, J., Usoskin, D., Xu, X., Wiesenfeld-Hallin, Z., Ernfors, P., 2011. Essential role of Ret for defining non-peptidergic nociceptor phenotypes and functions in the adult mouse. Eur. J. Neurosci. 33, 1385–1400. https://doi.org/10.1111/j.1460-9568.2011.07634.x

Freitag, F.B., Ahemaiti, A., Jakobsson, J.E.T., Weman, H.M., Lagerström, M.C., 2019. Spinal gastrin releasing peptide receptor expressing interneurons are controlled by local phasic and tonic inhibition. Sci. Rep. 9, 16573. https://doi.org/10.1038/s41598-019-52642-3

Ganley, R.P., Iwagaki, N., Del Rio, P., Baseer, N., Dickie, A.C., Boyle, K.A., Polgár, E., Watanabe, M., Abraira, V.E., Zimmerman, A., Riddell, J.S., Todd, A.J., 2015. Inhibitory Interneurons That Express GFP in the PrP-GFP Mouse Spinal Cord Are Morphologically Heterogeneous, Innervated by Several Classes of Primary Afferent and Include Lamina I Projection Neurons among Their Postsynaptic Targets. J. Neurosci. 35, 7626–7642. https://doi.org/10.1523/JNEUROSCI.0406-15.2015

Gao, T., Ma, H., Xu, B., Bergman, J., Larhammar, D., Lagerström, M.C., 2018. The Neuropeptide Y System Regulates Both Mechanical and Histaminergic Itch. J. Invest. Dermatol. 138, 2405–2411. https://doi.org/10.1016/j.jid.2018.05.008

Gao, Y.-J., Ji, R.-R., 2009. c-Fos and pERK, which is a better marker for neuronal activation and central sensitization after noxious stimulation and tissue injury? Open Pain J. 2, 11–17. https://doi.org/10.2174/1876386300902010011

Glasgow, S.M., Henke, R.M., MacDonald, R.J., Wright, C.V.E., Johnson, J.E., 2005. Ptf1a determines GABAergic over glutamatergic neuronal cell fate in the spinal cord dorsal horn. Development 132, 5461–5469. https://doi.org/10.1242/dev.02167

Gobel, S., 1978. Golgi studies of the neurons in layer II of the dorsal horn of the medulla (trigeminal nucleus caudalis). J. Comp. Neurol. 180, 395–413. https://doi.org/10.1002/cne.901800213

Gong, S., Zheng, C., Doughty, M.L., Losos, K., Didkovsky, N., Schambra, U.B., Nowak, N.J., Joyner, A., Leblanc, G., Hatten, M.E., Heintz, N., 2003. A gene expression atlas of the central nervous system based on bacterial artificial chromosomes. Nature 425, 917–925. https://doi.org/10.1038/nature02033

Goswami, S.C., Thierry-Mieg, D., Thierry-Mieg, J., Mishra, S., Hoon, M.A., Mannes, A.J., Iadarola, M.J., 2014. Itch-associated peptides: RNA-Seq and bioinformatic analysis of natriuretic precursor peptide B and gastrin releasing peptide in dorsal root and trigeminal ganglia, and the spinal cord. Mol. Pain 10, 44. https://doi.org/10.1186/1744-8069-10-44

Graham, B.A., Hughes, D.I., 2019. Rewards, perils and pitfalls of untangling spinal pain circuits. Curr. Opin. Physiol., Physiology of Pain 11, 35–41. https://doi.org/10.1016/j.cophys.2019.04.015

Grudt, T.J., Perl, E.R., 2002. Correlations between neuronal morphology and electrophysiological features in the rodent superficial dorsal horn. J. Physiol. 540, 189–207.

Guo, Z., Zhao, C., Huang, M., Huang, T., Fan, M., Xie, Z., Chen, Y., Zhao, X., Xia, G., Geng, J., Cheng, L., 2012. Tlx1/3 and Ptf1a Control the Expression of Distinct Sets of Transmitter and Peptide Receptor Genes in the Developing Dorsal Spinal Cord. J. Neurosci. 32, 8509–8520. https://doi.org/10.1523/JNEUROSCI.6301-11.2012

Gutierrez-Mecinas, M., Bell, A., Polgár, E., Watanabe, M., Todd, A.J., 2019a. Expression of Neuropeptide FF Defines a Population of Excitatory Interneurons in the Superficial Dorsal Horn of the Mouse Spinal Cord that Respond to Noxious and Pruritic Stimuli. Neuroscience 416, 281–293. https://doi.org/10.1016/j.neuroscience.2019.08.013

Gutierrez-Mecinas, M., Bell, A.M., Marin, A., Taylor, R., Boyle, K.A., Furuta, T., Watanabe, M., Polgár, E., Todd, A.J., 2017. Preprotachykinin A is expressed by a distinct population of excitatory neurons in the mouse superficial spinal dorsal horn including cells that respond to noxious and pruritic stimuli. Pain 158, 440–456. https://doi.org/10.1097/j.pain.0000000000000778

Gutierrez-Mecinas, M., Bell, A.M., Shepherd, F., Polgár, E., Watanabe, M., Furuta, T., Todd, A.J., 2019. Expression of cholecystokinin by neurons in mouse spinal dorsal horn. J. Comp. Neurol. 527, 1857–1871. https://doi.org/10.1002/cne.24657

Gutierrez-Mecinas, M., Davis, O., Polgár, E., Shahzad, M., Navarro-Batista, K., Furuta, T., Watanabe, M., Hughes, D.I., Todd, A.J., 2019b. Expression of Calretinin Among Different Neurochemical Classes of Interneuron in the Superficial Dorsal Horn of the Mouse Spinal Cord. Neuroscience 398, 171–181. https://doi.org/10.1016/j.neuroscience.2018.12.009

Gutierrez-Mecinas, M., Furuta, T., Watanabe, M., Todd, A.J., 2016a. A quantitative study of neurochemically defined excitatory interneuron populations in laminae I–III of the mouse spinal cord. Mol. Pain 12, 1744806916629065. https://doi.org/10.1177/1744806916629065

Gutierrez-Mecinas, M., Kuehn, E.D., Abraira, V.E., Polgár, E., Watanabe, M., Todd, A.J., 2016b. Immunostaining for Homer reveals the majority of excitatory synapses in laminae I–III of the mouse spinal dorsal horn. Neuroscience 329, 171–181. https://doi.org/10.1016/j.neuroscience.2016.05.009

Gutierrez-Mecinas, M., Polgár, E., Bell, A.M., Herau, M., Todd, A.J., 2018. Substance P-expressing excitatory interneurons in the mouse superficial dorsal horn provide a propriospinal input to the lateral spinal nucleus. Brain Struct. Funct. 223, 2377–2392. https://doi.org/10.1007/s00429-018-1629-x

Gutierrez-Mecinas, M., Watanabe, M., Todd, A.J., 2014. Expression of gastrin-releasing peptide by excitatory interneurons in the mouse superficial dorsal horn. Mol. Pain 10, 79. https://doi.org/10.1186/1744-8069-10-79

Hachisuka, J., Baumbauer, K.M., Omori, Y., Snyder, L.M., Koerber, H.R., Ross, S.E., 2016. Semi-intact ex vivo approach to investigate spinal somatosensory circuits. eLife 5. https://doi.org/10.7554/eLife.22866

Han, L., Ma, C., Liu, Q., Weng, H.-J., Cui, Y., Tang, Z., Kim, Y., Nie, H., Qu, L., Patel, K.N., Li, Z., McNeil, B., He, S., Guan, Y., Xiao, B., LaMotte, R.H., Dong, X., 2013. A subpopulation of nociceptors specifically linked to itch. Nat. Neurosci. 16, 174–182. https://doi.org/10.1038/nn.3289

Häring, M., Zeisel, A., Hochgerner, H., Rinwa, P., Jakobsson, J.E.T., Lönnerberg, P., Manno, G., Sharma, N., Borgius, L., Kiehn, O., Lagerström, M.C., Linnarsson, S., Ernfors, P., 2018. Neuronal atlas of the dorsal horn defines its architecture and links sensory input to transcriptional cell types. Nat. Neurosci. 1. https://doi.org/10.1038/s41593-018-0141-1

Heinke, B., Ruscheweyh, R., Forsthuber, L., Wunderbaldinger, G., Sandkühler, J., 2004. Physiological, neurochemical and morphological properties of a subgroup of GABAergic spinal lamina II neurones identified by expression of green fluorescent protein in mice. J. Physiol. 560, 249–266. https://doi.org/10.1113/jphysiol.2004.070540

Hokfelt, T., Kellerth, J.O., Nilsson, G., Pernow, B., 1975. Substance p: localization in the central nervous system and in some primary sensory neurons. Science 190, 889–890. https://doi.org/10.1126/science.242075

Huang, J., Polgár, E., Solinski, H.J., Mishra, S.K., Tseng, P.-Y., Iwagaki, N., Boyle, K.A., Dickie, A.C., Kriegbaum, M.C., Wildner, H., Zeilhofer, H.U., Watanabe, M., Riddell, J.S., Todd, A.J., Hoon, M.A., 2018. Circuit dissection of the role of somatostatin in itch and pain. Nat. Neurosci. 21, 707–716. https://doi.org/10.1038/s41593-018-0119-z

Huang, T., Lin, S.-H., Malewicz, N.M., Zhang, Yan, Zhang, Ying, Goulding, M., LaMotte, R.H., Ma, Q., 2019. Identifying the pathways required for coping behaviours associated with sustained pain. Nature 565, 86–90. https://doi.org/10.1038/s41586-018-0793-8

Hughes, D.I., Sikander, S., Kinnon, C.M., Boyle, K.A., Watanabe, M., Callister, R.J., Graham, B.A., 2012. Morphological, neurochemical and electrophysiological features of parvalbumin-expressing cells: a likely source of axo-axonic inputs in the mouse spinal dorsal horn. J. Physiol. 590, 3927–3951. https://doi.org/10.1113/jphysiol.2012.235655

Imlach, W.L., Bhola, R.F., Mohammadi, S.A., Christie, M.J., 2016. Glycinergic dysfunction in a subpopulation of dorsal horn interneurons in a rat model of neuropathic pain. Sci. Rep. 6, 37104. https://doi.org/10.1038/srep37104

Iwagaki, N., Ganley, R.P., Dickie, A.C., Polgár, E., Hughes, D.I., Del Rio, P., Revina, Y., Watanabe, M., Todd, A.J., Riddell, J.S., 2016. A combined electrophysiological and morphological study of neuropeptide Y–expressing inhibitory interneurons in the spinal dorsal horn of the mouse. Pain 157, 598–612. https://doi.org/10.1097/j.pain.0000000000000407

Iwagaki, N., Garzillo, F., Polgár, E., Riddell, J.S., Todd, A.J., 2013. Neurochemical characterisation of lamina II inhibitory interneurons that express GFP in the PrP-GFP mouse. Mol. Pain 9. https://doi.org/10.1186/1744-8069-9-56

Jessell, T., Tsunoo, A., Kanazawa, I., Otsuka, M., 1979. Substance P: Depletion in the dorsal horn of rat spinal cord after section of the peripheral processes of primary sensory neurons. Brain Res. 168, 247–259. https://doi.org/10.1016/0006-8993(79)90167-7

Jessell, T.M., 2000. Neuronal specification in the spinal cord: inductive signals and transcriptional codes. Nat. Rev. Genet. 1, 20–29. https://doi.org/10.1038/35049541

Ji, R.-R., Baba, H., Brenner, G.J., Woolf, C.J., 1999. Nociceptive-specific activation of ERK in spinal neurons contributes to pain hypersensitivity. Nat. Neurosci. 2, 1114–1119. https://doi.org/10.1038/16040

Kardon, A.P., Polgár, E., Hachisuka, J., Snyder, L.M., Cameron, D., Savage, S., Cai, X., Karnup, S., Fan, C.R., Hemenway, G.M., Bernard, C.S., Schwartz, E.S., Nagase, H., Schwarzer, C., Watanabe, M., Furuta, T., Kaneko, T., Koerber, H.R., Todd, A.J., Ross, S.E., 2014. Dynorphin Acts as a Neuromodulator to Inhibit Itch in the Dorsal Horn of the Spinal Cord. Neuron 82, 573–586. https://doi.org/10.1016/j.neuron.2014.02.046

Kebschull, J.M., 2019. DNA sequencing in high-throughput neuroanatomy. J. Chem. Neuroanat. 100, 101653. https://doi.org/10.1016/j.jchemneu.2019.101653

Kim, E.J., Jacobs, M.W., Ito-Cole, T., Callaway, E.M., 2016. Improved Monosynaptic Neural Circuit Tracing Using Engineered Rabies Virus Glycoproteins. Cell Rep. 15, 692–699. https://doi.org/10.1016/j.celrep.2016.03.067

Koch, S.C., Acton, D., Goulding, M., 2018. Spinal Circuits for Touch, Pain and Itch. Annu. Rev. Physiol. 80, 189–217. https://doi.org/10.1146/annurev-physiol-022516-034303

Koga, K., Yamagata, R., Kohno, K., Yamane, T., Shiratori-Hayashi, M., Kohro, Y., Tozaki-Saitoh, H., Tsuda, M., 2020. Sensitization of spinal itch transmission neurons in a mouse

model of chronic itch requires an astrocytic factor. J. Allergy Clin. Immunol. 145, 183-191.e10. https://doi.org/10.1016/j.jaci.2019.09.034

Lai, H.C., Seal, R.P., Johnson, J.E., 2016. Making sense out of spinal cord somatosensory development. Development 143, 3434–3448. https://doi.org/10.1242/dev.139592

Larsson, M., 2017. Pax2 is persistently expressed by GABAergic neurons throughout the adult rat dorsal horn. Neurosci. Lett. 638, 96–101. https://doi.org/10.1016/j.neulet.2016.12.015

Larsson, M., Broman, J., 2019. Synaptic Organization of VGLUT3 Expressing Low-Threshold Mechanosensitive C Fiber Terminals in the Rodent Spinal Cord. eNeuro 6. https://doi.org/10.1523/ENEURO.0007-19.2019

Lawson, S.N., Crepps, B.A., Perl, E.R., 1997. Relationship of substance P to afferent characteristics of dorsal root ganglion neurones in guinea-pig. J. Physiol. 505 (Pt 1), 177–191. https://doi.org/10.1111/j.1469-7793.1997.00177.x

Lee, H., Ko, M.-C., 2015. Distinct functions of opioid-related peptides and gastrin-releasing peptide in regulating itch and pain in the spinal cord of primates. Sci. Rep. 5, 11676. https://doi.org/10.1038/srep11676

Li, C., Wang, S., Chen, Y., Zhang, X., 2018. Somatosensory Neuron Typing with High-Coverage Single-Cell RNA Sequencing and Functional Analysis. Neurosci. Bull. 34, 200–207. https://doi.org/10.1007/s12264-017-0147-9

Li, C.-L., Li, K.-C., Wu, D., Chen, Y., Luo, H., Zhao, J.-R., Wang, S.-S., Sun, M.-M., Lu, Y.-J., Zhong, Y.-Q., Hu, X.-Y., Hou, R., Zhou, B.-B., Bao, L., Xiao, H.-S., Zhang, X., 2016. Somatosensory neuron types identified by high-coverage single-cell RNA-sequencing and functional heterogeneity. Cell Res. 26, 83–102. https://doi.org/10.1038/cr.2015.149

Light, A.R., Perl, E.R., 1979. Spinal termination of functionally identified primary afferent neurons with slowly conducting myelinated fibers. J. Comp. Neurol. 186, 133–150. https://doi.org/10.1002/cne.901860203

Liljencrantz, J., Olausson, H., 2014. Tactile C fibers and their contributions to pleasant sensations and to tactile allodynia. Front. Behav. Neurosci. 8. https://doi.org/10.3389/fnbeh.2014.00037

Lin, J.-T., Coy, D.H., Mantey, S.A., Jensen, R.T., 1995. Comparison of the peptide structural requirements for high affinity interaction with bombesin receptors. Eur. J. Pharmacol. 294, 55–69. https://doi.org/10.1016/0014-2999(95)00510-2

Liu, M.-Z., Chen, X.-J., Liang, T.-Y., Li, Q., Wang, M., Zhang, X.-Y., Li, Y.-Z., Sun, Q., Sun, Y.-G., 2019. Synaptic control of spinal GRPR+ neurons by local and long-range inhibitory inputs. Proc. Natl. Acad. Sci. 116, 27011–27017. https://doi.org/10.1073/pnas.1905658116

Liu, Q., Sikand, P., Ma, C., Tang, Z., Han, L., Li, Z., Sun, S., LaMotte, R.H., Dong, X., 2012. Mechanisms of itch evoked by β-alanine. J. Neurosci. Off. J. Soc. Neurosci. 32, 14532–14537. https://doi.org/10.1523/JNEUROSCI.3509-12.2012

Liu, Q., Tang, Z., Surdenikova, L., Kim, S., Patel, K.N., Kim, A., Ru, F., Guan, Y., Weng, H.-J., Geng, Y., Undem, B.J., Kollarik, M., Chen, Z.-F., Anderson, D.J., Dong, X., 2009. Sensory neuron-specific GPCRs Mrgprs are itch receptors mediating chloroquine-induced pruritus. Cell 139, 1353–1365. https://doi.org/10.1016/j.cell.2009.11.034

Liu, X.-Y., Wan, L., Huo, F.-Q., Barry, D.M., Li, H., Zhao, Z.-Q., Chen, Z.-F., 2014. B-type natriuretic peptide is neither itch-specific nor functions upstream of the GRP-GRPR signaling pathway. Mol. Pain 10, 4. https://doi.org/10.1186/1744-8069-10-4

Liu, Y., Latremoliere, A., Li, X., Zhang, Z., Chen, M., Wang, X., Fang, C., Zhu, J., Alexandre, C., Gao, Z., Chen, B., Ding, X., Zhou, J.-Y., Zhang, Y., Chen, C., Wang, K.H., Woolf, C.J., He, Z., 2018. Touch and tactile neuropathic pain sensitivity are set by corticospinal projections. Nature 561, 547–550. https://doi.org/10.1038/s41586-018-0515-2

Löken, L.S., Wessberg, J., Morrison, I., McGlone, F., Olausson, H., 2009. Coding of pleasant touch by unmyelinated afferents in humans. Nat. Neurosci. 12, 547–548. https://doi.org/10.1038/nn.2312

Lu, Y., Dong, H., Gao, Y., Gong, Y., Ren, Y., Gu, N., Zhou, S., Xia, N., Sun, Y.-Y., Ji, R.-R., Xiong, L., 2013. A feed-forward spinal cord glycinergic neural circuit gates mechanical allodynia. J. Clin. Invest. 123, 4050–4062. https://doi.org/10.1172/JCI70026

Lu, Y., Perl, E.R., 2005. Modular organization of excitatory circuits between neurons of the spinal superficial dorsal horn (laminae I and II). J. Neurosci. 25, 3900–3907. https://doi.org/10.1523/JNEUROSCI.0102-05.2005

Luo, L., Callaway, E.M., Svoboda, K., 2018. Genetic Dissection of Neural Circuits: A Decade of Progress. Neuron 98, 256–281. https://doi.org/10.1016/j.neuron.2018.03.040

Ma, C., Nie, H., Gu, Q., Sikand, P., Lamotte, R.H., 2012. In vivo responses of cutaneous C-mechanosensitive neurons in mouse to punctate chemical stimuli that elicit itch and nociceptive sensations in humans. J. Neurophysiol. 107, 357–363. https://doi.org/10.1152/jn.00801.2011

Mainen, Z.F., Sejnowski, T.J., 1996. Influence of dendritic structure on firing pattern in model neocortical neurons. Nature 382, 363–366. https://doi.org/10.1038/382363a0

Malmberg, A.B., Chen, C., Tonegawa, S., Basbaum, A.I., 1997. Preserved acute pain and reduced neuropathic pain in mice lacking PKCgamma. Science 278, 279–283. https://doi.org/10.1126/science.278.5336.279

Marvizón, J.C.G., Chen, W., Murphy, N., 2009. Enkephalins, dynorphins and β-endorphin in the rat dorsal horn: an immunofluorescence colocalization study. J. Comp. Neurol. 517, 51–68. https://doi.org/10.1002/cne.22130

Maxwell, D.J., Belle, M.D., Cheunsuang, O., Stewart, A., Morris, R., 2007. Morphology of inhibitory and excitatory interneurons in superficial laminae of the rat dorsal horn. J. Physiol. 584, 521–533. https://doi.org/10.1113/jphysiol.2007.140996

McDonald, T.J., Jörnvall, H., Nilsson, G., Vagne, M., Ghatei, M., Bloom, S.R., Mutt, V., 1979. Characterization of a gastrin releasing peptide from porcine non-antral gastric tissue. Biochem. Biophys. Res. Commun. 90, 227–233. https://doi.org/10.1016/0006-291X(79)91614-0

McKemy, D.D., 2012. The Molecular and Cellular Basis of Cold Sensation. ACS Chem. Neurosci. 4, 238–247. https://doi.org/10.1021/cn300193h

Melzack, R., Wall, P.D., 1965. Pain mechanisms: a new theory. Science 150, 971–979.

Minamino, N., Kangawa, K., Matsuo, H., 1984. Neuromedin B is a major bombesin-like peptide in rat brain: Regional distribution of neuromedin B and neuromedin C in rat brain, pituitary and spinal cord. Biochem. Biophys. Res. Commun. 124, 925–932. https://doi.org/10.1016/0006-291X(84)91046-5

Miraucourt, L.S., Dallel, R., Voisin, D.L., 2007. Glycine inhibitory dysfunction turns touch into pain through PKCgamma interneurons. PloS One 2, e1116. https://doi.org/10.1371/journal.pone.0001116

Mishra, S.K., Hoon, M.A., 2013. The Cells and Circuitry for Itch Responses in Mice. Science 340, 968–971. https://doi.org/10.1126/science.1233765

Mu, D., Deng, J., Liu, K.-F., Wu, Z.-Y., Shi, Y.-F., Guo, W.-M., Mao, Q.-Q., Liu, X.-J., Li, H., Sun, Y.-G., 2017. A central neural circuit for itch sensation. Science 357, 695–699. https://doi.org/10.1126/science.aaf4918

Müller, T., Anlag, K., Wildner, H., Britsch, S., Treier, M., Birchmeier, C., 2005. The bHLH factor Olig3 coordinates the specification of dorsal neurons in the spinal cord. Genes Dev. 19, 733–743. https://doi.org/10.1101/gad.326105

Müller, T., Brohmann, H., Pierani, A., Heppenstall, P.A., Lewin, G.R., Jessell, T.M., Birchmeier, C., 2002. The Homeodomain Factor Lbx1 Distinguishes Two Major Programs of Neuronal Differentiation in the Dorsal Spinal Cord. Neuron 34, 551–562. https://doi.org/10.1016/S0896-6273(02)00689-X

Nelson, T.S., Fu, W., Donahue, R.R., Corder, G.F., Hökfelt, T., Wiley, R.G., Taylor, B.K., 2019. Facilitation of neuropathic pain by the NPY Y1 receptor-expressing subpopulation of excitatory interneurons in the dorsal horn. Sci. Rep. 9, 7248. https://doi.org/10.1038/s41598-019-43493-z

Neumann, S., Braz, J.M., Skinner, K., Llewellyn-Smith, I.J., Basbaum, A.I., 2008. Innocuous, not noxious, input activates PKCgamma interneurons of the spinal dorsal horn via myelinated afferent fibers. J. Neurosci. 28, 7936–7944. https://doi.org/10.1523/JNEUROSCI.1259-08.2008

Nguyen, M.Q., Le Pichon, C.E., Ryba, N., 2019. Stereotyped transcriptomic transformation of somatosensory neurons in response to injury. eLife 8, e49679. https://doi.org/10.7554/eLife.49679

Nguyen, M.Q., Wu, Y., Bonilla, L.S., Buchholtz, L.J. von, Ryba, N.J.P., 2017. Diversity amongst trigeminal neurons revealed by high throughput single cell sequencing. PLOS ONE 12, e0185543. https://doi.org/10.1371/journal.pone.0185543

Nusbaum, M.P., Blitz, D.M., Marder, E., 2017. Functional consequences of neuropeptide and small-molecule co-transmission. Nat. Rev. Neurosci. 18, 389–403. https://doi.org/10.1038/nrn.2017.56

Pagani, M., Albisetti, G.W., Sivakumar, N., Wildner, H., Santello, M., Johannssen, H.C., Zeilhofer, H.U., 2019. How Gastrin-Releasing Peptide Opens the Spinal Gate for Itch. Neuron. https://doi.org/10.1016/j.neuron.2019.04.022

Pan, H., Fatima, M., Li, A., Lee, H., Cai, W., Horwitz, L., Hor, C.C., Zaher, N., Cin, M., Slade, H., Huang, T., Xu, X.Z.S., Duan, B., 2019. Identification of a Spinal Circuit for Mechanical and Persistent Spontaneous Itch. Neuron 103, 1135-1149.e6. https://doi.org/10.1016/j.neuron.2019.06.016

Parekh, R., Ascoli, G.A., 2013. Neuronal Morphology Goes Digital: A Research Hub for Cellular and System Neuroscience. Neuron 77, 1017–1038. https://doi.org/10.1016/j.neuron.2013.03.008

Paricio-Montesinos, R., Schwaller, F., Udhayachandran, A., Rau, F., Walcher, J., Evangelista, R., Vriens, J., Voets, T., Poulet, J.F.A., Lewin, G.R., 2020. The Sensory Coding of

Warm Perception. Neuron 106, 830-841.e3. https://doi.org/10.1016/j.neuron.2020.02.035

Peirs, C., Dallel, R., Todd, A.J., 2020. Recent advances in our understanding of the organization of dorsal horn neuron populations and their contribution to cutaneous mechanical allodynia. J. Neural Transm. 127, 505–525. https://doi.org/10.1007/s00702-020-02159-1

Peirs, C., Patil, S., Bouali-Benazzouz, R., Artola, A., Landry, M., Dallel, R., 2014. Protein kinase C gamma interneurons in the rat medullary dorsal horn: Distribution and synaptic inputs to these neurons, and subcellular localization of the enzyme. J. Comp. Neurol. 522, 393–413. https://doi.org/10.1002/cne.23407

Peirs, C., Seal, R.P., 2016. Neural circuits for pain: Recent advances and current views. Science 354, 578–584. https://doi.org/10.1126/science.aaf8933

Peirs, C., Williams, S.-P.G., Zhao, X., Walsh, C.E., Gedeon, J.Y., Cagle, N.E., Goldring, A.C., Hioki, H., Liu, Z., Marell, P.S., Seal, R.P., 2015. Dorsal Horn Circuits for Persistent Mechanical Pain. Neuron 87, 797–812. https://doi.org/10.1016/j.neuron.2015.07.029

Petitjean, H., Bourojeni, F.B., Tsao, D., Davidova, A., Sotocinal, S.G., Mogil, J.S., Kania, A., Sharif-Naeini, R., 2019. Recruitment of Spinoparabrachial Neurons by Dorsal Horn Calretinin Neurons. Cell Rep. 28, 1429-1438.e4. https://doi.org/10.1016/j.celrep.2019.07.048

Petitjean, H., Pawlowski, S.A., Fraine, S.L., Sharif, B., Hamad, D., Fatima, T., Berg, J., Brown, C.M., Jan, L.-Y., Ribeiro-da-Silva, A., Braz, J.M., Basbaum, A.I., Sharif-Naeini, R., 2015. Dorsal Horn Parvalbumin Neurons Are Gate-Keepers of Touch-Evoked Pain after Nerve Injury. Cell Rep. 13, 1246–1257. https://doi.org/10.1016/j.celrep.2015.09.080

Polavaram, S., Gillette, T.A., Parekh, R., Ascoli, G.A., 2014. Statistical analysis and data mining of digital reconstructions of dendritic morphologies. Front. Neuroanat. 8, 138. https://doi.org/10.3389/fnana.2014.00138

Polgár, E., Bell, A.M., Gutierrez-Mecinas, M., Dickie, A.C., Akar, O., Costreie, M., Watanabe, M., Todd, A.J., 2020. Substance P-expressing neurons in the superficial dorsal horn of the mouse spinal cord: insights into their functions and their roles in synaptic circuits. Neuroscience. https://doi.org/10.1016/j.neuroscience.2020.06.038

Polgár, E., Durrieux, C., Hughes, D.I., Todd, A.J., 2013a. A Quantitative Study of Inhibitory Interneurons in Laminae I-III of the Mouse Spinal Dorsal Horn. PLoS ONE 8, e78309. https://doi.org/10.1371/journal.pone.0078309

Polgár, E., Sardella, T.C.P., Tiong, S.Y.X., Locke, S., Watanabe, M., Todd, A.J., 2013b. Functional differences between neurochemically defined populations of inhibitory interneurons in the rat spinal dorsal horn. Pain 154, 2606–2615. https://doi.org/10.1016/j.pain.2013.05.001

Prescott, S.A., Koninck, Y.D., 2002. Four cell types with distinctive membrane properties and morphologies in lamina I of the spinal dorsal horn of the adult rat. J. Physiol. 539, 817–836. https://doi.org/10.1113/jphysiol.2001.013437

Punnakkal, P., von Schoultz, C., Haenraets, K., Wildner, H., Zeilhofer, H.U., 2014. Morphological, biophysical and synaptic properties of glutamatergic neurons of the mouse spinal dorsal horn. J. Physiol. 592, 759–776. https://doi.org/10.1113/jphysiol.2013.264937

Ramos-Álvarez, I., Moreno, P., Mantey, S.A., Nakamura, T., Nuche-Berenguer, B., Moody, T.W., Coy, D.H., Jensen, R.T., 2015. Insights into bombesin receptors and ligands: Highlighting recent advances. Peptides 72, 128–144. https://doi.org/10.1016/j.peptides.2015.04.026

Rexed, B., 1952. The cytoarchitectonic organization of the spinal cord in the cat. J. Comp. Neurol. 96, 415–495. https://doi.org/10.1002/cne.900960303

Ribeiro-da-Silva, A., Coimbra, A., 1982. Two types of synaptic glomeruli and their distribution in laminae I-III of the rat spinal cord. J. Comp. Neurol. 209, 176–186. https://doi.org/10.1002/cne.902090205

Ribeiro-da-Silva, A., Pioro, E.P., Cuello, A.C., 1991. Substance P- and enkephalin-like immunoreactivities are colocalized in certain neurons of the substantia gelatinosa of the rat spinal cord: an ultrastructural double-labeling study. J. Neurosci. 11, 1068–1080. https://doi.org/10.1523/JNEUROSCI.11-04-01068.1991

Roome, R.B., Bourojeni, F.B., Mona, B., Rastegar-Pouyani, S., Blain, R., Dumouchel, A., Salesse, C., Thompson, W.S., Brookbank, M., Gitton, Y., Tessarollo, L., Goulding, M., Johnson, J.E., Kmita, M., Chédotal, A., Kania, A., 2020. Phox2a defines a developmental origin of the anterolateral system in mice and humans. bioRxiv 2020.06.10.144659. https://doi.org/10.1101/2020.06.10.144659

Ross, S.E., Mardinly, A.R., McCord, A.E., Zurawski, J., Cohen, S., Jung, C., Hu, L., Mok, S.I., Shah, A., Savner, E.M., Tolias, C., Corfas, R., Chen, S., Inquimbert, P., Xu, Y., McInnes, R.R., Rice, F.L., Corfas, G., Ma, Q., Woolf, C.J., Greenberg, M.E., 2010. Loss of inhibitory interneurons in the dorsal spinal cord and elevated itch in Bhlhb5 mutant mice. Neuron 65, 886–898. https://doi.org/10.1016/j.neuron.2010.02.025

Sakai, K., Sanders, K.M., Lin, S.-H., Pavlenko, D., Funahashi, H., Lozada, T., Hao, S., Chen, C.-C., Akiyama, T., 2020. Low-threshold mechanosensitive VGLUT3-lineage sensory neurons mediate spinal inhibition of itch by touch. J. Neurosci. https://doi.org/10.1523/JNEUROSCI.0091-20.2020

Saleeba, C., Dempsey, B., Le, S., Goodchild, A., McMullan, S., 2019. A Student's Guide to Neural Circuit Tracing. Front. Neurosci. 13, 897. https://doi.org/10.3389/fnins.2019.00897

Salio, C., Aimar, P., Malapert, P., Moqrich, A., Merighi, A., 2020. Neurochemical and Ultrastructural Characterization of Unmyelinated Non-peptidergic C-Nociceptors and C-Low Threshold Mechanoreceptors Projecting to Lamina II of the Mouse Spinal Cord. Cell. Mol. Neurobiol. https://doi.org/10.1007/s10571-020-00847-w

Sathyamurthy, A., Johnson, K.R., Matson, K.J.E., Dobrott, C.I., Li, L., Ryba, A.R., Bergman, T.B., Kelly, M.C., Kelley, M.W., Levine, A.J., 2018. Massively Parallel Single Nucleus Transcriptional Profiling Defines Spinal Cord Neurons and Their Activity during Behavior. Cell Rep. 22, 2216–2225. https://doi.org/10.1016/j.celrep.2018.02.003

Schmidt, R., Schmelz, M., Forster, C., Ringkamp, M., Torebjörk, E., Handwerker, H., 1995. Novel classes of responsive and unresponsive C nociceptors in human skin. J. Neurosci. Off. J. Soc. Neurosci. 15, 333–341.

Seal, R.P., Wang, X., Guan, Y., Raja, S.N., Woodbury, C.J., Basbaum, A.I., Edwards, R.H., 2009. Injury-induced mechanical hypersensitivity requires C-low threshold mechanoreceptors. Nature 462, 651–655. https://doi.org/10.1038/nature08505

Serafin, E., Chamessian, A., Li, J., Zhang, X., McGann, A., Brewer, C., Berta, T., Baccei, M., 2019. Transcriptional profile of spinal dynorphin-lineage interneurons in the developing mouse. Pain Publish Ahead of Print. https://doi.org/10.1097/j.pain.0000000000001636

Sharif, B., Ase, A.R., Ribeiro-da-Silva, A., Séguéla, P., 2020. Differential Coding of Itch and Pain by a Subpopulation of Primary Afferent Neurons. Neuron 106, 940-951.e4. https://doi.org/10.1016/j.neuron.2020.03.021

Shekhar, K., Lapan, S.W., Whitney, I.E., Tran, N.M., Macosko, E.Z., Kowalczyk, M., Adiconis, X., Levin, J.Z., Nemesh, J., Goldman, M., McCarroll, S.A., Cepko, C.L., Regev, A., Sanes, J.R., 2016. Comprehensive Classification of Retinal Bipolar Neurons by Single-Cell Transcriptomics. Cell 166, 1308-1323.e30. https://doi.org/10.1016/j.cell.2016.07.054

Smith, K.M., Boyle, K.A., Madden, J.F., Dickinson, S.A., Jobling, P., Callister, R.J., Hughes, D.I., Graham, B.A., 2015. Functional heterogeneity of calretinin-expressing neurons in the mouse superficial dorsal horn: implications for spinal pain processing. J. Physiol. 593, 4319–4339. https://doi.org/10.1113/JP270855

Smith, K.M., Browne, T.J., Davis, O.C., Coyle, A., Boyle, K.A., Watanabe, M., Dickinson, S.A., Iredale, J.A., Gradwell, M.A., Jobling, P., Callister, R.J., Dayas, C.V., Hughes, D.I., Graham, B.A., 2019. Calretinin positive neurons form an excitatory amplifier network in the spinal cord dorsal horn. eLife 8, e49190. https://doi.org/10.7554/eLife.49190

Smith, K.M., Ross, S.E., 2020. Making connections: recent advances in spinal cord dorsal horn circuitry. Pain 161, S122. https://doi.org/10.1097/j.pain.0000000000001980

Snider, W.D., McMahon, S.B., 1998. Tackling Pain at the Source: New Ideas about Nociceptors. Neuron 20, 629–632. https://doi.org/10.1016/S0896-6273(00)81003-X

Solorzano, C., Villafuerte, D., Meda, K., Cevikbas, F., Bráz, J., Sharif-Naeini, R., Juarez-Salinas, D., Llewellyn-Smith, I.J., Guan, Z., Basbaum, A.I., 2015. Primary Afferent and Spinal Cord Expression of Gastrin-Releasing Peptide: Message, Protein, and Antibody Concerns. J. Neurosci. 35, 648–657. https://doi.org/10.1523/JNEUROSCI.2955-14.2015

Solway, B., Bose, S.C., Corder, G., Donahue, R.R., Taylor, B.K., 2011. Tonic inhibition of chronic pain by neuropeptide Y. Proc. Natl. Acad. Sci. 108, 7224–7229. https://doi.org/10.1073/pnas.1017719108

Spike, R.C., Puskár, Z., Andrew, D., Todd, A.J., 2003. A quantitative and morphological study of projection neurons in lamina I of the rat lumbar spinal cord. Eur. J. Neurosci. 18, 2433–2448. https://doi.org/10.1046/j.1460-9568.2003.02981.x

Spruston, N., 2008. Pyramidal neurons: dendritic structure and synaptic integration. Nat. Rev. Neurosci. 9, 206–221. https://doi.org/10.1038/nrn2286

Stantcheva, K.K., Iovino, L., Dhandapani, R., Martinez, C., Castaldi, L., Nocchi, L., Perlas, E., Portulano, C., Pesaresi, M., Shirlekar, K.S., Reis, F. de C., Paparountas, T., Bilbao, D., Heppenstall, P.A., 2016. A subpopulation of itch-sensing neurons marked by Ret and

somatostatin expression. EMBO Rep. 17, 585–600. https://doi.org/10.15252/embr.201540983

Sukhtankar, D.D., Ko, M.-C., 2013. Physiological Function of Gastrin-Releasing Peptide and Neuromedin B Receptors in Regulating Itch Scratching Behavior in the Spinal Cord of Mice. PLoS ONE 8, e67422. https://doi.org/10.1371/journal.pone.0067422

Sun, S., Xu, Q., Guo, C., Guan, Y., Liu, Q., Dong, X., 2017. Leaky Gate Model: Intensity-Dependent Coding of Pain and Itch in the Spinal Cord. Neuron 93, 840-853.e5. https://doi.org/10.1016/j.neuron.2017.01.012

Sun, Y.-G., Chen, Z.-F., 2007. A gastrin-releasing peptide receptor mediates the itch sensation in the spinal cord. Nature 448, 700–703. https://doi.org/10.1038/nature06029

Sun, Y.-G., Zhao, Z.-Q., Meng, X.-L., Yin, J., Liu, X.-Y., Chen, Z.-F., 2009. Cellular Basis of Itch Sensation. Science 325, 1531–1534. https://doi.org/10.1126/science.1174868

Tadros, M.A., Graham, B.A., Callister, R.J., 2018. Moving functional classification of dorsal horn neurons from art to science. J. Physiol. 596, 1543–1544. https://doi.org/10.1113/JP275870

Takanami, K., Sakamoto, H., Matsuda, K.I., Satoh, K., Tanida, T., Yamada, S., Inoue, K., Oti, T., Sakamoto, T., Kawata, M., 2014. Distribution of gastrin-releasing peptide in the rat trigeminal and spinal somatosensory systems. J. Comp. Neurol. 522, 1858–1873. https://doi.org/10.1002/cne.23506

Todd, A.J., 2017. Identifying functional populations among the interneurons in laminae I-III of the spinal dorsal horn. Mol. Pain 13, 1744806917693003. https://doi.org/10.1177/1744806917693003

Todd, A.J., 2010. Neuronal circuitry for pain processing in the dorsal horn. Nat. Rev. Neurosci. 11, 823–836. https://doi.org/10.1038/nrn2947

Todd, A.J., 1996. GABA and glycine in synaptic glomeruli of the rat spinal dorsal horn. Eur. J. Neurosci. 8, 2492–2498. https://doi.org/10.1111/j.1460-9568.1996.tb01543.x

Todd, A.J., Hughes, D.I., Polgár, E., Nagy, G.G., Mackie, M., Ottersen, O.P., Maxwell, D.J., 2003. The expression of vesicular glutamate transporters VGLUT1 and VGLUT2 in neurochemically defined axonal populations in the rat spinal cord with emphasis on the dorsal horn. Eur. J. Neurosci. 17, 13–27.

Todd, A.J., Sullivan, A.C., 1990. Light microscope study of the coexistence of GABA-like and glycine-like immunoreactivities in the spinal cord of the rat. J. Comp. Neurol. 296, 496–505. https://doi.org/10.1002/cne.902960312

Todd, A.J., Wang, F., 2020. Central Nervous System Pain Pathways, in: Wood, J. (Ed.), The Oxford Handbook of the Neurobiology of Pain. Oxford Handbooks. https://doi.org/10.1093/oxfordhb/9780190860509.013.5

Tyssowski, K.M., DeStefino, N.R., Cho, J.-H., Dunn, C.J., Poston, R.G., Carty, C.E., Jones, R.D., Chang, S.M., Romeo, P., Wurzelmann, M.K., Ward, J.M., Andermann, M.L., Saha, R.N., Dudek, S.M., Gray, J.M., 2018. Different Neuronal Activity Patterns Induce Different Gene Expression Programs. Neuron 98, 530-546.e11. https://doi.org/10.1016/j.neuron.2018.04.001

Usoskin, D., Furlan, A., Islam, S., Abdo, H., Lönnerberg, P., Lou, D., Hjerling-Leffler, J., Haeggström, J., Kharchenko, O., Kharchenko, P.V., Linnarsson, S., Ernfors, P., 2015. Unbiased classification of sensory neuron types by large-scale single-cell RNA sequencing. Nat. Neurosci. 18, 145–153. https://doi.org/10.1038/nn.3881

Vandewauw, I., De Clercq, K., Mulier, M., Held, K., Pinto, S., Van Ranst, N., Segal, A., Voet, T., Vennekens, R., Zimmermann, K., Vriens, J., Voets, T., 2018. A TRP channel trio mediates acute noxious heat sensing. Nature 555, 662–666. https://doi.org/10.1038/nature26137

Vrontou, S., Wong, A.M., Rau, K.K., Koerber, H.R., Anderson, D.J., 2013. Genetic identification of C fibres that detect massage-like stroking of hairy skin in vivo. Nature 493, 669–673. https://doi.org/10.1038/nature11810

Wada, E., Way, J., Lebacq-Verheyden, A.M., Battey, J.F., 1990. Neuromedin B and gastrin-releasing peptide mRNAs are differentially distributed in the rat nervous system. J. Neurosci. 10, 2917–2930.

Wang, F., Bélanger, E., Côté, S.L., Desrosiers, P., Prescott, S.A., Côté, D.C., De Koninck, Y., 2018. Sensory Afferents Use Different Coding Strategies for Heat and Cold. Cell Rep. 23, 2001–2013. https://doi.org/10.1016/j.celrep.2018.04.065

Wang, H., Zylka, M.J., 2009. Mrgprd-expressing polymodal nociceptive neurons innervate most known classes of substantia gelatinosa neurons. J. Neurosci. 29, 13202–13209. https://doi.org/10.1523/JNEUROSCI.3248-09.2009

Wang, Q., Zhang, X., He, X., Du, S., Jiang, Z., Liu, P., Qi, L., Liang, C., Gu, N., Lu, Y., 2020. Synaptic Dynamics of the Feed-forward Inhibitory Circuitry Gating Mechanical Allodynia in Mice. Anesthesiology 132, 1212–1228. https://doi.org/10.1097/ALN.0000000000003194

Wang, X., Zhang, J., Eberhart, D., Urban, R., Meda, K., Solorzano, C., Yamanaka, H., Rice, D., Basbaum, A.I., 2013. Excitatory Superficial Dorsal Horn Interneurons Are Functionally Heterogeneous and Required for the Full Behavioral Expression of Pain and Itch. Neuron 78, 312–324. https://doi.org/10.1016/j.neuron.2013.03.001

Wiesenfeld-Hallin, Z., Xu, X.-J., Hökfelt, T., 2002. The role of spinal cholecystokinin in chronic pain states. Pharmacol. Toxicol. 91, 398–403.

Wildner, H., Gupta, R.D., Bröhl, D., Heppenstall, P.A., Zeilhofer, H.U., Birchmeier, C., 2013. Genome-Wide Expression Analysis of Ptf1a- and Ascl1-Deficient Mice Reveals New Markers for Distinct Dorsal Horn Interneuron Populations Contributing to Nociceptive Reflex Plasticity. J. Neurosci. 33, 7299–7307. https://doi.org/10.1523/JNEUROSCI.0491-13.2013

Xing, Y., Chen, J., Hilley, H., Steele, H., Yang, J., Han, L., 2020. Molecular Signature of Pruriceptive MrgprA3+ Neurons. J. Invest. Dermatol. https://doi.org/10.1016/j.jid.2020.03.935

Xu, Y., Lopes, C., Wende, H., Guo, Z., Cheng, L., Birchmeier, C., Ma, Q., 2013. Ontogeny of Excitatory Spinal Neurons Processing Distinct Somatic Sensory Modalities. J. Neurosci. 33, 14738–14748. https://doi.org/10.1523/JNEUROSCI.5512-12.2013

Yang, Y., Li, Q., He, Q.-H., Han, J.-S., Su, L., Wan, Y., 2018. Heteromerization of μ-opioid receptor and cholecystokinin B receptor through the third transmembrane domain of the μ-opioid receptor contributes to the anti-opioid effects of cholecystokinin octapeptide. Exp. Mol. Med. 50, 1–16. https://doi.org/10.1038/s12276-018-0090-5

Yap, E.-L., Greenberg, M.E., 2018. Activity-Regulated Transcription: Bridging the Gap between Neural Activity and Behavior. Neuron 100, 330–348. https://doi.org/10.1016/j.neuron.2018.10.013

Yasaka, T., Kato, G., Furue, H., Rashid, M.H., Sonohata, M., Tamae, A., Murata, Y., Masuko, S., Yoshimura, M., 2007. Cell-type-specific excitatory and inhibitory circuits involving primary afferents in the substantia gelatinosa of the rat spinal dorsal horn in vitro. J. Physiol. 581, 603–618. https://doi.org/10.1113/jphysiol.2006.123919

Yasaka, T., Tiong, S.Y., Polgár, E., Watanabe, M., Kumamoto, E., Riddell, J.S., Todd, A.J., 2014. A putative relay circuit providing low-threshold mechanoreceptive input to lamina I projection neurons via vertical cells in lamina II of the rat dorsal horn. Mol. Pain 10, 3. https://doi.org/10.1186/1744-8069-10-3

Yasaka, T., Tiong, S.Y.X., Hughes, D.I., Riddell, J.S., Todd, A.J., 2010. Populations of inhibitory and excitatory interneurons in lamina II of the adult rat spinal dorsal horn revealed by a combined electrophysiological and anatomical approach. Pain 151, 475–488. https://doi.org/10.1016/j.pain.2010.08.008

Zeisel, A., Hochgerner, H., Lönnerberg, P., Johnsson, A., Memic, F., van der Zwan, J., Häring, M., Braun, E., Borm, L.E., La Manno, G., Codeluppi, S., Furlan, A., Lee, K., Skene, N., Harris, K.D., Hjerling-Leffler, J., Arenas, E., Ernfors, P., Marklund, U., Linnarsson, S., 2018. Molecular Architecture of the Mouse Nervous System. Cell 174, 999-1014.e22. https://doi.org/10.1016/j.cell.2018.06.021

Zhao, Z.-Q., Huo, F.-Q., Jeffry, J., Hampton, L., Demehri, S., Kim, S., Liu, X.-Y., Barry, D.M., Wan, L., Liu, Z.-C., Li, H., Turkoz, A., Ma, K., Cornelius, L.A., Kopan, R., Battey, J.F., Zhong, J., Chen, Z.-F., 2013. Chronic itch development in sensory neurons requires BRAF signaling pathways. J. Clin. Invest. 123, 4769–4780. https://doi.org/10.1172/JCI70528

Zhao, Z.-Q., Wan, L., Liu, X.-Y., Huo, F.-Q., Li, H., Barry, D.M., Krieger, S., Kim, S., Liu, Z.-C., Xu, J., Rogers, B.E., Li, Y.-Q., Chen, Z.-F., 2014. Cross-Inhibition of NMBR and GRPR Signaling Maintains Normal Histaminergic Itch Transmission. J. Neurosci. 34, 12402–12414. https://doi.org/10.1523/JNEUROSCI.1709-14.2014

Zylka, M.J., Rice, F.L., Anderson, D.J., 2005. Topographically distinct epidermal nociceptive circuits revealed by axonal tracers targeted to Mrgprd. Neuron 45, 17–25. https://doi.org/10.1016/j.neuron.2004.12.015